



Přírodovědecká
fakulta
Faculty
of Science

Jihočeská univerzita
v Českých Budějovicích
University of South Bohemia
in České Budějovice

Katedra experimentální biologie rostlin

Přírodovědecká fakulta

Jihočeská univerzita v Českých Budějovicích

**Zbraňové systémy v interakcích rostlin s patogeny:
zaostřeno na kyselinu salicylovou a mimobuněčné váčky**

Habilitační práce

Ing. Martin Janda, Ph.D.

2023

BaToVeZu za úsměvy, motivaci, toleranci, trpělivost a mnohé další ...

Poděkování

„To, že něco dokážeš vysvětlit, ještě neznamená, že to není zázrak.“

Velice rád bych poděkoval všem svým kolegům z ČR i ze zahraničí, se kterými jsem měl tu radost a možnost spolupracovat, sdílet své myšlenky, diskutovat a získávat finance na pokračování dalšího výzkumu. Hlavní spolupracovníky, kteří mají velkou zásluhu na tom, že jsem mohl napsat tuto habilitační práci, naleznete mezi mými spoluautory na publikacích. Dále bych chtěl poděkovat všem kolegům z Katedry experimentální biologie rostlin na PřF JU a všem svým studentům. Doufám, že jejich jména brzy naleznete mezi spoluautory na budoucích publikacích.

Dále bych chtěl poděkovat za podporu BaToVeZu, kterým tuto práci věnuji, rodičům a široké rodině.

Práce, která vedla k vytvoření habilitační práce, byla financovaná z institucionálních peněz VŠCHT v Praze, Ústavu experimentální botaniky AV ČR, Ludwig-Maximilians-Universität München, Přírodovědecké fakulty Jihočeské univerzity v Českých Budějovicích a účelovou podporou z grantů GAČR: P501/11/1654; P0501/12/1942; GA14-09685S; GA17-05151S, dále z financí poskytnutých MŠMT č.p.: CZ.02.2.69/0.0/0.0/17_050/0008485; CZ.02.2.69/0.0/0.0/18_053/0016975-1.

Obsah

Úvod do interakcí rostlin s patogeny: souboje na život a na smrt	1
1. „Závod ve zbrojení“	3
2. Hlavní aktéři „závodu ve zbrojení“	5
3. Rozpoznání útočníka	7
3.1. Plasmatická membrána	7
3.2. Cytosol	9
3.2.1 Efektorý	9
3.2.1.1 Přenos efektorů do buněk rostlin	10
3.2.2. Rozpoznání efektorů – R proteiny	13
4. Buněčná signalizace	14
4.1 Kalóza	18
4.2. Fytohormonální dráhy v imunitě rostlin – zaostřeno na kyselinu salicylovou	19
5. Všeho moc škodí aneb Kompromis mezi obranou a růstem rostliny	22
6. Závěr: minulost, současnost a budoucnost	24
Slovníček klíčových zkratek a pojmu	27
Seznam použité literatury	31
Přílohy	40
Přiložené vybrané původní výzkumné publikace autora habilitační práce	42

Úvod do interakcí rostlin s patogeny: souboje na život a na smrt

„Alea iacta est“

Při psaní tohoto textu jsem si již od počátku uvědomil (patrné i z tohoto úvodu), že často porovnávám a připodobňuji situaci u rostlin situacím, se kterými se setkáváme u nás, u lidí. Ač se to úplně neshoduje s klasickým vědeckým přístupem, rozhodl jsem se tato připodobnění v relativně hojně míře v textu využít, protože, kromě populárně naučných textů, nenalézám lepší přiležitost, kde takovéto své myšlenky rozvést a „hodit“ na papír. Klasický vědecký přístup v rámci mé habilitační práce představují publikované články, zatímco tento shrnující text by měl být přístupný i pro širší čtenářské publikum.*

Na rostliny, my lidé, nahlížíme všelijak. Dělají nám radost svou krásou a vůní, čehož využíváme, pokud chceme potěšit druhé. Pro mnohé z nás jsou zdrojem tolik potřebného chladu a svěžestí v letních měsících. Nebo, když je vidíme, si pomyslíme (s ohledem na probíhající klimatickou změnu), kolik asi pro nás nyní vyrábí kyslíku a kolik zabudovávají oxidu uhličitého. Ale především jsou pro všechny z nás zdrojem potravy, a to i kdybychom se cítili být „stoprocentními masožrouty“. Kolonizace souše rostlinami umožnila to, že si můžeme naši planetu užívat i my, lidé.

Málokdo jistě na rostliny nahlíží jako na nemilosrdná „monstra“, která jsou schopna v rámci svého přežití obětovat takřka cokoliv a neštítí se využít jakéhokoliv triku, sebevícce podlého a zákeřného k tomu aby se ubránila napadení. Máme spíše pocit, že je musíme opečovávat, protože jak by jinak mohli přežít v našem „nehostinném“ světě. Po celou dobu své výzkumné (ale i pedagogické) kariéry jsem se věnoval tématu interakcí rostlin s patogeny a zjistil jsem, že bychom se nemohli více mylit.

Rostliny nemohou z boje utéci, a i proto si ke svému přežití vyvinuly důmyslné obranné strategie, kterými odrazují, ale i ničí své případné protivníky. Mezi ně se řadí i mikroskopické patogeny z řad bakterií, hub či řasovek (oomycet). Tito, často neviditelní, tvorové také nejsou žádná „neviňátká“. Na rostliny útočí ve velkých množstvích, rychle se množí a jejich „zbraňové systémy“ se tak neustále zdokonalují a adaptují. Klíčem úspěchu rostliny jsou nejen neprostupné fyzické bariéry, jakými jsou kutikula, lignin, celulóza, či rozmanité všudypřítomné toxicke chemikálie, jako nikotin, tekutina v žahavých trichomech či glukosinoláty, ale i sofistikovaný imunitní systém. Klíčem k obraně jsou důmyslné detekční mechanismy, které následně spouští signalizaci (zde hraje významnou roli fytohormon kyselina salicylová), která má za následek produkci nových obranných látek. Aktivace imunitního systému vede v buňkách k přeskupení „vojsk“, kterým může být i pohyb celých organel, jako jsou chloroplasty. A může nezřídka končit i řízeným sebezničením buněk v okolí patogena s cílem zabránit jeho dalšímu šíření (Walters, 2017). Moderní výzkum ukázal, že rostliny s patogeny (mikroorganismy) vzájemně velmi intenzivně komunikují a vyměňují si mezi sebou molekuly, a to i cíleně. To může být klíčové v rozlišení přátel od nepřátel. Čím dál tím více se ukazuje, že v komunikaci mezi rostlinou a patogenem hrají roli malé RNA umožňující ovlivňovat expresi cílových genů u druhého organismu. V tomto dialogu mají nezastupitelnou roli mimobuněčné váčky sloužící k dopravě materiálu, které molekulám mohou poskytovat ochranu a přesné doručení (Huang, 2019).

Studium interakcí rostlin s patogeny není jen intelektuálním rozmarem hnaným lidskou touhou po poznání. Má to i svůj velmi praktický význam. S příchodem zemědělství, domestikací, šlechtěním kulturních plodin a výsevem monolitických velkých ploch jsme některým patogenům usnadnili práci, neboť vyšlechtěné rostliny mohou být za takových podmínek velmi zranitelné. V lidské historii způsobil neviditelný mikroorganismus nejednou fatální škody, které stály životy milionů lidí. Za příklad mohou sloužit římské slavnosti Robigalie, kdy Římané obětovali psa, aby bůh ochránil jejich úrodu před nemocemi, konkrétně většinou před rzí. Ve středověku bylo postrachem onemocnění zvané „oheň svatého Antonína“, za kterým nestál nikdo jiný než houbový patogen paličkovice nachová (*Claviceps purpurea*) napadající obilí. V devatenáctém století způsobila oomyceta *Phytophthora infestans* fatální neúrodu brambor v Irsku. To vedlo k tomu, že se irská populace čítající skoro 8 milionů obyvatel snížila přibližně až na polovinu. Ve čtyřicátých letech dvacátého století probíhal bengálský hladomor, za který mohla, mimo jiné, houba *Cochliobolus miyabeanus* způsobující hnědou skvrnitost rýže. V současnosti, především u nás v Evropě, nevnímáme nedostatek potravin jako hrozbu a patogenů na polích se děsí maximálně zemědělci. Za to vděčíme z velké části i intenzivnímu používání fungicidů a pesticidů, jejichž množství bychom velmi rádi viděli co nejnižší. Jenže, pokud je přestaneme používat a současně nevyvineme alternativu, čím je nahradit, mohou nás čekat, i z hlediska potravinové bezpečnosti, „zajímavé časy“. Už samotný probíhající konflikt na Ukrajině nám ukázal, že některé stabilní zdroje potravin nemusí být zdaleka tak stabilní, jak by se mohlo zdát.

Studium interakcí rostlin s patogeny a pochopení rostlinné imunity v součinnosti s novými biotechnologiemi, jako je dostupné sekvenování, tvorba syntetických mikrobiomů, či genomové editace, by nás mělo do budoucna posunout k udržitelnějšímu zemědělství. Například díky novinkám v genomových editacích můžeme naše znalosti o fungování rostlinné imunity rychle vyzkoušet v praxi a rostlinu rychle a efektivně vylepšit (způsob moderního šlechtění, který je v tuto chvíli zatím v EU na „černé listině“). Můžeme také hledat nové alternativní technologie, jakými může být například postříkem indukované umlčování genů (SIGS; *spray-induced gene silencing*) (Qiao, 2021).

V této práci se věnuji především dvěma aspektům interakcí rostlin s mikroorganismy, neboť ty byly hlavními tématy mého odborného zájmu a přiložených publikovaných studií: jevům týkajícím se více či méně signální dráhy fytohormonu kyseliny salicylové a vlastnostem mimobuněčných váčků produkovaných bakteriemi kolonizujícími rostliny, především patogenními. V následujícím textu jsem se snažil tato dvě téma zakomponovat do příběhu týkajícího se schopností rostlin bránit se napadení patogeny a naopak schopností patogenů být v infekci úspěšnými.

*Text je složen ze tří různých typů textu: hlavní text; poznámky (žluté rámečky) – doprovodné informace rozvádějící či komentující hlavní text. Přečtení hlavního textu je samosnosné i bez přečtení poznámek; příspěvky (zelené rámečky) – odkazují na mou výzkumnou práci a rozvádějí hlavní text v kontextu mého výzkumu.

1. Závod ve zbrojení

Stalo se již pravidlem, že se pojednání o rostlinné imunitě, či obecněji o interakcích rostlin s mikroorganismy, resp. patogeny, začíná tím, že rostliny nemohou z místa před útočníkem utéct. Díky diskusi se svými kolegy jsem si uvědomil, že to z hlediska obrany proti patogenům není až tak zásadní nevýhoda, neboť patogeny jsou malé (tj. nevidíme je) a kvůli své velikosti jsou v podstatě „všude“. Útěk by byl pro rostliny pravděpodobně veleúspěšnou strategií především v obraně proti živočišným škůdcům a býložravcům. Ať je to tak či onak, nic to nemění na tom, že se rostlina musí spolehnout na své obranné schopnosti a „zbraně“. Ty má po ruce buď neustále, nebo si je umí na počkání vyrobít.

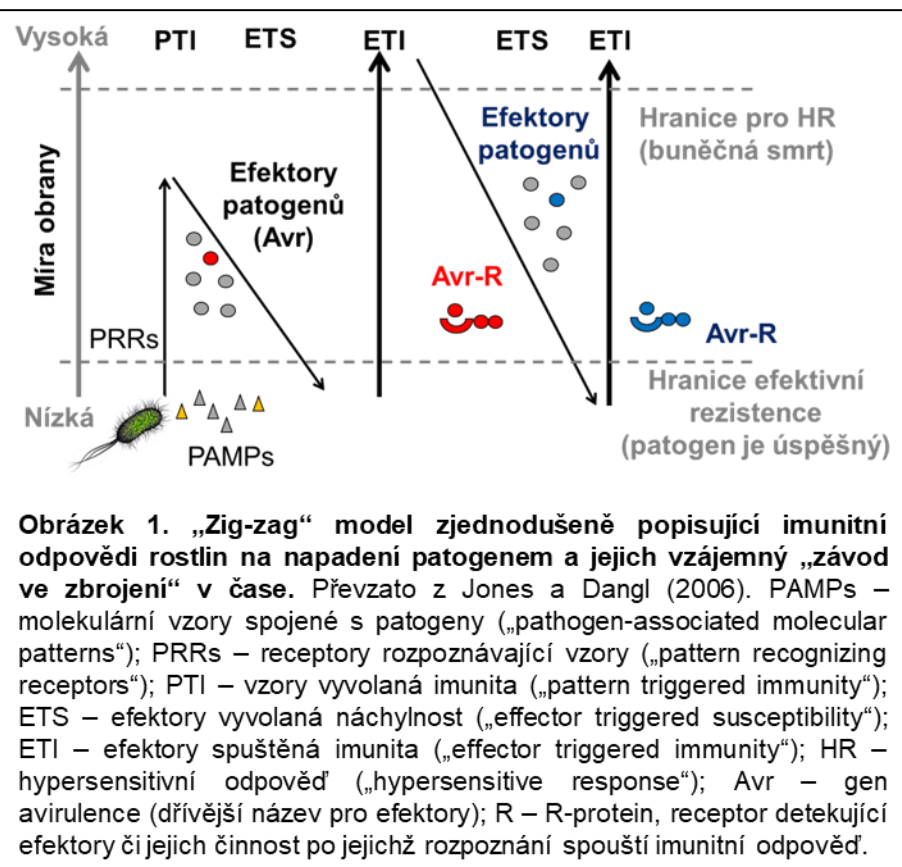
Souboj mezi rostlinou a patogenem prochází evolucí od počátku jejich setkání před stovkami milionů let. Rostliny se vyvíjí. Bleskurychle se však adaptují také patogeni. Zároveň se na stanovištích, kde rostlina roste, mohou objevovat úplně noví vetřelci (to se s globalizací a změnou klimatu děje a bude dít stále častěji). Tento neustále se vyvíjející „souboj“ mezi rostlinou a patogenem se velmi často v literatuře nazývá termínem „závod ve zbrojení“ (*arms race*). Jak rostlina, tak patogen se snaží vybavit lepšími a lepšími „zbraňovými systémy“, které jí umožní lépe a efektivněji se bránit a jemu naopak překonávat stále se zlepšující obranu rostliny a současně přežít její protiútoky^{poznámka 1}.

Stejně jako se vyvíjí vztah mezi rostlinou a patogenem, dozrává i náš pohled na tyto interakce^{příspěvek Živa 1/2020, strana 10}.

Pravděpodobně nejvlivnějším modelem znázorňujícím „závod ve zbrojení“ je tzv. „zig-zag“ model (Obr. 1), který zavedli ve svém přehledném článku pánorové Jonathan Jones z The Sainsbury Laboratory v Norwiche v Anglii a Jeffery Dangl z Duke University v USA (Jones, 2006). „Zig-zag“ model popisuje typy imunitní reakce rostliny na patogena, které jsou rozděleny podle molekul, jež jsou rostlinou rozpoznávány. Mohou jimi být konzervované molekuly typu PAMPs (molekulární vzory spojené s patogenem; *pathogen-associated molecular patterns*), či patogenem sekretované efektory. „Zig-zag“ model dále popisuje míru imunitní reakce a také to, jakým způsobem patogen tyto

Poznámka 1. Zajímavě do „závodu ve zbrojení“ vstoupil člověk. Ten již tisíce let domestikuje (a v blížší minulosti šlechtí) plodiny s cílem co nejvyššího výnosu. To ve většině případů vyústilo v kultivary, které rostou rychleji a produkují více. Na druhou stranu je rychlejší růst často spojen s tím, že je u těchto plodin významně snížena schopnost bránit se napadení patogenům. K náchylnosti pěstovaných plodin (a nebezpečí ztráty úrody v důsledku napadení patogeny) také velmi významně přispívá pěstování monokultur na velkých plochách. To úspěšnému patogenu proti danému kultivaru poskytuje v podstatě „ráj na zemi“ a my musíme vynakládat nemalé prostředky na postříky fungicidy a dalšími pesticidy. Šlechtění s cílem zásadně zvýšit obranyschopnost plodin je otázkou posledních dvou staletí. To souvisí s tím, že se dlouho nevěřilo tomu, že za nemoci rostlin mohou malé mikroorganismy, a dále s významným pokrokem našich znalostí v genetice, mikrobiologii, molekulární biologii (tj. velmi mladých vědeckých oborech), ale nesmíme opomenout i lepší vědomí o rostlinné fyziologii.

reakce obchází a jak na to následně reaguje rostlina. Zmíněný přehledový článek nese jednoduchý, ale v jistém smyslu komplikovaný název „Imunitní systém rostlin“ (Jones, 2006). Proč by to mělo být komplikované? Je nutné si uvědomit, že termín „imunita rostlin“ (*plant immunity*) nebyl všemi přijímán vřele (zejména imunology zabývajícími se živočichy). Nikdo již nezpochybňoval, že se rostlina napadením brání (a to velmi aktivně). Nicméně nazývat tuto obranu imunitou bylo pro některé kolegy příliš. Rostliny totiž nedisponují specializovanými imunitními buňkami či protilátkami. Tedy adaptivní imunitou tak, jak ji známe u živočichů (Ausubel, 2005). Ovšem stejně jako živočichové mají vrozenou (přirozenou) imunitu (Ausubel, 2005). A tu mají velmi propracovanou, protože na ní doslova závisí jejich život. Právě výše zmíněný článek od Jonesa a Dangla (vydaný v časopise *Nature*) s jednoduchým názvem „*The Plant Immune System*“ (Jones, 2006) výrazně přispěl k tomu, že je termín rostlinná imunita již široce akceptován napříč obory a že i my v současné době můžeme na její studium získávat zajímavé finanční prostředky.



Obrázek 1. „Zig-zag“ model zjednodušeně popisující imunitní odpovědi rostlin na napadení patogenem a jejich vzájemný „závod ve zbrojení“ v čase. Převzato z Jones a Dangl (2006). PAMPs – molekulární vzory spojené s patogeny („pathogen-associated molecular patterns“); PRRs – receptory rozpoznávající vzory („pattern recognizing receptors“); PTI – vzory vyvolaná imunita („pattern triggered immunity“); ETS – efektorové vyvolaná náchylnost („effector triggered susceptibility“); ETI – efektorové spuštěná imunita („effector triggered immunity“); HR – hypersensitivní odpověď („hypersensitive response“); Avr – gen avirulence (dřívější název pro efektor); R – R-protein, receptor detekující efektorové či jejich činnost po jejich rozpoznání spouští imunitní odpověď.

V rámci „ziz-zag“ modelu je imunitní reakce na napadení patogenem rozdělena v podstatě na dva typy. První se nazývá „vzory vyvolaná imunita“ (PTI; *Pattern Triggered Immunity*), slovo vzory se někdy nahrazuje termínem PAMPs. Tyto vzory reprezentují části proteinů, polysacharidů či lipidů, ale mohou to být i nízkomolekulární látky jako ATP. Druhým typem je imunita spuštěná efektorové (ETI; *Effector Triggered Immunity*). Ač se z modelu může zdát, že tyto dva typy imunitní reakce jsou vzájemně nezávislé a oddělené, není to pravdou. Objevuje se čím dál více důkazů o jejich propojenosti (Zhai, 2022), jejichž objevení vede ke snahám klasický „zig-zag“ model modifikovat tak, aby lépe reflektoval současné pokroky v poznání imunity rostlin (Cook, 2015; Lu, 2021). V rámci PTI jsou patogeni rozpoznáváni receptory

(PRRs; *Pattern Recognizing Receptors*) nalézajícími se většinou na plasmatické membráně rostlinné buňky. Tyto receptory rozpoznávají PAMPs, což jsou molekuly, bez nichž se patogen není schopen jednoduše obejít. Takovými molekulami jsou například flagelin, nenhoditelná součást bičíku (Zipfel, 2004), elongační faktor (Zipfel, 2006), klíčový pro translaci proteinů, či chitin (Miya, 2007), základní stavební kámen buněčných stěn hub. Výzkum zaměřený na nalezení nových „PAMPs“ a jejich receptorů je velmi intenzivní, což dokládá skoro exponenciální růst takto popsaných dvojic mezi lety 2012–2017 (Boutrot, 2017; Monaghan, 2012). Molekul PAMPs se patogen jen velice těžko zbavuje a je tedy nuten čelit jejich rozpoznání jinak. Čelí tomu tak, že syntetizuje a vypouští dovnitř buněk molekuly zvané efektory, které mají, mimo jiné, za úkol potlačovat reakce vyvolané při spuštění PTI. A právě rozpoznání takovýchto efektorů uvnitř buňky vede ke spuštění ETI (Obr. 1). To ukazuje, že rostliny mají receptory rozpoznávající patogeny i uvnitř buněk, tj. v cytosolu. Tyto receptory jsou nazývány R-proteiny a v obrázku 1 jsou označeny písmenem R.

Jestli v posledních letech nějaká událost „rozvířila vody“ na poli studia molekulárních interakcí rostlin s mikroorganismy, tak to byly dva články společně publikované v časopise *Science* v roce 2019, kde byl v řešitelských týmech stěžení postavou Jijie Chai (Wang, 2019a; Wang, 2019b). V článcích byl poprvé, za použití kryoelektronové mikroskopie, popsán detailní mechanismus rozpoznání efektoru R-proteinem s navržením následných buněčných dějů.

Ovšem závod ve zbrojení neprobíhá pouze jako součást rostlinné imunity. Vyvíjí se i, na první pohled, daleko zjevnější věci. Proti býložravcům například rostlina investuje do tvorby trnů a mnohých toxicických, či zpevňujících látek, jakými jsou alkaloidy či lignin. Je například známo, že akácie tvoří trny pouze do výšky, kam dosáhnou žirafy. Výše se jim prostě nevyplatí do tvorby trnů investovat energii. Současně bylo prokázáno, že pokud akácie rostou na území, kde tito býložravci nejsou, tak do tvorby trnů neinvestují prakticky vůbec. Kopřivy vytvářejí více žahavých trichomů na území, kde jsou pravidelně spásány kravami (Walters, 2017).

V tomto textu se však zaměřím pouze na interakce („závod ve zbrojení“) mezi rostlinami a mikroby, resp. patogeny. Dalším útočníkům neustále dotírajícím na rostliny, jako jsou háďátka, hmyz, býložravci, jiné rostliny a samozřejmě lidé, se v tomto textu věnovat nebudu.

2. Hlavní aktéři „závodu ve zbrojení“

„Kdo je kdo“

Ač jsem svým výzkumným zaměřením spíše rostlinný biolog než mikrobiolog a tato práce je součástí mé aspirace být habilitován v oboru *Fyziologie rostlin*, budu se snažit nenadřazovat v popisu onoho fascinujícího „závodu“ ani jedné ze stran konfliktu. I když srdečně stavět se na stranu bránícího, v tomto případě tedy většinou na stranu rostliny. A pokud se čtenáři bude zdát, že nadřuzuji, věřte, že to není cílené, ale pramení to z mých limitovaných znalostí.

Ve své výzkumné práci jsem se zabýval jak rostlinnou signalizací (výzkum týkající se fytohormonu kyseliny salicylové), tak patogenními „zbraněmi“, mimobuněčnými váčky.

Na jedné straně jsou rostliny, velmi rozmanitá říše, většinou mnohobuněčných, převážně fotosyntetizujících eukaryotických organismů, jichž je v současné době známo více než 300 000 druhů (CHRISTENHUSZ, 2016). Na přežití rostlin záleží i přežití nás živočichů, neboť rostliny ať už přímo nebo nepřímo představují esenciální zdroj potravy pro nás pro všechny. To je dáno jejich autotrofním způsobem života, kdy jsou schopny z anorganického oxidu uhličitého za využití světla a vody vytvářet organické molekuly, sacharidy. Proto je důležité znát co nejlépe, jak to rostliny dělají, že jsou schopné úspěšně čelit nepřízní prostředí, ve kterém se nacházejí. Nejvíce znalostí o průběhu „závodu ve zbrojení“ z hlediska rostliny známe díky výzkumu využívajícímu modelovou rostlinu *Arabidopsis thaliana* (huseníček rolní). Týká se to především znalostí procesů na buněčné úrovni. I já jsem v drtivé většině svých prací využíval huseníček. *A. thaliana* je hospodářsky i esteticky nevýznamná rostlina, ovšem jakožto modelový organismus s malým prostudovaným genomem a velmi dobře zavedenými molekulárními technikami je pro výzkum rostlin nepostradatelným společníkem (více o *A. thaliana* a historii jejího výzkumu v (Meyerowitz, 2001)).

Na straně druhé jsou patogenní mikroorganismy, patogeni, mezi které řadíme bakterie, oomycety, houby, ale i viry. Patogeny můžeme rozdělovat mnoha rozličnými způsoby, např. na prokaryotní a eukaryotní. Nebo jak již bylo zmíněno podle říše: na bakterie, houby, oomycety. Ale také například podle toho, jaký druh potravy patogen preferuje: živé pletivo rostliny (biotrofové), nebo mrtvé pletivo (nekrotrofové). Jsou ale i tací, kteří se v průběhu životního cyklu změní z biotrofů na nekrotrofy (hemibiotrofové) (Glazebrook, 2005). Všechna dělení dohromady slučují organismy s některými podobnými vlastnostmi. Na tom, jaké vlastnosti má patogen napadající rostlinu, závisí obrana dané rostliny. Jako příklad slouží imunita závislá na signalizaci zprostředkovávanou kyselinou salicylovou (SA), která je velmi efektivní v reakci na biotrofní patogeny, zatímco obrana závislá na signalizaci zprostředkovávanou kyselinou jasmonovou (JA) je účinná při napadení nekrotrofními patogeny (Glazebrook, 2005) a obráceně podle toho, na jakou rostlinu (skupinu rostlin) se patogen specializuje, bude i on vykazovat specifické vlastnosti.

Rostliny a patogeni jsou spolu v nepřetržitém kontaktu a jejich vzájemný vztah se neustále vyvíjí. Jak ale rostlina rozpozná, že ji právě napadl patogen?

3. Rozpoznání útočníka

„Pokyn k obraně“

Klíčovou událostí v případě obrany rostlin při napadení patogeny je jejich rozpoznání. Rostliny věnují svým rozpoznávacím systémům speciální pozornost a péči. Receptory rozpoznávající patogeny se nacházejí jak na povrchu (plasmatická membrána), tak uvnitř (cytosol) buněk.

3.1. Plasmatická membrána

„Hranice okupovaného území s rozmištěným mocným radarovým systémem“

Na plasmatické membráně se nalézají PRRs, které typicky rozpoznávají molekulární vzory útočníka, tj. PAMPs. Klasickou, dalo by se říci modelovou, dvojici PRR-PAMP představuje FLS2-Flg22. Jedná se o receptor rozpoznávající 22 aminokyselinový peptid (QRLSTGSRINSAKDDAAGLQIA) pocházející z flagelinu *Pseudomonas aeruginosa* (Trdá, 2014). Tato dvojice byla nejlépe prostudována u *A. thaliana*. První důkaz, že rostliny rozpoznávají flagelin podal Georg Felix v roce 1999 (Felix, 1999). Od té doby se stal flagelin pionýrem ve studiu molekulárních interakcí mezi PAMP a receptorem. Tým vedený prof. Thomasem Bollerem z Universität Basel ve Švýcarsku popsali, že rozpoznávaným epitopem flagelinu je výše zmíněný 22 aminokyselinový zbytek (Gómez-Gómez, 1999). Dále, že tento peptid je rozpoznáván receptorem FLS2 nacházejícím se v ekotypu *A. thaliana* Columbia 0, přičemž FLS2 se však přirozeně nenachází v ekotypu *A. thaliana* Wassilevskija (Zipfel, 2004). Tým okolo prof. Bollera dále prokázal, že ošetření flg22 před infekcí vede k vybuzení imunitní reakce a následné vyšší rezistenci rostlin (Zipfel, 2004). Experimenty prof. Robatzek demonstrovaly, že receptor FLS2 se nachází na plasmatické membráně a že po předání signálu o tom, že je přítomna bakterie, je FLS2 endocytován, tj. probíhá jeho recyklace na plasmatické membráně (Robatzek, 2006). FLS2 k následné signalizaci potřebuje při navázání flg22 navázat ještě koreceptor BAK1, který se váže současně k FLS2, ale i k části flg22 (Sun, 2013). BAK1 je mimochodem i koreceptorem pro receptor BRI1 detekující brassinosteroidy. Dlouho se mělo za to, že by mohl být klíčovou molekulou hrající roli v dialogu (kompromisu) rostliny mezi růstem a obranou (Li, 2002). (O tomto fenoménu blíže v kapitole 5). Nicméně experimenty prokázaly, že tomu tak není (Schwessinger, 2011). Zajímavostí je, že peptid flg22 se nachází ukryt uvnitř struktury flagelinu a není tudíž pro receptor přístupný. Trvalo bezmála 20 let, než se podařilo popsát mechanismus toho, jak je možné, že k tomuto peptidu má receptor v rostlině přístup (Buscaill, 2019)^{příspěvek Vesmír 99, 12, 2020/1}. V naší práci jsme flg22 také často využívali pro simulaci napadení rostliny bakteriálním patogenem (Janda, 2023; Kalachova, 2020; Janda, 2019; Kalachova, 2019). Tento přístup se postupně stal základním (ne-li prvním) krokem ve studiu těchto interakcí. V našem výzkumu (Janda, 2019) jsme prokázali, že receptor FLS2 je u *A. thaliana* pravděpodobně rychleji endocytován za zvýšené

teploty, resp. že za zvýšené teploty se ho nachází na plasmatické membráně méně, což vede k tomu, že rostlina se po působení vyšší teploty hůře brání napadení bakteriálním patogenem^{příspěvek 1}.

Nejen PAMPs jsou rozpoznávány na plasmatické membráně. Když se patogen snaží dostat dovnitř rostliny skrze kutikulu a buněčnou stěnu, nebo když produkce toxinů zničí buňku ve svém okolí, ocitnou se v mezibuněčném prostoru molekuly, které by tam za normálních okolností neměly být. Tyto molekuly se nazývají molekulární vzory spojené s nebezpečím (DAMPs, „Danger-Associated Molecular Patterns“). Mezi DAMPs se řadí oligomery kutinu z poškozené kutikuly, oligogalacturonidy z poškozené buněčné stěny, ATP, resp. eATP (extracelulární ATP) a další (Kanyuka, 2022). Rozpoznání PAMPs i DAMPs spouští velmi podobnou signalizaci, která je součástí aktivované imunitní odpovědi rostlin, ale o té podrobněji v kapitole 4^{příspěvek 2}. Protože jsou PAMPs i DAMPs relativně obecné molekuly, vede jejich rozpoznání ze své podstaty k univerzální a širokospektrální imunitní odpovědi, která se souhrnně nazývá PTI. Ovšem existuje i další, specifičtější, způsob rozpoznání napadení patogenů.

Příspěvek 1 Teplota a imunita. Rozvoj infekce u rostlin je charakterizován modelem tzv. „trojúhelníkem choroby“ („disease triangle“), který říká, že síla a závažnost choroby (úspěšnost patogena) závisí na druhu (genotypu), stáří a obecné fitness rostlin, dále na druhu (a množství) patogena a na prostředí, ve kterém se rostlina a patogen setkají. Z toho je patrné, že prostředí, tedy i teplota, hraje v interakcích rostlin s patogeny zásadní roli. Má teplota vliv i na imunitní reakce rostlin? Tato otázka je s přicházející klimatickou změnou o to aktuálnější. Z publikovaných výsledků bylo patrné, že vysoká teplota ovlivňuje obranné mechanismy u rostlin (Huot, 2017). V naší studii jsme popsali, že i krátké vystavení *A. thaliana* vysoké teplotě (rozmezí mezi 28°C – 42°C) vede k tomu, že při ošetření rostlin flg22 je potlačena produkce reaktivních forem kyslíku (ROS), která je za běžných podmínek typickým znakem rozpoznání flg22. Dále jsme pozorovali inhibici transkripce genů souvisejících s imunitní odpovědí rostlin (Janda, 2019). Tyto výsledky ukázaly, že je v našem případě potlačena signální dráha kyseliny salicylové (SA), důležitého fytohormonu účastníčícího se imunitních reakcí (více podrobností o SA v kapitole 4 nebo v našem přehledovém článku (Janda, 2015b)). Naše pozorování potvrdilo dřívější studie, které se zabývaly vlivem teploty na tuto signální dráhu. Dále nás zajímalo, co je důvodem, že je potlačena produkce ROS, která je po ošetření flg22 velmi rychlá (do deseti minut). Analyzovali jsme transkripci genu kódující receptor pro flg22, tj. FLS2. Zde jsme nepozorovali žádný efekt po vystavení zvýšené teplotě. Naopak jsme pomocí imunoblotové analýzy ukázali, že vystavení zvýšené teplotě vede ke snížení množství FLS2 na plasmatické membráně. Zvýšená teplota má tak pravděpodobně za následek zvýšenou endocytózu FLS2 z membrány nebo negativně ovlivňuje doručení nově produkovaného FLS2 na plasmatickou membránu. V dřívějších studiích zabývajících se vlivem vysoké teploty na infekci rostliny, konkrétně na patosystém *A. thaliana* – *Pst* DC3000, byla rostlina (a tedy i patogen) vystavena vyšší teplotě v průběhu infekce (Cheng, 2013). My jsme se rozhodli studovat, zda inhibice obranných schopností trvá i po vystavení vyšší teplotě a návratu do běžných pěstebních teplot. K našemu překvapení i 18 h po krátkém vystavení vyšší teplotě byly takto stresované rostliny více náchylné k napadení patogenem (Janda, 2019).

Příspěvek 2. Elicitory imunitních odpovědí rostlin. Nalézání molekul indukujících obranné reakce je dlouhodobě cílem nemála skupin, protože takové látky mohou mít potenciál při použití v zemědělství k ochraně plodin při napadení škůdci. Na Ústavu experimentální botaniky AV ČR jsem se zúčastnil výzkumu, který se zaměřil na testování efektu saponinů na interakci řepky olejky (*Brassica napus*) s jejím významným patogenem, způsobujícím fómové černání stonku, *Leptosphaeria maculans*. U saponinů, které jsou mimo jiné produkovaný rostlinami, je znám jejich antimikrobiální účinek. Ten jsme potvrdili také vůči *L. maculans*. Nejlépe se v tomto ohledu jeví saponin aescin. Proto nás nepřekvapilo, že při ošetření rostlin saponinu je infekce houbou nižší. Ovšem síla efektu byla výrazně vyšší, než jakou mělo použití komerčně dostupného fungicidu. Efekt byl naopak velmi podobný ošetření BTH, což je komerčně používaný induktor rezistence používaný pod názvem Bion®. Analyzovali jsme vliv aescinu na obranné mechanismy u řepky a překvapivě jsme prokázali, že aescin silně aktivuje její imunitní reakce. Aescin tak vykazuje zajímavý duální efekt. Fytohormonální analýza ukázala zvýšené množství SA. Proto jsme aescinem ošetřili také modelovou rostlinu *A. thaliana* a s využitím patosystému s bakterií *Pst DC3000* jsme prokázali, že aescin indukuje rezistenci i vůči bakteriálnímu patogenu (ačkoliv neměl antibakteriální účinek). Navíc jsme díky dostupným mutantním rostlinám prokázali, že aktivovaná obrana je závislá na funkční signální dráze SA (Trdá, 2019).

3.2. Cytosol

„Týl, velín. Tedy cíl“

Jedná se o rozpoznání, které probíhá uvnitř buňky, v cytosolu. I zde, možná překvapivě, dochází k rozpoznání napadení patogeny. Výše v textu jsem se zmiňoval, že patogeni s cílem zvýšit svou virulenci a úspěšnost infekce vypouštějí do rostlinných buněk molekuly nazývající se efektory.

3.2.1 Efektory

„Řízené střely patogenů“

Historie studia efektorů, jejich vlivu na rostlinu a obecně pohled na ně je fascinujícím, dynamickým příběhem obsahujícím zajímavé myšlenkové konstrukce, vynikající experimenty, nepřesnou a stále se vyvíjející nomenklaturu a překvapivé zvraty^{poznámka 2}. Současně je studium efektorů, mechanismu jejich účinku a jejich rozpoznání, jednoznačně téma přímo se dotýkající možných aplikací v rámci ochrany plodin proti patogenům. Potenciál se ještě více

projevuje především v kombinaci se současným pokrokem v genovém inženýrství (Van de Wouw, 2019).

Dříve byly efektory definovány jako molekuly potlačující imunitní (obrannou) odpověď rostliny, především PTI. Za příklad mohou sloužit tyto dobře charakterizované efektory z bakterie *Pseudomonas syringae* pv *tomato* DC3000 (*Pst DC3000*): AvrPto či AvrPtoB potlačující rozpoznání PAMPs PRR receptory, ale také komplex obsahující protein RIN4 regulující obranné reakce (Xin, 2013).

Nedávno se však ukázalo, že efektory nemusí nutně potlačovat imunitu, ale mohou pomáhat vytvořit příznivější prostředí k přežití a množení patogena. Za příklad slouží studie publikovaná v časopise Nature, která ukázala, že efektor HopM1 z *Pst DC3000* pomáhá patogenovi zajistit více vody v cytosolu (Xin, 2016)^{příspěvek Vesmír 96, 67, 2017/2}. Od té doby jsou efektory definovány šířejí jako molekuly pomáhající patogenům k infekci (virulenci) (El Kasmi, 2018)^{poznámka 3}. Jiným

zajímavým aspektem souboje o vlídnější vnitřní prostředí pro život patogena je regulace obsahu glukosy v mezibuněčném prostoru. Rostlinný glukosový transportér STP13 se ukazuje být zásadním ve snižování koncentrace glukosy v apoplastu. Současně se prokázalo, že množství glukózy ovlivňuje produkci a sekreci efektorů a že pokud gen *STP13* chybí, je rostlina náchylnější k napadení patogenem (Yamada, 2016)^{příspěvek Vesmír 96, 126, 2017/3}. Tyto práce dobře ilustrují, že „závod ve zbrojení“ se netýká jen vlastního arzenálu, ale cílí i na dostupnost živin.

3.2.1.1 Přenos efektorů do buněk rostlin

Jakým způsobem jsou efektori dopravovány do buněk? Různými způsoby, především v závislosti na druhu patogena, a zdaleka ne všechny teorie jsou uspokojivě prokázány experimentálně. Nejlépe prostudovaným způsobem dopravování bakteriálních efektorů je ten skrze sekreční systém třetího typu (T3SS) (Xin, 2018). U bakterií bylo popsáno šest sekrečních systémů (Green, 2016), z nichž právě T3SS je specialistou na transport efektorů do rostlinné buňky. Tento způsob transportu efektorů je u bakterií dominantní, pokud tedy daná bakterie disponuje T3SS. T3SS by se dal připodobnit

k dlouhé jehle vyrůstající z bakteriální buňky procházející skrze plasmatickou membránu rostlinné buňky a ústící v cytosolu, kam dopravuje efektoru (Cunnac, 2009). Houby a oomycety takovýmto útvarem, pokud je mi známo, nedisponují. Ty vytvářejí buněčnou strukturu zvanou haustorium. To se vchlipuje do plasmatické membrány rostlinné buňky (neproniká membránou) tak, aby byl co největší povrch haustoriu kontaktu s plasmatickou membránou. Plasmatická membrána rostliny obklopující haustorium se nazývá extrahaustoriální membrána

Poznámka 2. Na přednášce prof. Sophiena Kamouna, předního světového odborníka zabývajícího se efektoru, z The Sainsbury Laboratory v Norwichi (ORCID 0000-0002-0290-0315) jsem poprvé slyšel o konceptu, který nahlíží na efektor jako na rostlinný protein, i přestože jsou efektori produkované mikroorganismem (patogenem). Může se to zdát přitažené za vlasy, ale skrývá se za tím zajímavá logika. Efektor působí na rostlinu, nikoliv na patogena. Jeho aktivitou jsou tedy ovlivněny rostlinné procesy a vlastně své schopnosti projevuje až v rostlinné buňce, tudíž funguje jakožto rostlinný protein. Jistě by se takto neměl efektor definovat, ale myslím, že takovéto provokující myšlenkové konstrukce, které reflekují situaci v přírodě, vedou k tomu, že jsme schopni na danou problematiku nahlédnout z jiné perspektivy, což může vést k nečekaným objevům.

Poznámka 3. To, že jsou efektori definovány jako molekuly, které pomáhají virulenci, je logické, ale má to, z mého pohledu, jednu matoucí historickou souvislost, která může sloužit i jako výborný příklad toho, že i ve vědě velmi závisí na úhlu pohledu. Jedná se o to, že nemálo efektorových molekul má ve svém názvu Avr (od slova „avirulent“), např. u bakterie *Pseudomonas syringae* s touto předponou existuje alespoň sedm efektorů: AvrPto, AvrPtoB, AvrE, AvrPphB, AvrRps4, AvrRpt2, AvrRpm1 a AvrB (Xin, 2013). Tato předpona se v minulosti používala na základě faktu, že efektori byly popisovány z pohledu rostliny, tj. ve spojitosti se situací, že pokud měla rostlina odpovídající receptorový protein rozpoznávající daný efektor, byla vůči patogenovi mnohem rezistentnější. Přítomnost efektoru v patogenovi tak zapříčinila avirulenci. Na těchto pozorování vyrostla velmi úspěšná teorie popisující mechanismus obrany rostlin proti patogenům, a sice koncept rezistence „gen proti genu“ („Gene for gene theory“) vytvořená skvělým fytopatologem H. H. Florem (Flor, 1971). Když se ale na efektoru budeme dívat z hlediska definice, že pomáhají virulenci, těžko bychom je pojmenovali s předponou Avr.

(Mach, 2013). To, jakým způsobem jsou efektor využívány z haustoria přes membránu houby (či oomycety) a přes plasmatickou membránu rostlinné buňky (extrahaustoriální membránu), zatím není zcela jasné (Petre, 2014). Jeden z navržených mechanismů je transport díky mimobuněčným váčkům obsahujícím efektor (U. Stotz, 2022). Tyto váčky mohou splynout s plasmatickou membránou rostlinné buňky a tak vylít svůj obsah do cytosolu. Nicméně přesný mechanismus, jakým váčky, které jsou produkované patogeny mohou do rostliny doprovádat svůj náklad, není dosud zcela objasněn.

Využiji zmínky o mimobuněčných váčcích (EVs, „extracellular vesicles“) a popíši je blíže, neboť bakteriální mimobuněčné váčky jsou významnou součástí mého výzkumu^{příspěvek Vesmír 97, 554, 2018/10} (Janda, 2022; Janda, 2023).

S pokrokem v mikroskopických a molekulárních technikách se ukázalo, že pozorované váčky, které byly identifikovány již v polovině 20. století, nejsou artefaktem, ale i velmi aktivně produkovanými strukturami. Tvorba EVs byla od té doby popsána v podstatě u všech tříd organismů, od bakterií po savce. O EVs, jakožto o reálných (ne artificiálních) strukturách majících enzymatický a funkční potenciál, se začalo mluvit v 80. a 90. letech 20. století (Couch, 2021). U bakterií asociovaných s rostlinami (fytobakterií) byly EVs poprvé pozorovány u *Erwinia amylovora* v roce 1987 (Laurent, 1987). EVs jsou fosfolipidovou membránou ohrazené sférické struktury obsahující náklad pocházející z periplasmatického prostoru, ale i z cytosolu, poskytující přenášenému obsahu ochranu před vnějším prostředím, např. degradačními enzymy, jako jsou různé proteázy (McMillan, 2021a). Studium EVs se v posledních letech těší poměrně velkému zájmu, který je spojen s vysokými očekáváními jejich různorodých funkcí v rámci komunikace mezi organismy i v rámci jednoho mnohobuněčného organismu, a současně se pojí se zajímavým aplikačním potenciálem. Tento „boom“ souvisí i se snahou výzkum EVs co nejvíce standardizovat (Théry, 2018), protože studium EVs je velmi často spojeno s výzvami spojenými s jejich izolací a identifikací, či nedostatkem vlastního biologického materiálu, kdy se nezřídka v rámci pozorování nemusí jednat přímo o EVs, ale o artefakty (Théry, 2018). Navíc existují různé typy EVs a je vhodné udržovat správnou nomenklaturu, která je závislá na míře znalostí o daném typu pozorovaných EVs (Théry, 2018). Medicinální výzkum je v tomto ohledu oproti rostlinnému výzkumu o mnoho napřed, ale i tak již bylo jen u fytobakterií publikováno nejméně 29 studií věnujících se tématu EVs (Janda, 2022). V rámci výzkumu EVs se věnujeme různým tématům, jejich biogenezi (EVs mohou být produkovaný aktivně, či být vedlejším produktem buněčné smrti), stabilitě (ukazuje se, že EVs dokáží odolávat i velmi nepříznivým podmírkám a mohou být stabilnější, než bychom od nich očekávali), obsahu (víme, že EVs mohou obsahovat proteiny, nukleotidy včetně siRNA, toxiny, lipidy), efektu na cílový organismus (např. potlačení či indukce

imunitních reakcí, potlačení růstu a vývoje) (Janda, 2022; Cai, 2021; Van Niel, 2018). Je zřejmé, že očekávání,

které ohledně EVs máme, je poměrně vysoké, nicméně i kvůli jejich relativně náročnému studiu, je stále u EVs co objevovat. Při popisování efektů EVs je nutno experimenty pečlivě opakovat a navrhovat a tak se ne vždy zbavíme nejistoty, zda se nakonec nejedná o artefakt.

Příspěvek. 3 Mimobuněčné váčky (EVs) v interakcích rostlin s patogeny. V posledních letech se i pozornost vědců zabývajících se rostlinami a jejich interakcemi s mikroorganismy zaměřila na roli EVs v této komunikaci. Významnou roli by EVs mohly mít v doprovázení malých RNA mezi organismy (He, 2021). Při svém pobytu v laboratoři prof. Silke Robatzek na LMU jsem se věnoval vlastnostem EVs produkovaných fytopatogenní bakterií *Pst DC3000* a jejich vlivu na imunitní reakce *A. thaliana*. Jasně jsme demonstrovali produkci EVs při různých způsobech kultivace bakterie, ale také jsme jako první ukázali, že tento bakteriální patogen produkuje váčky i v průběhu infekce v apoplastu rostliny. Dále jsme prokázali imunogenní potenciál EVs (čímž jsme potvrdili předchozí studie) (Bahar, 2016), který je do značné míry závislý na přítomnosti flagelinu u váčků. V rámci tohoto pozorování stále nejsme schopni s jistotou říci, zda se jedná o artefakt způsobený kopurifikací flagelinu při izolaci EVs, nebo je efekt skutečně způsoben přítomností části flagelinu na izolovaných váčcích. V proteomické analýze jsme peptidy z flagelinu ve váčcích detekovali jako výrazně nabohacené. Proteomická analýza váčků navíc odhalila, že uvnitř váčků se mohou nalézat i bakteriální efektorů, čímž jsme doplnili i dříve publikované proteomické studie (Janda, 2022). Zajímavým zjištěním bylo, že by váčky mohly bakterii velmi dobře sloužit k získávání živin z apoplastu, konkrétně železa. Významně nabohacenými proteiny ve váčcích se ukázaly být proteiny související se siderophorovým transportem (Janda, 2023). Role a vlastnosti váčků u fytopakterií jsme shrnuli v přehledovém článku (Janda, 2022).

My jsme se zaměřili na studium EVs produkovaných fytopatogenní bakterií *Pst DC3000*, jejichž studiu se paralelně věnovala i skupina z Duke University v USA pod vedením prof. Kuehn, kteří publikovali jejich imunogenní efekt na rostliny v podstatě ve stejnou dobu, v jakou jsme my náš výzkum „vypustili do světa“ v preprint verzi (McMillan, 2021b; Janda, 2023). My jsme v našem výzkumu, nezávisle na americké skupině, dospěli k podobným výsledkům, ale současně ukazujeme některé rozdílnosti, které je nutno dále vysvetlit (Janda, 2023). V našem přístupu jsme se více zaměřili na biofyzikální vlastnosti váčků, jejich obsah a produkci přímo v rostline
^{příspěvek 3}.

Již dříve byl navržen možný přenos bakteriálních efektorů pomocí EVs i u fytopakterií. Tato hypotéza je podporována provedenými proteomickými studiemi zabývajícími se obsahem bakteriálních EVs. V těchto studiích byly uvnitř EVs identifikovány i efektorové (Janda, 2022)
^{příspěvek 3}.

3.2.2. Rozpoznání efektorů – R proteiny

„Protiraketový detekční systém“

Jak jsem popsal v předchozí kapitole, účinek efektorů může rozhodovat o „životě a smrti“ rostliny i patogena. Pokud má například bakterie *Pst DC3000* zablokovanou tvorbu nebo dopravu svých T3SS efektorů, tak je v podstatě neschopná infikovat *A. thaliana*. S funkčním efektorovým repertoárem je tato bakterie pro *A. thaliana* smrtelným nebezpečím (Xin, 2013; Xin, 2018). Patogeni se tak velmi často na sekreci efektorů spoléhají. Toho využívají rostliny a snaží se vytvořit detekční systémy monitorující přítomnost efektorů^{poznámka 4}. Efektory rozpoznávají většinou receptory nalézající se uvnitř buňky, v cytosolu. Jedná se o proteiny obsahující vazebnou doménu pro nukleotidy s částí obohacenou o leucin („Nucleotide-binding domain and leucin-rich repeat proteins“; NLRs). Toto rozpoznání vede ke spuštění tzv. ETI (obr. 1)^{poznámka 5}.

Je zajímavé, že jak PTI, tak ETI spouští podobné signalizační dráhy, které vedou k imunitní odpovědi (více v kapitole 4). Nicméně rozpoznání přítomnosti efektorů často vede k silnější odpovědi, která nezřídka ústí v hypersenzitivní odpověď (HR; „hypersensitivity response“), kdy rostlina lokálně usmrtí buňky s cílem zamezit dalšímu šíření patogena. Pochopení mechanismu, jak rostlina spouští tento typ buněčné smrti, bylo věnováno v posledních třiceti letech nemálo úsilí. Byly popsány důležité součásti signalizace, které přispívají k úspěšnému spuštění HR (Balint-Kurti, 2019). Významnou roli hraje produkce reaktivních forem kyslíku (ROS) (Zurbriggen, 2014) či funkční signalizace SA (Raffaele, 2006; Radojičić, 2018). Ovšem v roce 2019 došlo na tomto poli k zásadnímu objevu. S využitím kryoelektronové mikroskopie byl popsán přesný molekulární mechanismus rozpoznání efektoru. V tomto případě bylo popsáno rozpoznání zprostředkované proteinem ZAR1, řadícím se mezi NLR proteiny. ZAR1 nerozpoznává efektor přímo^{poznámka 4}, hlídá, zda není uridynilován protein PBL2. Uridynilaci PBL2 má totiž na svědomí efektor AvrRC. Ve chvíli, kdy AvrRC přidá uridynilový zbytek k PBL2, ZAR1 to detekuje, dochází k oligomerizaci ZAR1 a

Poznámka 4. Cíleně píše, že NLRs rozpoznávají „přítomnost efektorů“ nikoliv přímo efektory (tedy přímé rozpoznání konkrétního efektoru), protože v mikrobiální říši existuje nespočet efektorů a není v možnostech rostliny mít přímo proti každému z nich specifický receptor (každý mikrob má jiný repertoár efektorů, které se od sebe více či méně liší). K monitorování efektorů tak rostlina využívá několik „triků“, protože efektory s různorodou strukturou mohou mít jeden cíl účinku, tj. několik efektorů může cílit na degradaci stejněho proteinu, či potlačení / aktivaci některé konkrétní funkce. Jedná se o tyto způsoby rozpoznání: i) přímá vazba na efektor; ii) přímé monitorování dané funkce či proteinu zodpovědného za danou funkci; iii) vytvoření návnady pro efektor a monitorování změn u návnady. Díky tomu jsou NLRs velmi efektivním detekčním systémem v repertoáru rostliny (Cesari, 2018).

Poznámka 5. Na NLRs (tedy i na ETI) spoléhají rostliny daleko více než živočichové. Repertoár identifikovaných NLRs v rostlinách dosahuje několika stovek různých proteinů, zatímco u živočichů se často jedná o jednotky různých proteinů (huseníček 151, člověk 22) (Jones, 2016).

tvorbě tzv. resistosomu (Bi, 2021). Tako vzniklý resistosom tvoří uprostřed strukturu podobnou děravému hrotu, pro kterou byla navržena schopnost vytvářet póry v plasmatické membráně a tím přivodit buněčnou smrt (Förderer, 2022; Wang, 2019a; Wang, 2019b)^{poznámka 6}. Takovýto mechanismus by k buněčné smrti teoreticky nepotřeboval ani SA, ani ROS. Toto zjištění vedlo a vede k celé řadě otázek, kdy jednou z nich je, jak naložit s jasnými důkazy, že SA a ROS v aktivaci HR roli mají. Jako vysvětlení se nabízí možnost, že spouštěčem vedoucím k HR je rozpoznání efektoru a následná přímá smrt dané buňky. Dále následuje „vyliti“ obsahu této mrtvé buňky do apoplastu, kde jsou molekuly z vnitřku buňky rozpoznány, což vede dále k aktivaci a zesílení imunitní odpovědi (*de facto* rozpoznání DAMPs a tedy následná PTI) v přilehlých buňkách. Taková odpověď již vyžaduje funkční SA a ROS. Víme, že PTI sama o sobě HR často nevyvolává. Ovšem poslední navržené modely, které PTI a ETI významně propojují, než aby je škatulkovaly a oddělovaly od sebe, ukazují, že to nelze tak jednoznačně tvrdit (Cook, 2015; Lu, 2021). A nejde jen o modely. V roce 2021 byl v časopisu Nature publikován článek ukazující, že PRRs jsou nutné pro imunitu zprostředkovanou NLR (tedy přímé propojení klasicky definovaných PTI a ETI). Autoři současně prokázali, že signalizace spuštěná NLRs rychle posiluje expresi klíčových složek PTI. Jako jeden ze spojujících článků mezi PTI a ETI demonstrovali tvorbu ROS skrze NADPH oxidázu RboH (Yuan, 2021). To bylo potvrzeno a rozvedeno následnou prací (Zhai, 2022). Propojení mezi PTI a ETI vysvětluje, že v kombinaci s rozpoznáním efektoru je reakce na DAMPs (i PAMPs) tak silná, že dochází k HR.

Poznámka 6. Studium NLRs, jejich nová identifikace a popis mechanismu jejich účinku má a může mít nedocenitelný potenciál v zefektivnění šlechtění rostlin pro zlepšení rezistence proti cílovému patogenu. Již dříve byly úspěšné šlechtitelské projekty vnášející vybraný NLR do náhylné plodiny (Ellis, 2014). Ovšem, jak se ukázalo, vnesení pouze jednoho nového NLR není sázkou na jistotu. Ve většině případů je patogen schopen během 3-5 let rezistenci závislou na jednom konkrétním NLR obejít, proto je nyní snahou vnést do plodiny více nových NLR naráz, tzv. *stacking gene strategy*. Ukazuje se, že takto vytvořenou rezistenci je pro patogena v podstatě nemožné obejít (Zhu, 2012; Halpin, 2005).

4. Buněčná signalizace

„Spojařina v obraně rostlin“

V předchozím textu jsem představil možnosti detekce napadení patogeny. V této kapitole se zaměřím na následnou buněčnou signalizaci. Imunitní odpověď, ať už spuštěná rozpoznáním PAMPs, nebo efektorů, obsahuje typické události, které se dají rozdělit z hlediska jejich časoprostorového uspořádání (hezké schéma pro takové časoprostorové rozdělení reakcí v rámci PTI poskytuje přehledový článek (Ben Khaled, 2015)). Z hlediska „závodu ve zbrojení“

je znalost imunitní signalizace důležitá i proto, že účinek efektorů cílí v podstatě na všechny součásti této signalizace.

Po rozpoznání PAMPs na plasmatické membráně dochází k navázání receptoru s PAMP na koreceptor, což má za následek následnou fosforylací cílových proteinů. Imunitní odpověď se snaží postupně v rámci signalizace snížit její komplexitu. Od velmi různorodých PRRs (jichž se může v buňce nalézat poměrně vysoký počet) po fytohormonální signalizaci, či MAPK kaskádu^{poznámka 7}. Prvním krokem ke zjednodušení je právě využití koreceptorů. Tyto koreceptory jsou funkční pro více PRRs. Typickým příkladem je koreceptor BAK1, který je zásadní pro spuštění signalizace po rozpoznání flg22, ale je současně koreceptorem pro EFR1 a další PRRs, které se specializují na rozpoznání PAMPs proteinové povahy (Yasuda, 2017). Na plasmatické membráně dochází během jednotek minut k otevření kanálů umožňujících příliv vápenatých iontů (Ca^{2+}) do cytosolu. Signál na stres se může šířit celou rostlinou, přičemž sledování koncentrace Ca^{2+} iontů umožňuje monitoring signalizace. Např. při poranění byl prokázán glutamát, aby zprostředkovatel signálu do dalších částí rostliny při odpovědi na poranění. Glutamát je rozpoznán receptory na povrchu buněk a to spouští zvýšení koncentrace Ca^{2+} iontů uvnitř cytosolu. Takový signál prochází rostlinou během několika minut, přičemž rostlina koncentraci Ca^{2+} iontů v cytosolu velmi aktivně hlídá a jejich zvýšení je tak pouze dočasné (Toyota, 2018).

Zvýšení koncentrace vápenatých iontů aktivuje (nebo minimálně přispívá k aktivaci) následné procesy. Jedním z nich je zvýšená produkce ROS v apoplastu, která probíhá přibližně po deseti minutách po detekci patogena. U *A. thaliana* za tuto událost odpovídají NADPH oxidázy lokalizované na plasmatické membráně. Konkrétně se jedná o RbohD a RbohF oxidázy (*NADPH/Respiratory burst oxidase protein D (nebo F)*). Tyto oxidázy produkují do apoplastu superoxidový radikál, který je velmi reaktivní a v apoplastu se za přítomnosti superoxid dismutázy přeměňuje na peroxid vodíku. Tyto ROS mohou mít jak signalizační funkci, tak mohou samy o sobě působit antimikrobiálně (Qi, 2017). Pro nás výzkumníky je tato událost užitečná analyticky, protože byla vyvinuta technika stanovující apoplastický H_2O_2 na základě luminiscence s využitím roztoku luminolu (Smith, 2014). Tato technika je velmi rychlá a levná a kvalitativně velmi vypovídající. Slouží dobře prvnímu screeningu, zda je či není spuštěná

Poznámka 7. O tom, že následná signalizace po rozpoznání PAMPs pomocí PRR je mezi různými čeleděmi rostlin velmi konzervovaná, poskytuje důkazy studie, ve které vědci vložili receptor pro elongační faktor (EFR1) z *A. thaliana* (brukvovité) do rajče (lilkovité). Elongační faktor (EF-Tu) je rozpoznáván pouze u brukvovitých. Kontrolní a transgenní rostliny rajče ošetřili fytopatogenní bakterií *Ralstonia solanaceae*. Výsledky byly jednoznačné, transgenní rostliny byly daleko více rezistentní než kontrolní. To přineslo několik důležitých poznatků: i) rostliny si jsou schopny zabudovat funkční PRR z jiné čeledi; ii) imunitní signalizace je mezi čeleděmi velmi konzervovaná, tj. stačí rozpoznání PRR z jiné čeledi a je spuštěna fungující imunitní odpověď; iii) odhalení vysokého potenciálu daného výzkumu pro zlepšení ochrany rostlin proti patogenům (Lacombe, 2010).

imunitní odpověď. Tuto analýzu ve svých experimentech velmi rád používám, např. (Janda, 2019). V současnosti jsme například díky této metodě provedli u nás v laboratoři screening různých druhů rostlin na reakci na flagelin^{příspěvek 4} a hodláme s tím pokračovat, např. u vodních masožravých rostlin ve spolupráci s dr. Lubomírem Adamcem (Botanický ústav AV ČR, Třeboň). V případě pozitivní reakce těchto rostlin na flg22 budeme mít náhle v ruce světově unikátní modelový systém pro studium imunity u vodních rostlin, což je pole v našem oboru neprobádané. Produkce ROS není závislá pouze na Ca^{2+} iontech. Po navázání koreceptoru, jako příklad opět uvedeme BAK1, k PRR receptoru dochází k fosforylací RbohD a tím její aktivaci (Kadota, 2014; Lee, 2020). V podobném čase jako je tvorba ROS v apoplastu je pozorovatelná také jeho alkalizace (Felix, 1999).

V průběhu desítek minut po rozpoznání patogena dochází k další významné buněčné události, reorganizaci aktinového cytoskeletu (Henty-Ridilla, 2013). Aktinový cytoskelet hraje v rostlinné buňce zásadní roli v cíleném dopravování molekul a tzv. váčkovém transportu („vesicle trafficking“). Je již relativně dlouho známo, že v případě napadení rostliny houbovým patogenem je aktinová síť v okolí haustoria, resp. extrahaustoriální membrány, zhuštěna a aktinová vlákna jsou nasměrována tak, aby bylo možno dopravit co nejvíce materiálu do místa napadení (Li, 2019). Aktinový cytoskelet tak hraje roli jako fyzická bariéra, ale i jako „dopravní síť“, která umožňuje zásobovat místo napadení komponenty potřebnými pro tvorbu kalózy či jinými, s obranou souvisejícími, látkami, jako je PEN3 protein, hrající klíčovou roli v nehostitelské odolnosti rostlin (*non-host resistance*) (Wang, 2022). Experimenty využívající jak farmakologického přístupu (ošetření chemikáliemi depolymerizující aktinová vlákna), tak genetického přístupu (mutantní rostlinky *A. thaliana*), prokázaly, že rostlinky s ovlivněnou funkcí aktinového cytoskeletu jsou více náchylné na napadení patogeny (Henty-Ridilla, 2013; Wang, 2022; Porter, 2016; Sun, 2018).

V průběhu řešení své dizertační práce jsem se účastnil výzkumu, který ukázal, že při rozrušení aktinových vláken s využitím chemikálií latrunculin B a cytochalasin E dochází u *A. thaliana* k zajímavé události, a sice ke zvýšené transkripci genů souvisejících s imunitou, a to především se signální drahou SA (Matoušková, 2014; Janda, 2014). Tento objev nás vedl k testování hypotézy, že rostlinná buňka hlídá integritu svých aktinových vláken, a pokud je tato integrita narušena, tak buňka má za to, že je napadena patogenem a spouští imunitní odpověď. K této hypotéze nás také vedl fakt, že u bakterie *Pst DC3000* byl identifikován efektor (HopW1), který depolymerizaci aktinového cytoskeletu zapříčinuje (Jelenska, 2015). Situace v našich myslích velmi připomínala možný způsob detekce patogena pomocí NLR hlídajícího funkční aktinový cytoskelet. Skutečně jsme ukázali, že depolymerizace aktinového cytoskeletu může vést ke zvýšení rezistence vůči patogenům (ne striktně jen k vyšší náchylnosti, jak bylo

doposud uváděno) a že za touto indukovanou rezistencí stojí aktivace signální dráhy SA (Leontovyčová, 2019; Leontovyčová, 2020).

Klíčovou roli ve výsledku pozorovaného efektu, tedy náchylnost vs. rezistence, hraje čas^{příspěvek 5}.

S dopravou materiálu a reorganizací cytoskeletu může souviset obohacení PRRs v rámci mikrodomén na plasmatické membráně (Bücherl, 2017; Grönner, 2022). V rámci imunitní signalizace jsou následně PRRs endocytovány a degradovány (Beck, 2012) (Frescatada-Rosa, 2015). Aktinový cytoskelet hraje důležitou roli v uzavírání průduchů a plasmodesmat, k čemuž také dochází po rozpoznání patogena (Zou, 2021).

V průběhu 15–60 minut od detekce patogena je aktivována MAP-kinázová kaskáda. Jedná se o velmi konzervovaný způsob signalizace závislý na fosforylace a defosforylace MAP-kináz (MAPK). Tuto signalizaci využívají i živočichové a není specifická jen pro reakci na biotický stres. MAPK hrají roli i v reakcích na abiotické stresy. To, co se liší, jsou jednotlivé konkrétní MAPK, které za daného stresu podléhají fosforylace (Sun, 2022). Jedná se o úspěšný způsob signalizace i z toho pohledu, že je relativně snadno regulovatelný a dá se díky němu signál napadení efektivně amplifikovat a cílit (Zhang, 2022). Ve svém výzkumu jsem se ale MAPK signalizaci nikdy nevěnoval.

V průběhu prvních hodin po rozpoznání patogena dochází ke dvěma událostem, které hrály (a hrají) v mému výzkumu významnou roli: zvýšení akumulace kalózy (kap. 4.1) a spuštění fytohormonálních drah, především signální dráhy SA (kap. 4.2).

Příspěvek 4. Reakce rostlin na flg22. Na rozdíl např. od elongačního faktoru, který je, zdá se, rozpoznáván pouze u brukvovitých, je flg22 rozpoznáván napříč rostlinnými čeleděmi. Z našich předběžných výsledků využívajících měření tvorby apoplastických ROS se současně zdá, že ne všechny druhy rostlin ze stejných čeledí musí nutně reagovat na flg22. (Příloha 1).

Příspěvek 5. Indukce rezistence rostlin vyvolaná rozrušením (změnou dynamiky aktinových vláken). Až do našich experimentů panoval široce přijímaný konsensus, že depolymerizace aktinového cytoskeletu následně vede ke zvýšené náchylnosti rostlin vůči patogenům (Li, 2019). My jsme si v roce 2014 všimli, že rozrušení aktinového cytoskeletu aktivuje signální dráhu SA (Matoušková, 2014; Janda, 2014). Tuto myšlenku jsme dále rozvedli v článku (Leontovyčová, 2019), kde jsme ukázali, že pokud rostliny vystavíte podmínkám depolymerizujícím aktinový cytoskelet den před infekcí patogenem, tak dochází překvapivě ke zvýšené rezistenci vůči napadení. Zvýšená rezistence je závislá na aktivaci signální dráhy SA. Důvodem našich protichůdných pozorování vůči konsensu v literatuře je čas. V předchozích studiích byly rostliny ošetřovány látkami depolymerizujícími aktinová vlákna současně s jejich inokulací patogeny (Henty-Ridilla, 2013), zatímco my jsme depolymerizovali aktin dříve a dali jsme tak rostlině čas na to, aby aktivovala signální dráhu SA. V naší práci jsme ukázali, že rezistence je indukovaná proti různým druhům patogenů. Studiovali jsme dva různé patosystémy: *A. thaliana* s bakteriálním patogenem *Pst DC3000* a *B. napus* (řepka olejka) s houbovým patogenem *Leptosphaeria maculans* (Leontovyčová, 2019).

4.1 Kalóza

„obranný val“

Kalóza je polysacharid skládající se stejně jako celulóza z monomerů glukózy. Ovšem v celulóze se jedná o β -1,4-glukan, zatímco kalóza je β -1,3-glukan. Akumulace kalózy je při napadení patogenem výrazně zvýšená, a to především v místech kde k napadení došlo. V případě napadení houbovým patogenem vzniká tzv. papila, což je útvar, ve kterém je kalóza nabohacena. Papila slouží k zabránění penetrace houbového patogena s cílem zabránit vytvoření haustoria (Hückelhoven, 2014). Kalóza také hraje důležitou roli v uzavírání plasmodesmat, což hraje například významnou roli v zabránění šíření virové infekce rostlinou (Liu, 2021). Současně je detekce akumulace kalózy využívána jako jedna ze screeningových metod aktivované imunity, neboť i ošetření flg22 (a jinými PAMPs) vede k významné akumulaci kalózy (Luna, 2011). Takto jsme ji ve svých experimentech využívali i my, např. (Kalachova, 2019; Kalachova, 2020), avšak to se změnilo ve chvíli, kdy jsme zjistili vyšší akumulaci kalózy také u námi studovaného dvojnásobného mutanta *A. thaliana* s vyřazenými geny kódujícími isoformy $\beta 1$ a $\beta 2$ fosfatidyl inositol-4-kinázy (*pi4k $\beta 1\beta 2$*). U tohoto mutanta jsme dále popsali vyšší koncentraci SA, trpasličí vzrůst, vyšší rezistenci vůči bakteriální infekci a zvýšenou akumulaci ROS (Šašek, 2014). Za nestresových podmínek je akumulace kalózy u *pi4k $\beta 1\beta 2$* závislá na zvýšené koncentraci SA. Avšak při působení patogena *Blumeria graminis*, pro nějž není *A. thaliana* hostitelskou rostlinou, se ukázalo, že kalóza akumulovaná v papilách je na

Přispěvek 6. Jevy závislé a nezávislé na zvýšené koncentraci SA u dvojnásobného mutanta *pi4k $\beta 1\beta 2$* . Isoformy PI4K $\beta 1$ a PI4K $\beta 2$ hrají roli ve váčkovém transportu, tedy ve velmi obecném ději ovlivňujícím v buňce nepřeberné množství procesů (Antignani, 2015; Preuss, 2006; Kang, 2011; Lin, 2019). Současně rostliny se zablokovanými geny kódujícími tyto dvě isoformy (*pi4k $\beta 1\beta 2$*) vykazují zvýšenou koncentraci SA (Šašek, 2014), jejíž signální dráha také ovlivňuje v rostlině mnoho reakcí. Proto jsme se pokusili zjistit, jaké fenotypové projevy souvisí exklusivně s mutacemi v kinázách bez přispění zvýšené koncentrace SA (SA-nezávislé jevy) a které projevy jsou naopak důsledkem zvýšené koncentrace SA (SA-závislé jevy). K tomuto rozlišení efektů jsme použili set vytvořených násobných mutantů modifikujících koncentraci SA v rostlině. Vnesli jsme do *pi4k $\beta 1\beta 2$* gen kódující SA hydroxylázu z bakterie *Pseudomonas putida* (*NahG*), čímž vznikl mutant *NahG/pi4k $\beta 1\beta 2$* , který má koncentraci SA podobnou planě rostoucí *A. thaliana* (Šašek, 2014; Pluhařová, 2019). Dále jsme do *pi4k $\beta 1\beta 2$* vnesli mutaci v genu kódujícím ICS1 (tzv. *sid2* mutant), který je zásadní pro biosyntézu SA. Vznikl mutant *sid2/pi4k $\beta 1\beta 2$* , který vykazoval obdobné množství SA jako planě rostoucí *A. thaliana* (Šašek, 2014; Pluhařová, 2019). Na těchto rostlinách jsme provedli experimenty sledující jejich rezistenci vůči biotrofu (oomyceta *Hyaloperenospora arabidopsisidis*), hemibiotrofu (bakterie *Pseudomonas syringae*) a vůči nekrotrofu (houba *Botrytis cinerea*). Ukázali jsme, že *pi4k $\beta 1\beta 2$* je více rezistentní vůči všem těmto patogenům a tato rezistence je závislá na SA. Stejně tak jako akumulace kalózy za nestresových podmínek. K našemu překvapení se však ukázalo, že při ošetření houbou *Blumeria graminis*, pro kterou není *A. thaliana* hostitelskou rostlinou, je akumulace kalózy v papile nezávislá na zvýšené koncentraci SA. Současně byly mutantní rostliny *pi4k $\beta 1\beta 2$* náchylnější k penetraci houbou a tento jev byl také nezávislý na množství SA, protože náchylnější byly i mutantní rostliny *sid2/pi4k $\beta 1\beta 2$* (Kalachova, 2020).

SA nezávislá příspěvek⁶. Na akumulaci kalózy jsme se zaměřili blíže. V *A. thaliana* je kalóza syntáza kódována dvanácti isoformami (Chen, 2014). Nicméně je známo, že za akumulaci kalózy v reakci na biotický stres je zodpovědná kalóza syntáza 12, která byla původně nazvána PMR4 (*powdery mildew resistance 4*) a pod tímto označením je doposud převážně označována ve studiích zabývajících se interakcemi rostlin s mikroorganismy (Ellinger, 2013; Nishimura, 2003; Vogel, 2000)^{poznámka 8}. Zkřížili jsme *pi4kβ1β2* s mutantní rostlinou *pmr4-1*, která má zablokovanou tvorbu PMR4 s cílem zjistit, zda je akumulace kalózy u *pi4kβ1β2* závislá na této isoformě kalóza syntázy. K našemu překvapení se ukázalo, že homozygotní linie *pmr4/pi4kβ1β2* jsou výrazně zakrslého růstu (prakticky nerostou, *data neukázána*). Je

Poznámka 8. Matoucí situace okolo pojmenování kalóza syntázy 12 není v biologii nikterak výjimečná. Původní pojmenování proteinu (genu) je často spojeno s typem experimentu, při kterém byl daný gen identifikován. V tomto případě se jednalo o screening množství náhodně zmutovaných *A. thaliana* na rezistenci vůči padlí (Vogel, 2000). Mezi nalezenými geny hrajícími důležitou roli pro rezistenci byla i zmíněná kalosa synthasa 12, která byla v té době nazvána „*powdery mildew resistance 4*“ (PMR4). V té době se nevědělo o její funkci v biosyntéze kalosy, na to se přišlo až později. Tento protein se v literatuře vyskytuje dokonce ještě pod jedním názvem GLS5 (Ellinger, 2014).

stále zatím otázkou, co za daný efekt na růst a vývoj u tohoto trojnásobného mutanta může. Současně se ukázalo, že kombinace mutací v PMR4, v PI4Kβ1 a v PI4Kβ2 způsobuje nemendelovské štěpné poměry pro *pmr4/pi4kβ1β2*. Na tomto tématu v současnosti spolupracujeme s Dr. Tetianou Kalachovou z Ústavu experimentální botaniky AV ČR, která je vedoucí tohoto směru výzkumu.

4.2. Fytohormonální dráhy v imunitě rostlin – zaostřeno na kyselinu salicylovou

„Dobrý sluha, zlý pán“

Fytohormony, dříve nazývané růstové regulátory rostlin, hrají v signalizačních procesech rostlin zásadní roli. Nejlépe probádanými a známými fytohormony jsou pravděpodobně auxiny a cytokininy. Těmi se ale v této práci nechci zabývat, protože hlavní roli v signalizaci při biotickém stresu, tj. při napadení patogenem, hraje „triumvirát“ fytohormonů: kyselina salicylová (SA), kyselina jasmonová (JA) a etylén (ET). Je zajímavé, že rostliny rozlišují, kterou signalizaci (který fytohormon) upřednostní na základě toho, jaký patogen rostlinu napadl.

Tradičně se udává (a je na to téma publikováno mnoho studií), že při napadení biotrofními patogeny je spuštěna signální dráha SA, zatímco při napadení nekrotrofními patogeny se spouští signální dráhy JA a ET, přičemž mezi SA a JA byl prokázán antagonistický vztah, tj. pokud je

Poznámka 9. Typickým znakem fytohormonálních signalizací je, že se nejedná o samostatné entity, ale spíše o propletenc různých událostí ovlivňující různými vazbami jednu druhou (Pieterse, 2009). Z toho důvodu je stále třeba mít na mysli, že, i když hovoříme o třech fytohormonech majících roli v reakcích na biotický stres, neznamená to, že by se ostatní fytohormony těchto reakcí neúčastnily. Účastní, ale zatím jejich role nebyla zdaleka tak dobře popsána jako u „triumvirátu“ SA, JA a ET.

jedna z drah aktivována, tak inhibuje druhou dráhu (pro zájemce doporučuji ke čtení vynikající přehledové články na toto téma (Glazebrook, 2005) (Pieterse, 2009; Aerts, 2021))^{poznámka 9}. Toto rozdělení podporuje i to, že signální dráha SA hraje významnou roli při spuštění buněčné smrti (hypersensitivní odpovědi) (Radojičić, 2018) a bylo by tedy pro rostlinu krajně nebezpečné aktivovat tuto dráhu proti nekrotrofům, kteří by ze spuštěné HR profitovali. Ovšem nic není černobílé a existují studie, které ukazují, že i rostliny se zvýšenou SA byli rezistentnější vůči nekrotrofním patogenům (Ferrari, 2003; Nováková, 2014), což jsme ukázali i v naší studii (Kalachova, 2020). Více světla do studia zapojení fytohormonálních drah při interakcích rostlin s patogeny vnesl článek s relativně jednoduchou myšlenkou – sledovat akumulaci SA a JA v čase a prostoru v rámci listu. Autoři využili jako nástroj k pozorování akumulace SA a JA dostupné transgenní linie *A. thaliana*, které měly vneseny geny reagující na koncentraci SA (*PR1*) a JA (*VSP1*) spojené s fluorescenční značkou. Tyto transgenní rostliny autoři infikovali patogenní bakterií a pozorovali v čase průběh infekce a intenzitu fluorescence, která odpovídala indukci zmíněných genů a tedy, velmi pravděpodobně, i produkci SA a JA. Výsledek byl poměrně překvapivý, i když ne nelogický. Ukázalo se, že v rámci listu byla zvýšena akumulace obou fytohormonů, ale akumulace SA a JA byla od sebe lokalizačně oddělena. Koncentrace SA se zvyšovala v těsné blízkosti napadení. JA se hromadila za hranicí akumulace SA a ve zbytku listu (Betsuyaku, 2018). Výsledky tedy opět poukázaly na antagonismus obou drah, ale současně nás upozornily na fakt, že bychom měli být velmi obezřetní v tom, jaké části rostliny, či dokonce listu analyzujeme. Jako vysvětlení, proč rostlina reaguje na napadení bakterií aktivací obou fytohormonálních drah, se jeví, že v blízkosti patogena rostlina sází na to, že to bude biotrof, kdo ji infikuje, a tedy indukuje SA, protože buněčná smrt, na které by se SA podílela, by proliferaci biotrofního patogena jistě zastavila. Pro případ, že by se ale jednalo o nekrotrofa a SA by nebyla účinná, se rostlina připravuje tak, že v dalších částech listu aktivuje dráhu JA, která je proti nekrotrofům účinná

^{příspěvek Vesmír 97, 126, 2018/3.}

Pro studium zapojení zmíněných fytohormonálních drah (SA, JA, ET) v rostlinné imunitě byl, dle mého názoru, stěžejní článek z roku 2009 od Kenichi Tsudy (Tsuda, 2009). V rámci práce na tomto článku byli vytvořeni čtverní mutanti *A. thaliana* (a všechny kombinace dvojnásobných a trojnásobných mutantů) se zablokovanými geny důležitými pro biosyntézu či odpověď na SA (*sid2*; mutant se zablokovanou isochorismát syntázou 1 – klíčový protein v biosyntéze SA, (Wildermuth, 2001)), JA (*dde2*, mutant se zablokovaným AOS tj. „*allene oxide synthase*“ – klíčový protein v biosyntéze JA, (Von Malek, 2002)); ET (*ein2*; mutant se zablokovaným „*ethylene insensitive protein 2*“ – protein klíčový v signalizaci v odpovědi na etylén (Alonso, 1999)) a *pad4*, což je také významný protein v rostlinné imunitě zčásti se překrývající se signální drahou SA (Jirage, 1999). V článku mimo jiné prokázali, že zmíněné

(zablokované) čtyři součásti rostlinné imunity odpovídají zhruba za 85 % intenzity imunitní odpovědi spuštěné flg22 (což approximovali obecně ke spuštěné PTI) stejně jako při rozpoznání AvrRpt2 efektoru (což approximovali obecně ke spuštěné ETI). Tento článek tak také poukázal na významný překryv v signalizaci PTI a ETI. Současně je vytvořená kolekce mutantů vynikajícím

Poznámka 10. Je možné, že to, co nyní částečně popisujeme jako samozřejmost, důležitost ICS1 pro biosyntézu SA v rostlinách, není zdaleka tak univerzální, jak by se mohlo zdát. Jak mi při osobní komunikaci sdělil dr. Hirofumi Nakagami z Ústavu Maxe Plancka pro šlechtění rostlin v Kolíně nad Rýnem, zdá se, že ICS1 a jeho důležitost je typická pro brukvovité, ale nikoliv pro jiné rostlinné čeledi. To, že se role ICS1 může přečeňovat, plyne z faktu, že tento typ výzkumu je zatím stále nejpokročilejší u modelové rostliny *A. thaliana*, která patří mezi brukvovité.

nástrojem pro další výzkum, což se prokázalo v následných pracích Kenichi Tsudy (ORCID: 0000-0001-7074-0731). I my jsme v našem výzkumu tuto kolekci využili. Shodou okolností jsme pozorovali, že infekce klíčních rostlin *A. thaliana* rostoucích za sterilních podmínek na pevném médiu bakterií *Pst* DC3000 vede k tomu, že se zvýší a prodlouží růst kořenových vlásků. Chtěli jsme vědět, zda v tom hrají roli fytohormony, a proto jsme daný jev analyzovali u kolekce „deps“ mutantů (*dde2/ein2/pad4/sid2*). Ukázalo se, že zásadní roli pro tvorbu kořenových vlásků má ET (Pečenková, 2017). Role ET byla již známa i bez spojitosti s biotickým stresem (Růžička, 2007; Qin, 2019). Je otázkou, zda je to skutečně ET, co je aktivováno po rozpoznání infekce kořeny.

Ve svém výzkumu jsem se již od bakalářské práce věnoval více či méně procesům v rostlinách týkajících se SA^{příspěvek Vesmír 98, 454, 2019}⁷. Biosyntéza SA probíhá v rostlinách dvěma drahami (Dempsey, 2011). První je závislá na fenylalanin amonium lyáze (PAL). druhá je závislá na enzymu isochorismát syntáze 1 (ICS1)

a část této biosyntetické dráhy probíhá v chloroplastech. Biosyntetická dráha závislá na ICS1 je odpovědná za přibližně 90 % nově syntetizované SA po napadení bakteriálním patogenem (Wildermuth, 2001)^{poznámka 10}. Po rozpoznání napadení patogenem je spuštěna dimerizace proteinů PAD4 a EDS1, která vede k tomu, že je aktivována dráha využívající ICS1, což vede k vyšší koncentraci SA^{příspěvek}⁷. SA se váže na proteiny NPR („nonexpressor of pathogenesis-related genes“), které byly identifikovány jako receptory pro SA.

Příspěvek 7 Co všechno indukuje tvorbu kyseliny salicylové? V našem výzkumu jsme nezřídka sledovali, že velmi různorodé podmínky/ošetření/mutace jsou schopny indukovat akumulaci SA. Mutant *pi4kβ1β2* (Šašek, 2014; Kalachova, 2020), depolymerizace aktinového cytoskeletu (ošetření latrunculinem B a cytochalasinem E) (Leontovyčová, 2019), ošetření saponinem aescinem (Trdá, 2019). V současné době se pokoušíme o sumarizaci doposud známých podmínek vedoucích k akumulaci SA, kde chceme poskytnout seznamy mutantů, abiotických stresů, biotických stresů a chemikálií, jež vedou ke zvýšené akumulaci SA u *A. thaliana*. Bude publikováno v připravovaném přehledovém článku.

Prostřednictvím NPR je zprostředkován účinek SA na změnu transkriptomu v rostlině (Wang, 2020a; Spoel, 2009; Kumar, 2022). Zvýšená koncentrace SA má za následek, že oligomerní

protein NPR1 je monomerizován a následně přechází do jádra, kde ovlivňuje transkripci (Kumar, 2022; Mou, 2003). Ve své dizertační práci jsem popsal možné zapojení fosfolipázy D v této signalizaci. Ukázali jsme, že ošetření *n*-butanolem, inhibitorem fosfolipázy D, inhibuje tvorbu NPR1 monomeru a jeho akumulaci v jádře rostlinné buňky (Janda, 2015a).

Poznámka 11. V 90. letech 20. století se mělo za to, že nezbytným mobilním signálem pro SAR je SA (Métraux, 1990). Nicméně elegantní pokusy využívající roubování, provedené na přelomu tisíciletí, ukázaly, že SA je důležitá pro funkčnost SAR, ale přitom není zmíněným mobilním signálem (Vernooij, 1994). Od té doby bylo publikováno několik molekul, které jako mobilní signál v SAR slouží (Kachroo, 2020). Tento výzkum má i významnou českou stopu, kdy jako takový signál byla demonstrována kyselina pipekolová v článku Hany Návarové (Návarová, 2012).

SA, přesnější by bylo mluvit o signální dráze závislé na SA, je mocná zbraň. Jak bylo zmíněno výše, je důležitou molekulou v ustanovení hypersensitivní odpovědi a tedy v obraně proti biotrofním patogenům. Dále je nepostradatelnou součástí tzv. systémově získané rezistence (SAR)^{poznámka 11}, což je událost, kdy napadení jednoho listu rostliny patogenem vyšle signál do dalších částí rostliny, které tím připraví na případný následující útok patogena. Tato vzdálená, doposud nenapadená pletiva jsou tak lépe připravena na napadení a při něm spouští intenzivnější a rychlejší obrannou odpověď (Kachroo, 2020). Právě popsání zapojení SA v SAR v roce 1990 (Métraux, 1990; Malamy, 1990) bylo spouštěčem zvýšeného zájmu o SA jakožto součásti obrany rostlin při napadení patogeny (Gaffney, 1993). Současně všechny doposud popsané mutantní rostliny *A. thaliana* vykazující zvýšenou koncentraci SA mají vyšší

Příspěvek 8 Kyselina salicylová a růst.
Tomuto tématu se věnuji dlouhodobě a vše začalo publikací popisující inhibici růstu u *pi4kβ1β2*. Jednoznačně jsme prokázali, že zásadní vliv má zvýšená aktivace signální dráhy SA (Šašek, 2014). Tímto jsem se začal aktivně zajímat o mutanty *A. thaliana* se zvýšenou koncentrací SA, což vyústilo ve vytvoření kolekce 18 genotypů pro studium vlivu vysoké SA na růst (Pluhařová, 2019). U *pi4kβ1β2* jsme nevěděli, co přesně aktivuje v *pi4kβ1β2* tuto signální dráhu. PI4Kβ1 a PI4Kβ2 hrají významnou roli ve váčkovém transportu (Kang, 2011), proto jsme se zaměřili na možné ovlivnění aktivity PRR receptorů, u kterých je váčkový transport významným činitelem. Vytvořili jsme sadu trojnásobných mutantů, kdy jsme *pi4kβ1β2* zkřížili s mutantními rostlinami se zablokovanou tvorbou vybraných PRRs a jejich koreceptorů, jako např. *bak1*. Avšak žádný z vytvořených mutantů nenavrzel zpátky růst *pi4kβ1β2* a tedy tento přístup nepřinesl popis mechanismu, jak je biosyntéza SA v *pi4kβ1β2* aktivována. V současné době se na JU zaměřujeme na možnost vlivu uzavřených průduchů na růst *A. thaliana* v důsledku vysoké akumulace SA (data neukázána).

rezistenci k testovaným patogenům (Janda, 2015b). Ovšem vysoký obsah SA má i svou stinnou stránku, všechny tyto mutantní rostliny jsou trpasličího vzrůstu (více v kap. 5)^{příspěvek 8}.

5. Všechno moc škodí aneb Kompromis mezi obranou a růstem rostliny

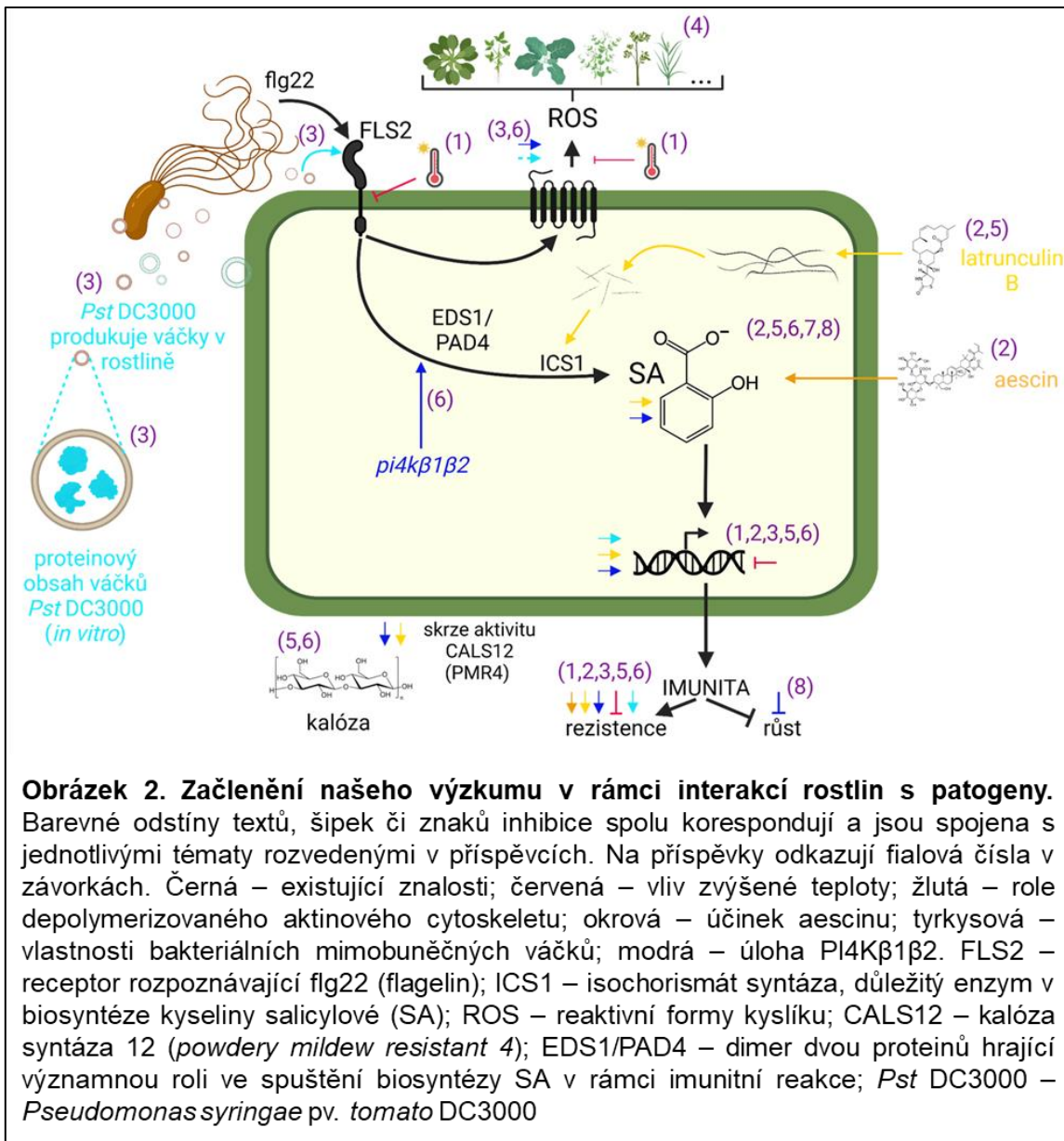
„2 % HDP“

Vyspělé státy si hlídají své výdaje na obranu a v rámci NATO mají jasné definovaný mandatorní výdaj na obranu v % HDP. Uvědomují si, že je na obranu třeba dávat tolik, aby to co nejvíce snížilo možnost napadení a v případě napadení zvýšilo pravděpodobnost úspěšné obrany a současně aby tyto výdaje neohrozily hospodářské fungování státu. Je zde vždy kompromis mezi tím, kolik investovat do ministerstva obrany a kolik např. do školství či kultury. A míra kompromisu je silně závislá na podmírkách, za jakých je rozpočet tvořen. Stejně tak to mají, pravděpodobně, i rostliny.

Rostlina se musí umět rozhodnout, zda investovat do obrany či do růstu, přičemž se ukazuje, že se snaží v rámci kompromisu investovat co nejúčinněji do obojího a být schopna upřednostnit růst nebo obranu jen v případech, kdy je to nutné (He, 2022). O tom, že aktivovaná imunitní odpověď potlačuje růst, se ví již od 90. let 20. století a důkazy o tomto jevu přinesly studie zabývající se různými aspekty rostlinné imunity.

Obligátním důkazem, že aktivace imunity inhibuje vzrůst, je klasický test inhibice růstu klíčních rostlin po ošetření některým PAMPs, typicky flg22. Takto ošetřené klíční rostliny *A. thaliana* po týdnu dosahují zpravidla 20–40 % hmotnosti neošetřených rostlin v závislosti na koncentraci PAMP (Gómez-Gómez, 1999). Takový test jsme využili i v naší studii týkající se efektu bakteriálních váčků na rostlinu (Janda, 2023). V naší současné práci se věnujeme reakcím máku setého (*Papaver somniferum*) na flagelin a ukazuje se, že ošetření máku flagelinem také vede k inhibici růstu (*data neukázána*). Ačkoliv se o fenoménu kompromisu mezi růstem a obranou (*growth–defense tradeoff*) napsalo již mnoho, o přesném mechanismu, který za ním stojí, víme zatím relativně málo. A to i přes nemalé úsilí jej objasnit. Je velmi pravděpodobné, že za tento kompromis bude zodpovědných více jevů naráz. Velmi významným přispěvatelem je bezpochyby komunikace mezi fytohormony a vzájemné ovlivnění jejich druh (Huot, 2014). V naší laboratoři se tomuto fenoménu také nadále věnujeme, a to především ve spojitosti s SA, protože jsme prokázali u dvojnásobných mutantních rostlin *A. thaliana* s nefunkčními fosfatidyl inositol-4-kinázami $\beta 1$ a $\beta 2$ (*pi4k $\beta 1\beta 2$*), že jejich výrazná inhibice růstu je způsobena nadměrnou koncentrací SA, resp. funkční signální dráhou SA a aktivovanou imunitou (Šašek, 2014)^{příspěvek 8}.

Klasickou odpověďí, proč rostliny s aktivovanou imunitou jsou nižšího vzrůstu, je, že mají omezené zdroje energie, a pokud je tedy rostlina využívá k obraně, nemůže je plně využít k růstu (Huot, 2014). Logická a jistě do značné míry pravdivá odpověď. Nicméně my jsme se rozhodli, že prostudujeme jeden mírně opomíjený fenomén, a sice že zvýšená koncentrace SA vede k uzavření průduchů (Wang, 2020b), což by podle nás mohlo souviseť nejen s přesměrováním využití dostupných zdrojů, ale současně i k nižší dostupnosti zdrojů (CO₂), což by také přispívalo k nižšímu růstu. U mutantů se zvýšenou akumulací SA jsme měřili jejich uzavřenosť průduchů a asimilaci CO₂ a zjistili jsme, že je u nich dostupnost CO₂ skutečně významně omezena (*data neukázána*).



6. Závěr: minulost, současnost a budoucnost

„Závod ve zbrojení“ mezi rostlinami a patogeny nikdy nekončí. Má ale bezpochyby svá pravidla a vymezené bitevní pole. Vzhledem k výzvám, které na nás klade klimatická změna a zvyšující se světová populace, je více než žádoucí „pravidlům závodu“ co nejvíce porozumět a využít naše poznatky v zemědělství k ochraně plodin proti patogenům. Zlepšení ochrany by mělo zvýšit výnosy a udržitelnost zemědělství. Prostor k výzkumu je stále veliký a s novými možnostmi, jakými je např. editování genomů (především s využitím technologie na základě CRISPR-Cas), se jeví možné aplikace využívající znalostí základního výzkumu ještě více na dosah ruky.

Ve svém výzkumu **jsem se doposud věnoval** především dvěma dílcům tématům souvisejícím se „závodem ve zbrojení“ mezi rostlinou a patogenem:

1) Rolí kyseliny salicylové v signalizaci rostlin (tj. součásti rostlinného „zbraňového systému“)

- Věnovali jsme se propojení fosfolipidového signálního systému se signalizací SA, kde jsme prokázali souvislost s fosfolipázou D, nespecifickou fosfolipázou C2 a fosfatidylinositol-4-kinázami β 1 a β 2 (Janda, 2015a; Šašek, 2014; Kalachova, 2020; Kalachova, 2019; Janda, 2013; Krčková, 2018; Junková, 2021).
- Přišli jsme na dva nové stimuly vedoucí k nadprodukci SA: ošetření saponinem aescinem (Trdá, 2019) a latrunculinem B (depolymerizace aktinového cytoskeletu) (Leontovyčová, 2019; Matoušková, 2014).
- Ve výzkumu aktinového cytoskeletu jsme jako první popsali, že rozrušení aktinových vláken nemusí nutně vést k větší náchylnosti plodin, ale naopak může zvýšit rezistenci (Leontovyčová, 2020; Leontovyčová, 2019) a naznačili jsme spojení s fosfoinositidy (Kalachova, 2019).
- Prokázali jsme, že krátkodobé vystavení *A. thaliana* vyšší teplotě potlačuje imunitní reakce související s SA a navíc vede ke snížení přítomnosti receptoru FLS2 na plasmatické membráně. To vše má za následek vyšší náchylnost rostlin vystavených teplotnímu stresu vůči *Pst DC3000* (Janda, 2019).
- Vytvořili jsme kolekci mutantních rostlin *A. thaliana* se změněnou koncentrací SA, jakožto nástroj pro další výzkum signalizace SA (Pluhařová, 2019). Tuto kolekci v současnosti v laboratoři intenzivně využíváme.

2) Bakteriálním mimobuněčným váčkům, jejich obsahu a vlivu na rostlinu a její imunitu (tj. součásti „zbraňového systému“ patogena).

- Popsali jsme biofyzikální vlastnosti izolovaných váčků produkovaných patogenní bakterií *Pst DC3000*, přičemž jsme jejich produkci potvrzili jak *in vitro*, tak v průběhu infekce v rostlině (Janda, 2023).
- Provedli jsme proteomickou analýzu váčků *Pst DC3000* a porovnali naše výsledky s dostupnými proteomickými analýzami jiných mimobuněčných váčků produkovaných jinými bakteriemi (Janda, 2022). Tyto výsledky ukázaly možnost využití váčků při získávání železa z apoplastu (Janda, 2023).
- Prokázali jsme imunogenní efekt váčků na rostlinu, který je závislý na receptoru FLS2, tj. na přítomnosti flagelinu. Zde z mého pohledu stále panuje nejistota, zda se jedná opravdu o efekt váčků nebo o artefakt jejich purifikace (Janda, 2023).

V současnosti se u nás v laboratoři věnujeme vlivu SA na růst rostlin, kdy se zaměřujeme především na možnost snížené dostupnosti CO₂ v důsledku vyšší koncentrace SA. Dále jsme, v souvislosti s SA, rozšířili naši pozornost na ovlivnění kutikuly v případě aktivované imunity.

K oběma témtu tématům mě přivedl tradiční výzkum prováděný na Katedře experimentální biologie rostlin na PřF JU, který se týká průduchů, fotosyntézy a kutikuly. Mým cílem je jeho propojení s mou expertizou v rámci rostlinné imunity. V tématech souvisejících s SA blízce spolupracujeme s Ústavem experimentální botaniky AV ČR.

Při zavádění pěstebních metod v naší laboratoři jsme shodou okolností přišli na to, že vysoká koncentrace SA inhibuje tvorbu antokyanů. Tento fenomén se v současnosti snažíme popsat a poslat k publikaci (příloha 2).

Díky obdrženému MSCA stipendiu pokračujeme ve výzkumu mimobuněčných bakteriálních váčků, kde se zaměřujeme především na podmínky ovlivňující intenzitu produkce váčků u bakterií kolonizujících rostliny. Zde blízce spolupracujeme s laboratoří prof. Silke Robatzek z LMU v Mnichově.

Významným rozšířením našeho vědeckého zájmu je zacílení na jinou rostlinu, než je modelový huseníček. Předmětem našeho zájmu je především zemědělská plodina mák setý (*Papaver somniferum*), kde blízce spolupracujeme s laboratoří prof. Vladislava Čurna z Fakulty zemědělské a technologické na JU a rozvíjíme spolupráci s Výzkumným ústavem olejin v Opavě (OSEVA PRO s.r.o). Cílem tohoto výzkumu je komplexně se zaměřit na molekulární interakce máku s patogeny, tj. na „závod ve zbrojení“ mezi mákem a jeho patogeny. Dlouhodobě naší vizí spojenou s výzkumem máku je vyvinutí nového (nových) přístupu(ů) k jeho ochraně proti patogenům a škůdcům. K tomu bychom chtěli využít tři přístupy: genové editace; ošetření s využitím exRNA v liposomech; rychlou diagnostiku patogenů na polích. V souvislosti s naším zájmem o mák předpokládám, že do budoucna se zaměření laboratoře více přiblíží aplikovanému typu výzkumu (lépe řečeno výzkumu na rozhraní základního a aplikovaného výzkumu). Nejnovějším malým projektem naší laboratoře je spolupráce s dr. Lubomírem Adamcem z Botanického ústavu AV ČR v Třeboni, kdy máme v plánu, hned jak to kultivační podmínky dovolí, se zaměřit na imunitní reakce vodních masožravých rostlin.

Věřím, že náš výzkum (ať už jakákoli jeho část) **v budoucnosti** přinese zlepšení ochrany plodin na našich polích, ať už díky lepší znalosti signální dráhy kyseliny salicylové, mimobuněčných váčků, či detailním znalostem imunitních reakcí máku a jeho interakcí s patogeny a škůdci.

Slovníček klíčových zkrátek pojmu

A. thaliana	Huseníček rolní, také chudina rolní, je drobná dvouděložná efemérní plevelná rostlina z čeledi brukvovitých, která se používá jako modelový organismus v molekulární genetice rostlin [1].
AOS	Zásadní enzym v biosyntéze kyseliny jasmonové. U <i>A. thaliana</i> se mutant se zablokovanou AOS nazývá <i>dde2</i> (<i>ALLEN OXIDE SYNTHASE</i> ; EC 4.2.2.92).
Biotrof	Organismus, který žije a rozmnožuje se výhradně v jiném živém organismu. Jeho výživa je zcela závislá na hostiteli. Příkladem mohou být houby způsobující rostlinné choroby padlí a rez [2].
DAMPs	Molekulární vzory spojené s nebezpečím (poraněním) (<i>Danger (damage)-associated molecular patterns</i>). DAMPs jsou molekuly pocházející z rostliny, ale jsou rozpoznávány receptory na plasmatické membráně a spouští imunitní odpověď (podobně jako PAMPs). Příklady takových molekul jsou extracelulární ATP, oligogalakturonidy (z buněčné stěny) či monomery kutinu.
deps	<i>dde2/ein2/pad4/sid2</i> -Čtverný mutant <i>A. thaliana</i> vytvořený Dr Kenichi Tsudou se zablokovanými geny kódujícími enzymy nutné pro imunitní reakce. Konkrétně pro dráhu kyseliny salicylové (<i>sid2</i> ; zablokovaný <i>ICS1</i>), kyseliny jasmonové (<i>dde2</i> ; zablokovaný <i>AOS</i>), etylénu (<i>ein2</i> ; zablokovaný <i>EIN2</i>), a imunitního sektoru závislého na <i>PAD4</i> (<i>pad4</i>).
EDS1/PAD4	Proteiny, které v případě spuštění imunitní odpovědi tvoří heterodimery a jsou zodpovědné za předání signálu pro zvýšení koncentrace kyseliny salicylové (<i>ENHANCED DISEASE SUSCEPTIBILITY 1 / PHYTOALEXIN DEFICIENT 4</i>).
Efektor	Molekula, kterou využívá rostlinný patogen při infekci určitého druhu rostliny. Pomocí takové molekuly mohou patogeny účinně potlačovat imunitní odpověď infikované rostliny [2].
EIN2	Klíčový protein pro přenos signálu zprostředkovávaný etylénem (<i>ETHYLENE INSENSITIVE 2</i>).
Elongační faktor (EF-Tu)	Elongační faktory jsou proteiny, které v průběhu translace pomáhají a řídí elongaci peptidového řetězce.
ET	Etylén. Plynný fytohormon mající významnou roli v obranných reakcích rostlin při napadení patogeny.
ETI	Efektory spuštěná imunita (<i>effector triggered immunity</i>). Tento typ imunitní reakce je spuštěn rozpoznáním efektoru R proteinem (NLR receptorem) v cytosolu rostlinné buňky.
EVs	Mimobuněčné váčky (<i>extracellular vesicles</i>)
Flg22	QRLSTGSRINSAKDDAAGLQIA; Strukturní protein, který je hlavní součástí bakteriálního bičíku. Rozeznává ho imunitní systém rostliny a hraje roli účinného elicitoru imunitní odpovědi [2].
FLS2	Receptor rozpoznávající flg22 (<i>FLAGELLIN-SENSITIVE 2</i>)
Fytobakterie	Bakterie kolonizující rostlinky
Hemibiotrof	Obvykle houbový patogen, který začíná životní cyklus jako biotrof a následně se přepne do životního stylu nekrotrofa. Během biotrofické fáze patogen poškodí hostitelskou rostlinu jen minimálně. Po přepnutí do nekrotrofické fáze ničí buňky i pletiva rostliny [2].

HR	Hypersenzitivní odpověď (<i>hypersensitive response</i>). Událost, kdy rostlina v reakci na napadení patogenem vyvolá kontrolovanou buněčnou smrt u buněk vyskytujících se v okolí napadení patogenem.
ICS	ISOCHORISMÁT SYNTÁZA (<i>ISOCHORISMATE SYNTHASE</i>), enzym klíčový pro biosyntézu kyseliny salicylové v reakci na napadení patogenem.
JA	Kyselina jasmonová (<i>jasmonic acid</i>). Důležitý fytohormon v obranných reakcích rostlin při napadení patogeny. JA je účinná především v obraně proti nekrotrofům a herbivorům.
MAPK	Kinázy aktivované mitogenem (<i>mitogen-activated protein kinase</i>). Typická součást signalizačních kaskád jak u rostlin, tak u živočichů.
Nehostitelská rezistence	Fenomenologická definice: schopnost všech genotypů rostlinného druhu poskytnout odolnost vůči všem genotypům druhu patogenu, přičemž odolnost často znamená neschopnost patogenu dokončit svůj asexuální nebo sexuální životní cyklus na daném rostlinném druhu [3]. Pokud vás více zajímají molekulární aspekty tohoto druhu rezistence, doporučuji přehledový článek Panstruga a Moscou (2020) [4]. (<i>Nonhost resistance</i>)
Nekrotrof	Parazitický organismus, jako je houba nebo bakterie, který likviduje buňky a tělo hostitele, například pletiva rostliny, protože se živí mrtvým materiélem. Příkladem nekrotrofa je plíseň šedá (<i>Botrytis cinerea</i>) [2].
NLRs	Receptory s doménou vázající nukleotidy a doménou bohatou na leucin. (<i>nucleotide-binding oligomerization domain-like receptors</i> , nebo <i>NOD-like receptors</i>). Jsou to receptory nalézající se v cytosolu a rozpoznávající efektory. V literatuře je často používán jako synonymum termín R protein.
NPR	Proteiny klíčové ve zprostředkování signalizace závislé na kyselině salicylové (<i>NONEXPRESSOR OF PR GENES</i>).
PAL	FENYLALANIN AMONIAK LYÁZA (<i>PHENYLALANIN AMMONIA-LYASE</i> ; EC 4.3.1.24). Klíčový enzym pro biosyntézu kyseliny salicylové u dráhy, která je nezávislá na ICS. U brukvovitých není tato dráha tolik významná při napadení patogeny, zatímco u jiných čeledí se zdá, že je její role významnější.
PAMPs	Molekulární vzory spojené s patogeny (<i>pathogen-associated molecular patterns</i>), někdy také uváděny jako MAMPs (molekulární vzory spojené s mikrobami). PAMPs jsou molekuly z patogena, které jsou rozpoznávány receptory (PRRs) na plasmatické membráně. Jedná se o molekuly, kterých se patogen nemůže jednoduše zbavit (jsou pro jeho život esenciální). Příkladem PAMPs jsou flg22, elf18 či oligomery chitinu.
patogen	Biologický faktor, jako je například bakterie, virus, oomycenta nebo houba, který může narušit život hostitele a vyvolat onemocnění [2].
patosystém	Subsystém ekosystému zahrnující parazitické vztahy mezi organismy. V případě, že se jedná o rostlinný patosystém, tak je hostitelským organismem rostlina.
PRRs	Receptory rozpoznávající vzory (<i>pattern recognizing receptors</i>), někdy také receptory rozpoznávající PAMPs, neboť slovo vzory v názvu PRRs značí, že tyto receptory rozpoznávají molekuly, jako jsou PAMPs, MAMPs či DAMPs. Většinou se tyto receptory nacházejí na plasmatické membráně.

Pst DC3000	Bakterie <i>Pseudomonas syringae</i> pv <i>tomato</i> DC3000. Modelový bakteriální patogen schopný infikovat <i>A. thaliana</i> . Současně významný patogen rajčete.
PTI	Imunita spuštěná vzory (někdy také nazývána imunita spuštěná PAMPs; <i>pattern (PAMP) triggered immunity</i>). Tento typ imunitní reakce proběhne po rozpoznání molekulárního vzory pomocí PRRs na plasmatické membráně.
R proteiny	Viz NLRs
RbohD(F)	NADPH oxidáza. (<i>Respiratory burst oxidase homolog protein D (or F)</i>). Enzym nalézající se na plasmatické membráně odpovědný za produkci superoxidového radikálu po spuštění imunitní odpovědi, např. po rozpoznání flg22 pomocí receptoru FLS2.
Rezistence	Schopnost rostliny omezit růst a vývoj patogenu. Na rozdíl od imunity není rezistence „všechno, nebo nic“, ale může představovat celou škálu odpovědí rostliny. Například účinná rezistence může vést k tomu, že rozvoj nemoci nedoprovází žádné nápadné symptomy. Naopak u rostlin se slabou rezistencí si patogen může dělat, co chce, a v takovém případě obvykle dochází k rozvoji symptomů onemocnění [2].
Rezistozom	Struktura, o níž se předpokládá, že rostlinám propůjčuje odolnost vůči chorobám. Tento termín byl zaveden v souvislosti s popsáním mechanismu, jakým R protein ZAR1 reaguje na rozpoznání efektoru, kdy ZAR1 vytvoří oligomer uspořádaný do struktury umožňující narušit plasmatickou membránu.
ROS	Reaktivní formy kyslíku (<i>reactive oxygen species</i>). Typickými ROS jsou H_2O_2 či O_2^- .
SA	Kyselina salicylová (<i>salicylic acid</i>). Kyselina 2-hydroxybenzoová. Fytohormon mající významnou roli v obraně rostlin proti patogenům, především biotrofům.
SAR	Systémově získaná rezistence (<i>systemic acquired resistance</i>). Událost, kdy je informace o napadení v jednom listu rostliny přenesena do jiného nenapadeného listu, čímž dojde k aktivaci (budoucímu zesílení) imunitní odpovědi v těchto nenapadených částech rostliny, a pokud je takováto část rostliny následně napadena patogenem, je rostlina vůči němu více rezistentní. Významnou roli v SAR hraje SA.
Symbióza	Těsný a často dlouhodobý vztah mezi organismy různých druhů. Existují různé typy symbiotických vztahů, včetně mutualismu, který je přínosný pro oba partnery, komensalismu, kdy jeden z partnerů profituje a druhý není vztahem příliš ovlivněn, a parazitismu, kdy se jeden z partnerů přizívá na úkor druhého [2].
T3SS	Bakteriální sekreční systém typ 3 (<i>type 3 secretion system</i>). Jedná se o strukturu, díky níž bakterie dopravují efektory dovnitř rostlinné buňky. Struktura připomíná jehlu, která projde plasmatickou membránou a umožní tak dopravovat do cytosolu efektory.
Virulentní	Pojem vyjadřující schopnost patogenu vyvolat infekci, často závažnou [2].
Vnímavost	Pojem užívaný v souvislosti s rezistencí při popisu schopnosti organismu omezit růst a vývoj útočníka. Pro každý stupeň rezistence existuje odpovídající stupeň vnímavosti. Například rostlinu, která vykazuje nízkou úroveň rezistence vůči určitému patogenu a umožňuje mu tak, aby kolonizoval její pletiva a dokončil svůj životní cyklus, je možné označit za vysoko vnímavou [2].

ZAR1	R-protein, na němž byl poprvé popsán molekulární mechanismus rozpoznání efektoru pomocí NLR (<i>ZYGOTIC ARREST 1</i>).
„Zig-zag“ model	Model průběhu imunitní reakce představený pány Jonathanem Jonesem a Jeffem Danglem v roce 2006. Tento model zjednodušeně popisuje PTI a ETI.

[1] https://cs.wikipedia.org/wiki/Hlavn%C3%A9_AD_strana; [2] Český překlad knihy *Rostlina jako pevnost od Dale Walterse. Na překladu jsem se podílel a kniha vyjde v roce 2023*; [3] Heath MC. (2000) doi: 10.1016/s1369-5266(00)00087-x; [4] Panstruga R, Moscou MJ. (2020) doi: 10.1094/MPMI-06-20-0161-CR.

Seznam použité literatury

- AERTS, Niels, Marciel PEREIRA MENDES a Saskia VAN WEES, 2021. Multiple levels of crosstalk in hormone networks regulating plant defense. *The Plant Journal* [online]. **105**(2), 489-504 [cit. 2023-02-26]. ISSN 0960-7412. Dostupné z: doi:10.1111/tpj.15124
- ALONSO, Jose, Takashi HIRAYAMA, Gregg ROMAN, Saeid NOURIZADEH a Joseph ECKER, 1999. EIN2, a Bifunctional Transducer of Ethylene and Stress Responses in Arabidopsis. *Science* [online]. **284**(5423), 2148-2152 [cit. 2023-02-26]. ISSN 0036-8075. Dostupné z: doi:10.1126/science.284.5423.2148
- AUSUBEL, Frederick M, 2005. Are innate immune signaling pathways in plants and animals conserved?. *Nature Immunology* [online]. **6**(10), 973-979 [cit. 2023-02-24]. ISSN 1529-2908. Dostupné z: doi:10.1038/ni1253
- BALINT-KURTI, Peter, 2019. The plant hypersensitive response: concepts, control and consequences. *Molecular Plant Pathology* [online]. [cit. 2023-02-26]. ISSN 1464-6722. Dostupné z: doi:10.1111/mpp.12821
- BECK, Martina, Ji ZHOU, Christine FAULKNER, Daniel MACLEAN a Silke ROBATZEK, 2012. Spatio-Temporal Cellular Dynamics of the Arabidopsis Flagellin Receptor Reveal Activation Status-Dependent Endosomal Sorting. *The Plant Cell* [online]. **24**(10), 4205-4219 [cit. 2023-02-24]. ISSN 1040-4651. Dostupné z: doi:10.1105/tpc.112.100263
- BEN KHALED, Sara, Jelle POSTMA a Silke ROBATZEK, 2015. A Moving View: Subcellular Trafficking Processes in Pattern Recognition Receptor-Triggered Plant Immunity. *Annual Review of Phytopathology* [online]. **53**(1), 379-402 [cit. 2023-02-26]. ISSN 0066-4286. Dostupné z: doi:10.1146/annurev-phyto-080614-120347
- BETSUYAKU, Shigeyuki, Shinpei KATO, Yumiko TAKEBAYASHI, Hitoshi SAKAKIBARA, Nobuhiko NOMURA a Hiroo FUKUDA, 2018. Salicylic Acid and Jasmonic Acid Pathways are Activated in Spatially Different Domains Around the Infection Site During Effector-Triggered Immunity in *Arabidopsis thaliana*. *Plant and Cell Physiology* [online]. **59**(1), 8-16 [cit. 2023-02-26]. ISSN 0032-0781. Dostupné z: doi:10.1093/pcp/pcx181
- BI, Guozhi, Min SU, Nan LI et al., 2021. The ZAR1 resistosome is a calcium-permeable channel triggering plant immune signaling. *Cell* [online]. **184**(13), 3528-354112 [cit. 2023-05-02]. ISSN 00928674. Dostupné z: doi:10.1016/j.cell.2021.05.003
- BOUTROT, Freddy a Cyril ZIPFEL, 2017. Function, Discovery, and Exploitation of Plant Pattern Recognition Receptors for Broad-Spectrum Disease Resistance. *Annual Review of Phytopathology* [online]. **55**(1), 257-286 [cit. 2023-02-18]. ISSN 0066-4286. Dostupné z: doi:10.1146/annurev-phyto-080614-120106
- BÜCHERL, Christoph, Iris JARSCH, Christian SCHUDOMA et al., 2017. Plant immune and growth receptors share common signalling components but localise to distinct plasma membrane nanodomains. *eLife* [online]. **6** [cit. 2023-02-26]. ISSN 2050-084X. Dostupné z: doi:10.7554/eLife.25114
- BUSCAILL, Pierre, Balakumaran CHANDRASEKAR, Nattapong SANGUANKIATTICHAI et al., 2019. Glycosidase and glycan polymorphism control hydrolytic release of immunogenic flagellin peptides. *Science* [online]. **364**(6436) [cit. 2023-02-24]. ISSN 0036-8075. Dostupné z: doi:10.1126/science.aav0748
- CAI, Qiang, Baoye HE, Shumei WANG, Stephen FLETCHER, Dongdong NIU, Neena MITTER, Paul BIRCH a Hailing JIN, 2021. Message in a Bubble: Shutting Small RNAs and Proteins Between Cells and Interacting Organisms Using Extracellular Vesicles. *Annual Review of Plant Biology* [online]. **72**(1), 497-524 [cit. 2023-02-25]. ISSN 1543-5008. Dostupné z: doi:10.1146/annurev-arplant-081720-010616

COOK, David, Carl MESARICH a Bart THOMMA, 2015. Understanding Plant Immunity as a Surveillance System to Detect Invasion. *Annual Review of Phytopathology* [online]. **53**(1), 541-563 [cit. 2023-02-18]. ISSN 0066-4286. Dostupné z: doi:10.1146/annurev-phyto-080614-120114

COUCH, Yvonne, Edit BUZÀS, Dolores DI VIZIO et al., 2021. A brief history of nearly EV-erything – The rise and rise of extracellular vesicles. *Journal of Extracellular Vesicles* [online]. **10**(14) [cit. 2023-02-25]. ISSN 2001-3078. Dostupné z: doi:10.1002/jev2.12144

CUNNAC, Sébastien, Magdalén LINDEBERG a Alan COLLMER, 2009. Pseudomonas syringae type III secretion system effectors: repertoires in search of functions. *Current Opinion in Microbiology* [online]. **12**(1), 53-60 [cit. 2023-02-25]. ISSN 13695274. Dostupné z: doi:10.1016/j.mib.2008.12.003

DEMPSEY, D'Maris, A. VLOT, Mary WILDERMUTH a Daniel KLESSIG, 2011. Salicylic Acid Biosynthesis and Metabolism. *The Arabidopsis Book* [online]. **9** [cit. 2023-02-26]. ISSN 1543-8120. Dostupné z: doi:10.1199/tab.0156

EL KASMI, Farid, Diana HORVATH a Thomas LAHAYE, 2018. Microbial effectors and the role of water and sugar in the infection battle ground. *Current Opinion in Plant Biology* [online]. **44**, 98-107 [cit. 2023-02-25]. ISSN 13695266. Dostupné z: doi:10.1016/j.pbi.2018.02.011

ELLINGER, Dorothea, Marcel NAUMANN, Christian FALTER, Claudia ZWIKOWICS, Torsten JAMROW, Chithra MANISSERI, Shauna SOMERVILLE a Christian VOIGT, 2013. Elevated Early Callose Deposition Results in Complete Penetration Resistance to Powdery Mildew in *Arabidopsis*. *Plant Physiology* [online]. **161**(3), 1433-1444 [cit. 2023-02-26]. ISSN 1532-2548. Dostupné z: doi:10.1104/pp.112.211011

FELIX, Georg, Juliana DURAN, Sigrid VOLKO a Thomas BOLLER, 1999. Plants have a sensitive perception system for the most conserved domain of bacterial flagellin. *The Plant Journal* [online]. **18**(3), 265-276 [cit. 2023-02-24]. ISSN 09607412. Dostupné z: doi:10.1046/j.1365-313X.1999.00265.x

FERRARI, Simone, Julia PLOTNIKOVA, Giulia DE LORENZO a Frederick AUSUBEL, 2003. *Arabidopsis* local resistance to *Botrytis cinerea* involves salicylic acid and camalexin and requires EDS4 and PAD2, but not SID2, EDS5 or PAD4. *The Plant Journal* [online]. **35**(2), 193-205 [cit. 2023-02-26]. ISSN 09607412. Dostupné z: doi:10.1046/j.1365-313X.2003.01794.x

FÖRDERER, Alexander, Dongli YU, Ertong LI a Jijie CHAI, 2022. Resistosomes at the interface of pathogens and plants. *Current Opinion in Plant Biology* [online]. **67** [cit. 2023-02-26]. ISSN 13695266. Dostupné z: doi:10.1016/j.pbi.2022.102212

FRESCATADA-ROSA, Márcia, Silke ROBATZEK a Hannah KUHN, 2015. Should I stay or should I go? Traffic control for plant pattern recognition receptors. *Current Opinion in Plant Biology* [online]. **28**, 23-29 [cit. 2023-02-26]. ISSN 13695266. Dostupné z: doi:10.1016/j.pbi.2015.08.007

GAFFNEY, Thomas, Leslie FRIEDRICH, Bernard VERNOOIJ et al., 1993. Requirement of Salicylic Acid for the Induction of Systemic Acquired Resistance. *Science* [online]. **261**(5122), 754-756 [cit. 2023-05-02]. ISSN 0036-8075. Dostupné z: doi:10.1126/science.261.5122.754

GLAZEBROOK, Jane, 2005. Contrasting Mechanisms of Defense Against Biotrophic and Necrotrophic Pathogens. *Annual Review of Phytopathology* [online]. **43**(1), 205-227 [cit. 2023-02-24]. ISSN 0066-4286. Dostupné z: doi:10.1146/annurev.phyto.43.040204.135923

GÓMEZ-GÓMEZ, Lourdes, Georg FELIX a Thomas BOLLER, 1999. A single locus determines sensitivity to bacterial flagellin in *Arabidopsis thaliana*. *The Plant Journal* [online]. **18**(3), 277-284 [cit. 2023-02-24]. ISSN 09607412. Dostupné z: doi:10.1046/j.1365-313X.1999.00451.x

GREEN, Erin, Joan MECSAS a Indira KUDVA, 2016. Bacterial Secretion Systems: An Overview. *Microbiology Spectrum* [online]. **4**(1) [cit. 2023-02-25]. ISSN 2165-0497. Dostupné z: doi:10.1128/microbiolspec.VMBF-0012-2015

GRONNIER, Julien, Christina FRANCK, Martin STEGMANN et al., 2022. Regulation of immune receptor kinase plasma membrane nanoscale organization by a plant peptide hormone and its receptors. *eLife* [online]. **11** [cit. 2023-02-26]. ISSN 2050-084X. Dostupné z: doi:10.7554/eLife.74162

HENTY-RIDILLA, Jessica, Masaki SHIMONO, Jiejie LI, Jeff CHANG, Brad DAY, Christopher STAIGER a Jian-Min ZHOU, 2013. The Plant Actin Cytoskeleton Responds to Signals from Microbe-Associated Molecular Patterns. *PLoS Pathogens* [online]. **9**(4) [cit. 2023-02-26]. ISSN 1553-7374. Dostupné z: doi:10.1371/journal.ppat.1003290

HE, Zuhua, Shanice WEBSTER a Sheng HE, 2022. Growth–defense trade-offs in plants. *Current Biology* [online]. **32**(12), 634-639 [cit. 2023-02-26]. ISSN 09609822. Dostupné z: doi:10.1016/j.cub.2022.04.070

HUANG, Chien-Yu, Huan WANG, Po HU, Rachael HAMBY a Hailing JIN, 2019. Small RNAs – Big Players in Plant-Microbe Interactions. *Cell Host & Microbe* [online]. **26**(2), 173-182 [cit. 2023-05-02]. ISSN 19313128. Dostupné z: doi:10.1016/j.chom.2019.07.021

HÜCKELHOVEN, Ralph, 2014. The effective papilla hypothesis. *New Phytologist* [online]. **204**(3), 438-440 [cit. 2023-02-21]. ISSN 0028-646X. Dostupné z: doi:10.1111/nph.13026

HUOT, Bethany, Jian YAO, Beronda MONTGOMERY a Sheng HE, 2014. Growth–Defense Tradeoffs in Plants: A Balancing Act to Optimize Fitness. *Molecular Plant* [online]. **7**(8), 1267-1287 [cit. 2023-02-26]. ISSN 16742052. Dostupné z: doi:10.1093/mp/ssu049

CHEN, Xiong-Yan a Jae-Yean KIM, 2014. Callose synthesis in higher plants. *Plant Signaling & Behavior* [online]. **4**(6), 489-492 [cit. 2023-02-26]. ISSN 1559-2324. Dostupné z: doi:10.4161/psb.4.6.8359

CHRISTENHUSZ, MAARTEN a JAMES BYNG, 2016. The number of known plants species in the world and its annual increase. *Phytotaxa* [online]. **261**(3), 201-217 [cit. 2023-02-24]. ISSN 1179-3163. Dostupné z: doi:10.11646/phytotaxa.261.3.1

JANDA, Martin, Lucie LAMPAROVÁ, Alžběta ZUBÍKOVÁ, Lenka BURKETOVÁ, Jan MARTINEC a Zuzana KRČKOVÁ, 2019. Temporary heat stress suppresses PAMP-triggered immunity and resistance to bacteria in *Arabidopsis thaliana*. *Molecular Plant Pathology* [online]. **20**(7), 1005-1012 [cit. 2023-02-21]. ISSN 1464-6722. Dostupné z: doi:10.1111/mpp.12799

JANDA, Martin, Jindříška MATOUŠKOVÁ, Lenka BURKETOVÁ a Olga VALENTOVÁ, 2014. Interconnection between actin cytoskeleton and plant defense signaling. *Plant Signaling & Behavior* [online]. **9**(11) [cit. 2023-02-26]. ISSN 1559-2324. Dostupné z: doi:10.4161/15592324.2014.976486

JANDA, Martin, Severine PLANCHAINS, Nabila DJAFI, Jan MARTINEC, Lenka BURKETOVA, Olga VALENTOVA, Alain ZACHOWSKI a Eric RUELLAND, 2013. Phosphoglycerolipids are master players in plant hormone signal transduction. *Plant Cell Reports* [online]. **32**(6), 839-851 [cit. 2023-02-28]. ISSN 0721-7714. Dostupné z: doi:10.1007/s00299-013-1399-0

JANDA, Martin a Silke ROBATZEK, 2022. Extracellular vesicles from phytobacteria: Properties, functions and uses. *Biotechnology Advances* [online]. **58** [cit. 2023-02-21]. ISSN 07349750. Dostupné z: doi:10.1016/j.biotechadv.2022.107934

JANDA, Martin a Eric RUELLAND, 2015b. Magical mystery tour: Salicylic acid signalling. *Environmental and Experimental Botany* [online]. **114**, 117-128 [cit. 2023-02-10]. ISSN 00988472. Dostupné z: doi:10.1016/j.envexpbot.2014.07.003

JANDA, Martin, Katarzyna RYBAK, Katarzyna MENG et al., 2023. Biophysical and proteomic analyses of *Pseudomonas syringae* pv tomato DC3000 extracellular vesicles suggest adaptive functions during plant infection. *MBio (in press)* [online]. Dostupné z: doi:10.1101/2021.02.08.430144 (preprint verze na BioRxiv)

JANDA, Martin, Vladimír ŠAŠEK, Hana CHMELAŘOVÁ, Jan ANDREJCH, Miroslava NOVÁKOVÁ, Jana HAJŠLOVÁ, Lenka BURKETOVÁ a Olga VALENTOVÁ, 2015a. Phospholipase D affects translocation

of NPR1 to the nucleus in *Arabidopsis thaliana*. *Frontiers in Plant Science* [online]. **6** [cit. 2023-02-26]. ISSN 1664-462X. Dostupné z: doi:10.3389/fpls.2015.00059

JELENSKA, Joanna, Yongsung KANG a Jean GREENBERG, 2015. Plant pathogenic bacteria target the actin microfilament network involved in the trafficking of disease defense components. *BioArchitecture* [online]. **4**(4-5), 149-153 [cit. 2023-02-26]. ISSN 1949-0992. Dostupné z: doi:10.4161/19490992.2014.980662

JIRAGE, Dayadevi, Tina TOOTLE, T. REUBER, Louise FROST, Bart FEYS, Jane PARKER, Frederick AUSUBEL a Jane GLAZEBROOK, 1999. *Arabidopsis thaliana* PAD4 encodes a lipase-like gene that is important for salicylic acid signaling. *Proceedings of the National Academy of Sciences* [online]. **96**(23), 13583-13588 [cit. 2023-02-26]. ISSN 0027-8424. Dostupné z: doi:10.1073/pnas.96.23.13583

JONES, Jonathan a Jeffery DANGL, 2006. The plant immune system. *Nature* [online]. **444**(7117), 323-329 [cit. 2023-02-10]. ISSN 0028-0836. Dostupné z: doi:10.1038/nature05286

JUNKOVÁ, Petra, Michaela NEUBERGEROVÁ, Tetiana KALACHOVA, Olga VALENTOVÁ a Martin JANDA, 2021. Regulation of the microsomal proteome by salicylic acid and deficiency of phosphatidylinositol-4-kinases $\beta 1$ and $\beta 2$ in *Arabidopsis thaliana*. *PROTEOMICS* [online]. **21**(5) [cit. 2023-02-28]. ISSN 1615-9853. Dostupné z: doi:10.1002/pmic.202000223

KADOTA, Yasuhiro, Jan SKLENAR, Paul DERBYSHIRE et al., 2014. Direct Regulation of the NADPH Oxidase RBOHD by the PRR-Associated Kinase BIK1 during Plant Immunity. *Molecular Cell* [online]. **54**(1), 43-55 [cit. 2023-02-26]. ISSN 10972765. Dostupné z: doi:10.1016/j.molcel.2014.02.021

KACHROO, Aardra a Pradeep KACHROO, 2020. Mobile signals in systemic acquired resistance. *Current Opinion in Plant Biology* [online]. **58**, 41-47 [cit. 2023-02-26]. ISSN 13695266. Dostupné z: doi:10.1016/j.pbi.2020.10.004

KALACHOVA, Tetiana, Martin JANDA, Vladimír ŠAŠEK et al., 2020. Identification of salicylic acid-independent responses in an *Arabidopsis* phosphatidylinositol 4-kinase beta double mutant. *Annals of Botany* [online]. **125**(5), 775-784 [cit. 2023-02-26]. ISSN 0305-7364. Dostupné z: doi:10.1093/aob/mcz112

KALACHOVA, Tetiana, Hana LEONTOVYČOVÁ, Oksana IAKOVENKO et al., 2019. Interplay between phosphoinositides and actin cytoskeleton in the regulation of immunity related responses in *Arabidopsis thaliana* seedlings. *Environmental and Experimental Botany* [online]. **167** [cit. 2023-02-13]. ISSN 00988472. Dostupné z: doi:10.1016/j.envexpbot.2019.103867

KANYUKA, Kostya, Kim HAMMOND-KOSACK, Giulia DE LORENZO a Felice CERVONE, 2022. Plant immunity by damage-associated molecular patterns (DAMPs). *Essays in Biochemistry* [online]. **66**(5), 459-469 [cit. 2023-02-25]. ISSN 0071-1365. Dostupné z: doi:10.1042/EBC20210087

KRČKOVÁ, Zuzana, Daniela KOCOURKOVÁ, Michal DANĚK et al., 2018. The *Arabidopsis thaliana* non-specific phospholipase C2 is involved in the response to *Pseudomonas syringae* attack. *Annals of Botany* [online]. **121**(2), 297-310 [cit. 2023-02-28]. ISSN 0305-7364. Dostupné z: doi:10.1093/aob/mcx160

KUMAR, Shivesh, Raul ZAVALIEV, Qinglin WU et al., 2022. Structural basis of NPR1 in activating plant immunity. *Nature* [online]. **605**(7910), 561-566 [cit. 2023-02-26]. ISSN 0028-0836. Dostupné z: doi:10.1038/s41586-022-04699-w

LAURENT, Jacqueline, J. PAULIN a J. ZUCCA, 1987. Ultrastructural study of *Erwinia amylovora* strains: Effect of culture conditions and fixation procedures. *Protoplasma* [online]. **139**(1), 1-8 [cit. 2023-02-25]. ISSN 0033-183X. Dostupné z: doi:10.1007/BF01417529

LEE, DongHyuk, Neeraj LAL, Zuh-Jyh LIN et al., 2020. Regulation of reactive oxygen species during plant immunity through phosphorylation and ubiquitination of RBOHD. *Nature Communications* [online]. **11**(1) [cit. 2023-02-26]. ISSN 2041-1723. Dostupné z: doi:10.1038/s41467-020-15601-5

LEONTOVYČOVÁ, Hana, Tetiana KALACHOVA a Martin JANDA, 2020. Disrupted actin: a novel player in pathogen attack sensing?. *New Phytologist* [online]. **227**(6), 1605-1609 [cit. 2023-02-26]. ISSN 0028-646X. Dostupné z: doi:10.1111/nph.16584

LEONTOVYČOVÁ, Hana, Tetiana KALACHOVA, Lucie TRDÁ et al., 2019. Actin depolymerization is able to increase plant resistance against pathogens via activation of salicylic acid signalling pathway. *Scientific Reports* [online]. **9**(1) [cit. 2023-02-10]. ISSN 2045-2322. Dostupné z: doi:10.1038/s41598-019-46465-5

LI, Jia, Jiangqi WEN, Kevin LEASE, Jason DOKE, Frans TAX a John WALKER, 2002. BAK1, an Arabidopsis LRR Receptor-like Protein Kinase, Interacts with BRI1 and Modulates Brassinosteroid Signaling. *Cell* [online]. **110**(2), 213-222 [cit. 2023-02-24]. ISSN 00928674. Dostupné z: doi:10.1016/S0092-8674(02)00812-7

LI, Pai a Brad DAY, 2019. Battlefield Cytoskeleton: Turning the Tide on Plant Immunity. *Molecular Plant-Microbe Interactions®* [online]. **32**(1), 25-34 [cit. 2023-02-26]. ISSN 0894-0282. Dostupné z: doi:10.1094/MPMI-07-18-0195-FI

LIU, Jie, Lin ZHANG a Dawei YAN, 2021. Plasmodesmata-Involved Battle Against Pathogens and Potential Strategies for Strengthening Hosts. *Frontiers in Plant Science* [online]. **12** [cit. 2023-02-26]. ISSN 1664-462X. Dostupné z: doi:10.3389/fpls.2021.644870

LUNA, Estrella, Victoria PASTOR, Jérôme ROBERT, Victor FLORS, Brigitte MAUCH-MANI a Jurriaan TON, 2011. Callose Deposition: A Multifaceted Plant Defense Response. *Molecular Plant-Microbe Interactions®* [online]. **24**(2), 183-193 [cit. 2023-02-26]. ISSN 0894-0282. Dostupné z: doi:10.1094/MPMI-07-10-0149

LU, You a Kenichi TSUDA, 2021. Intimate Association of PRR- and NLR-Mediated Signaling in Plant Immunity. *Molecular Plant-Microbe Interactions®* [online]. **34**(1), 3-14 [cit. 2023-02-18]. ISSN 0894-0282. Dostupné z: doi:10.1094/MPMI-08-20-0239-IA

MACH, Jennifer, 2013. Border Patrol on the Extrahaustorial Membrane: Arabidopsis Resistance Protein RPW8.2 Activates Targeted, Postpenetration Defenses. *The Plant Cell* [online]. **25**(10), 3638-3638 [cit. 2023-02-25]. ISSN 1040-4651. Dostupné z: doi:10.1105/tpc.113.251014

MALAMY, Jocelyn, John CARR, Daniel KLESSIG a Ilya RASKIN, 1990. Salicylic Acid: A Likely Endogenous Signal in the Resistance Response of Tobacco to Viral Infection. *Science* [online]. **250**(4983), 1002-1004 [cit. 2023-05-02]. ISSN 0036-8075. Dostupné z: doi:10.1126/science.250.4983.1002

MATOUŠKOVÁ, Jindřiška, Martin JANDA, Radovan FIŠER et al., 2014. Changes in actin dynamics are involved in salicylic acid signaling pathway. *Plant Science* [online]. **223**, 36-44 [cit. 2023-02-26]. ISSN 01689452. Dostupné z: doi:10.1016/j.plantsci.2014.03.002

MCMILLAN, Hannah, Sophia ZEBELL, Jean RISTAINO, Xinnian DONG a Meta KUEHN, 2021b. Protective plant immune responses are elicited by bacterial outer membrane vesicles. *Cell Reports* [online]. **34**(3) [cit. 2023-02-25]. ISSN 22111247. Dostupné z: doi:10.1016/j.celrep.2020.108645

MCMILLAN, Hannah a Meta KUEHN, 2021a. The extracellular vesicle generation paradox: a bacterial point of view. *The EMBO Journal* [online]. **40**(21) [cit. 2023-05-02]. ISSN 0261-4189. Dostupné z: doi:10.15252/embj.2021108174

MÉTRAUX, J., H. SIGNER, J. RYALS et al., 1990. Increase in Salicylic Acid at the Onset of Systemic Acquired Resistance in Cucumber. *Science* [online]. **250**(4983), 1004-1006 [cit. 2023-05-02]. ISSN 0036-8075. Dostupné z: doi:10.1126/science.250.4983.1004

MEYEROWITZ, Elliot M., 2001. Prehistory and History of Arabidopsis Research. *Plant Physiology* [online]. **125**(1), 15-19 [cit. 2023-02-24]. ISSN 1532-2548. Dostupné z: doi:10.1104/pp.125.1.15

MIYA, Ayako, Premkumar ALBERT, Tomonori SHINYA et al., 2007. CERK1, a LysM receptor kinase, is essential for chitin elicitor signaling in Arabidopsis. *Proceedings of the National Academy of Sciences*

[online]. **104**(49), 19613-19618 [cit. 2023-02-18]. ISSN 0027-8424. Dostupné z: doi:10.1073/pnas.0705147104

MONAGHAN, Jacqueline a Cyril ZIPFEL, 2012. Plant pattern recognition receptor complexes at the plasma membrane. *Current Opinion in Plant Biology* [online]. **15**(4), 349-357 [cit. 2023-02-18]. ISSN 13695266. Dostupné z: doi:10.1016/j.pbi.2012.05.006

MOU, Zhonglin, Weihua FAN a Xinnian DONG, 2003. Inducers of Plant Systemic Acquired Resistance Regulate NPR1 Function through Redox Changes. *Cell* [online]. **113**(7), 935-944 [cit. 2023-02-26]. ISSN 00928674. Dostupné z: doi:10.1016/S0092-8674(03)00429-X

NISHIMURA, Marc, Mónica STEIN, Bi-Huei HOU, John VOGEL, Herb EDWARDS a Shauna SOMERVILLE, 2003. Loss of a Callose Synthase Results in Salicylic Acid-Dependent Disease Resistance. *Science* [online]. **301**(5635), 969-972 [cit. 2023-02-26]. ISSN 0036-8075. Dostupné z: doi:10.1126/science.1086716

NOVÁKOVÁ, Miroslava, Vladimír ŠAŠEK, Petre DOBREV, Olga VALENTOVÁ a Lenka BURKETOVÁ, 2014. Plant hormones in defense response of Brassica napus to Sclerotinia sclerotiorum – Reassessing the role of salicylic acid in the interaction with a necrotroph. *Plant Physiology and Biochemistry* [online]. **80**, 308-317 [cit. 2023-02-26]. ISSN 09819428. Dostupné z: doi:10.1016/j.plaphy.2014.04.019

PEČENKOVÁ, Tamara, Martin JANDA, Jitka ORTMANNOVÁ, Vladimíra HAJNÁ, Zuzana STEHLÍKOVÁ a Viktor ŽÁRSKÝ, 2017. Early Arabidopsis root hair growth stimulation by pathogenic strains of Pseudomonas syringae. *Annals of Botany* [online]. **120**(3), 437-446 [cit. 2023-02-26]. ISSN 0305-7364. Dostupné z: doi:10.1093/aob/mcx073

PETRE, Benjamin, Sophien KAMOUN a John McDOWELL, 2014. How Do Filamentous Pathogens Deliver Effector Proteins into Plant Cells?. *PLoS Biology* [online]. **12**(2) [cit. 2023-02-25]. ISSN 1545-7885. Dostupné z: doi:10.1371/journal.pbio.1001801

PIETERSE, Corné, Antonio LEON-REYES, Sjoerd VAN DER ENT a Saskia VAN WEES, 2009. Networking by small-molecule hormones in plant immunity. *Nature Chemical Biology* [online]. **5**(5), 308-316 [cit. 2023-02-26]. ISSN 1552-4450. Dostupné z: doi:10.1038/nchembio.164

PLUHAŘOVÁ, Kamila, Hana LEONTOVYČOVÁ, Věra STOUDKOVÁ et al., 2019. "Salicylic Acid Mutant Collection" as a Tool to Explore the Role of Salicylic Acid in Regulation of Plant Growth under a Changing Environment. *International Journal of Molecular Sciences* [online]. **20**(24) [cit. 2023-02-12]. ISSN 1422-0067. Dostupné z: doi:10.3390/ijms20246365

PORTER, Katie a Brad DAY, 2016. From filaments to function: The role of the plant actin cytoskeleton in pathogen perception, signaling and immunity. *Journal of Integrative Plant Biology* [online]. **58**(4), 299-311 [cit. 2023-02-26]. ISSN 1672-9072. Dostupné z: doi:10.1111/jipb.12445

QIAO, Lulu, Chi LAN, Luca CAPRIOTTI et al., 2021. Spray-induced gene silencing for disease control is dependent on the efficiency of pathogen RNA uptake. *Plant Biotechnology Journal* [online]. **19**(9), 1756-1768 [cit. 2023-05-02]. ISSN 1467-7644. Dostupné z: doi:10.1111/pbi.13589

QI, Junsheng, Jinlong WANG, Zhizhong GONG a Jian-Min ZHOU, 2017. Apoplastic ROS signaling in plant immunity. *Current Opinion in Plant Biology* [online]. **38**, 92-100 [cit. 2023-02-26]. ISSN 13695266. Dostupné z: doi:10.1016/j.pbi.2017.04.022

QIN, Hua, Lina HE a Rongfeng HUANG, 2019. The Coordination of Ethylene and Other Hormones in Primary Root Development. *Frontiers in Plant Science* [online]. **10** [cit. 2023-02-26]. ISSN 1664-462X. Dostupné z: doi:10.3389/fpls.2019.00874

RADOJIČIĆ, Ana, Xin LI a Yuelin ZHANG, 2018. Salicylic Acid: A Double-Edged Sword for Programed Cell Death in Plants. *Frontiers in Plant Science* [online]. **9** [cit. 2023-02-26]. ISSN 1664-462X. Dostupné z: doi:10.3389/fpls.2018.01133

RAFFAELE, Sylvain, Susana RIVAS a Dominique ROBY, 2006. An essential role for salicylic acid in AtMYB30-mediated control of the hypersensitive cell death program in Arabidopsis. *FEBS Letters*

[online]. **580**(14), 3498-3504 [cit. 2023-02-26]. ISSN 00145793. Dostupné z: doi:10.1016/j.febslet.2006.05.027

ROBATZEK, Silke, Delphine CHINCHILLA a Thomas BOLLER, 2006. Ligand-induced endocytosis of the pattern recognition receptor FLS2 in Arabidopsis. *Genes & Development* [online]. **20**(5), 537-542 [cit. 2023-02-24]. ISSN 0890-9369. Dostupné z: doi:10.1101/gad.366506

RŮŽIČKA, Kamil, Karin LJUNG, Steffen VANNESTE, Radka PODHORSKÁ, Tom BEECKMAN, Jiří FRIML a Eva BENKOVÁ, 2007. Ethylene Regulates Root Growth through Effects on Auxin Biosynthesis and Transport-Dependent Auxin Distribution. *The Plant Cell* [online]. **19**(7), 2197-2212 [cit. 2023-02-26]. ISSN 1532-298X. Dostupné z: doi:10.1105/tpc.107.052126

SCHWESSINGER, Benjamin, Milena ROUX, Yasuhiro KADOTA, Vardis NTOUKAKIS, Jan SKLENAR, Alexandra JONES, Cyril ZIPFEL a David GUTTMAN, 2011. Phosphorylation-Dependent Differential Regulation of Plant Growth, Cell Death, and Innate Immunity by the Regulatory Receptor-Like Kinase BAK1. *PLoS Genetics* [online]. **7**(4) [cit. 2023-02-24]. ISSN 1553-7404. Dostupné z: doi:10.1371/journal.pgen.1002046

SMITH, John a Antje HEESE, 2014. Rapid bioassay to measure early reactive oxygen species production in Arabidopsis leave tissue in response to living *Pseudomonas syringae*. *Plant Methods* [online]. **10**(1) [cit. 2023-02-26]. ISSN 1746-4811. Dostupné z: doi:10.1186/1746-4811-10-6

SPOEL, Steven, Zhonglin MOU, Yasuomi TADA, Natalie SPIVEY, Pascal GENSCHIK a Xinnian DONG, 2009. Proteasome-Mediated Turnover of the Transcription Coactivator NPR1 Plays Dual Roles in Regulating Plant Immunity. *Cell* [online]. **137**(5), 860-872 [cit. 2023-02-26]. ISSN 00928674. Dostupné z: doi:10.1016/j.cell.2009.03.038

SUN, He, Zhu QIAO, Khi CHUA et al., 2018. Profilin Negatively Regulates Formin-Mediated Actin Assembly to Modulate PAMP-Triggered Plant Immunity. *Current Biology* [online]. **28**(12), 1882-1895 [cit. 2023-02-26]. ISSN 09609822. Dostupné z: doi:10.1016/j.cub.2018.04.045

SUN, Tongjun a Yuelin ZHANG, 2022. MAP kinase cascades in plant development and immune signaling. *EMBO reports* [online]. **23**(2) [cit. 2023-02-26]. ISSN 1469-221X. Dostupné z: doi:10.15252/embr.202153817

SUN, Yadong, Lei LI, Alberto MACHO, Zhifu HAN, Zehan HU, Cyril ZIPFEL, Jian-Min ZHOU a Jijie CHAI, 2013. Structural Basis for flg22-Induced Activation of the Arabidopsis FLS2-BAK1 Immune Complex. *Science* [online]. **342**(6158), 624-628 [cit. 2023-02-24]. ISSN 0036-8075. Dostupné z: doi:10.1126/science.1243825

ŠAŠEK, Vladimír, Martin JANDA, Elise DELAGE et al., 2014. Constitutive salicylic acid accumulation in pi4k III β1β2 Arabidopsis plants stunts rosette but not root growth. *New Phytologist* [online]. **203**(3), 805-816 [cit. 2023-02-10]. ISSN 0028-646X. Dostupné z: doi:10.1111/nph.12822

THÉRY, Clotilde, Kenneth WITWER, Elena AIKAWA et al., 2018. Minimal information for studies of extracellular vesicles 2018 (MISEV2018): a position statement of the International Society for Extracellular Vesicles and update of the MISEV2014 guidelines. *Journal of Extracellular Vesicles* [online]. **7**(1) [cit. 2023-02-25]. ISSN 2001-3078. Dostupné z: doi:10.1080/20013078.2018.1535750

TOYOTA, Masatsugu, Dirk SPENCER, Satoe SAWAI-TOYOTA, Wang JIAQI, Tong ZHANG, Abraham KOO, Gregg HOWE a Simon GILROY, 2018. Glutamate triggers long-distance, calcium-based plant defense signaling. *Science* [online]. **361**(6407), 1112-1115 [cit. 2023-02-26]. ISSN 0036-8075. Dostupné z: doi:10.1126/science.aat7744

TRDÁ, Lucie, Olivier FERNANDEZ, Freddy BOUTROT et al., 2014. The grapevine flagellin receptor Vv FLS 2 differentially recognizes flagellin-derived epitopes from the endophytic growth-promoting bacterium Burkholderia phytofirmans and plant pathogenic bacteria. *New Phytologist* [online]. **201**(4), 1371-1384 [cit. 2023-02-24]. ISSN 0028-646X. Dostupné z: doi:10.1111/nph.12592

TRDÁ, Lucie, Martin JANDA, Denisa MACKOVÁ, Romana POSPÍCHALOVÁ, Petre DOBREV, Lenka BURKETOVÁ a Pavel MATUŠINSKY, 2019. Dual Mode of the Saponin Aescin in Plant Protection:

Antifungal Agent and Plant Defense Elicitor. *Frontiers in Plant Science* [online]. **10** [cit. 2023-02-21]. ISSN 1664-462X. Dostupné z: doi:10.3389/fpls.2019.01448

TSUDA, Kenichi, Masanao SATO, Thomas STODDARD, Jane GLAZEBROOK, Fumiaki KATAGIRI a Gregory COPENHAVER, 2009. Network Properties of Robust Immunity in Plants. *PLoS Genetics* [online]. **5**(12) [cit. 2023-02-26]. ISSN 1553-7404. Dostupné z: doi:10.1371/journal.pgen.1000772

U. STOTZ, Henrik, Dominik BROTHERTON a Jameel INAL, 2022. Communication is key: extracellular vesicles as mediators of infection and defence during host–microbe interactions in animals and plants. *FEMS Microbiology Reviews* [online]. **46**(1) [cit. 2023-02-25]. ISSN 1574-6976. Dostupné z: doi:10.1093/femsre/fuab044

VAN DE WOUW, Angela a Alexander IDNURM, 2019. Biotechnological potential of engineering pathogen effector proteins for use in plant disease management. *Biotechnology Advances* [online]. **37**(6) [cit. 2023-02-25]. ISSN 07349750. Dostupné z: doi:10.1016/j.biotechadv.2019.04.009

VAN NIEL, Guillaume, Gisela D'ANGELO a Graça RAPOSO, 2018. Shedding light on the cell biology of extracellular vesicles. *Nature Reviews Molecular Cell Biology* [online]. **19**(4), 213-228 [cit. 2023-02-25]. ISSN 1471-0072. Dostupné z: doi:10.1038/nrm.2017.125

VOGEL, John a Shauna SOMERVILLE, 2000. Isolation and characterization of powdery mildew-resistant *Arabidopsis* mutants. *Proceedings of the National Academy of Sciences* [online]. **97**(4), 1897-1902 [cit. 2023-02-26]. ISSN 0027-8424. Dostupné z: doi:10.1073/pnas.030531997

VON MALEK, Bernadette, Eric VAN DER GRAAFF, Kay SCHNEITZ a Beat KELLER, 2002. The *Arabidopsis* male-sterile mutant dde2-2 is defective in the ALLENE OXIDE SYNTHASE gene encoding one of the key enzymes of the jasmonic acid biosynthesis pathway. *Planta* [online]. **216**(1), 187-192 [cit. 2023-02-26]. ISSN 0032-0935. Dostupné z: doi:10.1007/s00425-002-0906-2

WALTERS, Dale, 2017. *Fortress plant: how to survive when everything wants to eat you*. New York, NY: Oxford University Press. ISBN 9780198745600.

WANG, Hui-Qin, Li-Ping SUN, Li-Xiao WANG et al., 2020b. Ethylene mediates salicylic-acid-induced stomatal closure by controlling reactive oxygen species and nitric oxide production in *Arabidopsis*. *Plant Science* [online]. **294** [cit. 2023-02-26]. ISSN 01689452. Dostupné z: doi:10.1016/j.plantsci.2020.110464

WANG, Jingyi, Na LIAN, Yue ZHANG, Yi MAN, Lulu CHEN, Haobo YANG, Jinxing LIN a Yanping JING, 2022. The Cytoskeleton in Plant Immunity: Dynamics, Regulation, and Function. *International Journal of Molecular Sciences* [online]. **23**(24) [cit. 2023-02-26]. ISSN 1422-0067. Dostupné z: doi:10.3390/ijms232415553

WANG, Jizong, Meijuan HU, Jia WANG et al., 2019a. Reconstitution and structure of a plant NLR resistosome conferring immunity. *Science* [online]. **364**(6435) [cit. 2023-02-18]. ISSN 0036-8075. Dostupné z: doi:10.1126/science.aav5870

WANG, Jizong, Jia WANG, Meijuan HU et al., 2019b. Ligand-triggered allosteric ADP release primes a plant NLR complex. *Science* [online]. **364**(6435) [cit. 2023-02-18]. ISSN 0036-8075. Dostupné z: doi:10.1126/science.aav5868

WANG, Wei, John WITHERS, Heng LI et al., 2020a. Structural basis of salicylic acid perception by *Arabidopsis* NPR proteins. *Nature* [online]. **586**(7828), 311-316 [cit. 2023-02-26]. ISSN 0028-0836. Dostupné z: doi:10.1038/s41586-020-2596-y

WILDERMUTH, Mary, Julia DEWDNEY, Gang WU a Frederick AUSUBEL, 2001. Isochorismate synthase is required to synthesize salicylic acid for plant defence. *Nature* [online]. **414**(6863), 562-565 [cit. 2023-02-26]. ISSN 0028-0836. Dostupné z: doi:10.1038/35107108

XIN, Xiu-Fang a Sheng HE, 2013. *Pseudomonas syringae* pv. *tomato* DC3000: A Model Pathogen for Probing Disease Susceptibility and Hormone Signaling in Plants. *Annual Review of Phytopathology*

[online]. **51**(1), 473-498 [cit. 2023-02-25]. ISSN 0066-4286. Dostupné z: doi:10.1146/annurev-phyto-082712-102321

XIN, Xiu-Fang, Brian KVITKO a Sheng HE, 2018. *Pseudomonas syringae*: what it takes to be a pathogen. *Nature Reviews Microbiology* [online]. **16**(5), 316-328 [cit. 2023-02-25]. ISSN 1740-1526. Dostupné z: doi:10.1038/nrmicro.2018.17

XIN, Xiu-Fang, Kinya NOMURA, Kyaw AUNG et al., 2016. Bacteria establish an aqueous living space in plants crucial for virulence. *Nature* [online]. **539**(7630), 524-529 [cit. 2023-02-25]. ISSN 0028-0836. Dostupné z: doi:10.1038/nature20166

YAMADA, Kohji, Yusuke SAIJO, Hirofumi NAKAGAMI a Yoshitaka TAKANO, 2016. Regulation of sugar transporter activity for antibacterial defense in *Arabidopsis*. *Science* [online]. **354**(6318), 1427-1430 [cit. 2023-02-25]. ISSN 0036-8075. Dostupné z: doi:10.1126/science.aaah5692

YASUDA, Shigetaka, Kentaro OKADA a Yusuke SAIJO, 2017. A look at plant immunity through the window of the multitasking coreceptor BAK1. *Current Opinion in Plant Biology* [online]. **38**, 10-18 [cit. 2023-02-26]. ISSN 13695266. Dostupné z: doi:10.1016/j.pbi.2017.04.007

YUAN, Minhong, Zeyu JIANG, Guozhi BI et al., 2021. Pattern-recognition receptors are required for NLR-mediated plant immunity. *Nature* [online]. **592**(7852), 105-109 [cit. 2023-02-26]. ISSN 0028-0836. Dostupné z: doi:10.1038/s41586-021-03316-6

ZHAI, Keran, Di LIANG, Helin LI et al., 2022. NLRs guard metabolism to coordinate pattern- and effector-triggered immunity. *Nature* [online]. **601**(7892), 245-251 [cit. 2023-05-02]. ISSN 0028-0836. Dostupné z: doi:10.1038/s41586-021-04219-2

ZHANG, Mengmeng a Shuqun ZHANG, 2022. Mitogen-activated protein kinase cascades in plant signaling. *Journal of Integrative Plant Biology* [online]. [cit. 2023-02-26]. ISSN 1672-9072. Dostupné z: doi:10.1111/jipb.13215

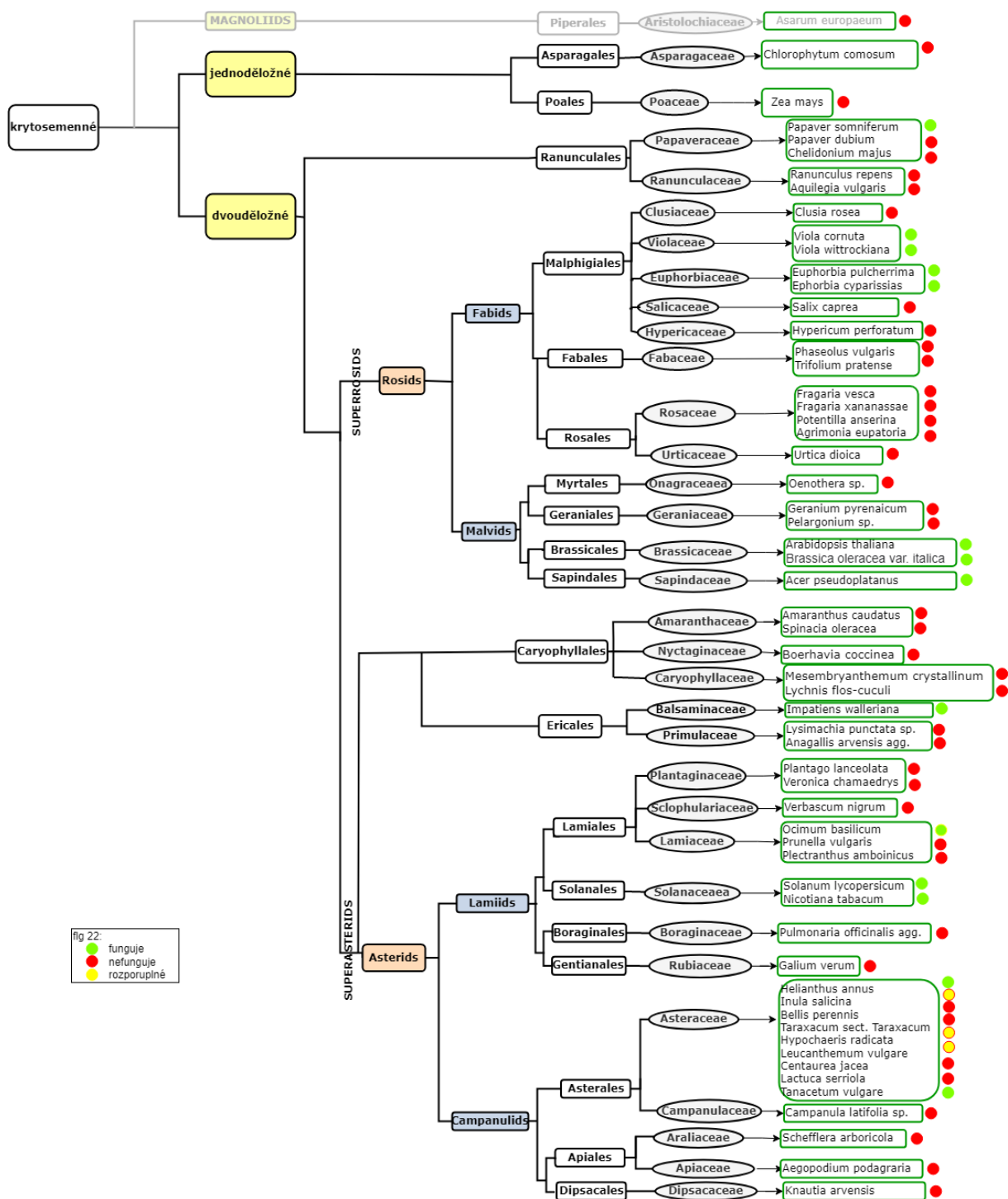
ZIPFEL, Cyril, Gernot KUNZE, Delphine CHINCHILLA, Anne CANIARD, Jonathan JONES, Thomas BOLLER a Georg FELIX, 2006. Perception of the Bacterial PAMP EF-Tu by the Receptor EFR Restricts Agrobacterium-Mediated Transformation. *Cell* [online]. **125**(4), 749-760 [cit. 2023-02-18]. ISSN 00928674. Dostupné z: doi:10.1016/j.cell.2006.03.037

ZIPFEL, Cyril, Silke ROBATZEK, Lionel NAVARRO, Edward OAKELEY, Jonathan JONES, Georg FELIX a Thomas BOLLER, 2004. Bacterial disease resistance in *Arabidopsis* through flagellin perception. *Nature* [online]. **428**(6984), 764-767 [cit. 2023-02-18]. ISSN 0028-0836. Dostupné z: doi:10.1038/nature02485

ZOU, Minxia, Mengmeng GUO, Zhaoyang ZHOU, Bingxiao WANG, Qing PAN, Jiajing LI, Jian-Min ZHOU a Jiejie LI, 2021. MPK3- and MPK6-mediated VLN3 phosphorylation regulates actin dynamics during stomatal immunity in *Arabidopsis*. *Nature Communications* [online]. **12**(1) [cit. 2023-02-26]. ISSN 2041-1723. Dostupné z: doi:10.1038/s41467-021-26827-2

ZURBRIGGEN, Matias, Néstor CARRILLO a Mohammad-Reza HAJIREZAEI, 2014. ROS signaling in the hypersensitive response. *Plant Signaling & Behavior* [online]. **5**(4), 393-396 [cit. 2023-02-26]. ISSN 1559-2324. Dostupné z: doi:10.4161/psb.5.4.10793

PŘÍLOHY



Příloha 1. Reakce rostlin z různých čeledí na flg22. Screening prováděný pomocí metody analyzující tvorbu apoplastických ROS (Smith, 2014). Červeně jsou znázorněny rostliny, které na ošetření flg22 nereagovali. Zeleně jsou znázorněny rostliny, které na ošetření flg22 reagovali opakovatelně a jednoznačně. Žlutě jsou znázorněny rostliny, u nichž v rámci opakování došlo k rozporuplným výsledkům. Tyto výsledky získala doktorandka Tereza Kalistová z mé skupiny (doposud nepublikováno).



Příloha 2 Vysoká koncentrace kyseliny salicylové (SA) inhibuje tvorbu antokyanů.
 Genotypy WT, NahG, NahG/pi4k β 1 β 2 a bon1/snc1-11 mají normální nebo nižší koncentraci SA. Genotypy fah1/fah2, pi4k β 1 β 2 a bon1 mají vysokou koncentraci SA (doposud nepublikováno).

Následují původní výzkumné publikace autora habilitační práce v pořadí, jak jsou zmínovány v příspěvcích (zelené rámečky) v této habilitační práci.

Short communication

Temporary heat stress suppresses PAMP-triggered immunity and resistance to bacteria in *Arabidopsis thaliana*

MARTIN JANDA^{1†}, LUCIE LAMPAROVÁ^{1,2†}, ALŽBĚTA ZUBÍKOVÁ², LENKA BURKETOVÁ²,
JAN MARTINEC² AND ZUZANA KRČKOVÁ^{2,*}

¹University of Chemistry and Technology Prague, Technická 5, Prague 6 – Dejvice, 166 282, Czech Republic

²The Czech Academy of Sciences, Institute of Experimental Botany, Rozvojová 263, Prague 6 – Lysolaje, 165 00, Czech Republic

SUMMARY

Recognition of pathogen-associated molecular patterns (PAMPs) is crucial for plant defence against pathogen attack. The best characterized PAMP is flg22, a 22 amino acid conserved peptide from flagellin protein. In *Arabidopsis thaliana*, flg22 is recognized by the flagellin sensing 2 (FLS2) receptor. In this study, we focused on biotic stress responses triggered by flg22 after exposure to temporary heat stress (HS). It is important to study the reactions of plants to multiple stress conditions because plants are often exposed simultaneously to a combination of both abiotic and biotic stresses. Transient early production of reactive oxygen species (ROS) is a well-characterized response to PAMP recognition. We demonstrate the strong reduction of flg22-induced ROS production in *A. thaliana* after HS treatment. In addition, a decrease in FLS2 transcription and a decrease of the FLS2 presence at the plasma membrane are shown after HS. In summary, our data show the strong inhibitory effect of HS on flg22-triggered events in *A. thaliana*. Subsequently, temporary HS strongly decreases the resistance of *A. thaliana* to *Pseudomonas syringae*. We propose that short exposure to high temperature is a crucial abiotic stress factor that suppresses PAMP-triggered immunity, which subsequently leads to the higher susceptibility of plants to pathogens.

Keywords: *Arabidopsis thaliana*, flagellin sensing 2 receptor, flg22, heat stress, PAMP-triggered immunity, *Pseudomonas syringae*, reactive oxygen species.

Plants are exposed to different environmental stresses that often occur simultaneously. Due to their sessile disposition, plants had to develop strategies to adapt to multi-stress conditions. Nowadays, as the case of global warming becomes a very important issue, the studies of how high temperatures impact on

plant resistance to pathogens are of the highest interest. Indeed, it is not exceptional now that even in the relatively mild climate areas temperature rises up to 40 °C or that the night and day temperature difference exceeds a variance of about 30 °C. This unstable temperature influences plant-pathogen interactions amongst other stresses (Hua, 2013; Velásquez *et al.*, 2018).

A typical response to pathogen attack is the activation of plant immunity. It consists of two layers: PTI (PAMP-triggered immunity) and ETI (effector-triggered immunity) (Jones and Dangl, 2006). PTI involves the recognition of conserved pathogen-associated molecular patterns (PAMPs) acting as elicitors. Typical PAMPs include flagellin, peptidoglycan, Tu elongation factor, lipopolysaccharides, chitin and glucans. PAMPs are recognized at the plasma membrane (PM) by specific pattern recognition receptors (PRRs) (Boller and Felix, 2009; Trda *et al.*, 2015). The best characterized plant PRR is flagellin sensing 2 (FLS2) that recognizes a conserved 22 amino acid peptide (flg22) from bacterial flagellin (Gomez-Gomez *et al.*, 1999; Zipfel *et al.*, 2004). Flg22 recognition leads to the production of reactive oxygen species (ROS), nitric oxide, ion fluxes, cytoskeletal remodelling, stomatal closure, activation of protein phosphorylation cascades and increased levels of phytohormones (salicylic acid [SA], jasmonic acid [JA] and ethylene) (Bigeard *et al.*, 2015). Subsequently, the transcription of defence genes is induced, followed by the expression of antimicrobial compounds and the strengthening of the cell wall by the accumulation of callose (Boller and Felix, 2009; Muthamilarasan and Prasad, 2013). Pathogenic organisms have developed special molecules, called effectors, to overcome PTI. Effectors are recognized by the receptor proteins (mostly intracellular) commonly called R-proteins. This recognition leads to ETI responses that are similar to PTI, but are often stronger and could result in the hypersensitive reaction (HR) (Chisholm *et al.*, 2006; Coll *et al.*, 2011; Cui *et al.*, 2015; He *et al.*, 2006). In this study, we focused on the effect of temporary heat stress (HS) on *Arabidopsis thaliana* PTI and the resistance to *Pseudomonas syringae* pv. *tomato* (*Pst*) DC3000.

* Correspondence: Email: krckova@ueb.cas.cz

†These authors contributed equally to the study.

Several studies focused on the relationship between HS and plant immunity. However, until now most studies used 'long-term' exposure to HS in their experiments, such as 1 day or constitutive growth under mildly elevated temperature (approximately 28 °C) (Cheng *et al.*, 2013; Wang *et al.*, 2009; Zhu *et al.*, 2010). Based on a gene transcription and mitogen-activated protein kinase (MAPK) activation analysis, it was shown that PTI is activated within a temperature interval of 23 °C–32 °C with the peak at 28 °C (Cheng *et al.*, 2013). We were then interested in situations, while plants suffered more severe HS than a mildly elevated temperature. In this study, we show that short exposure to high temperature suppressed typical PTI responses. The ROS production, one of the best characterized responses to pathogen attack, increased after exposure to flg22 (Smith and Heese, 2014), as well as after HS (Volkov *et al.*, 2006; Wang *et al.*, 2014). We observed that the exposure of 4-week-old *A. thaliana* leaf discs to 42 °C for 45 min almost blocks the transient flg22-induced ROS production, which normally occurs within approximately 12 min (Methods S1, Fig. 1A). The exposure of the leaf discs to HS alone increased ROS production as late as in 40 min after exposure to 42 °C (Fig. 1A inset). It confirms a distinct origin of ROS in the response of plant immunity and in reaction to HS. The HS-induced inhibition of flg22-induced ROS production is time-dependent; 15 min at 42 °C was not enough to suppress ROS production, but when the leaf discs were exposed to HS for 30 min, the maximum ROS value was reduced to 13% and even nearly blocked after 45 min exposure (Fig. 1B). The reduction of the flg22-induced ROS production after HS might be the consequence of damage to plants by applied HS. Therefore, we tested whether the reduction is reversible. Leaf discs were returned after exposure to HS (45 min at 42 °C) to the control conditions (22 °C) for either 1 h or 2 h, and flg22-induced ROS production was then monitored. In this case, ROS production did not fully recover (Fig. 1C). However, it was clear, and the recovery reached over 30% of the control. This suggests that HS did not cause any pathological or devastating changes to the plants under our experimental conditions. In addition, we found the same trend for lower temperatures, but a longer exposure time was needed. Flg22-induced ROS production was severely decreased when the leaf discs were maintained at 37 °C for 120 min. After 360 min at 32 °C or 28 °C, the ROS production decreased to 14% or 65%, respectively (Figs 1D and S1). To address the specificity of the studied phenomenon, we tested another well-known PTI-triggering elicitor, a peptide from the N-terminus of EF-Tu (elf18). Elf18-triggered responses are similar to the flg22-triggered ones (Henty-Ridilla *et al.*, 2014; Kunze *et al.*, 2004). In this study, HS induced the inhibition of elf18-induced ROS production similarly to that of flg22. The elf18-induced ROS production was reduced to 4% after 45 min at 42 °C, and after 2 h, the recovery reached 36% of the control and to 8% after 120 min at 37 °C, and after 2 h, the recovery reached 33% of the control (Fig. S2). We show

that temporary HS has a robust inhibitory effect on PTI-induced ROS production.

Flg22-triggered ROS production starts with the recognition of flg22 by its plasma membrane-localized receptor FLS2. In its non-activated state, FLS2 constitutively cycles between the PM and early endosome compartments (Beck *et al.*, 2012; Robatzek *et al.*, 2006; Zipfel *et al.*, 2004). Thus, the HS-induced decrease of flg22-triggered ROS production might be caused by the decrease of FLS2 transcription or by altered FLS2 cycling. We observed that the transcription level of *FLS2* decreased after 30 min and 45 min at 42 °C and after 120 min at 37 °C (Fig. 2A, Methods S1, Table S3). Transcriptional levels increased back to the original level after 2 h at 22 °C after HS (Fig. 2B). These results demonstrate the transient effect of temporary exposure to high temperature on *FLS2* transcription. To study the effect of HS on FLS2 protein level, we used plants harbouring *pFLS2::FLS2-GFP-HA* (Beck *et al.*, 2012). A Western blot analysis of the PM fractions isolated from control and heat stressed plants (42 °C at 1 h) show a decreased level of FLS2 at the PM after HS (Fig. 2C). We used plants harbouring *p35S::FLOT2:GFP*, another PM protein (Daněk *et al.*, 2016; Junková *et al.*, 2018) to figure out whether the decrease of protein association with PM is a general effect of HS. In plants exposed to HS (1 h at 42 °C) FLOT2-GFP level was not decreased in comparison to control conditions (Fig. S3). The specific decrease of FLS2 at PM after HS implies a mechanism by which HS suppresses flagellin-activated responses. We suggest that the HS inhibited the *FLS2* transcription and decreased the amount of FLS2 at the PM, which results in the inhibition of flg22-induced ROS production. This decrease of *FLS2* transcription after HS was transient, as well as the flg22-induced ROS production (Figs 1 and 2).

Furthermore, we wondered whether other PTI-induced genes were inhibited by the temporary HS. We analysed the transcription of two genes (*FRK1* and *ICS1*) activated after the recognition of flg22 (Swain *et al.*, 2015; Tsuda *et al.*, 2008; Wildermuth *et al.*, 2001; Yeh *et al.*, 2015). It was reported that *FRK1* transcription is activated early upon the recognition of the PAMPs (including flg22), and its transcription is enhanced by temperatures between 25 °C–32 °C during the response to flg22 (Cheng *et al.*, 2013). However, the authors used *A. thaliana* protoplasts exposed to 32 °C for just 15 min, 3 h before flg22 treatment. In our experiments, *FRK1* transcription was transiently but inhibited by the exposure to 42 °C for 45 min (Fig. 2D,E). This inconsistency indicates a very important role of timing and/or difference between basal and elicited responses of immune components upon HS. *ICS1* is one of the crucial components of the SA biosynthetic pathway (Wildermuth *et al.*, 2001). *ICS1* transcription induced by flg22 (or *Pst* DC3000) is strongly inhibited at 30 °C followed by a decrease of SA concentration (Huot *et al.*, 2017). In our conditions, the transcription of *ICS1* decreased at a later time during the recovery phase after HS (42 °C at 45 min) (Fig. 2E). This is

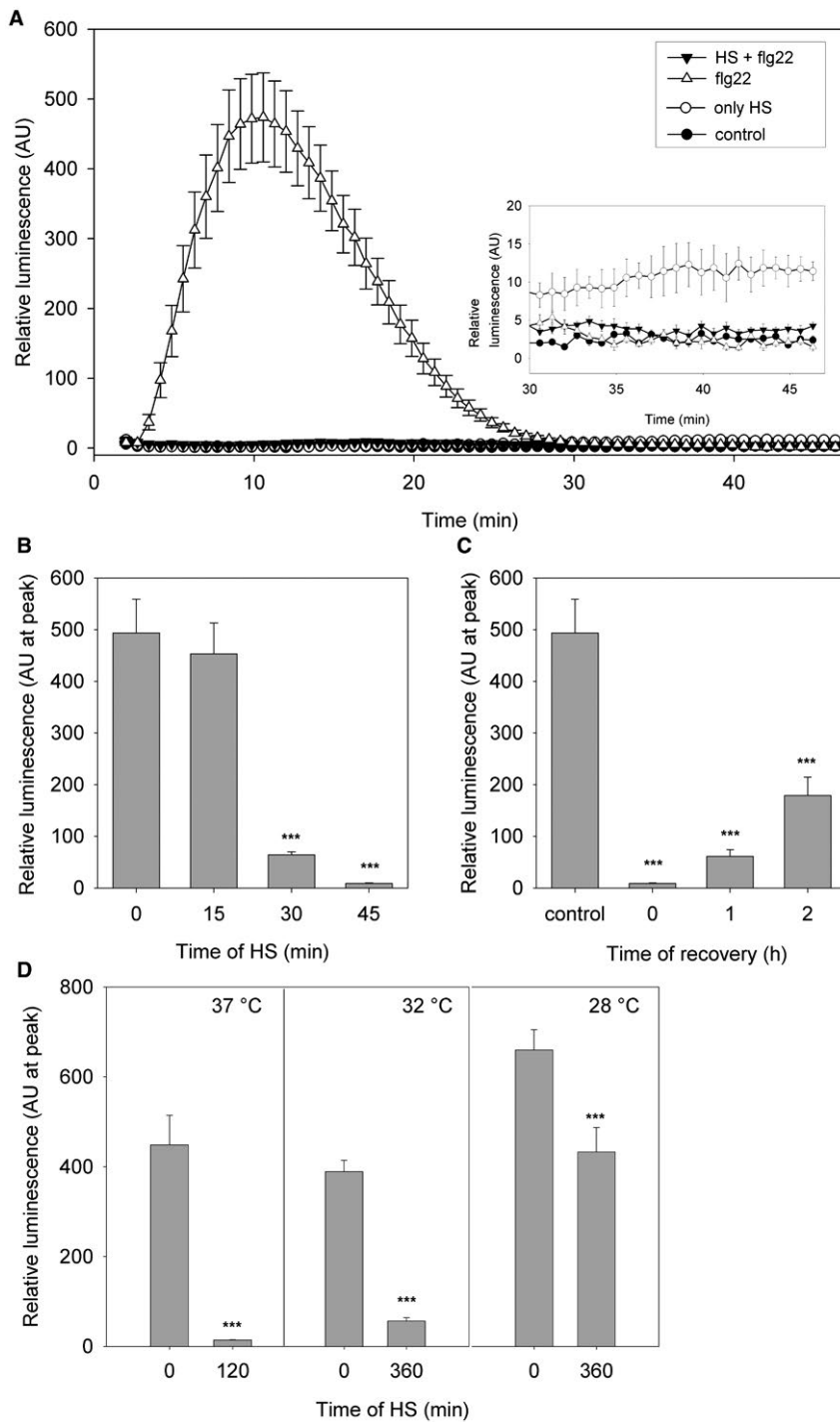


Fig. 1 Oxidative burst triggered by the combination of HS and 100 nM flg22. The ROS production was measured by luminol-dependent chemiluminescence counting in leaf discs from 4-week-old *Arabidopsis thaliana*. A) The ROS production kinetics monitored over 45 min after 100 nM flg22 (white triangle), after HS (42 °C at 45 min; white circle), after HS with a follow-up treatment with flg22 (black triangle) and in control conditions (black circle). B) ROS production (represented by the peak luminescence) was measured after the addition of 100 nM flg22. The discs were pre-treated with HS (15 min, 30 min and 45 min at 42 °C) or kept in control conditions (0 h). C) Recovery of the ROS production (represented by the peak luminescence) was measured after the addition of 100 nM flg22. The discs were pre-treated with HS (45 min at 42 °C) or kept in control conditions. ROS production was measured immediately after HS (0 h), or the discs were returned to the control conditions for 1 h or 2 h and then measured. D) ROS production (represented by the peak luminescence) was measured after the addition of 100 nM flg22. The discs were pre-treated with HS (120 min at 37 °C, 360 min at 32 °C and 360 min at 28 °C) or kept in control conditions (0 h). The data represent the means + SE; $n = 8$ leaf discs in one biological experiment. The experiment was repeated three times independently with similar results. Asterisks indicate that the mean value is significantly different from the control conditions without HS (two-tailed Student's *t*-test, $n = 8$, *** $P < 0.001$). HS, heat stress; ROS, reactive oxygen species; SE, standard error.

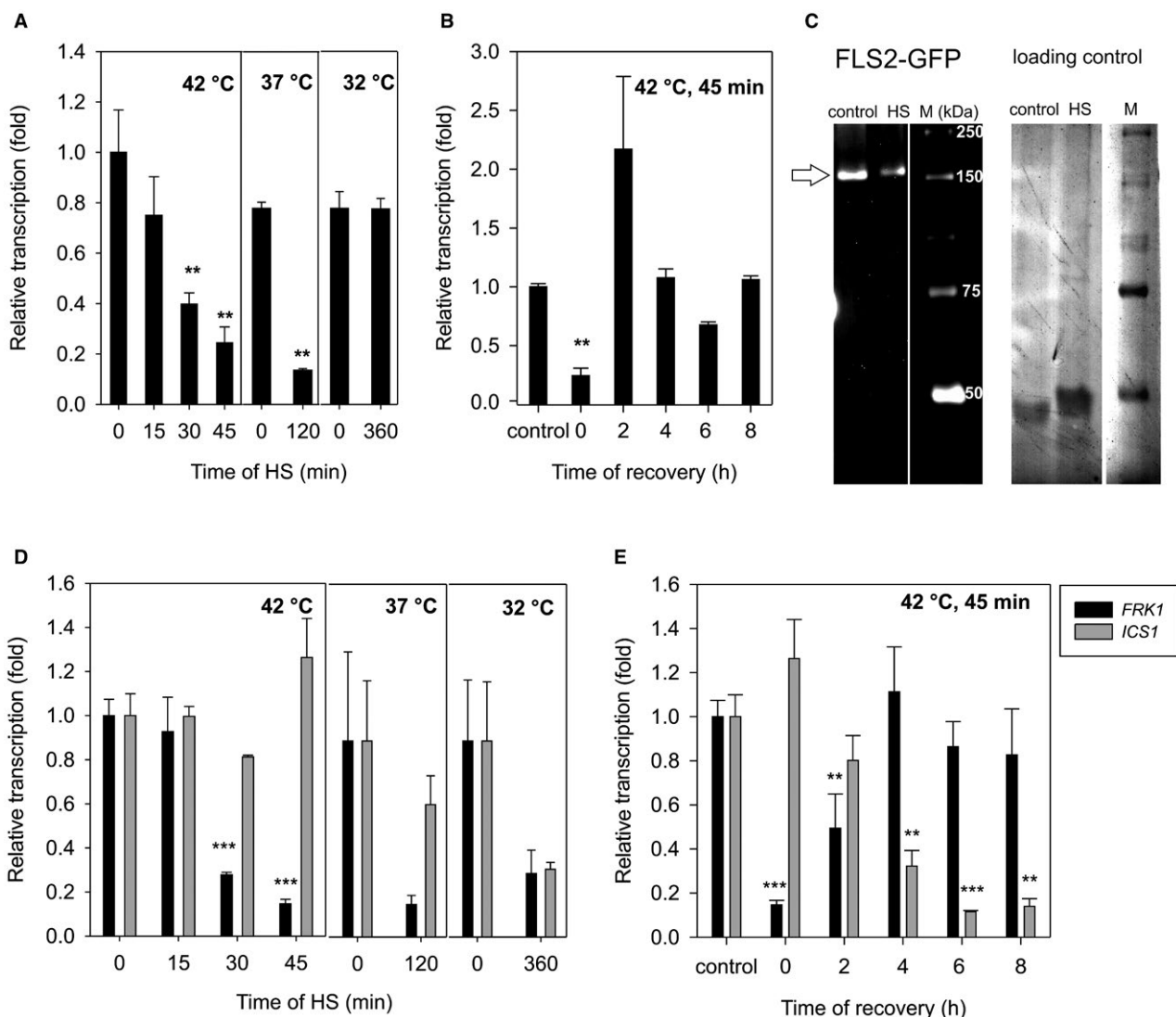


Fig. 2 Analysis of *FLS2*, *FRK1* and *ICS1* transcription and the level of *FLS2* at the PM after HS. Discs of 4-week-old *Arabidopsis thaliana* leaves were subjected to HS and transcript levels of the *FLS2* (A, B), *FRK1* and *ICS1* (D, E) were measured by quantitative real-time PCR. (A, D) Leaf discs were stressed for 15 min, 30 min and 45 min at 42 °C; 120 min at 37 °C and 360 min at 32 °C. (B, E) Leaf discs were stressed for 45 min at 42 °C and were returned to the control conditions for 2 h, 4 h, 6 h and 8 h. *TIP41* was used as a reference gene. The data represent the means + SE; $n = 3$ discrete samples from one biological experiment. The experiment was repeated three times independently with similar results. Asterisks indicate that the mean value is significantly different from the control conditions (two-tailed Student's *t*-test, $n = 3$, ** $P < 0.01$, *** $P < 0.001$). (C) Western blot analysis of the PM was performed. The PM was purified from a 4-week-old leaf of *A. thaliana* plants harbouring pFLS2::FLS2-GFP-HA. These plants were treated with either HS (42 °C at 1 h) or kept in control conditions. The GFP tag was detected using anti-GFP antibody. Loading controls of proteins on membrane were visualized using Novex reversible membrane protein stain. HS, heat stress; FLS, flagellin-sensitive2; FRK1, FLG22-induced receptor-like kinase1; GFP, green fluorescent protein; ICS1, isochromate synthase 1; M, marker; PCR, polymerase chain reaction; PM, plasma membrane; SE, standard error.

consistent with the slower transcriptional reaction of this gene in comparison to *FRK1* (Denoux *et al.*, 2008; Hunter *et al.*, 2013). To study whether the PTI-activated gene transcription response is generally suppressed after HS, we performed *in silico* gene transcription analysis using Genevestigator (Hruz *et al.*, 2008). We selected 20 genes connected with plant immunity in general and with PTI in particular (Table S1) (Muthamilarasan and Prasad, 2013). Genes specifically connected to PTI include *FLS2*, *BAK1*

and *BIK1*. PTI overlaps with ETI signalling with the activation of such genes as those involved in the MAPK cascade (*MKK4*, *MEKK1*, *MKK1* and *MPK4*) and *WRKY* transcription factors (Pandey and Somssich, 2009). *EDS1*, *PAD4* and *SAG101* proteins that mediate the SA-signalling result in *PR* (pathogenesis related) and *NPR* (nonexpressor of pathogenesis-related genes 1) induced transcription (Makandar *et al.*, 2015). Using Genevestigator, we show that those genes have higher transcription after differential

treatment with flg22 (Fig. S4). However, the transcription of these genes was largely inhibited in the experiments where the plants were exposed to high temperature (Fig. S4). Figure S4 also shows an example of genes activated by HS (*HSFA7A*, *HSA32*, *HSP18* and *HSP70*). Our analysis is consistent with that of Huot *et al.* (2017) who showed that after benzothiadiazole (a functional analogue of SA) treatment, a high proportion of the induced genes was suppressed at 30 °C, including *PR1*, *PR2*, *ICS1*, *SARD1*, *EDS1*, *PAD4*, *WRKY18* and *WRKY60*. Overall, the transcription of the flg22-activated genes is inhibited by temporary HS.

In addition to ROS production and the transcription of defence-related genes, the PTI response is characterized by callose deposition. Zhang *et al.* (2007) showed that respiratory burst oxidase homolog D (RbohD) regulates cell wall defence exemplified by callose deposition. Callose deposition is influenced by the SA-signalling pathway (Huot *et al.*, 2017; Yi *et al.*, 2014). We performed our experiments on leaf discs from 4-week-old plants as used for the ROS measurement. We induced callose formation by flg22 treatment in the leaf discs. We observed that the callose formation decreased to 60% when the leaf discs were exposed to HS (42 °C for 1 h) and treated with flg22 at 22 °C for 24 h compared to the control conditions at 22 °C (Fig. S5). Consistently with the results from Huot *et al.* (2017), callose accumulation was almost blocked when the treatment with flg22 was performed under the heat conditions (37 °C; Fig. S5), but in this case, the leaf discs were constantly subjected to high temperature (24 h).

To summarize, our results show that temporary HS caused the inhibition of the early flg22-triggered responses of plant immunity (ROS production and *FLS2* transcription), as well as later responses (transcriptional activation of genes of plant immunity pathways and callose deposition).

As a final point, we wanted to determine if temporary HS could also affect the resistance of *A. thaliana* to *Pst* DC3000. The inhibitory effect of longer exposure (24 h or more) to mildly elevated temperature on plant immunity, especially on the SA-signalling pathway, had been shown. Mutants with elevated SA production, such as *bon1*, *cpr1* and *snc1*, are very good examples. The dwarf phenotype of these mutants and SA production was suppressed during constant growth at 28 °C (Bowling *et al.*, 1994; Felix *et al.*, 1999; Hammoudi *et al.*, 2018; Ichimura *et al.*, 2006; Janda and Ruelland, 2015; Yang and Hua, 2004; Zhang *et al.*, 2003). The exposure to mildly elevated temperature (28 °C–30 °C) also inhibits *A. thaliana* resistance to *Pst* DC3000 (Huot *et al.*, 2017; Menna *et al.*, 2015; Wang *et al.*, 2009; Xin *et al.*, 2018). It must be noted that in those studies, the plants were exposed to elevated temperature also after the treatment with *Pst* DC3000. Therefore, it is difficult to conclude that the higher susceptibility is caused solely by HS because the bacteria were also affected by elevated temperature.

In this study, we used a higher temperature for the temporary exposure of plants (1 h at 42 °C and 2 h at 37 °C) before bacterial treatment. After HS, the plants were kept in control conditions (22 °C at 18 h), subsequently infiltrated with *Pst* DC3000 and maintained at 22 °C. As a result, in our experimental design *Pst* DC3000 propagation was not affected by the high temperature and all the observed effects on *Pst* DC3000 growth *in planta* came from the changes in host metabolism. To overcome the immunity connected with stomata closure, which could be affected by higher temperature, we infiltrated *Pst* DC3000 directly into the apoplast. Indeed, we demonstrated that *A. thaliana* plants exposed to 42 °C or 37 °C were more susceptible to *Pst* DC3000 comparing to the control (Fig. 3A). The bacterial growth in plants at 42 °C and 37 °C was fourfold higher than at 22 °C.

To determine if the effect of a long recovery from HS on resistance exists at the level of ROS production, we treated whole plants with HS (1 h at 42 °C; 2 h at 37 °C), cut the leaf discs and left them at 22 °C for 18 h. In this case, the ROS production was decreased to 50% at the plants treated with 42 °C and to 68% at the plants treated with 37 °C (Fig. 3B). It means that temporary HS led to the significant inhibition of flg22-induced ROS production.

To address whether full recovery after HS is possible, we returned plants after exposure to HS (2 h at 37 °C or 1 h at 42 °C) to the control conditions (22 °C) for 24 h, cut the leaf discs and left them at 22 °C for 18 h. Indeed, we were able to detect the full recovery for the 37 °C treated plants and 70% recovery for the plants exposed to 42 °C (Fig. S6). We wondered whether the general physiological parameters were affected in our HS conditions. To study this, we measured ion leakage at 24 h after HS using a COND70 conductivity meter (XS Instruments) (Prerostova *et al.*, 2018) and detected no difference between control and HS-treated plants (Table S2). In addition 6 days after the HS exposure (1 h at 42 °C) plants still looked like control plants (Fig. S7). This indicates that used mild HS conditions did not cause severe damage on plants.

It is possible, that the inhibition of PTI is one of the reasons why plants are vulnerable to pathogen attack even 18 h after the exposure to high temperature. Huot *et al.* (2017) showed decreased resistance of *A. thaliana* after *Pst* DC3000 infection, but only when the plants were maintained at 30 °C. However, when plants were exposed to 30 °C for 2 days before infiltration and subsequently subjected to 23 °C, there was no detectable difference in the infection development comparing to the control plants. It might seem that just temporary mild HS is not sufficient to affect resistance. Alternatively, here we show that temporary effect of higher temperatures (37 °C and 42 °C) decreased the resistance of *A. thaliana* to *Pst* DC3000 without the influence of temperature on the pathogen.

In conclusion, here we provide the evidence that the modulation of plant metabolism by HS leads to higher susceptibility

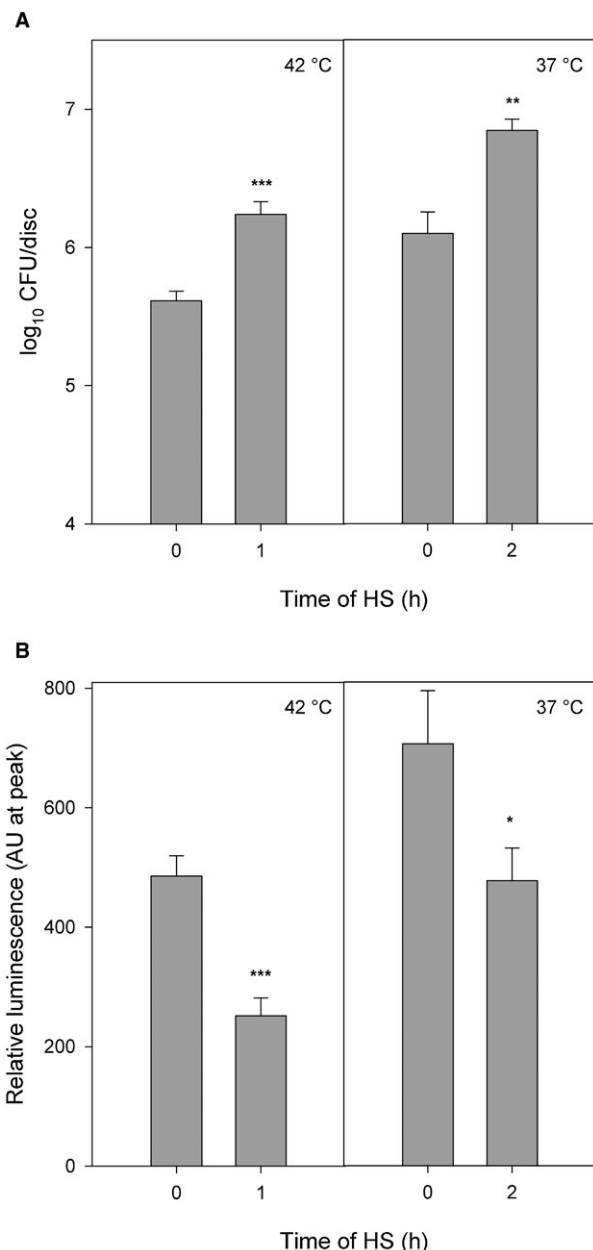


Fig. 3 Resistance to *Pst* DC3000 and the oxidative burst triggered by flg22 after temporary HS. (A) Four-week-old *Arabidopsis thaliana* plants were kept at 42 °C for 1 h and at 37 °C for 2 h. The recovery phase took 18 h in control conditions before treatment with *Pst* DC3000. Control plants were continuously cultivated at 22 °C. Leaf discs were harvested 3 days after inoculation with *Pst* DC3000. The data represent the means + SE; $n = 4$ from four biological experiments. (B) The plants were exposed to 42 °C for 1 h and 37 °C for 2 h. After HS, the leaf discs were cut and returned to 22 °C for 18 h. ROS production (represented by the peak luminescence) was measured after the addition of 100 nM flg22. The data represent means + SE; $n = 12$ discs. The experiment was repeated three times independently with similar results. The asterisks represent statistically significant changes between the heat and control conditions (* $P < 0.5$, ** $P < 0.01$, *** $P < 0.001$; two-tailed Student's *t*-test). CFU, colony-forming units; HS, heat stress; *Pst*, *Pseudomonas syringae* pv. *tomato*, ROS, reactive oxygen species; SE, standard error.

to the bacterial pathogen (Fig. 3). We present a broad study of flg22-triggered ROS production upon short exposure to high temperatures, which demonstrated a strong inhibitory effect of temporary HS on ROS production. In parallel, the transcription of the genes activated by flg22 was inhibited after HS. We suggest that these processes play an important role in the decreased amount of FLS2 at the PM after HS. From those results, it could be stated that HS significantly influences the PTI and resistance to *Pst* DC3000 in *A. thaliana*.

ACKNOWLEDGEMENTS

The authors would like to thank Tereza Podmanická and Romana Pospíchalová for their extremely helpful technical support; Dr Kenichi Tsuda from MPIPZ Cologne for providing the strain of *Pst* DC3000; and Professor Silke Robatzek from LMU Munich for providing pFLS2::FLS2-GFP-HA. Martin Janda and Lucie Lamparová would like to thank the leader of their laboratory Professor Olga Valentová. The work was supported by the Ministry of Education, Youth and Sports of CR from European Regional Development Fund-Project 'Centre for Experimental Plant Biology': No. CZ.02. 1.01/0.0/0.0/16_019/0000738 and Postdoctoral Fellowship programme of the Czech Academy of Sciences (L200381652) and specific University of Chemistry and Technology research of the Czech Republic (MSMT Nos 20-SVV/2017 and 21-SVV/2018).

ACCESSION NUMBERS

FLS2, At5g46330; FRK1, At2g19190; ICS1, At1g74710; and TIP41, At4g34270.

REFERENCES

- Beck, M., Zhou, J., Faulkner, C., MacLean, D. and Robatzek, S. (2012) Spatio-temporal cellular dynamics of the *Arabidopsis* flagellin receptor reveal activation status-dependent endosomal sorting. *Plant Cell*, **24**, 4205–4219.
- Bigard, J., Colcombet, J. and Hirt, H. (2015) Signaling mechanisms in pattern-triggered immunity (PTI). *Mol. Plant*, **8**, 521–539.
- Boller, T. and Felix, G. (2009) A renaissance of elicitors: Perception of microbe-associated molecular patterns and danger signals by pattern-recognition receptors. *Annu. Rev. Plant Biol.*, **60**, 379–406.
- Bowling, S.A., Guo, A., Cao, H., Gordon, A.S., Klessig, D.F. and Dong, X.I. (1994) A mutation in *Arabidopsis* that leads to constitutive expression of systemic acquired-resistance. *Plant Cell*, **6**, 1845–1857.
- Cheng, C., Gao, X.Q., Feng, B.M., Sheen, J., Shan, L.B. and He, P. (2013) Plant immune response to pathogens differs with changing temperatures. *Nat. Commun.*, **4**, 1–9.
- Chisholm, S.T., Coaker, G., Day, B. and Staskawicz, B.J. (2006) Host-microbe interactions: Shaping the evolution of the plant immune response. *Cell*, **124**, 803–814.
- Coll, N.S., Epple, P. and Dangl, J.L. (2011) Programmed cell death in the plant immune system. *Cell Death Differ.*, **18**, 1247–1256.
- Cui, H., Tsuda, K. and Parker, J.E. (2015) Effector-triggered immunity: From pathogen perception to robust defense. *Annu. Rev. Plant Biol.*, **66**, 487–511.

- Daněk, M., Valentová, O. and Martinec, J. (2016) Flotillins, Erlins, and HIRs: From Animal Base Camp to Plant New Horizons. *Crit. Rev. Plant Sci.* **35**, 191–214.
- Denoux, C., Galletti, R., Mammarella, N., Gopalan, S., Werck, D., De Lorenzo, G., Ferrari, S., Ausubel, F.M. and Dewdney, J. (2008) Activation of defense response pathways by OGs and Flg22 elicitors in *Arabidopsis* seedlings. *Mol. Plant*, **1**, 423–445.
- Felix, G., Duran, J.D., Volko, S. and Boller, T. (1999) Plants have a sensitive perception system for the most conserved domain of bacterial flagellin. *Plant J.* **18**, 265–276.
- Gomez-Gomez, L., Felix, G. and Boller, T. (1999) A single locus determines sensitivity to bacterial flagellin in *Arabidopsis thaliana*. *Plant J.* **18**, 277–284.
- Hammoudi, V., Fokkens, L., Beerens, B., Vlachakis, G., Chatterjee, S., Arroyo-Mateos, M., Wackers, P.F.K., Jonker, M.J. and van den Burg, H.A. (2018) The *Arabidopsis* SUMO E3 ligase SIZ1 mediates the temperature dependent trade-off between plant immunity and growth. *PLoS Genet.* **14**, e1007157.
- He, P., Shan, L., Lin, N.-C., Martin, G.B., Kemmerling, B., Nurnberger, T. and Sheen, J. (2006) Specific bacterial suppressors of MAMP signaling upstream of MAPKKK in *Arabidopsis* innate immunity. *Cell*, **125**, 563–575.
- Henty-Ridilla, J.L., Li, J.J., Day, B. and Staiger, C.J. (2014) Actin depolymerizing FACTOR4 regulates actin dynamics during innate immune signaling in *Arabidopsis*. *Plant Cell*, **26**, 340–352.
- Hruz, T., Laule, O., Szabo, G., Wessendorp, F., Bleuler, S., Oertle, L., Widmayer, P., Gruissem, W. and Zimmermann, P. (2008) Genevestigator V3: A reference expression database for the meta-analysis of transcriptomes. *Adv. Bioinformatics*, 2008, Article ID 420747.
- Hua, J. (2013) Modulation of plant immunity by light, circadian rhythm, and temperature. *Curr. Opin. Plant Biol.* **16**, 406–413.
- Hunter, L.J.R., Westwood, J.H., Heath, G., Macaulay, K., Smith, A.G., MacFarlane, S.A., Palukaitis, P. and Carr, J.P. (2013) Regulation of RNA-dependent RNA polymerase 1 and isochorismate synthase gene expression in *Arabidopsis*. *PLoS ONE*, **8**, 1–10.
- Huot, B., Castroverde, C.D.M., Velasquez, A.C., Hubbard, E., Pulman, J.A., Yao, J., Childs, K.L., Tsuda, K., Montgomery, B.L. and He, S.Y. (2017) Dual impact of elevated temperature on plant defence and bacterial virulence in *Arabidopsis*. *Nat. Commun.* **8**, 1808.
- Ichimura, K., Casais, C., Peck, S.C., Shinozaki, K. and Shirasu, K. (2006) MEKK1 is required for MPK4 activation and regulates tissue-specific and temperature-dependent cell death in *Arabidopsis*. *J. Biol. Chem.* **281**, 36969–36976.
- Janda, M. and Ruelland, E. (2015) Magical mystery tour: Salicylic acid signalling. *Environ. Exp. Bot.* **114**, 117–128.
- Jones, J.D.G. and Dangl, J.L. (2006) The plant immune system. *Nature*, **444**, 323–329.
- Junková, P., Daněk, M., Kocourková, D., Brouzdová, J., Kroumanová, K., Zelazny, E., Janda, M., Hynek, R., Martinec, J. and Valentová, O. (2018) Mapping of plasma membrane proteins interacting with *Arabidopsis thaliana* Flotillin 2. *Front. Plant Sci.* **9**, 991.
- Kunze, G., Zipfel, C., Robatzek, S., Niehaus, K., Boller, T. and Felix, G. (2004) The N terminus of bacterial elongation factor Tu elicits innate immunity in *Arabidopsis* plants. *Plant Cell*, **16**, 3496–3507.
- Makandar, R., Nalam, V.J., Chowdhury, Z., Sarowar, S., Klossner, G., Lee, H., Burdan, D., Trick, H.N., Gobbato, E., Parker, J.E. and Shah, J. (2015) The combined action of enhanced disease susceptibility1, phytoalexin deficient4, and senescence-associated101 promotes salicylic acid-mediated defenses to limit *Fusarium graminearum* infection in *Arabidopsis thaliana*. *Mol. Plant-Microbe Interact.* **28**, 943–953.
- Menna, A., Nguyen, D., Guttman, D.S. and Desveaux, D. (2015) Elevated temperature differentially influences effector-triggered immunity outputs in *Arabidopsis*. *Front. Plant Sci.* **6**, 995.
- Muthamilarasan, M. and Prasad, M. (2013) Plant innate immunity: An updated insight into defense mechanism. *J. Biosci.* **38**, 433–449.
- Pandey, S.P. and Somssich, I.E. (2009) The role of WRKY transcription factors in plant immunity. *Plant Physiol.* **150**, 1648–1655.
- Prerostova, S., Kramna, B., Dobrev, P.I., Gaudinova, A., Marsik, P., Fiala, R., Knirsch, V., Vanek, T., Kuresova, G. and Vankova, R. (2018) Organ-specific hormonal cross-talk in phosphate deficiency. *Environ. Exp. Bot.* **153**, 198–208.
- Robatzek, S., Chinchilla, D. and Boller, T. (2006) Ligand-induced endocytosis of the pattern recognition receptor FLS2 in *Arabidopsis*. *Genes Dev.* **20**, 537–542.
- Smith, J.M. and Heese, A. (2014) Rapid bioassay to measure early reactive oxygen species production in *Arabidopsis* leave tissue in response to living *Pseudomonas syringae*. *Plant Methods*, **10**, 6.
- Swain, S., Singh, N. and Nandi, A.K. (2015) Identification of plant defence regulators through transcriptional profiling of *Arabidopsis thaliana* cdd1 mutant. *J. Biosci.* **40**, 137–146.
- Trda, L., Boutrot, F., Claverie, J., Brule, D., Dorey, S. and Poinsot, B. (2015) Perception of pathogenic or beneficial bacteria and their evasion of host immunity: pattern recognition receptors in the frontline. *Front. Plant Sci.* **6**, 219.
- Tsuda, K., Sato, M., Glazebrook, J., Cohen, J.D. and Katajiri, F. (2008) Interplay between MAMP-triggered and SA-mediated defense responses. *Plant J.* **53**, 763–775.
- Velásquez, A.C., Castroverde, C.D.M. and He, S.Y. (2018) Plant-Pathogen Warfare under Changing Climate Conditions. *Curr. Biol.* **28**, R619–R634.
- Volkov, R.A., Panchuk, I.I., Mullineaux, P.M. and Schoffl, F. (2006) Heat stress-induced H₂O₂ is required for effective expression of heat shock genes in *Arabidopsis*. *Plant Mol. Biol.* **61**, 733–746.
- Wang, Y., Bao, Z.L., Zhu, Y. and Hua, J. (2009) Analysis of temperature modulation of plant defense against biotrophic microbes. *Mol. Plant-Microbe Interact.* **22**, 498–506.
- Wang, L., Guo, Y., Jia, L., Chu, H., Zhou, S., Chen, K., Wu, D. and Zhao, L. (2014) Hydrogen peroxide acts upstream of nitric oxide in the heat shock pathway in *Arabidopsis* seedlings. *Plant Physiol.* **164**, 2184–2196.
- Wildermuth, M.C., Dewdney, J., Wu, G. and Ausubel, F.M. (2001) Isochorismate synthase is required to synthesize salicylic acid for plant defense. *Nature*, **414**, 562–565.
- Xin, X.-F., Kvittko, B. and He, S.Y. (2018) *Pseudomonas syringae*: what it takes to be a pathogen. *Nat. Rev. Microbiol.* **16**, 316–328.
- Yang, S.H. and Hua, J. (2004) A haplotype-specific Resistance gene regulated by BONZAI1 mediates temperature-dependent growth control in *Arabidopsis*. *Plant Cell*, **16**, 1060–1071.
- Yeh, Y.-H., Chang, Y.-H., Huang, P.-Y., Huang, J.-B. and Zimmerli, L. (2015) Enhanced *Arabidopsis* pattern-triggered immunity by overexpression of cysteine-rich receptor-like kinases. *Front. Plant Sci.* **6**, 322.
- Yi, S.Y., Shirasu, K., Moon, J.S., Lee, S.G. and Kwon, S.Y. (2014) The Activated SA and JA signaling pathways have an influence on flg22-triggered oxidative burst and callose deposition. *PLoS ONE*, **9**, e88951.
- Zhang, Y.L., Goritschnig, S., Dong, X.N. and Li, X. (2003) A gain-of-function mutation in a plant disease resistance gene leads to constitutive activation of downstream signal transduction pathways in suppressor of npr1-1, constitutive 1. *Plant Cell*, **15**, 2636–2646.
- Zhang, J., Shao, F., Cui, H., Chen, L.J., Li, H.T., Zou, Y., Long, C.Z., Lan, L.F., Chai, J.J., Chen, S., Tang, X.Y. and Zhou, J.M. (2007) A *Pseudomonas syringae* effector inactivates MAPKs to suppress PAMP-induced immunity in plants. *Cell Host & Microbe*, **1**, 175–185.
- Zhu, Y., Qian, W.Q. and Hua, J. (2010) Temperature modulates plant defense responses through NB-LRR proteins. *PLoS Pathog.* **6**, e1000844.
- Zipfel, C., Robatzek, S., Navarro, L., Oakeley, E.J., Jones, J.D.G., Felix, G. and Boller, T. (2004) Bacterial disease resistance in *Arabidopsis* through flagellin perception. *Nature*, **428**, 764–767.

SUPPORTING INFORMATION

Additional supporting information may be found in the online version of this article at the publisher's web site:

Fig. S1 Oxidative burst triggered by the combination of HS and 100 nM flg22. The ROS production was measured by luminol-dependent chemiluminescence counting in leaf discs from 4-week-old *A. thaliana*. ROS production (represented by the peak luminescence) was measured after the addition of 100 nM flg22. The discs were pre-treated with HS (90 min and 120 min at 37 °C, 60; 120 min and 360 min at 32 °C; and 60 min, 120 min and 360 min at 28 °C) or kept in control conditions (0 h). The data represent the means + SE; $n = 8$ leaf discs in one biological experiment. The experiment was repeated two times independently with similar results. Asterisks indicate that the mean value is significantly different from the control conditions without HS (two-tailed Student's *t*-test, $n = 8$, * $P < 0.05$, *** $P < 0.001$). HS, heat stress; ROS, reactive oxygen species; SE, standard error.

Fig. S2 Oxidative burst triggered by the combination of HS and 100 nM elf18. The ROS production was measured using luminol-dependent chemiluminescence counting in leaf discs from 4-week-old *A. thaliana*. ROS production (represented by the peak luminescence) was measured after the addition of 100 nM elf18. The discs were pre-treated with HS (45 min at 42 °C or 120 min at 37 °C) or kept in control conditions. The production of ROS was measurement immediately after HS (0 h), or the discs were returned to the control conditions for 1 h or 2 h. The data represent the means + SE; $n = 8$ leaf discs in one biological experiment. The experiment was repeated twice independently with similar results. Asterisks indicate that the mean value is significantly different from the control conditions without HS (two-tailed Student's *t*-test, $n = 8$, ** $P < 0.01$, *** $P < 0.001$). HS, heat stress; ROS, reactive oxygen species, SE, standard error.

Fig. S3 The level of FLOT2 at the PM after HS. Western blot analysis of the PM was performed. The PM was purified from leaf of 4-week-old *A. thaliana* plants harbouring p35S::FLOT2:GFP. Amount of protein was 2.7 µg per lane. These plants were treated with either HS (42 °C for 1 h) or kept in control conditions. Immunoblotting analysis of FLOT2 with GFP tag was detected using anti-GFP antibody. Loading controls of proteins on membrane were visualized using Novex reversible membrane protein stain. HS, heat stress; FLOT2, flotillin 2; GFP, green fluorescent protein; PM, plasma membrane.

Fig. S4 *In silico* analysis of the transcription of genes involved in plant immunity and HS. Transcription pattern of plant immunity response genes in *A. thaliana*. Diagrams show that selected genes responded differently to treatment by flg22 and HS. Experimental data were performed using Genevestigator (<http://www.genevestigator.com>). For list of genes see Table S1. HS, heat stress.

Fig. S5 Callose deposition triggered by the combination of HS and flg22. Callose was stained with aniline blue and observed using fluorescent microscopy. The graph displays the amount of callose spots per 1 disc from 4-week old *A. thaliana* plants treated with flg22 (100 nM, grey box) or without flg22 (black box) and with HS, A) 1 h at 42 °C and B) 2 h at 37 °C; 24 h at 37 °C. Treatment with flg22 took 24 h, and HS was applied either 1 h before the addition of flg22 (in the case of 1 h at 42 °C or 2 h at 37 °C treatment) or simultaneously with the flg22 treatment (in the case of 24 h at 37 °C). The data represent the means + SD; $n = 30$ leaf discs. One biological experiment was comprised of ten leaf discs. Values with different letters differed significantly at $P < 0.05$ based on a one-way analysis of variance (ANOVA) with a post-hoc Tukey HSD test. HS, heat stress, SD, standard deviation.

Fig. S6 Oxidative burst triggered by flg22 after temporary HS. Four-week-old *A. thaliana* plants were exposed to 42 °C for 1 h and 37 °C for 2 h. After HS the plants were put back to the control conditions for 24 h. After that the leaf discs were cut and returned to 22 °C for 18 h. ROS production (represented by the peak luminescence) was measured after the addition of 100 nM flg22. The data represent means + SE; $n = 12$ discs. The experiment was repeated three times independently with similar results. The asterisks represent statistically significant changes between the heat and control conditions (* $P < 0.05$; two-tailed Student's *t*-test). HS, heat stress; ROS, reactive oxygen species, SE, standard error.

Fig. S7 The phenotype of *A. thaliana* after heat stress (HS). Four-week-old *A. thaliana* plants were kept at 42 °C for 1 h and put back to the control conditions; 6 days after HS the pictures were taken.

Table S1 The phenotype of *A. thaliana* after heat stress (HS). Four-week-old *A. thaliana* plants were kept at 42 °C for 1 h and put back to the control conditions; 6 days after HS the pictures were taken.

Table S2 Ion leakage 24 h after heat stress (HS) measured with a conductivity metre.

Table S3 Sequence of specific primers.

Methods S1 Experimental procedures.



Dual Mode of the Saponin Aescin in Plant Protection: Antifungal Agent and Plant Defense Elicitor

Lucie Trdá^{1*}, Martin Janda^{1,2,3}, Denisa Macková^{1,2}, Romana Pospíchalová¹, Petre I. Dobrev⁴, Lenka Burketová¹ and Pavel Matušinsky^{5,6}

¹ Laboratory of Pathological Plant Physiology, Institute of Experimental Botany of The Czech Academy of Sciences, Prague, Czechia, ² Laboratory of Plant Biochemistry, Department of Biochemistry and Microbiology, University of Chemistry and Technology Prague, Prague, Czechia, ³ Department Genetics, Faculty of Biology, Biocenter, Ludwig-Maximilian-University of Munich (LMU), Martinsried, Germany, ⁴ Laboratory of Hormonal Regulations in Plants, Institute of Experimental Botany of The Czech Academy of Sciences, Prague, Czechia, ⁵ Department of Plant Pathology, Agrotest Fyto, Ltd, Kroměříž, Czechia, ⁶ Department of Botany, Faculty of Science, Palacký University in Olomouc, Olomouc, Czechia

OPEN ACCESS

Edited by:

Ivan Baccelli,
Istituto per la Protezione sostenibile
delle Piante,
Sede Secondaria Firenze,
Italy

Reviewed by:

Eugenio Llorens,
Tel Aviv University, Israel
Hidenori Matsui,
Okayama University, Japan

***Correspondence:**

Lucie Trdá
lucie.trda@gmail.com;
trdal@ueb.cas.cz

Specialty section:

This article was submitted to
Plant Microbe Interactions,
a section of the journal
Frontiers in Plant Science

Received: 16 August 2019

Accepted: 17 October 2019

Published: 28 November 2019

Citation:

Trdá L, Janda M, Macková D,
Pospíchalová R, Dobrev PI,
Burketová L and Matušinsky P (2019)
Dual Mode of the Saponin Aescin in
Plant Protection: Antifungal Agent
and Plant Defense Elicitor.
Front. Plant Sci. 10:1448.
doi: 10.3389/fpls.2019.01448

Being natural plant antimicrobials, saponins have potential for use as biopesticides. Nevertheless, their activity in plant-pathogen interaction is poorly understood. We performed a comparative study of saponins' antifungal activities on important crop pathogens based on their effective dose (EC_{50}) values. Among those saponins tested, aescin showed itself to be the strongest antifungal agent. The antifungal effect of aescin could be reversed by ergosterol, thus suggesting that aescin interferes with fungal sterols. We tested the effect of aescin on plant-pathogen interaction in two different pathosystems: *Brassica napus* versus (fungus) *Leptosphaeria maculans* and *Arabidopsis thaliana* versus (bacterium) *Pseudomonas syringae* pv *tomato* DC3000 (*Pst* DC3000). We analyzed resistance assays, defense gene transcription, phytohormonal production, and reactive oxygen species production. Aescin activated *B. napus* defense through induction of the salicylic acid pathway and oxidative burst. This defense response led finally to highly efficient plant protection against *L. maculans* that was comparable to the effect of fungicides. Aescin also inhibited colonization of *A. thaliana* by *Pst* DC3000, the effect being based on active elicitation of salicylic acid (SA)-dependent immune mechanisms and without any direct antibacterial effect detected. Therefore, this study brings the first report on the ability of saponins to trigger plant immune responses. Taken together, aescin in addition to its antifungal properties activates plant immunity in two different plant species and provides SA-dependent resistance against both fungal and bacterial pathogens.

Keywords: *Brassica napus*, *Leptosphaeria maculans*, salicylic acid, fungicide, *Pseudomonas syringae*, *Arabidopsis thaliana*, EC_{50}

INTRODUCTION

Crop production is hampered by numerous plant diseases caused by diverse pathogenic microorganisms, such as fungi, bacteria or pests, affecting yield, harvest quality and safety. Although pesticides are currently employed to control crop pathogens and pests, growing problems of fungal resistance to fungicides appear to pose a serious future threat to agriculture (Fisher et al., 2018).

Moreover, alternatives to fungicides are needed that are less harmful to health and the environment. These might include more intensive employment of biological control, greater crop diversity (Zhu et al., 2000), or developing safer compounds with new modes of action (Burketová et al., 2015). Higher plants could constitute a great source of such compounds. Most plants produce a wide variety of antimicrobial secondary metabolites, including alkaloids, flavonoids, terpenes, organic acids, essential oils, and saponins that are involved in plant defense responses essential for plant protection against microbial or pest attack (Osbourne, 1996; Field et al., 2006; da Cruz Cabral et al., 2013; Matušinský et al., 2015).

Saponins occur in a wide range of plant species (Price et al., 1987; Moses et al., 2014). They comprise a structurally diverse family of triterpenoids, steroids or steroid-like glycoalkaloids (Podolak et al., 2010; Moses et al., 2014). Saponins exhibit amphiphilic properties that are due to the linkage of a lipophilic triterpene derivative (sapogenin) to one or more hydrophilic glycoside moieties. Historically, plant extracts from *Saponaria officinalis* have been used for their soap properties (Hostettmann and Marston, 1995). Saponins have a broad spectrum of activities in living organisms. They are generally antimicrobial against bacteria and fungi invading plants (Gruiz, 1996; Zablotowicz et al., 1996; Papadopoulou et al., 1999; Barile et al., 2007; Hoagland, 2009; Moses et al., 2014), but they were also effectively applied against microbes associated with animals (Yang et al., 2006; Saleem et al., 2010). Furthermore, saponins exert insecticidal (Nielsen et al., 2010; Singh and Kaur, 2018), antiviral (Zhao et al., 2008), and molluscicidal (Huang et al., 2003) activities, as well as allelopathic activity towards other plant species (Waller et al., 1993).

Saponins are mainly considered to comprise a part of plants' antimicrobial defense system. The underlying mechanisms of their activity are understood to be based on their ability to form complexes with sterols present in the membrane of microorganisms and consequently to cause membrane perturbation (Steel and Drysdale, 1988; Morrissey and Osbourne, 1999; Augustin et al., 2011; Sreij et al., 2019). The antifungal activity of saponins has been known for decades (Turner, 1960; Wolters, 1966; Gruiz, 1996) and their activity against fungal plant pathogens of crops has been reported previously. For example, minutaside saponins and sapogenins, alliogenin, and neoalligenin, isolated from the bulbs of *Allium minutiflorum* showed antimicrobial activity against various soil-borne and air-borne fungal pathogens (Barile et al., 2007). Saponin alliospiroside extracted from *Allium cepa* protected strawberry plants against *Colletotrichum gloeosporioides*, thus indicating a potential to control anthracnose of the plant (Teshima et al., 2013). To date, however, only limited work has been reported toward quantifying antifungal activity against phytopathogenic fungi by establishing EC₅₀ values (Saniewska et al., 2006; Porsche et al., 2018), and parallel comparisons with fungicides are often lacking. Moreover, effects on plants have been tested only by several studies (Hoagland et al., 1996; Hoagland, 2009). The goal of the present study was to investigate the potential of plant saponins as an alternative to fungicide treatment on crops.

We focus here mainly on the pathosystem of the crop *Brassica napus* (oilseed rape) and its devastating fungal hemibiotrophic

pathogen *Leptosphaeria maculans*, an infectious agent of phoma stem canker in oilseed rape. Plants face microbial infections through an efficient immune system. Plant immunity is very complex, consisting of pathogen recognition by plant immune receptors, signaling events, such as reactive oxygen species (ROS) production or MAP kinase activation, which ultimately triggers such defense mechanisms as changes in gene transcription resulting in expression of antimicrobial proteins, phytohormone production, or callose accumulation (Dodds and Rathjen, 2010; Cook et al., 2015; Trdá et al., 2015). Signaling pathways of phytohormones, such as salicylic acid (SA), jasmonic acid (JA) or ethylene (ET) cross-communicate allowing the plant to finely regulate its immune responses (Glazebrook, 2005; Pieterse et al., 2009). Immune responses have been previously studied in *B. napus* (Šašek et al., 2012a; Šašek et al., 2012b; Lloyd et al., 2014; Nováková et al., 2014).

Plant treatment with diverse agents, including microbe-derived compounds, phytohormones and synthetic chemicals, can induce resistance to subsequent pathogen invasion both locally and systemically (Walters et al., 2013; Burketová et al., 2015). Such resistance, called systemic acquired resistance (SAR), is among others mediated and dependent on SA. SAR was inhibited in *npr1* or *ics1* mutant plants (Kachroo and Robin, 2013). SAR-inducing chemicals are employed in pest control. Benzothiadiazole (BTH) is a functional analog of salicylic acid (SA) and a synthetic inducer of resistance to pathogens (Friedrich et al., 1996; Walters et al., 2013). BTH activates the *B. napus* immune system and provides protection against *L. maculans* (Šašek et al., 2012a). We have previously shown that the phytohormone salicylic acid (SA) plays an important role upon *L. maculans* infection (Šašek et al., 2012b). SA's role in plant immunity is well established (Tsuda et al., 2013; Janda and Ruelland, 2015). Although SA can be involved also in response to some necrotrophic pathogens (Nováková et al., 2014), it is mostly connected with defense against biotrophic microorganisms (Glazebrook, 2005). Substantial knowledge about SA's role in plant disease resistance comes from studies using a model pathosystem involving *A. thaliana* and the bacteria *Pseudomonas syringae* pv tomato DC3000 (*Pst* DC3000) (Katagiri et al., 2002; Xin and He, 2013; Xin et al., 2018; Leontovýčová et al., 2019).

Here, we present a comprehensive and comparative study of antifungal activities against crop pathogens of three terpenoid saponins in comparison to fungicides in commercial use. We chose aescin as the best antifungal agent and further characterized its activity in plants. We show that aescin triggers plant defense by activating the SA pathway and oxidative burst, ultimately leading to highly efficient resistance of *B. napus* against the fungus *L. maculans*. The level of protection it provides is comparable to that of fungicides. In *A. thaliana*, aescin induces SA-dependent resistance to *Pst* DC3000. Therefore, we provide here evidence of aescin's dual mode of action in plant defense.

MATERIAL AND METHODS

Fungal Isolates and Cultivation

Fungal isolates (with the exception of *L. maculans* JN2) were acquired in the territory of the Czech Republic from

symptomatic crop tissue in the field during the period 2002–2015. *Microdochium nivale* (Mn177 and Mn30) and *Oculimacula yallundae* (Oy19 and Oy221) were isolated from the stem bases of wheat in 2013 (Matušinský et al., 2017). *Zymoseptoria tritici* (Zt88 and Zt96) was collected from the leaves of winter wheat in 2013, and *Fusarium culmorum* strains (Fc107 and Fc289) were collected from wheat grains after harvest in 2010 and 2002, respectively (Matušinský et al., 2015). *Pyrenophora teres* (Ptt52 and Ptt17) and *Ramularia collo-cygni* (Rcc11 and Rcc41) were collected from leaves of spring barley in 2013. *L. maculans* (Lm170, Lm1-Lm4) isolates were collected from leaves of oilseed rape during 2014–2015.

Pyrenophora teres and *R. collo-cygni* conidia were transferred from the symptomatic leaves to Petri dishes with potato dextrose agar (PDA) media containing 50 µg·ml⁻¹ of ampicillin. Conidia were spread over the surface of media and cultivated for 24–96 h at 18°C. Single-spore microcolonies were transferred into new Petri dishes. In the case of *L. maculans*, a single pycnidium from a symptomatic leaf was transferred to a droplet of sterile water on a glass microscope slide. The pycnidium was crushed by a cover glass and a part of the conidia was spread using a sterile needle over a solid PDA medium. After 3 days at 18°C in darkness, single microcolonies were transferred to new PDA plates. The *L. maculans* isolate JN2, also referred to as v23.1.2 (Balesdent et al., 2001; Šašek et al., 2012b), was used for most of the assays. Conidia of isolates JN2 and JN2-sGFP (JN2 transformed using a pCAMBgfp construct (Šašek et al., 2012a) were obtained from sporulating mycelium 10 days old kept under a 14h/10h light/dark regime (150 µE·m⁻²·s⁻¹, 22°C, 70% relative humidity) in a cultivation chamber as described by Šašek et al. (2012b). Conidia were stored in concentration 10⁸ conidia·ml⁻¹ at -20°C for up to 6 months.

Antifungal and Antibacterial Assays

The radial growth of fungal mycelium was analyzed on PDA plates using the agar dilution method. Mycelial discs, 2 mm in diameter, were cut from the margins of colonies 5 days old and transferred to medium supplemented with streptomycin sulfate (50 µg·ml⁻¹) and saponins (0, 10, 25, 50, and 100 µg·ml⁻¹). After incubation at 18°C in darkness for 3 days in cases of rapidly growing fungi (*F. culmorum*, *L. maculans*, *M. nivale*, and *P. teres*) and 14 days in case of slowly growing fungi (*O. yallundae*, *R. collo-cygni*, and *Z. tritici*), the colony diameters were measured and compared to control plates lacking a saponin. Each isolate was analyzed in four technical replicates (four mycelial discs per plate) and in three independent biological experiments.

The conidial growth of *L. maculans* JN2-GFP isolate was analyzed in Gamborg B5 medium (Duchefa) supplemented with 0.3% (w/v) sucrose and 10 mM MES buffer (pH 6.8) at the final concentration of 2500 conidia per well of black 96-well plate (Nunc®). Aescin was used in the concentration range 0–100 µg·ml⁻¹. Plates were incubated in darkness at 26°C for 4 days. Fluorescence was measured in eight wells for each treatment using a Tecan F200 fluorescence reader (Tecan, Männedorf, Switzerland) with 485/20 nm excitation filter and 535/25 nm emission filter. For both assays, the final concentration of EtOH

in all treatments was 1% (v/v). Effective dose (EC₅₀) values were calculated by probit analysis (Finney, 1971) using Biostat software (AnalystSoft Inc., Walnut, CA, USA). For microscopic analysis, the content of each well was transferred to a microscopic slide and observed under a Leica DM 5000 B fluorescence microscope (Leica, Germany).

To monitor antibacterial activity of aescin, a fresh bacterial suspension (OD₆₀₀ of 0.005) in liquid LB medium was prepared from *Pst* DC3000 culture grown overnight on LB agar plates. Aescin (10 µg·ml⁻¹) or EtOH (0.1%) was added to this suspension and OD₆₀₀ was measured after 24 h, with three independent samples being used for each treatment.

Fungal Treatment for Gene Expression

For gene expression, 10⁷ conidia of JN2-GFP were grown in 100 ml of Gamborg B5 medium (Duchefa, G0210, Haarlem, The Netherlands) supplemented with 3% (w/v) sucrose and 10 mM MES (pH 6.8) in Erlenmeyer flasks. Cultures were kept at 26°C in darkness and at constant shaking of 130 rpm in an orbital shaker (JeioTech, Seoul, Korea). The culture at day 7 was treated in sterile conditions with aescin, fungicide, or control (EtOH). The concentration of EtOH solvent was identical in each treatment. Samples were collected after 24 hours of treatment and processed as described for plant samples.

Plant Cultivation and Treatment

Brassica napus plants of cultivar (cv.) Columbus were grown in perlite nourished with Steiner's nutrient solution (Steiner, 1984) under a 14 h/10 h light/dark regime (25°C and 150 µE·m⁻²·s⁻¹/22°C) and 30–50% relative humidity in a cultivation room. In all assays, chemical treatment was applied to 10 days old plants. Treatment was infiltrated into the abaxial side of cotyledons using a 1 ml plastic needless syringe. At least six plants were used for each sample.

Arabidopsis thaliana Col-0 and NahG transgenic plants (Delaney et al., 1994) were grown in soil. Surface-sterilized seeds were sown in Jiffy 7 peat pellets and the plants cultivated under a short-day photoperiod (10 h/14 h light/dark regime) at 100–130 µE·m⁻²·s⁻¹, 22°C and 70% relative humidity. They were watered with fertilizer-free distilled water as necessary. Plants 4 weeks old were used for all assays. Treatment was applied to three fully developed leaves from one plant, using a 1 ml needless syringe. At least six plants were used for each sample.

Except from concentration dependent assays, aescin was used at 25 µg·ml⁻¹ and 10 µg·ml⁻¹ concentrations for *B. napus* and *A. thaliana*, respectively. Treatment at these concentrations caused no evident leaf chlorosis symptoms. As a control treatment, EtOH at a corresponding concentration was used.

Plant Resistance Assays

For *B. napus*-*L. maculans* resistance assays, cotyledons were pre-treated with diverse treatments 4 days prior to infection. Upon infection, the pre-treated cotyledons of *B. napus* plants 14 days old were infiltrated by an aqueous conidial suspension of *L. maculans* JN2-GFP (10⁵ conidia·ml⁻¹) as described by Šašek et al.

(2012a) using a 1 ml needleless syringe. Prior to inoculation true leaves were removed from plants to avoid cotyledon senescence. At least 12 plants were used per condition. The cotyledons were assessed 11 days after inoculation. The cotyledon areas and lesion areas therein were measured by image analysis using APS Assess 2.0 software (American Phytopathological Society, St. Paul, MN, USA). The relative lesion area was then calculated as the ratio of lesion area to whole leaf area. The hyphal colonization of cotyledons was assessed under a Leica DM5000 B fluorescence microscope (Leica, Germany).

For *A. thaliana* – *P. syringae* pv. tomato DC3000 resistance assays, leaves were pre-treated with aescin 24 h prior to infection. The bacteria *Pst* DC3000 was cultivated overnight on lysogeny broth (LB) agar plates with rifampicin at 26°C, then resuspended in 10 mM MgCl₂ to an OD₆₀₀ of 0.005. The bacterial suspension was infiltrated into three fully developed pre-treated leaves from one plant, using a 1 ml needless syringe. After 3 days, cut leaf discs (one disc per leaf, 0.6 cm in diameter) were collected from infected tissue, with three leaves from a single plant representing one sample. To determine bacterial content in leaves at 0 dpi, samples were collected 1 h after bacterial infiltration. Tissue was homogenized in tubes with silica beads using a FastPrep-24 instrument (MP Biomedicals, Santa Ana, CA, USA). The resulting homogenate was serially diluted and transferred onto LB agar plates with rifampicin. Grown bacterial colonies were counted after 24 h of incubation at 26°C.

Reactive Oxygen Species Detection

Treated cotyledons were detached and infiltrated under vacuum with diaminobenzidine tetrahydrochloride (DAB; Šašek et al., 2012b) aqueous solution (10 mg·ml⁻¹, Sigma-Aldrich), with DAB being solubilized in dimethylformamide. Cotyledons were kept in humid conditions in darkness at room temperature until reddish-brown staining appeared. Chlorophyll was removed using 96% EtOH, after which cotyledons were rehydrated and scanned.

Analysis of Plant Hormones

Levels of plant hormones were determined 24 hours post treatment in *B. napus* cotyledons. In each sample, 150 mg of fresh material from plant tissue was pooled from eight different plants, as previously described (Dobrev and Kaminek, 2002). Briefly, samples were homogenized with extraction reagent methanol/H₂O/formic acid (15:4:1, v:v:v) supplemented with stable isotope-labeled internal standards, each at 10 pmol per sample. Clarified supernatants were subjected to solid-phase extraction using Oasis MCX cartridges (Waters Co., Milford, MA, USA), eluates were evaporated to dryness, and the generated solids were dissolved in 30 µL of 15% (v/v) acetonitrile in water. Quantification was done on an Ultimate 3000 high-performance liquid chromatograph (HPLC; Dionex, Bannockburn, IL, USA) coupled to a 3200 Q TRAP hybrid triple quadrupole/linear ion trap mass spectrometer (MS; Applied Biosystems, Foster City, CA, USA), as described by Djilianov et al. (2013). Metabolite levels were expressed in pmol·g⁻¹ fresh weight.

Gene Expression Analysis

Samples (both plant and fungi) were collected 24 hours post treatment. At least six plants were used for each sample for gene expression. Total RNA was isolated from 100 mg of frozen plant tissue or fungal mycelium using a Spectrum Plant Total RNA Kit (Sigma-Aldrich, St. Louis, MO, USA). Next, 1 µg of RNA was treated with a DNA-free Kit (Ambion, Austin, TX, USA) and reverse transcribe to cDNA with M-MLV RNase H Minus Point Mutant reverse transcriptase (Promega Corp., Fitchburg, WI, USA) and anchored oligo dT₂₁ primer (Metabion, Martinsried, Germany). Gene transcription was quantified by q-PCR using LightCycler 480 SYBR Green I Master kit and LightCycler 480 (Roche, Basel, Switzerland). The PCR conditions were: 95°C for 10 minutes, followed by 45 cycles of 95°C for 10 s, 55°C for 20 s, and 72°C for 20 s, followed by a melting curve analysis. Relative transcription was calculated with efficiency correction and normalization to the corresponding housekeeping gene for each organism. LmERG3 (Q8J207) and LmERG11 (Q8J1Y7) proteins were retrieved from the Uniprot database and primers were designed for the corresponding genes using PerlPrimer v1.1.21 (Marshall, 2004). Primers are listed in Supplementary Table 1.

Chemical Treatments

Saponins aescin (E1378), hederagenin (H3916), and soyasaponin I (S9951), and fungicides metconazole, fluconazole, boscalid, and fluopyram (all purchased from Sigma-Aldrich, St. Louis, MO, USA) were dissolved in 99.8% ethanol (EtOH) as 10 mg·ml⁻¹ stock solution. Tebuconazole, in the form of the commercially formulated product Horizon 250 EW (Bayer CropScience, Germany), was also prepared as 10 mg·ml⁻¹ stock solution in EtOH. Ergosterol (Sigma, St. Louis, MO, USA) was prepared as 5 mM stock solution in EtOH and used at the final concentration of 25 µg·ml⁻¹. Benothiadiazole (BTH) was used in the form of the commercially formulated product Bion 50 WG (Syngenta, Switzerland) and prepared directly into the working solutions. The commercial peptide flg22 (EZBiolab) was diluted in Milli-Q water and used at the final concentration of 1 µM. All stock solutions were stored at -20°C.

Statistical Analyses

If not stated otherwise, all experiments were repeated independently three times, with at least three independent samples (from independent biological material, cultivated under the same conditions). Using Statistica 12 software, statistical analyses were performed either by paired two-tailed Student's *t*-test or by analysis of variance in conjunction with Tukey's honestly significant difference multiple mean comparison *post hoc* test (*P* < 0.05).

RESULTS

Aescin Has the Highest Antifungal Activity Among Tested Saponins

Although saponins are well known to have antifungal activity (Gruiz, 1996; Moses et al., 2014), only very limited data is available

quantifying saponin antifungal activity by establishing EC₅₀ values. We screened antifungal activity of the triterpenoid plant saponins aescin (from *Aesculus hippocastanum*), soyasaponin (from *Glycine max*), and hederagenin (from *Hedera helix*) against important fungal pathogens (*O. yallundae*, *M. nivale*, *Z. tritici*, *P. teres*, *R. collo-cygni*, *F. culmorum*, and *L. maculans*). These fungi infect such crop plants as wheat, barley, or oilseed rape. Our fungal collection consists of various naturally occurring isolates for each pathogen. To calculate EC₅₀ values, we assessed the radial mycelial growth on solid media plates supplemented with saponins. All tested saponins displayed significant antifungal activity, with aescin's activity being the most efficient (Figure 1A). Differences in species sensitivity to saponins were observed (Figure 1A). As further analyzed for aescin, the activity on isolates varied among species but was mostly conserved within a given fungal species (Figure 1B). The fungi most sensitive to saponins were *M. nivale*, *P. teres*, and *L. maculans*, while *O. yallundae*, *R. collo-cygni*, *Z. tritici*, and *F. culmorum* showed only minor growth inhibition (Figures 1A, B; Table 1). Accordingly, while aescin EC₅₀ values for *P. teres*, *M. nivale*, and *L. maculans* isolates occurred in the range of 11–21 µg·ml⁻¹, 7–29 µg·ml⁻¹, and

25–33 µg·ml⁻¹, respectively, EC₅₀ values for more-resistant fungal isolates exceeded 100 µg·ml⁻¹ and could not be calculated precisely due to concentration limitations caused by saponin solubility (Table 1). It is noteworthy that fungal sensitivity (Figure 1B) did not correlate with hyphal thickness (Supplementary Figure 1A). Correlation between fungal growth rate and fungal sensitivity was observed, however, with the slowly growing isolates being the most resistant (Supplementary Figure 1B). In summary, all tested saponins inhibited growth of phytopathogenic fungi in a species-dependent manner, with the strongest growth inhibition provided by aescin.

Aescin Antifungal Activity Is Lower Than That of Commercial Fungicides

The biological activity of aescin was further studied on *L. maculans*, which is a destructive pathogen of *B. napus*. The antifungal activities (EC₅₀ values) of aescin and synthetic fungicides were first compared. Several fungicides of different classes were tested, including triazolic sterol inhibitor tebuconazole, commonly used for *B. napus* protection against phoma stem canker (Child

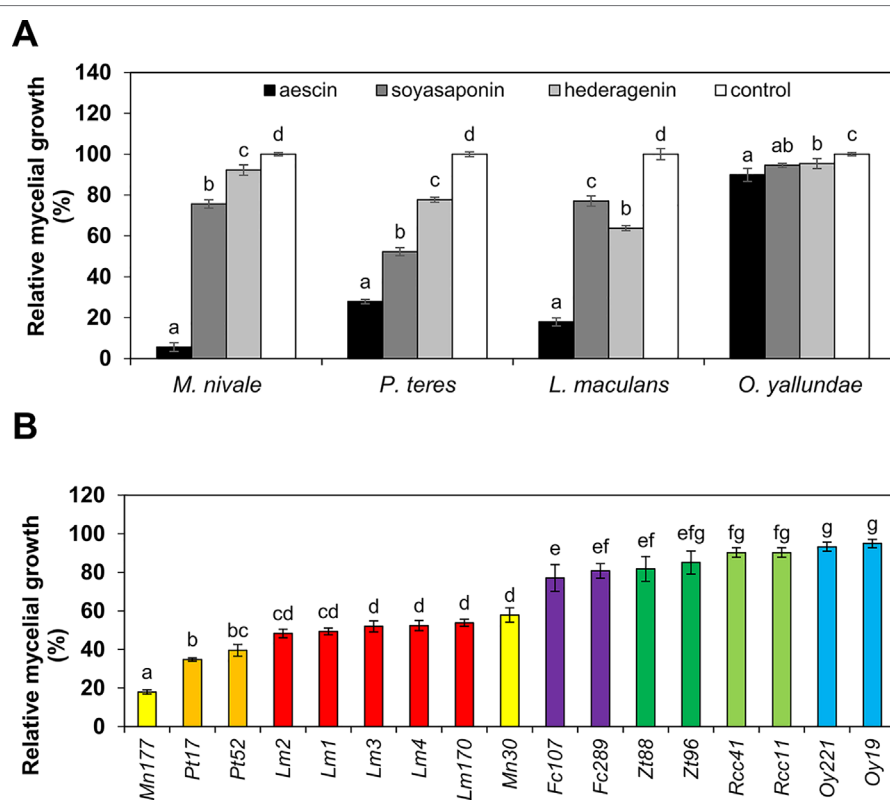


FIGURE 1 | Saponins inhibit mycelial growth of crop pathogens *in vitro* in a species-dependent manner. Relative growth of different fungal species assessed as percentage diameter of fungal colony cultivated on PDA medium supplemented with saponins. The control treatment (without saponins) was set as 100%. **(A)** Growth on aescin (black bars), soyasaponin (dark gray bars), and hederagenin (light gray bars) at 100 µg·ml⁻¹, or on a control (without saponin; white bars). The following fungal isolates were used: Mn177, Pt52, Lm1, and Oy19. **(B)** Growth on aescin at the 25 µg·ml⁻¹ rate compared to control-treated fungi. All data represent means ± SE from three independent experiments. Different letters above bars illustrate significant differences using ANOVA test in conjunction with Tukey's honestly significant difference multiple mean comparison post hoc test ($P < 0.05$). For (A), the statistical analyses were carried out separately within each fungal species (Fc, *Fusarium culmorum*; Lm, *Leptosphaeria maculans*; Mn, *Microdochium nivale*; Oy, *Oculimacula yallundae*; Pt, *Pyrenophora teres*; Rcc, *Ramularia collo-cygni*; Zt, *Zymoseptoria tritici*).

TABLE 1 | Effective dose (EC_{50}) values of saponins against pathogenic fungi.

Fungal species	Isolate	EC_{50} [$\mu\text{g}\cdot\text{ml}^{-1}$]		
		Aescin	Soyasaponin	Hederagenin
<i>Microdochium nivale</i>	Mn30	29.40 ± 6.01	na	na
	Mn177	6.74 ± 0.84	>100.00	>100.00
<i>Pyrenophora teres</i>	Pt17	11.40 ± 9.51	na	na
	Pt52	20.79 ± 5.14	97.61 ± 8.83	> 100.00
<i>Leptosphaeria maculans</i>	Lm170	31.71 ± 3.29	na	na
	Lm1	28.62 ± 10.03	>100.00	>100.00
	Lm2	25.21 ± 3.25	na	na
	Lm3	33.11 ± 6.49	na	na
	Lm4	25.52 ± 0.88	na	na
<i>Fusarium culmorum</i>	Fc107	>100.00	na	na
	Fc289	>100.00	na	na
<i>Zymoseptoria tritici</i>	Zt88	>100.00	na	na
	Zt96	>100.00	na	na
<i>Ramularia collo cygni</i>	Rcc11	>100.00	na	na
	Rcc41	>100.00	na	na
<i>Oculimacula yallundae</i>	Oy19	>100.00	>100.00	>100.00
	Oy221	>100.00	na	na

EC_{50} values [$\mu\text{g}\cdot\text{ml}^{-1}$] calculated by probit analysis for combinations of a given fungal pathogenic isolate and a given saponin, assessed as inhibition of mycelial radial growth on PDA medium with saponin. Data are expressed as means ± SE from three experiments. Cases of $EC_{50} > 100.00$ indicate that precise values above $100 \mu\text{g ml}^{-1}$ could not be calculated. na, not analyzed.

et al., 1993). For this purpose, fungal growth was measured as GFP fluorescence of germinating conidia of the *L. maculans* JN2 isolate expressing GFP (JN2-GFP) (Balesdent et al., 2001; Šašek et al., 2012a). In this setup, aescin was fully fungitoxic to the conidia at concentrations above $50 \mu\text{g}\cdot\text{ml}^{-1}$ (Figure 2A) and demonstrated EC_{50} of $28.79 \mu\text{g}\cdot\text{ml}^{-1}$ (Figures 2A, B) that was in agreement with EC_{50} obtained for the *L. maculans* field isolates (Table 1). EC_{50} values for the fungicides were mostly in a range from $0.018 \mu\text{g}\cdot\text{ml}^{-1}$ to $0.087 \mu\text{g}\cdot\text{ml}^{-1}$, with metconazole being the most efficient (Figure 2B). On the other hand, fluconazole, was the least efficient ($EC_{50} = 2.33 \mu\text{g}\cdot\text{ml}^{-1}$; Figure 2B). Overall, aescin inhibits conidial and mycelial growth of *L. maculans* *in vitro* and demonstrates antifungal activity 1 to 3 orders of magnitude lower than that of fungicides.

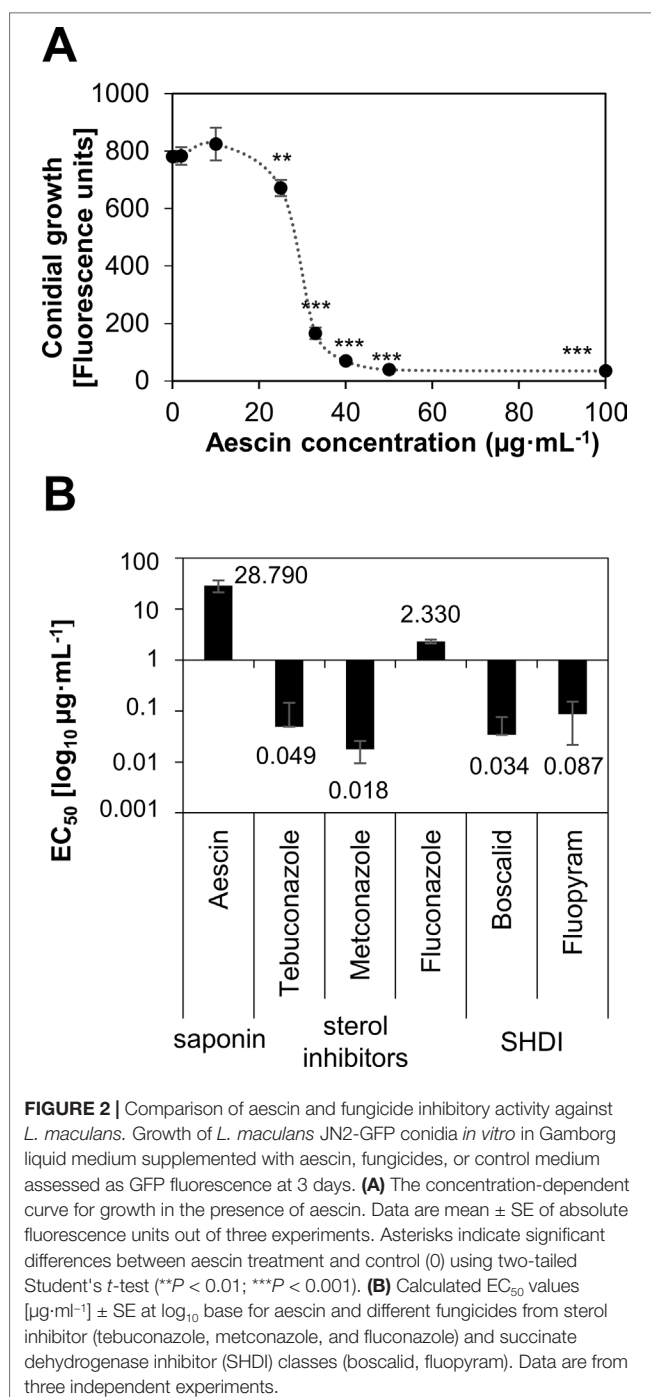
Antifungal Activity of Aescin Against *L. Maculans* Occurs Through Its Interaction With Sterols

Aescin's antimicrobial effect occurs through interference with membranes and interaction with sterols (Morrissey and Osbourn, 1999; Sreij et al., 2019). Therefore, we tested aescin's activity in the presence of ergosterol, a sterol naturally present in fungal membranes. Ergosterol markedly restored the growth of *L. maculans* JN2-GFP in the presence of aescin at all the inhibiting concentrations (Figure 3A), which was confirmed also by microscopic analysis of hyphae (Figure 3B) (Supplementary Figure 2). Growth inhibition caused by metconazole could not be reversed by the ergosterol supply (Figure 3C). Ergosterol itself did not significantly affect fungal growth (concentration 0 of Figures 3A, C). Inasmuch as triazole fungicides block biosynthesis of ergosterol (Sanati et al., 1997), transcription of *LmErg3* and *LmErg11* genes, identified as involved in ergosterol biosynthesis in *L. maculans* (Griffiths and Howlett, 2002), was

assessed following aescin treatment of the fungus. The effect of aescin or fungicides was observed in 7-day-old *L. maculans* culture 24 h post treatment. While metconazole induced transcription of *LmErg3* and *LmErg11* genes by 7 times and 27 times, respectively, in excess of the control, aescin did not significantly upregulate transcription of these genes (Figure 3D). The data show that aescin interfered with the fungal ergosterol but not directly with its biosynthesis.

Aescin Pretreatment Confers Resistance in *B. napus* Against *L. maculans*

Given the antifungal activity of aescin, we further investigated whether pretreatment with aescin could efficiently protect *B. napus* against *L. maculans*. Pretreatment of *B. napus* cotyledons by leaf infiltration with aescin at rates of $25 \mu\text{g}\cdot\text{ml}^{-1}$ and $10 \mu\text{g}\cdot\text{ml}^{-1}$ 3 days prior to inoculation with *L. maculans* JN2-GFP efficiently reduced the cotyledon area covered by necrotic lesions (Figures 4A, B). The effect was comparable to those provided both by the fungicide metconazole at rate $2 \mu\text{g}\cdot\text{ml}^{-1}$ and the plant defense inducer benzothiadiazole (BTH) at rate $30 \mu\text{M}$. BTH activates the *B. napus* immune system and provides protection against *L. maculans* (Šašek et al., 2012a). The protection provided by aescin was even more efficient than that induced by the fungicide tebuconazole at rate $2 \mu\text{g}\cdot\text{ml}^{-1}$. Aescin's protection was concentration dependent, and no significant effect was observed with aescin at the $2 \mu\text{g}\cdot\text{ml}^{-1}$ level. Microscopic analyses (Figure 4C) revealed only a few restricted GFP-fluorescent hyphal zones in aescin- and metconazole-pretreated cotyledons, while the control treatment displayed extensive hyphal network all over the infected cotyledon and corresponding to the localization of necroses. We also showed that foliar spray of aescin aqueous solution is protective (Supplementary Figure 3), although higher concentration may be required compared to when



infiltration is used. Taken together, our data demonstrate that aescin protects *B. napus* against *L. maculans* by inhibiting tissue colonization by fungal hyphae and necrosis formation. It is noteworthy that the treatment with aescin at concentration 25 $\mu\text{g}\cdot\text{mL}^{-1}$ decreased cotyledon growth to a similar extent as did 30 μM BTH (Supplementary Figure 4). At higher concentrations (above 50 $\mu\text{g}\cdot\text{mL}^{-1}$), aescin caused chlorosis and necroses on leaves (Supplementary Figure 4). Treatment with 10 $\mu\text{g}\cdot\text{mL}^{-1}$ of aescin caused no obvious effects on cotyledon fitness (Supplementary

Figure 4), however, and this concentration was still able to reduce *L. maculans* infection (Figure 4A).

Aescin Induces Defense Responses in *L. Maculans*, Governed by SA Pathway and Oxidative Burst

The fact that aescin can provide a higher level of plant protection than do fungicides having more potent antifungal activity suggested a possibility that aescin stimulates plant defense. Therefore, transcription of plant defense marker genes was determined in cotyledons 6 h and 24 h after treatment with aescin or BTH (Figure 5A). At both time points, aescin upregulated transcription of *BnPR1* and SA-specific transcription factor *BnWRKY70* genes previously characterized as being marker genes of activated SA pathway in *B. napus* (Šašek et al., 2012b). At 24 h, the level of induction was similar to that of BTH, but aescin and BTH induced defense genes with different kinetics. In contrast to BTH, aescin also upregulated transcription of the SA-biosynthetic gene for isochorismate synthase 1 (*BnICS1*). Given the strong induction of *BnICS1* transcription, aescin's capacity to stimulate SA production was tested and compared to that of flg22, a well-characterized microbe-associated molecular pattern (MAMP) activating SA pathway in *A. thaliana* (Tsuda et al., 2008; Lloyd et al., 2014). Aescin application at the 25 $\mu\text{g}\cdot\text{mL}^{-1}$ rate to cotyledons led to a massive increase in SA 24 h after treatment, with SA content reaching even higher levels than those seen following treatment with 1 μM flg22 (Figure 5B). Other tested phytohormone metabolites were altered not at all or only slightly by aescin (Figure 5C). Aescin caused mild decrease in the *cis*-OPDA metabolite, the JA precursor (Dave and Graham, 2012), and auxin forms. In summary, based on gene transcription analysis and phytohormone measurement, it was apparent that aescin treatment activated the SA pathway.

Further defense responses were analyzed in aescin-treated *B. napus* cotyledons. At 24 h following treatment aescin triggered accumulation of ROS compared to the control treatment, as was visualized by brown-reddish precipitates in DAB staining assay (Figure 5D). The accumulation was induced to a similar extent as was that for the flg22 treatment and was concentration dependent (Supplementary Figure 5). Accordingly, at 24 h post treatment, aescin induced transcription of respiratory burst oxidase homolog *RbohD* and *RbohF* genes coding NADPH oxidases responsible for ROS production in plants after exposure to MAMPs (Torres et al., 2005; Qi et al., 2017) (Figure 5E). The fungicides tebuconazole and metconazole did not elicit transcription of any defense genes, nor did they trigger oxidative burst in *B. napus* cotyledons (Supplementary Figures 6A, B).

Aescin-Induced SA-Dependent Resistance to Bacterial Pathogen in *A. thaliana*

To exclude that the phenomenon of aescin-activated immunity is specific to the *B. napus*-*L. maculans* system, the activity of aescin was investigated also in an *A. thaliana* model system challenged by a hemibiotrophic bacterial pathogen, *Pst* DC3000. After 24 h of treatment with aescin at the 10 $\mu\text{g}\cdot\text{mL}^{-1}$ level, there

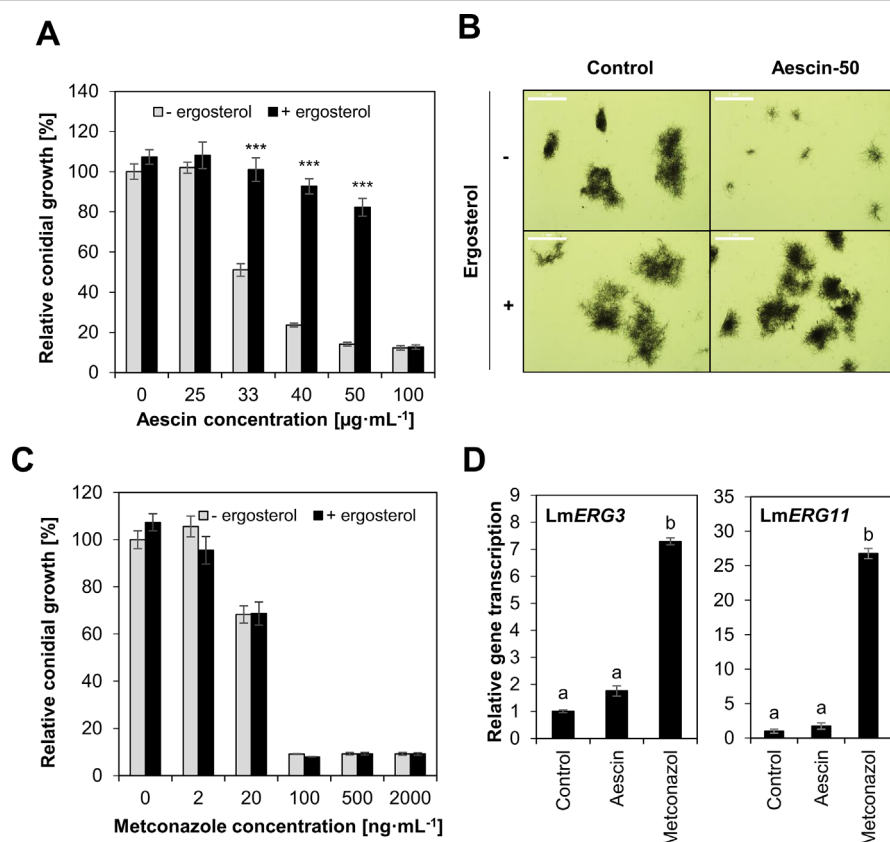


FIGURE 3 | Ergosterol reverts aescin-mediated growth inhibition of *L. maculans*. **(A–C)**, Growth of *L. maculans* JN2-GFP conidia *in vitro* in Gamborg liquid medium supplemented with aescin (**A**, **B**) or metconazole (**C**) in absence (gray bars) or presence (black bars) of ergosterol (25 $\mu\text{g}\cdot\text{mL}^{-1}$). **(A, C)** Data are expressed as relative fluorescence units at 4 days of growth compared to control (0) without ergosterol, set as 100%. Data are expressed as means \pm SE from three independent experiments. Asterisks indicate significant differences (** $P < 0.001$; two-tailed Student's *t*-test) between treatments with and without ergosterol for each concentration of aescin or metconazole. **(B)** Light microscopy of germinating hyphae at control and aescin at 50 $\mu\text{g}\cdot\text{mL}^{-1}$ rate at 5 days of growth in presence or absence of ergosterol (25 $\mu\text{g}\cdot\text{mL}^{-1}$). Scale bar corresponds to 1 mm. **(D)** Relative transcription of ergosterol biosynthetic genes *LmERG3* and *LmERG11* at mycelium 7 days old and treated with aescin (100 $\mu\text{g}\cdot\text{mL}^{-1}$) or metconazole (2 $\mu\text{g}\cdot\text{mL}^{-1}$) for 24 h. Gene transcription was analyzed by qPCR, normalized to *LmTubulin*, then compared to control treatment. Data represent mean \pm SE from one biological experiment (three biological replicates) representative of three. Different letters above bars illustrate significant differences using ANOVA test in conjunction with Tukey's honestly significant difference multiple mean comparison post hoc test ($P < 0.05$).

was upregulated transcription of *AtPR1* and *AtICS1* genes in *A. thaliana* leaves (**Figure 6A**). Aescin pretreatment for 24 h also led to induced resistance against bacterium *Pst* DC3000, observed as substantial decrease of both disease symptoms and bacterial titers in infected leaves (**Figure 6B**). For direct investigation of possible SA involvement in aescin-triggered resistance to *Pst* DC3000, we used NahG transgenic plants, in which low endogenous SA levels are maintained through the expression of SA-hydroxylase (Delaney et al., 1994). In NahG plants, the effect of aescin-induced resistance against *Pst* DC3000 was lost (**Figure 6B**).

Aescin did not impact the growth of *Pst* DC3000 cultivated *in vitro* (**Supplementary Figure 7A**). It also did not affect the bacterial titers in aescin-pretreated leaves sampled 1 h after infection with *Pst* DC3000 (**Supplementary Figure 7B**). In addition, co-inoculation of *A. thaliana* plants simultaneously with *Pst* DC3000 bacterium and aescin did not affect the bacterial colonization in the infected leaves (**Supplementary Figure 7C**).

These data suggest that the bacterial resistance provided by aescin in *A. thaliana* is not due to a direct antibacterial effect. Together, these data show increased resistance of *A. thaliana* against *Pst* DC3000 induced by aescin treatment, which possibly acts through activating SA-dependent immune pathways.

DISCUSSION

Currently, field crops are protected from fungal pathogens by such fungicide compounds as benzimidazoles, sterol biosynthesis inhibitors, strobilurins, or succinate dehydrogenase inhibitors. Because the occurrence of synthetic pesticide residues is progressively degrading the health of living organisms and the environment even as fungicide resistance is developing, there is a clear need to discover "greener" antifungal agents. Our study was focused on plant-derived saponins as hypothetical new plant protectants.

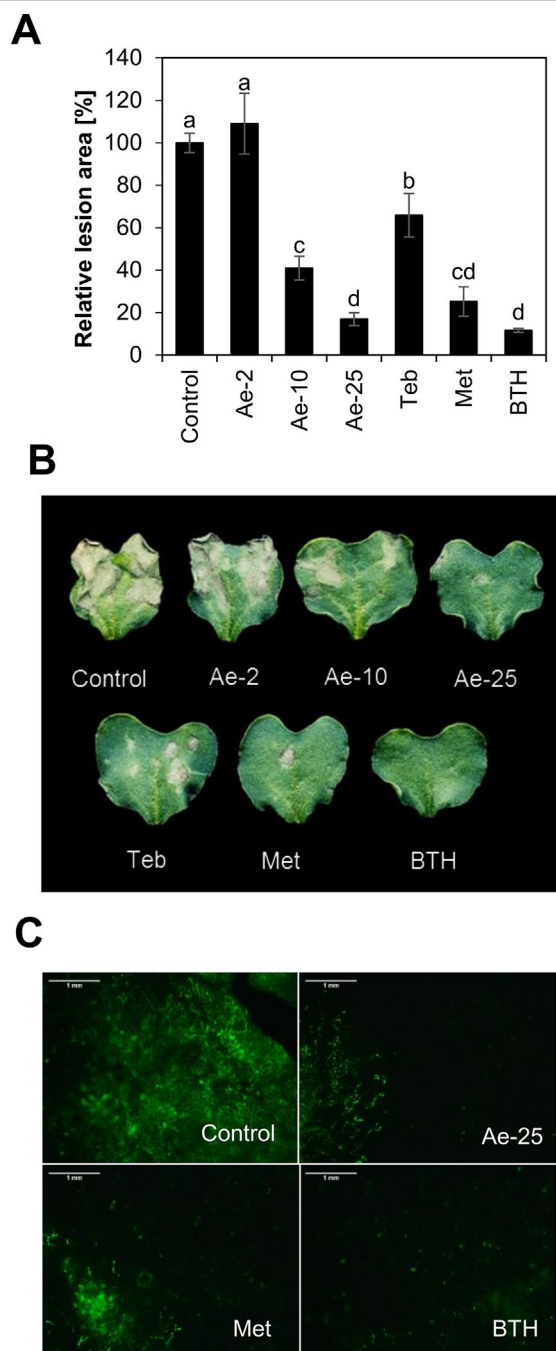


FIGURE 4 | Aescin pretreatment provides *B. napus* with efficient resistance against *L. maculans*. Cotyledons of *B. napus* were infiltrated by aqueous solutions of aescin (Ae; at 2, 10, and 25 $\mu\text{g}\cdot\text{ml}^{-1}$), tebuconazole, metconazole (Teb and Met; both at 2 $\mu\text{g}\cdot\text{ml}^{-1}$), BTH (30 μM), or a control 3 days prior to being infiltrated by conidial suspension of *L. maculans* JN2-GFP. The outcome was assessed at 12 days. **(A)** Quantification of the relative lesion area by image analysis is expressed as percentage. Control treatment was set as 100%. Data represent means \pm SE from five independent experiments. Different letters above bars illustrate significant differences using ANOVA test in conjunction with Tukey's honestly significant difference multiple mean comparison post hoc test ($P < 0.05$). **(B)** Panel with representative infected cotyledons. **(C)** Hyphal spread of JN2-GFP fungus in infected cotyledons. Scale bar corresponds to 1 mm.

Aescin: A Potent Antifungal Saponin

The effect of saponins on fungi has been widely studied (Gruiz, 1996; Barile et al., 2007; Hoagland, 2009; Saha et al., 2010; Teshima et al., 2013). Heretofore, however, there has been only few comprehensive studies of saponin activity against phytopathogens, including to determine EC₅₀ values and compare more deeply saponin efficiency with that of synthetic fungicides.

EC₅₀ values in the ranges 181–678 $\mu\text{g}\cdot\text{ml}^{-1}$ and 230–455 $\mu\text{g}\cdot\text{ml}^{-1}$ have been reported for the inhibitory activity of saponins of *Sapindus mukorossi* and *Diploknema butyracea*, respectively, on mycelial growth of phytopathogens *Rhizoctonia* sp. and *Sclerotinia* sp. (Saha et al., 2010). Minutosides extracted from *A. minutiflorum* have been shown to be highly inhibitory to spore germination of soil- and air-borne fungi (*Fusarium oxysporum*, *F. solani*, *Pythium ultimum*, *Rhizoctonia solani*, *Botrytis cinerea*, *Alternaria alternata*, *A. porri*, and *Trichoderma harzianum*) at 10–1000 $\mu\text{g}\cdot\text{ml}^{-1}$, depending upon the individual fungal species and saponin (Barile et al., 2007). The antifungal activity of aescin, a saponin from horse chestnut *Aesculus hippocastanum*, has been characterized only poorly. Previous studies have reported both antibacterial activity of β -aescin towards soil *Rhizobium* bacteria (Zablotowicz et al., 1996) and its antifungal activity against *Candida* sp. (Franiczek et al., 2015). However, knowledge as to aescin's activity against phytopathogens has not previously been presented. Here, we tested the antifungal effect of aescin on seven species of phytopathogenic fungi causing crop losses in cereals and rapeseed. The activity was also tested in comparison to that of soyasaponin, hederagenin, and synthetic fungicides.

We have shown here that aescin displayed strong inhibitory effect against fungal growth, significantly impeding mycelial growth in all tested fungal isolates (Figure 1A). Aescin was highly active against *M. nivale*, *P. teres*, and *L. maculans*, exhibiting EC₅₀ values below 50 $\mu\text{g}\cdot\text{ml}^{-1}$ (Table 1). Aescin also exhibited greater antifungal activity than did the other two saponins tested, soyasaponin and hederagenin (Figure 1A, Table 1). In light of these results and those of previous studies on other saponins, aescin emerges as a potent antifungal saponin. A parallel comparison of aescin's inhibitory activity with those of synthetic commercial fungicides was carried out on germinating *L. maculans* conidia. Aescin's EC₅₀ was from 1 to 3 orders of magnitude greater in comparison to that of fungicides (Figure 2). Co-treatment with ergosterol, which reverses the effect of aescin but not the effect of fungicides, showed aescin to have a different mode of action on membranes compared to that of fungicides (Figures 3A, C).

We observed aescin activity to be variable in different fungal species, while it was mostly conserved among isolates within a given species (Figure 1B). Compared to other fungi, *O. yallundae* isolates were the most resistant to aescin and the other tested saponins (Figure 1, Table 1). This general resistance of *O. yallundae* independent of saponin type (Figure 1A) may reflect its different fungal morphology and physiology. A correlation was observed between growth rate and fungal sensitivity, and *O. yallundae* is a slowly growing fungus (Supplementary Figure 1). Furthermore, saponin-resistant fungi may contain membranes with low sterol content (Arneson and Durbin,

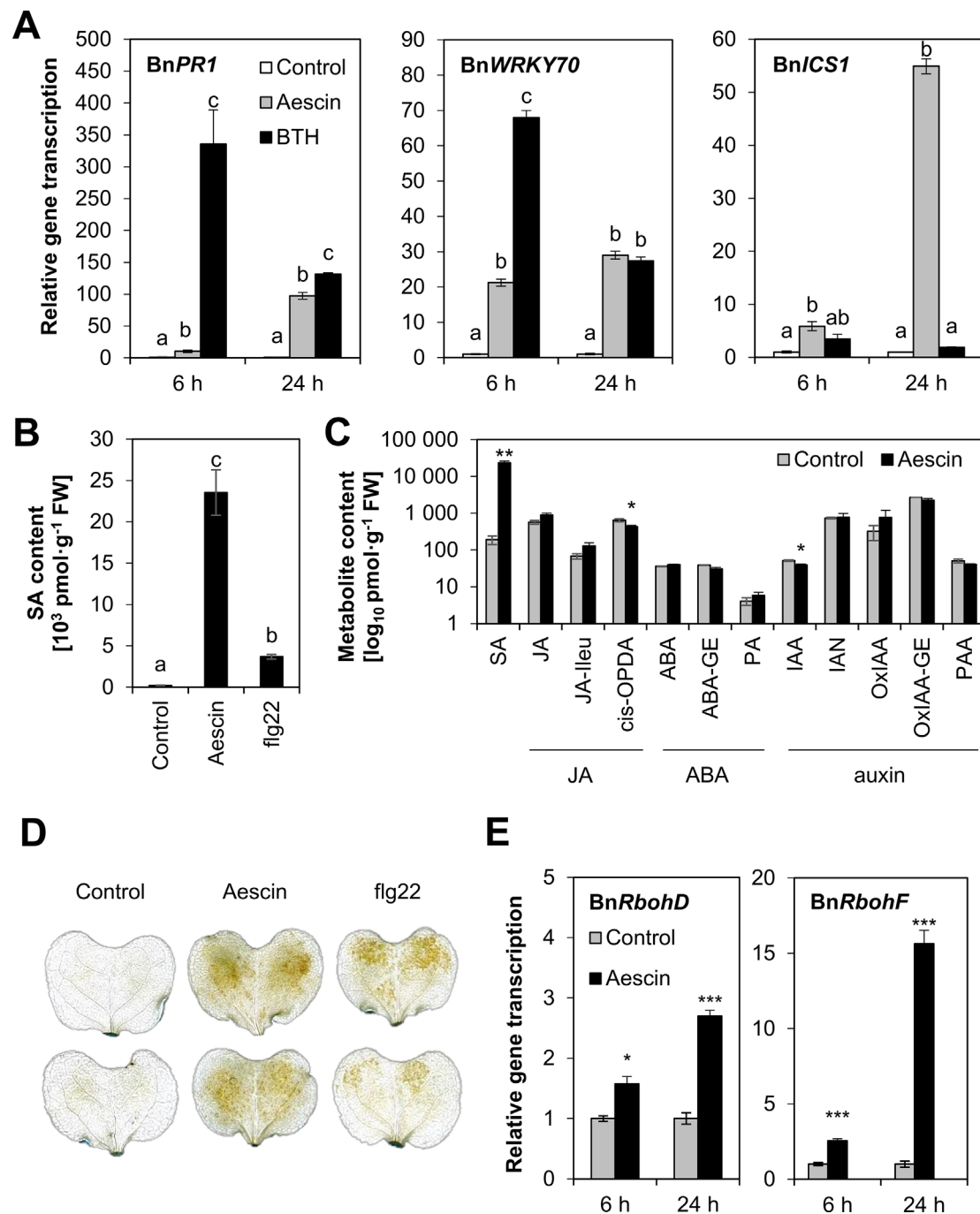


FIGURE 5 | Aescin treatment triggers defense responses in *B. napus*. Cotyledons of *B. napus* were infiltrated by aqueous solutions of aescin (25 $\mu\text{g} \cdot \text{ml}^{-1}$), BTH (30 μM), flg22 (1 μM), or a control treatment. **(A)** Gene transcription of pathogenesis-related *BnPR1*, *BnWRKY70*, and *isochorismate-synthase 1 BnICS1* was analyzed by qPCR after 6 and 24 h of treatment, normalized to *BnActin* and *BnTIP41*, and compared to the corresponding control at 6 or 24 h (set as 1). Data represent mean \pm SE from one biological experiment (four biological replicates), representative of three. **(B, C)** Content of salicylic acid (SA; **B**) and SA, JA, ABA- and auxin-derived hormones in plant tissue expressed as $\text{pmol} \cdot \text{g}^{-1}$ fresh weight \pm SE was measured after 24 h. Data are means of four biological replicates. Experiment was repeated twice. SA, salicylic acid; JA, jasmonic acid; JA-Ile, JA-isoleucine; cis-OPDA, cis-12-oxo-phytodienoic acid; ABA, abscisic acid; ABA-GE, ABA-glucose ester; PA, phaseic acid; IAA, indole-3-acetic acid; OxIAA, oxo-IAA; OxIAA-GE, oxo-IAA-glucose ester; IAN, indole-3-acetonitrile; PAA, phenylacetic acid. **(D)** Oxidative burst visualized by DAB staining at 24 h post treatment. Images are representative of three experiments. **(E)** Transcription of respiratory burst oxidase homolog *RbohD* and *RbohF* genes following aescin treatment was analyzed at 6 or 24 h by qPCR, normalized to *BnActin* and *BnTIP41*, and compared to the corresponding control (set as 1). Data represent means \pm SE from one biological experiment (four biological replicates) representative of three. For **(A)** and **(B)**, different letters above bars illustrate significant differences using ANOVA test in conjunction with Tukey's honestly significant difference multiple mean comparison post hoc test ($P < 0.05$). For **(A)**, the statistical analyses were carried out separately within each time point. For **(C)** and **(E)**, asterisks indicate significant differences between control and a given treatment ($*P < 0.05$; $**P < 0.01$; $***P < 0.001$; two-tailed Student's *t*-test).

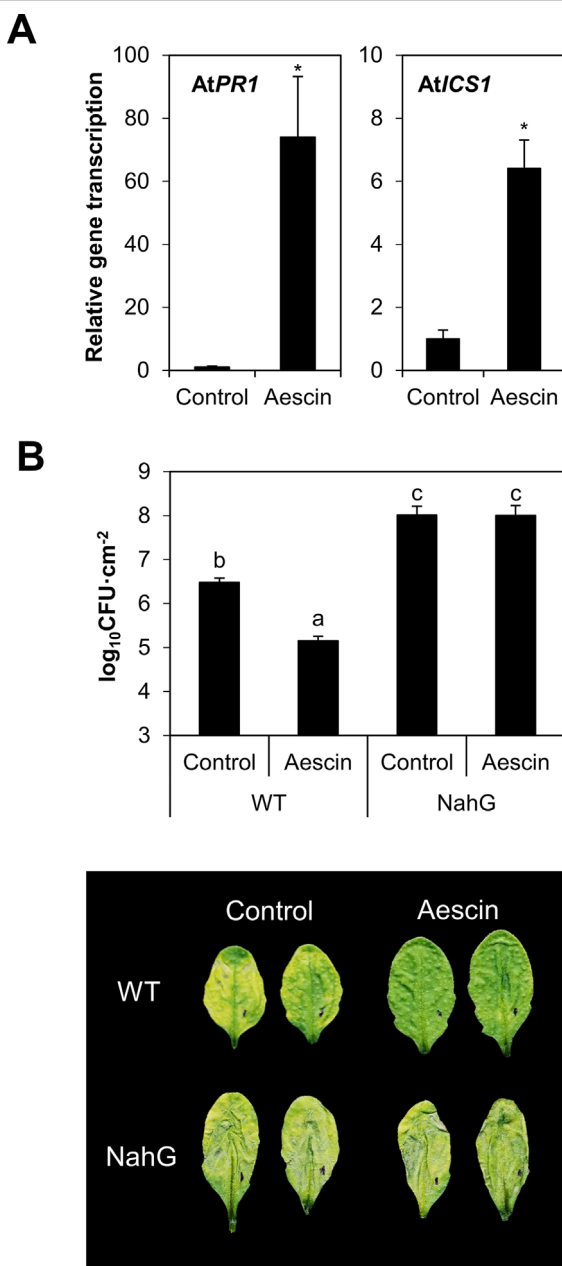


FIGURE 6 | Aescin pretreatment triggers defense gene transcription in *A. thaliana* and resistance against bacteria *Pseudomonas syringae* pv. *tomato* DC3000 (Pst DC3000). Leaves of *Arabidopsis* plants were infiltrated by aqueous solutions of aescin ($10 \mu\text{g}\cdot\text{ml}^{-1}$) or a control treatment. **(A)** Gene transcription of pathogenesis-related *AtPR1* and isochorismate-synthase 1 *AtICS1* was analyzed by qPCR after 24 h of treatment, normalized to *AtTIP41*, then compared to the control. Data represent mean \pm SE from one biological experiment (four biological replicates), representative of three. Asterisks indicate significant differences $*P < 0.05$; two-tailed Student's *t*-test. **(B)** Bacterial growth of *Pst* DC3000 bacteria at 3 days post inoculation in infected leaves of wild type (WT) or NahG transgenic plants pretreated by aescin or control for 24 h. **(upper)** Bacterial titers within leaves. Data represent means of colony forming units (CFU) per $\text{cm}^2 \pm$ SE from six independent replicates of one experiment, representative of three. Different letters above bars illustrate statistical difference between samples using ANOVA with a Tukey honestly significant difference multiple mean comparison post hoc test ($P < 0.01$). **(lower)** A representative leaf for each treatment is shown.

1967; Barile et al., 2007) or fungal sterols with moieties bound only weakly by saponins (Steel and Drysdale, 1988). In general, fungi with defective sterol biosynthesis or in the presence of sterol inhibitors are more resistant to saponins (Olsen, 1973; Defago and Kern, 1983). Moreover, some fungi can cleave sugar moieties of saponins, thereby resulting in non-toxic molecules. For some saponins, a C3-attached sugar moiety or moieties can be critical for both permeabilizing membrane and antifungal properties of saponins (Morrissey and Osbourn, 1999). For instance, *Gaeumannomyces graminis* and *Gibberella pulicaris* produce avenacinase and alpha-chaconinase, respectively, and these detoxify their hosts' saponins (Bowyer et al., 1995; Becker and Weltring, 1998). To sum up, our study characterizes the fungistatic activity of aescin on different phytopathogenic fungi and provides a parallel comparison to fungicides.

Aescin: A Potent Plant Disease Control Agent

The role of saponins as plant-protecting compounds has been shown. Namely, avenacin triterpene glycosides protect oat roots against soil-borne fungal pathogens such as the *Gaeumannomyces graminis* causing disease "take all" in cereals (Papadopoulou et al., 1999). Saponin alliospiroside extracted from *A. cepa* protects strawberry plants against *C. gloeosporioides*, the causal agent of anthracnose (Teshima et al., 2013). Beta-amyrin-derived triterpene glycosides confer resistance in *Barbarea vulgaris* against flea beetle (*Phyllotreta nemorum*) (Nielsen et al., 2010). Here, we showed that pretreatment of *B. napus* cotyledons with aescin led to strong concentration-dependent plant protection against infection by the hemibiotrophic fungus *L. maculans* that causes phoma stem canker. This was demonstrated also by the reduced hyphal spread and necrosis formation in infected cotyledons pretreated with aescin (Figure 4).

Aescin induced transcription of SA-dependent genes in *B. napus*. Namely, aescin led to increased transcription of the SA biosynthetic gene *BnICS1* (Figure 5A) and caused great accumulation of SA (Figure 5B). Additionally, aescin triggered oxidative burst, as demonstrated by ROS accumulation and upregulated transcription of *BnRbohD* and *BnRbohF* genes (Figure 5E). Both SA and oxidative stress have antimicrobial properties (Lamb and Dixon, 1997). Aescin's dual mode of action combining antifungal and induced plant immune responses led to a very efficient inhibition of blackleg disease on *B. napus*. Aescin treatment provided plant resistance to a similar extent as did the fungicide metconazole or BTH (Figure 4A), a potent plant immunity inducer (Zhou and Wang, 2018). The key role played by triggering immunity in aescin-induced *B. napus* protection is seen in the fact that metconazole is greater than 1000 times more effective in its antifungal activity against *L. maculans* compared to aescin (Figures 2B and 3A, C). Overall, then, the plant defense activation may be an important part – and perhaps the crucial part – of aescin-induced plant protection. In the animal kingdom, various studies have shown that saponins induce immunity in vertebrates. Indeed, they are commonly used as vaccine adjuvants (Sun et al., 2009; Moses et al., 2014) because they stimulate antibody production (Soltysik et al., 1995),

production of cytotoxic T-lymphocytes or induce inflammasome (Marty-Roix et al., 2016). To the best of our knowledge, we are the first to show that saponins may induce plant immune responses.

SA Pathway: Target of Aescin-Triggered Immunity

Our data show that aescin activates the plant immune system, and specifically the SA pathway, in both *B. napus* and *A. thaliana*. The SA pathway was shown to be the main defense route activated in *B. napus* upon *L. maculans* infection (Potlakayala et al., 2007; Šašek et al., 2012b). Various microorganisms evolved strategies to disrupt SA-mediated defense (Qi et al., 2018). Some *L. maculans* effectors, such as AvrLm4-7, may target this pathway to weaken the host immune system (Nováková et al., 2016). *B. napus* plants transformed with the salicylate hydroxylase gene *nahG* have been shown to have compromised systemic acquired resistance against *L. maculans* and *P. syringae* pv. *maculicola* (Potlakayala et al., 2007). In comparison with SA, other tested phytohormone metabolites were not or much less affected in *B. napus*. Slight decrease in *cis*-OPDA metabolite might be caused by SA-mediated repression on JA pathways, as has been described for *A. thaliana* (Pieterse et al., 2009; Dave and Graham, 2012).

The crucial role of SA in aescin-triggered plant resistance against pathogens was shown using the *A. thaliana*-*P. syringae* model pathosystem (Katagiri et al., 2002). Leaf pretreatment with aescin strongly inhibited *Pst* DC3000 infection (Figure 6B). The protective effect of aescin relied on the active defense mechanisms of *A. thaliana* inasmuch as aescin did not exhibit direct antibacterial properties (Supplementary Figure 7B). Accordingly, the treatment with aescin simultaneously with the infection had no effect on *Pst* DC3000 infection (Supplementary Figure 7A), thus suggesting some time is required to activate the plant defense. Furthermore, NahG plants defective in SA pathway showed no effect of aescin on the bacterial infection (Figure 6B), thus demonstrating that a functional SA pathway is indispensable for aescin-induced *A. thaliana* resistance against *Pst* DC3000.

In conclusion, we report here broad-spectrum antifungal activity of aescin and the new finding that aescin elicits defense responses in *B. napus* and *A. thaliana* by triggering the SA pathway and oxidative burst. These responses lead ultimately to highly efficient protection of *B. napus* against the fungus *L. maculans* and of *A. thaliana* against the bacteria *Pst* DC3000. The effect of aescin against *L. maculans* is of an extent comparable to that provided by fungicide protection. Additionally, we showed that aescin provides protective activity as a foliar spray. Taken

together, our results suggest that aescin may constitute an attractive bioactive molecule with dual mode of action that could be found suitable for field application.

DATA AVAILABILITY STATEMENT

The datasets generated for this study are available on request to the corresponding author.

AUTHOR CONTRIBUTIONS

LT and PM designed the experiments. LT, MJ, DM, RP, PD, and PM performed the experiments. LT, MJ, PD and PM analyzed the data. LT, MJ, and PM wrote the manuscript. LB revised the manuscript and provided a methodological and knowledge platform for studying the *L. maculans* and *B. napus* interaction, finances, and lab space for a substantial part of the work. All the authors discussed the results and commented on the manuscript.

FUNDING

The research leading to these results was supported by projects QJ1310226, QK1910197, MZE-RO1118, TA ČR GAMA PP1 TG03010009, by the Ministry of Education, Youth and Sports of the Czech Republic from the European Regional Development Fund-Project 'Centre for Experimental Plant Biology': No. CZ.02. 1.01/0.0/0.0/16_019/0000738, and the European Structural and Investment Funds, OP RDE-funded project 'CHEMFELLS4UCTP' (No. CZ.02.2.69/0.0/0.0/17_050/0008485).

ACKNOWLEDGMENTS

The authors would like to thank T. Rouxel for *L. maculans* JN2 isolate, Andrea Kung Wai and English Editorial Services for editing, and Iva Trdá for her technical assistance that enabled us to complete the manuscript.

SUPPLEMENTARY MATERIAL

The Supplementary Material for this article can be found online at: <https://www.frontiersin.org/articles/10.3389/fpls.2019.01448/full#supplementary-material>

REFERENCES

- Arneson, P. A., and Durbin, R. D. (1967). Hydrolysis of tomatine by *Septoria lycopersici*: a detoxification mechanism. *Phytopathology* 57, 1358–1360.
- Augustin, J. M., Kuzina, V., Andersen, S. B., and Bak, S. (2011). Molecular activities, biosynthesis and evolution of triterpenoid saponins. *Phytochemistry* 72 (6), 435–457. doi: 10.1016/j.phytochem.2011.01.015
- Balesdent, M. H., Attard, A., Ansan-Melayah, D., Delourme, R., Renard, M., and Rouxel, T. (2001). Genetic control and host range of avirulence toward *Brassica napus* Cultivars Quinta and Jet Neuf in *Leptosphaeria maculans*. *Phytopathology* 91 (1), 70–76. doi: 10.1094/PHYTO.2001.91.1.70
- Barile, E., Bonanomi, G., Antignani, V., Zolfaghari, B., Sajjadi, S. E., Scala, F., et al. (2007). Saponins from *Allium minutiflorum* with antifungal activity. *Phytochemistry* 68 (5), 596–603. doi: 10.1016/j.phytochem.2006.10.009
- Becker, P., and Weltring, K. M. (1998). Purification and characterization of alpha-chaconinase of *Gibberella pulicaris*. *FEMS Microbiol. Lett.* 167, 197–202. doi: 10.1111/j.1574-6968.1998.tb13228.x

- Bowyer, P., Clarke, B. R., Lunness, P., Daniels, M. J., and Osbourn, A. E. (1995). Host-range of a plant-pathogenic fungus determined by a Saponin detoxifying enzyme. *Science* 267, 371–374. doi: 10.1126/science.7824933
- Burketová, L., Trdá, L., Ott, P. G., and Valentová, O. (2015). Bio-based resistance inducers for sustainable plant protection against pathogens. *Biotechnol. Adv.* 33 (6 Pt 2), 994–1004. doi: 10.1016/j.biotechadv.2015.01.004
- Child, R. D., Evans, D. E., Allen, J., and Arnold, G. M. (1993). Growth responses in oilseed rape (*Brassica napus* L.) to combined applications of the triazole chemicals triapenthenol and tebuconazole and interactions with gibberellin. *Plant Growth Regul.* 13 (2), 203–212. doi: 10.1007/BF00024263
- Cook, D. E., Mesarich, C. H., and Thomma, B. P. (2015). Understanding plant immunity as a surveillance system to detect invasion. *Annu. Rev. Phytopathol.* 53, 541–563. doi: 10.1146/annurev-phyto-080614-120114
- da Cruz Cabral, L., Fernandez Pinto, V., and Patriarca, A. (2013). Application of plant derived compounds to control fungal spoilage and mycotoxin production in foods. *Int. J. Food Microbiol.* 166 (1), 1–14. doi: 10.1016/j.ijfoodmicro.2013.05.026
- Dave, A., and Graham, I. A. (2012). Oxylipin signaling: a distinct role for the Jasmonic acid precursor cis-(+)-12-Oxo-Phytodienoic Acid (cis-OPDA). *Front. Plant Sci.* 3, 42. doi: 10.3389/fpls.2012.00042
- Defago, G., and Kern, H. (1983). Induction of *Fusarium-solani* mutants insensitive to Tomatine, their pathogenicity and aggressiveness to tomato fruits and pea-plants. *Physiol. Plant Pathol.* 22, 29–37. doi: 10.1016/S0048-4059(83)81035-2
- Delaney, T. P., Uknas, S., Vernooy, B., Friedrich, L., Weymann, K., Negrotto, D., et al. (1994). A central role of salicylic Acid in plant disease resistance. *Science* 266 (5188), 1247–1250. doi: 10.1126/science.266.5188.1247
- Djiljanov, D. L., Dobrev, P. I., Moyanova, D. P., Vankova, R., Georgieva, D. T., Gajdošová, S., et al. (2013). Dynamics of endogenous phytohormones during desiccation and recovery of the resurrection plant species *Haberlea rhodopensis*. *J. Plant Growth Regul.* 32, 564–574. doi: 10.1007/s00344-013-9323-y
- Dobrev, P. I., and Kaminek, M. (2002). Fast and efficient separation of cytokinins from auxin and abscisic acid and their purification using mixed-mode solid-phase extraction. *J. Chromatogr. A* 950 (1–2), 21–29. doi: 10.1016/S0021-9673(02)00024-9
- Dodds, P. N., and Rathjen, J. P. (2010). Plant immunity: towards an integrated view of plant-pathogen interactions. *Nat. Rev. Genet.* 11 (8), 539–548. doi: 10.1038/nrg2812
- Field, B., Jordán, F., and Osbourn, A. (2006). First encounters—deployment of defence-related natural products by plants. *New Phytol.* 172 (2), 193–207. doi: 10.1111/j.1469-8137.2006.01863.x
- Finney, D. J. (1971). *Probit Analysis*. Cambridge: Cambridge University Press.
- Fisher, M. C., Hawkins, N. J., Sanglard, D., and Gurr, S. J. (2018). Worldwide emergence of resistance to antifungal drugs challenges human health and food security. *Science* 360 (6390), 739–742. doi: 10.1126/science.aap7999
- Franiczek, R., Glensk, M., Krzyzanowska, B., and Włodarczyk, M. (2015). beta-Aescin at subinhibitory concentration (sub-MIC) enhances susceptibility of *Candida glabrata* clinical isolates to nystatin. *Med. Mycol.* 53, 845–851. doi: 10.1093/mmy/mvy035
- Friedrich, L., Lawton, K., Ruess, W., Masner, P., Specker, N., Rella, M. G., et al. (1996). A benzothiadiazole derivative induces systemic acquired resistance in tobacco. *Plant J.* 10, 61–70. doi: 10.1046/j.1365-313X.1996.10010061.x
- Glazebrook, J. (2005). Contrasting mechanisms of defense against biotrophic and necrotrophic pathogens. *Annu. Rev. Phytopathol.* 43, 205–227. doi: 10.1146/annurev.phyto.43.040204.135923
- Griffiths, K. M., and Howlett, B. J. (2002). Transcription of sterol Delta(5,6)-desaturase and sterol 14alpha-demethylase is induced in the plant pathogenic ascomycete, *Leptosphaeria maculans*, during treatment with a triazole fungicide. *FEMS Microbiol. Lett.* 217 (1), 81–87. doi: 10.1111/j.1574-6968.2002.tb11459.x
- Gruiz, K. (1996). Fungitoxic activity of saponins: practical use and fundamental principles. *Adv. Exp. Med. Biol.* 404, 527–534. doi: 10.1007/978-1-4899-1367-8_43
- Hoagland, R. E., Zablotowicz, R. M., and Reddy, K. N., (1996). "Studies of the Phytotoxicity of Saponins on Weed and Crop Plants," in *Saponins Used in Food and Agriculture. Advances in Experimental Medicine and Biology*, vol. 405 . Eds. Waller, G. R., and Yamasaki, K. (Boston, MA: Springer). doi: 10.1007/978-1-4613-0413-5_6
- Hoagland, R. E. (2009). Toxicity of tomatine and tomatidine on weeds, crops and phytopathogenetic fungi. *Allelopathy* J. 23 (2), 425–436.
- Hostettmann, K., and Marston, A., (1995). *Saponins*. Cambridge University Press. doi: 10.1017/CBO9780511565113
- Huang, H. C., Liao, S. C., Chang, F. R., Kuo, Y. H., and Wu, Y. C. (2003). Molluscicidal saponins from *Sapindus mukorossi*, inhibitory agents of golden apple snails, *Pomacea canaliculata*. *J. Agric. Food Chem.* 51 (17), 4916–4919. doi: 10.1021/jf0301910
- Janda, M., and Ruelland, E. (2015). Magical mystery tour: Salicylic acid signaling. *Environ. Exp. Bot.* 114, 117–128. doi: 10.1016/j.envexpbot.2014.07.003
- Kachroo, A., and Robin, G. P. (2013). Systemic signaling during plant defense. *Curr. Opin. Plant Biol.* 16, 527–533.
- Katagiri, F., Thilimony, R., He, S. Y. (2002). The *Arabidopsis thaliana*-*pseudomonas syringae* interaction. *Arabidopsis Book.* 1, e0039. doi: 10.1199/tab.0039
- Lamb, C., and Dixon, R. A. (1997). The oxidative burst in plant disease resistance. *Annu. Rev. Plant Physiol. Plant Mol. Biol.* 48, 251–275. doi: 10.1199/tab.0039
- Leontovčová, H., Kalachová, T., Trdá, L., Pospišalová, R., Lamparová, L., Dobrev, P. I., et al. (2019). Actin depolymerization is able to increase plant resistance against pathogens via activation of salicylic acid signalling pathway. *Sci. Rep.* 9 (1), 10397. doi: 10.1038/s41598-019-46465-5
- Lloyd, S. R., Schoonbeek, H. J., Trick, M., Zipfel, C., and Ridout, C. J. (2014). Methods to study PAMP-triggered immunity in *Brassica* species. *Mol. Plant Microbe Interact.* 27 (3), 286–295. doi: 10.1094/MPMI-05-13-0154-FI
- Marshall, O. J. (2004). PerlPrimer: cross-platform, graphical primer design for standard, bisulphite and real-time PCR. *Bioinformatics* 20 (15), 2471–2472. doi: 10.1093/bioinformatics/bth254
- Marty-Roix, R., Vladimer, G. I., Pouliot, K., Weng, D., Buglione-Corbett, R., West, K., et al. (2016). Identification of QS-21 as an inflammasome-activating molecular component of saponin adjuvants. *J. Biol. Chem.* 291 (3), 1123–1136. doi: 10.1074/jbc.M115.683011
- Matušinský, P., Švačinová, I., Jonavičienė, A., and Tvarůžek, L. (2017). Long-term dynamics of causative agents of stem base diseases in winter wheat and reaction of Czech *Oculimacula* spp. and *Microdochium* spp. populations to prochloraz. *Eur. J. Plant Pathol.* 148, 199–206. doi: 10.1007/s10658-016-1082-8
- Matušinský, P., Zouhar, M., Pavela, R., and Nový, P. (2015). Antifungal effect of five essential oils against important pathogenic fungi of cereals. *Ind. Crops Prod.* 67, 208–215. doi: 10.1016/j.indcrop.2015.01.022
- Morrissey, J. P., and Osbourn, A. E. (1999). Fungal resistance to plant antibiotics as a mechanism of pathogenesis. *Microbiol. Mol. Biol. Rev.* 63 (3), 708–724.
- Moses, T., Papadopoulou, K. K., and Osbourn, A. (2014). Metabolic and functional diversity of saponins, biosynthetic intermediates and semi-synthetic derivatives. *Crit. Rev. Biochem. Mol. Biol.* 49 (6), 439–462. doi: 10.3109/10409238.2014.953628
- Nielsen, J. K., Nagao, T., Okabe, H., and Shinoda, T. (2010). Resistance in the plant, *Barbarea vulgaris*, and counter-adaptations in flea beetles mediated by saponins. *J. Chem. Ecol.* 36 (3), 277–285. doi: 10.1007/s10886-010-9758-6
- Nováková M., Šašek V., Dobrev PI., Valentová O., Burketová L. (2014). Plant hormones in defense response of *Brassica napus* to *Sclerotinia sclerotiorum* - reassessing the role of salicylic acid in the interaction with a necrotroph. *Plant Physiol. Biochem.* 80, 308–317. doi: 10.1016/j.jplphys.2014.04.019
- Nováková M., Šašek V., Trdá, L., Krutinová, H., Mongin, T., Valentová, O., et al. (2016). Leptosphaeria maculans effector AvrLm4-7 affects salicylic acid (SA) and ethylene (ET) signalling and hydrogen peroxide (H2O2) accumulation in *Brassica napus*. *Mol. Plant Pathol.* 17, 818–831. doi: 10.1111/mpp.12332
- Olsen, R. A. (1973). Triterpeneglycosides as inhibitors of fungal growth and metabolism.6. Effect of Aescin on fungi with reduced sterol contents. *Physiol. Plant* 29, 145–149. doi: 10.1111/j.1399-3054.1973.tb03082.x
- Osbourn, A. (1996). Saponins and plant defence - A soap story. *Trends Plant Sci.* 1, 4–9. doi: 10.1016/S1360-1385(96)80016-1
- Papadopoulou, K., Melton, R. E., Leggett, M., Daniels, M. J., and Osbourn, A. E. (1999). Compromised disease resistance in saponin-deficient plants. *Proc. Natl. Acad. Sci. U.S.A.* 96, 12923–12928. doi: 10.1073/pnas.96.22.12923
- Pieterse, C. M., Leon-Reyes, A., Van der Ent, S., and Van Wees, S. C. (2009). Networking by small-molecule hormones in plant immunity. *Nat. Chem. Biol.* 5 (5), 308–316. doi: 10.1038/nchembio.164

- Podolak, I., Galanty, A., and Sobolewska, D. (2010). Saponins as cytotoxic agents: a review. *Phytochem. Rev.* 9 (3), 425–474. doi: 10.1007/s11101-010-9183-z
- Porsche, F. M., Molitor, D., Beyer, M., Charton, S., Andre, C., and Kollar, A. (2018). Antifungal activity of saponins from the fruit pericarp of *Sapindus mukorossi* against *Venturia inaequalis* and *Botrytis cinerea*. *Plant Dis.* 102 (5), 991–1000. doi: 10.1094/PDIS-06-17-0906-RE
- Potlakayala, S. D., Reed, D. W., Covello, P. S., and Fobert, P. R. (2007). Systemic acquired resistance in canola is linked with pathogenesis-related gene expression and requires salicylic acid. *Phytopathology* 97, 794–802. doi: 10.1094/PHYTO-97-7-0794
- Price, K. R., Johnson, I. T., Fenwick, G. R., and Malinow, M. R. (1987). The chemistry and biological significance of saponins in foods and feedingstuffs. *Crit. Rev. Food Sci. Nutr.* 26 (1), 27–135. doi: 10.1080/10408398709527461
- Qi, J., Wang, J., Gong, Z., and Zhou, J. M. (2017). Apoplastic ROS signaling in plant immunity. *Curr. Opin. Plant Biol.* 38, 92–100. doi: 10.1016/j.pbi.2017.04.022
- Qi, G., Chen, J., Chang, M., Chen, H., Hall, K., Korin, J., et al. (2018). Pandemonium breaks out: disruption of salicylic acid-mediated defense by plant pathogens. *Mol. Plant* 11 (12), 1427–1439. doi: 10.1016/j.molp.2018.10.002
- Saha, S., Walia, S., Kumar, J., and Parmar, B. S. (2010). Structure-biological activity relationships in triterpenic saponins: the relative activity of protobassic acid and its derivatives against plant pathogenic fungi. *Pest Manage. Sci.* 66, 825–831. doi: 10.1002/ps.1947
- Saleem, M., Nazir, M., Ali, M. S., Hussain, H., Lee, Y. S., Riaz, N., et al. (2010). Antimicrobial natural products: an update on future antibiotic drug candidates. *Nat. Prod. Rep.* 27 (2), 238–254. doi: 10.1039/B916096E
- Sanati, H., Belanger, P., Fratti, R., and Ghannoum, M. (1997). A new triazole, voriconazole (UK-109,496), blocks sterol biosynthesis in *Candida albicans* and *Candida krusei*. *Antimicrob. Agents Chemother.* 41, 2492–2496. doi: 10.1128/AAC.41.11.2492
- Saniewska, A., Jarecka, A., Bialy, Z., and Jurzysta, M. (2006). Antifungal activity of saponins originated from *Medicago hybrida* against some ornamental plant pathogens. *Acta Agrobotanica* 59 (2), 51–58. doi: 10.5586/aa.2006.061
- Šašek, V., Nováková, M., Dobrev, P. I., Valentová, O., and Burkotová, L. (2012a). β-aminobutyric acid protects *Brassica napus* plants from infection by *Leptosphaeria maculans*. Resistance induction or a direct antifungal effect? *Eur. J. Plant Pathol.* 133, 279–289. doi: 10.1007/s10658-011-9897-9
- Šašek, V., Nováková, M., Jindřichová, B., Boka, K., Valentová, O., and Burkotová, L. (2012b). Recognition of avirulence gene AvrLm1 from hemibiotrophic ascomycete *Leptosphaeria maculans* triggers salicylic acid and ethylene signaling in *Brassica napus*. *Mol. Plant Microbe Interact.* 25, 1238–1250. doi: 10.1094/MPMI-02-12-0033-R
- Singh, B., and Kaur, A. (2018). Control of insect pests in crop plants and stored food grains using plant saponins: a review. *LWT* 87, 93–101. doi: 10.1016/j.lwt.2017.08.077
- Soltysik, S., Wu, J. Y., Recchia, J., Wheeler, D. A., Newman, M. J., Coughlin, R. T., et al. (1995). Structure-function studies of Qs-21 adjuvant - assessment of triterpene aldehyde and glucuronic-acid roles in adjuvant function. *Vaccine* 13, 1403–1410. doi: 10.1016/0264-410X(95)00077-E
- Sreij, R., Dargel, C., Schweins, R., Prevost, S., Dattani, R., and Hellweg, T. (2019). Aescin-cholesterol complexes in DMPC model membranes: a DSC and temperature-dependent scattering study. *Sci. Rep.* 9 (1), 5542. doi: 10.1038/s41598-019-41865-z
- Steel, C. C., and Drysdale, R. B. (1988). Electrolyte leakage from plant and fungal tissues and disruption of liposome membranes by alpha-tomatine. *Phytochemistry* 27, 1025–1030. doi: 10.1016/0031-9422(88)80266-8
- Steiner, A. A. (1984). The Universal Nutrient Solution. *Proceedings of IWOSC 6th International Congress on Soilless Culture*, Netherlands: Wageningen. pp. 633–650, Wageningen, Netherlands. doi: 10.1016/j.vaccine.2009.01.091
- Sun, H. X., Xie, Y., and Ye, Y. P. (2009). Advances in saponin-based adjuvants. *Vaccine* 27, 1787–1796. doi: 10.1016/j.vaccine.2009.01.091
- Teshima, Y., Ikeda, T., Imada, K., Sasaki, K., El-Sayed, M. A., Shigyo, M., et al. (2013). Identification and biological activity of antifungal saponins from shallot (*Allium cepa* L. Aggregatum group). *J. Agric. Food Chem.* 61 (31), 7440–7445. doi: 10.1021/jf401720q
- Torres, M. A., Jones, J. D., and Dangl, J. L. (2005). Pathogen-induced, NADPH oxidase-derived reactive oxygen intermediates suppress spread of cell death in *Arabidopsis thaliana*. *Nat. Genet.* 37 (10), 1130–1134. doi: 10.1038/ng1639
- Trdá, L., Boutrot, F., Claverie, J., Brûlé, D., Dorey, S., and Poinsot, B. (2015). Perception of pathogenic or beneficial bacteria and their evasion of host immunity: pattern recognition receptors in the frontline. *Front. Plant Sci.* 6, 219. doi: 10.3389/fpls.2015.00219
- Tsuda, K., Sato, M., Glazebrook, J., Cohen, J. D., and Katagiri, F. (2008). Interplay between MAMP-triggered and SA-mediated defense responses. *Plant J.* 53 (5), 763–775. doi: 10.1111/j.1365-313X.2007.03369.x
- Tsuda, K., Mine, A., Bethke, G., Igarashi, D., Botanga, C. J., Tsuda, Y., et al. (2013). Dual regulation of gene expression mediated by extended MAPK activation and salicylic acid contributes to robust innate immunity in *Arabidopsis thaliana*. *PLoS Genet.* 9 (12), e1004015. doi: 10.1371/journal.pgen.1004015
- Turner, E. M. C. (1960). The nature of the resistance of oats to the take-all fungus. Distribution of the inhibitor in oat seedlings. *J. Exp. Bot.* 11, 403–412. doi: 10.1093/jxb/11.3.403
- Waller, G. R., Jurzysta, M., and Thorne, R. L. Z. (1993). Allelopathic activity of root Saponins from Alfalfa (*Medicago Sativa* L) on weeds and wheat. *Bot. Bull. Acad. Sin.* 34, 1–11.
- Walters, D. R., Ratssep, J., and Havis, N. D. (2013). Controlling crop diseases using induced resistance: challenges for the future. *J. Exp. Bot.* 64, 1263–1280. doi: 10.1093/jxb/ert026
- Wolters, B. (1966). [On antimicrobial activity of plant steroids and triterpenes]. *Planta Med.* 14, 392–399. doi: 10.1055/s-0028-1100066
- Xin, X. F., and He, S. Y. (2013). *Pseudomonas syringae* pv. *tomato* DC3000: a model pathogen for probing disease susceptibility and hormone signaling in plants. *Annu. Rev. Phytopathol.* 51, 473–498. doi: 10.1146/annurev-phyto-082712-102321
- Xin, X. F., Kvítko, B., and He, S. Y. (2018). *Pseudomonas syringae*: what it takes to be a pathogen. *Nat. Rev. Microbiol.* 16 (5), 316–328. doi: 10.1038/nrmicro.2018.17
- Yang, C. R., Zhang, Y., Jacob, M. R., Khan, S. I., Zhang, Y. J., and Li, X. C. (2006). Antifungal activity of C-27 steroid saponins. *Antimicrob. Agents Chemother.* 50 (5), 1710–1714. doi: 10.1128/AAC.50.5.1710-1714.2006
- Zablotowicz, R. M., Hoagland, R. E., and Wagner, S. C. (1996). Effect of saponins on the growth and activity of rhizosphere bacteria. *Saponins Used Food Agric.* 405, 83–95. doi: 10.1007/978-1-4613-0413-5_8
- Zhao, Y. L., Cai, G. M., Hong, X., Shan, L. M., and Xiao, X. H. (2008). Anti-hepatitis B virus activities of triterpenoid saponin compound from *Potentilla anserine* L. *Phytomedicine* 15 (4), 253–258. doi: 10.1016/j.phymed.2008.01.005
- Zhu, Y., Chen, H., Fan, J., Wang, Y., Li, Y., Chen, J., et al. (2000). Genetic diversity and disease control in rice. *Nature* 406 (6797), 718–722. doi: 10.1038/35021046
- Zhou, M., and Wang, W. (2018). Recent advances in synthetic chemical inducers of plant immunity. *Front. Plant Sci.* 9, 1–10. doi: 10.3389/fpls.2018.01613

Conflict of Interest: Author Pavel Matusinsky is employed by company Agrotest Fyto, Ltd. The remaining authors declare that the research was conducted in the absence of any commercial or financial relationships that could be construed as a potential conflict of interest.

Copyright © 2019 Trdá, Janda, Macková, Pospíchalová, Dobrev, Burkotová and Matušinský. This is an open-access article distributed under the terms of the Creative Commons Attribution License (CC BY). The use, distribution or reproduction in other forums is permitted, provided the original author(s) and the copyright owner(s) are credited and that the original publication in this journal is cited, in accordance with accepted academic practice. No use, distribution or reproduction is permitted which does not comply with these terms.

Biophysical and proteomic analyses of *Pseudomonas syringae* pv. *tomato* DC3000 extracellular vesicles suggest adaptive functions during plant infection

Martin Janda,^{1,2,3} Katarzyna Rybak,¹ Laura Krassini,¹ Chen Meng,⁴ Oséias Feitosa-Junior,¹ Egidio Stigliano,^{5,6} Beata Szulc,¹ Jan Sklenar,⁵ Frank L.H. Menke,⁵ Jacob G. Malone,^{6,7} Andreas Brachmann,¹ Andreas Klingl,¹ Christina Ludwig,⁴ Silke Robatzek^{1,5}

AUTHOR AFFILIATIONS See affiliation list on p. 22.

ABSTRACT Vesiculation is a process employed by Gram-negative bacteria to release extracellular vesicles (EVs) into the environment. EVs from pathogenic bacteria play functions in host immune modulation, elimination of host defenses, and acquisition of nutrients from the host. Here, we observed EV production of the bacterial speck disease causal agent, *Pseudomonas syringae* pv. *tomato* (*Pto*) DC3000, as outer membrane vesicle release. Mass spectrometry identified 369 proteins enriched in *Pto* DC3000 EVs. The EV samples contained known immunomodulatory proteins and could induce plant immune responses mediated by bacterial flagellin. Having identified two biomarkers for EV detection, we provide evidence for *Pto* DC3000 releasing EVs during plant infection. Bioinformatic analysis of the EV-enriched proteins suggests a role for EVs in antibiotic defense and iron acquisition. Thus, our data provide insights into the strategies this pathogen may use to develop in a plant environment.

IMPORTANCE The release of extracellular vesicles (EVs) into the environment is ubiquitous among bacteria. Vesiculation has been recognized as an important mechanism of bacterial pathogenesis and human disease but is poorly understood in phytopathogenic bacteria. Our research addresses the role of bacterial EVs in plant infection. In this work, we show that the causal agent of bacterial speck disease, *Pseudomonas syringae* pv. *tomato*, produces EVs during plant infection. Our data suggest that EVs may help the bacteria to adapt to environments, e.g., when iron could be limiting such as the plant apoplast, laying the foundation for studying the factors that phytopathogenic bacteria use to thrive in the plant environment.

KEYWORDS extracellular vesicles, EVs, *Pto* DC3000, proteomics, pattern-triggered immunity, PTI, nanoparticle tracking analysis, NTA, *Arabidopsis thaliana*

Successful colonization of hosts depends on the ability of microbes to defend themselves against host immune responses and acquire nutrients. Bacterial pathogens use macromolecular translocation systems and deliver virulence proteins, so-called effectors, to circumvent host immunity (1). *Pseudomonas syringae* pv. *tomato* (*Pto*) DC3000 is the causal agent of bacterial speck, a common disease that affects tomato production worldwide (2, 3). *Pto* DC3000 is a Gram-negative bacterium that invades through openings in the plant surface and propagates in the apoplast, where it takes up nutrients and proliferates (4–6). Plants respond rapidly to colonization by microbes, activating interlinked innate defense strategies (7), which can broadly be categorized into pattern-triggered immunity (PTI) activated by pathogen-associated molecular patterns (PAMPs) and effector-triggered immunity induced upon recognition

Invited Editor Hailing Jin, University of California Berkeley, Berkeley, California, USA

Editor Regine Kahmann, Max Planck Institute for Terrestrial Microbiology, Marburg, Germany

Address correspondence to Silke Robatzek, robatzek@bio.lmu.de.

Katarzyna Rybak and Laura Krassini contributed equally to this article.

The authors declare no conflict of interest.

See the funding table on p. 22.

Received 6 January 2023

Accepted 3 May 2023

Published 27 June 2023

Copyright © 2023 Janda et al. This is an open-access article distributed under the terms of the Creative Commons Attribution 4.0 International license.

of virulence factors or their actions (8, 9). Virulence of *Pto* DC3000 largely depends on the type III secretion system and its secreted effectors (10–13).

The survival of infectious Gram-negative bacteria is greatly enhanced by releasing extracellular vesicles (EVs), a process widely studied in the context of bacteria pathogenic to humans (14). EVs are cytosol-containing membrane “nano” spheres that provide selection, storage, and protection against degradation of enclosed cargoes in a highly dynamic and environmental cue-responsive manner (14–16). EVs can differ in biophysical parameters like size and charge, as well as in cargo composition and biogenesis. Gram-negative bacteria actively form EVs by budding and shedding the outer membrane (OM), producing so-called outer membrane vesicles (OMVs) (17, 18). Outer–inner membrane vesicles (OIMVs) have also been described, involving a different mode of release such as endolysin-triggered cell lysis (19, 20). As insufficient biomarkers are available to convincingly probe their origin, in particular for *P. syringae*, we will collectively refer to these vesicles as EVs.

During infection, bacterial EVs can counteract the effect of antimicrobial peptides (21). They also perform immunomodulatory functions by delivering virulence factors to recipient cells resulting in immune suppression (22), despite having the capacity to activate defenses due to their immunogenic cargoes (22–24). Elongation factor Tu (EF-Tu) and lipopolysaccharides (LPS) are abundant components of EVs from *P. syringae*, *Xanthomonas campestris*, *X. oryzae*, and *Xylella fastidiosa* (25–28). Both represent PAMPs, with EV-associated EF-Tu shown to activate a prototypic PTI response in a receptor-dependent manner (25, 29). EVs isolated from pathogenic *Pto* DC3000 and the commensal *P. fluorescens* were shown to induce immunity, protecting plants against *Pto* DC3000 infection (30). These studies hint at some contrasting roles that EVs from bacterial phytopathogens could play during plant infection (23).

Here, we used biophysical and biochemical analysis to describe *Pto* DC3000 EVs and to gain insights into their role during infection. Analysis of *Pto* DC3000 cellular, OM and EV proteomes by mass spectrometry identified 369 EV-enriched proteins. The potential function of these proteins was assessed using bioinformatic analysis as well as exploring plant immune responses to EVs and the presence of EVs *in planta* by establishing OprF and β-lactamase as EV biomarkers. These findings expand our understanding of the functions of EVs in bacterial infection of plants.

RESULTS

Pto DC3000 bacteria vesiculate and produce EVs in culture

We first examined the morphology of *Pto* DC3000 cells grown in liquid cultures by scanning electron microscopy (SEM). The bacteria displayed multiple spherical structures protruding from their cell surfaces, with diameters in the range of 20–120 nm with a median around 35 nm (Fig. 1A; Fig. S1A and B). These vesicle-like structures appeared to be released from the surface, as similarly sized vesicular structures could also be observed in the vicinity of the bacteria.

To determine whether these structures were released, supernatants of *Pto* DC3000 cultures were processed and examined before (fluid sample) and after centrifugation (gradient-collected sample) (Fig. S1C). Density gradient centrifugation is used to separate EVs from other extracellular materials (31). Gradient-collected vesicles were analyzed by SEM, which revealed numerous spherical structures (Fig. 1B). Vesicle diameters ranged between 25 and 170 nm with a median around 80 nm (Fig. S1D). Co-purifying filamentous structures could also be detected (Fig. 1B). Transmission electron microscopy (TEM) analysis-sectioned *Pto* DC3000 samples showed several structures reminiscent of budding vesicles from the bacterial OM (Fig. 1C and D). This suggests that *Pto* DC3000 can produce EVs in the form of OMVs (17, 18).

Nanoparticle tracking analysis (NTA) was used to measure particle size (median diameter and distribution), particle surface charge (mean ζ -potential), and particle number (concentration). In this size analysis, both sample types exhibited a polydisperse-sized population of spherical structures with a diameter ranging from ~50 to 200 nm and

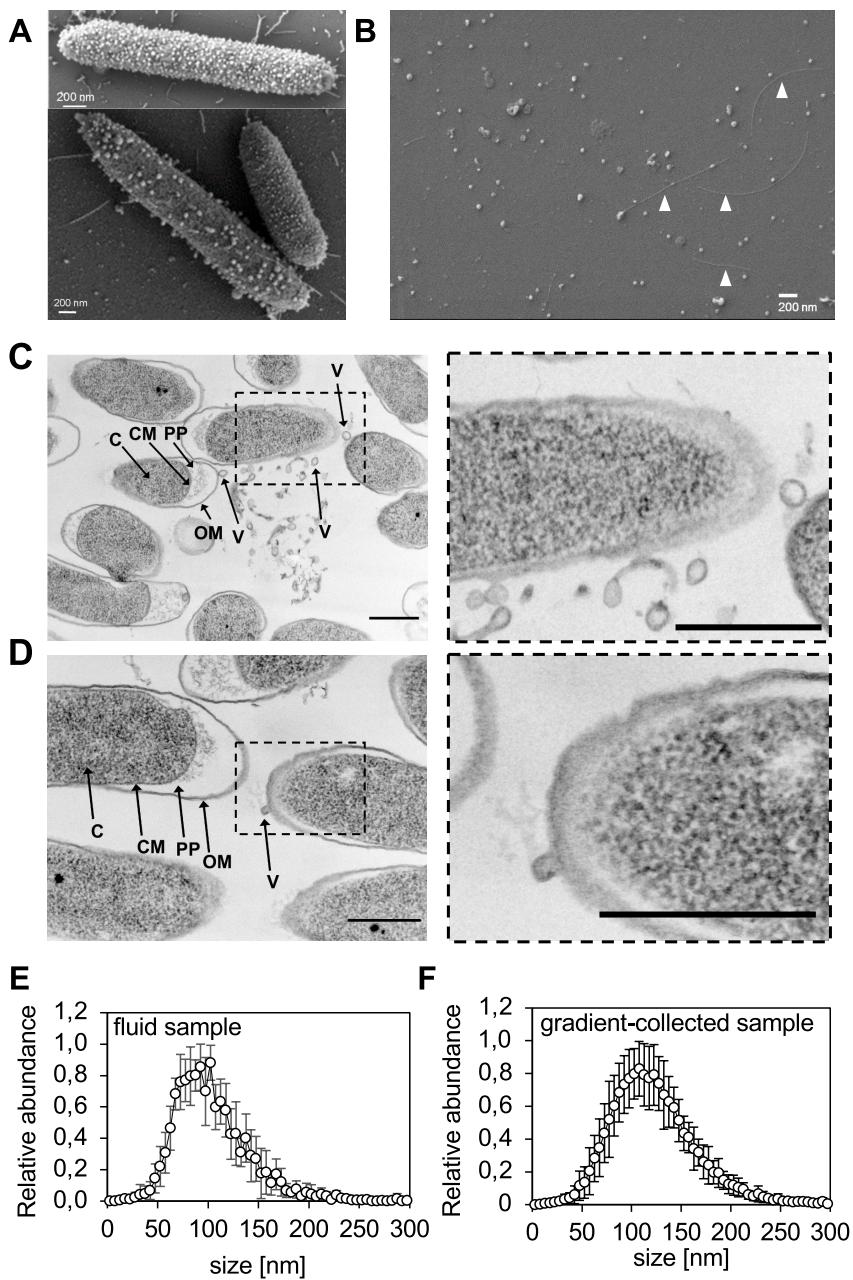


FIG 1 *Pto* DC3000 release extracellular vesicles in the form of OMVs. (A) Representative SEM micrographs of planktonic *Pto* DC3000 grown in liquid culture $1.5\text{--}2 \times 10^9$ cfu/mL (SEM was done in three biological repeats and in all repeats EVs were observed). (B) Representative SEM micrograph of gradient-enriched *Pto* DC3000 EVs purified from planktonic culture ($1.5\text{--}2 \times 10^9$ cfu/mL); arrowheads point at filamentous structures co-purifying with the vesicles (SEM was done in three biological repeats). For A and B scale bars = 200 nm. (C and D) Left panel shows representative transmission electron microscopy (TEM) micrographs from planktonic *Pto* DC3000 cultures ($1.5\text{--}2 \times 10^9$ cfu/mL). C, cytoplasm; CM, cytoplasmic membrane; PP, periplasm; V, vesicle. For C and D scale bars = 500 nm. (C) A lot of smaller and larger vesicles in proximity to cells. It is important to note that the larger vesicle-like structures could also represent debris of dead cells. (D) Budding vesicle in the right part of the micrograph. Dashed boxes indicate enlarged regions of the micrographs shown in the right panel. TEM was performed from three biologically independent bacterial samples. (E) Size profile of EVs from *Pto* DC3000 planktonic cultures in fluid samples ($3.75\text{--}5.5 \times 10^9$ cfu/mL); the values represent mean and standard deviations from 13 biologically independent samples. (F) Size profile of gradient-collected EVs from planktonic *Pto* DC3000 cultures ($1.5\text{--}2 \times 10^9$ cfu/mL); the values represent mean and standard deviations from 20 biologically independent samples.

median sizes of 100 and 115 nm for fluid samples and gradient-collected samples, respectively (Fig. 1E and F). It is possible that conditions used for SEM and NTA differ in their capacity to hydrate the vesicles and/or that NTA underestimates smaller particles (32).

To determine whether EV production is an active process, EVs were quantified from culture supernatants of *Pto* DC3000 over cultivation time, with increasing particle numbers observed with bacterial density (Fig. S2A and B). Calculation of the amount of EVs produced per bacterium showed that numbers were similar between growth stages (Fig. S2A and B). The median diameter and ζ -potential of EVs were mostly comparable across growth stages, yet differed slightly between the sample types (Fig. S2C and D). Albeit we cannot exclude the possibility that vesicles could be derived, e.g., from exploding cells (20), the vesicles recovered from culture samples appeared to be predominantly produced by bacteria as an active process since the number of dead cells from planktonic cultures was little compared with heat killing (Fig. S2E), which also caused higher particle numbers (Fig. S2F). This is consistent with the observations from TEM (Fig. 1C and D).

EVs from cultured *Pto* DC3000 are enriched in 369 proteins

To gain insights into the biogenesis and functions of *Pto* DC3000 EVs, we characterized the proteome of EVs using liquid chromatography-based tandem mass spectrometry (LC-MS/MS). To this end, we cultivated *Pto* DC3000 in a rich, yet iron-limited medium, allowing for high bacterial growth and thus EV yield as well as considering iron limitation in the leaf apoplast during pathogen infection (25, 33). The *Pto* DC3000 EV-associated proteins were isolated from *Pto* DC3000 cultures by gradient enrichment. In parallel, we determined the proteomes of whole cells (WC) and OM preparations. We detected the highest number of proteins from the WC sample ($n = 1,587$), followed by the EV sample ($n = 890$) and 212 proteins in OM samples (Fig. 2A; Table S1). In total, 2,898 proteins were identified over all samples, of which 1,899 proteins were identified at least in three of the four samples per sample type (WC, EV, or OM). These proteins were taken forward for further analysis (Table S1). Similar protein intensity distributions were obtained for all samples [label-free quantification (LFQ) values were generated by MaxQuant, Fig. S3], and the four replicate measurements per sample type fell into sample clusters on the first and second principal components, suggesting a systematic difference in the proteomes of these three sample types (Fig. 2B). By comparing the proteomes of EV and WC, we identified 369 EV-enriched proteins, consisting of 162 proteins exclusively identified in at least 3 replicates of EV sample (EV unique detected; Fig. 2C) and 207 proteins significantly higher in the EV compared with WC (Fig. 2C; Table S1). Next, we analyzed the proteomics data (i) using computational approaches (bioinformatics and database searches) and (ii) building on current knowledge (EV biogenesis and immunomodulatory activities).

Pto DC3000 EVs are enriched in proteins with predicted roles in transport and antimicrobial peptide resistance

We performed a gene set analysis on the 369 EV-enriched proteins to examine the biological processes, cellular component, and molecular function in which these proteins are involved [from gene ontology (GO)] (34, 35). In total, 20 GO terms were significantly enriched [Fig. 3A through C; false discovery rate (FDR) <0.05; DAVID bioinformatics resources] (36, 37). Eight terms were found in the category “biological process,” out of which, four terms were associated with “cellular processes” related to cell division, shape, and cell wall remodeling. An increasing release of EVs was observed in cells that grow at exponential phase, likely due to an increased turnover of peptidoglycan during cell division (38). Three terms were connected to the general process of “transport,” including transmembrane transport, intracellular transmembrane transport, and protein transport by the Sec complex (Fig. 3A; Table S2). This suggests a specific and/or selective mechanism for the delivery of protein cargoes into EVs. Indeed, classification of the proteins

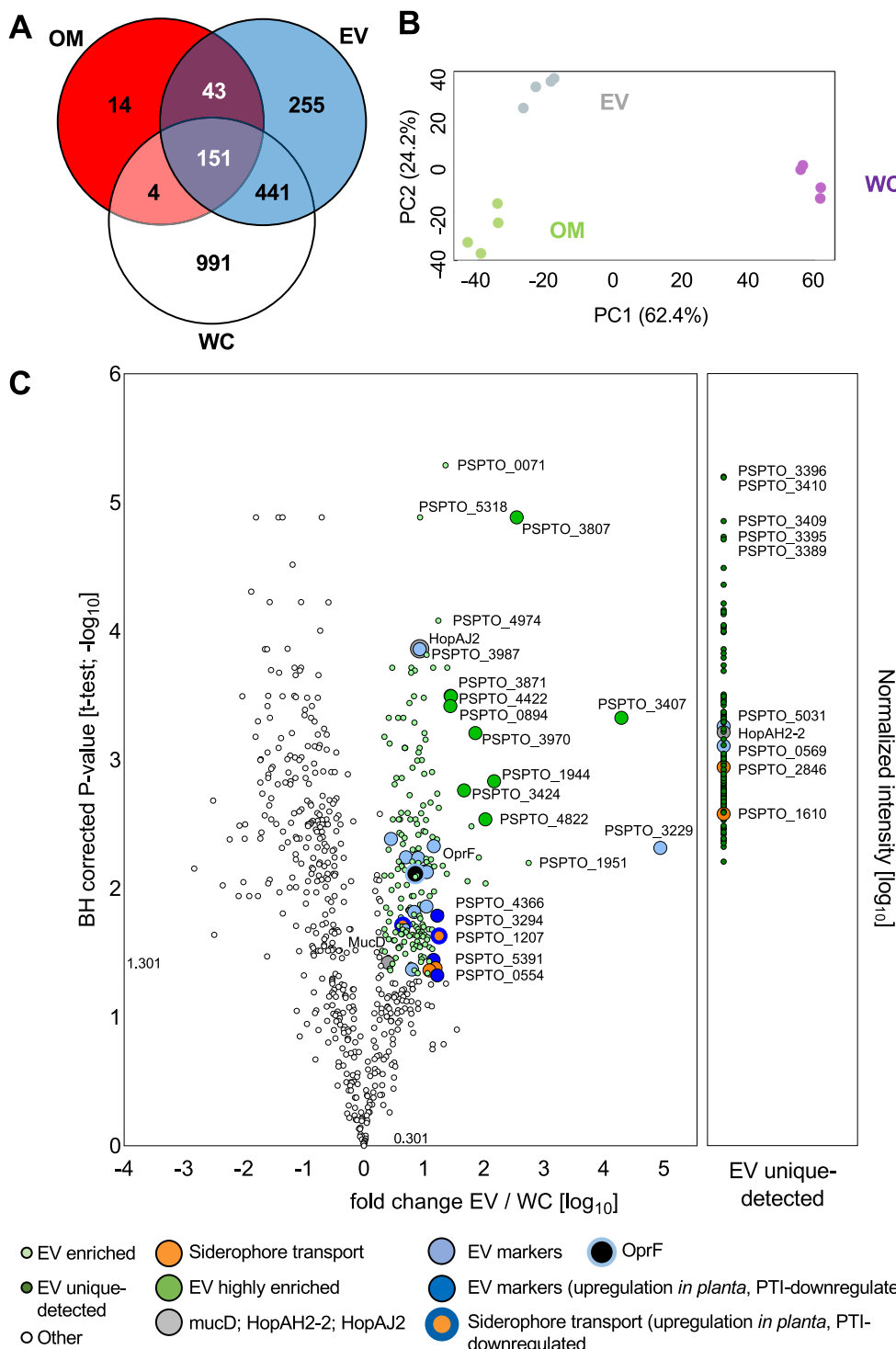


FIG 2 Proteomic analysis identifies 369 proteins enriched in *Pto* DC3000 EVs. (A) Comparison of proteins detected in *Pto* DC3000 WC lysate, OM, and EV. Proteomic analysis was done using four biologically independent samples. (B) Principal component analysis of identified proteins. (C) Volcano plot comparing EV and WC proteomes. EV-enriched proteins were defined in two categories: (i) fold change EV/WC >2 and false discovery rate < 0.05 (*t*-test); (ii) measured in three replicates in EV but not in WC. In addition, the mean intensity in EV protein needs to be in the top 50% of all proteins, so only high-intensity proteins in EV are selected. Four types of proteins enriched or unique detected in EVs were highlighted: proteins related to virulence; proteins related to siderophore transport; candidate EV biomarkers; and proteins highly enriched in EVs compared with WC.

enriched in EVs by putative subcellular localization revealed distinct localization profiles compared with WC and OM proteins. While 66% of WC proteins were cytoplasmic, about half (51%) of the EV-enriched proteins were cytoplasmic membrane associated, with the next largest known class being OM associated (11%) (Fig. S3C). This is consistent with the four terms found in the category “cellular component,” connected to the general compartment “membrane,” including OM and plasma membrane (Fig. 3B). Combining the data from proteomics and TEM, it may suggest that *Pto* DC3000 produces EVs in the form of both OMVs and OIMVs, as previously described for the closely related species *P. aeruginosa* (20). The category “molecular function” was enriched in eight terms, including processes associated with peptidoglycan synthesis also found in the “biological process” category, and siderophore transport (Fig. 3C). Siderophores are secondary metabolites that can sequester iron. Bacteria secrete siderophores under iron-limiting environments, improving iron uptake and thereby contributing to bacterial survival (39). The enrichment of siderophore transport proteins in *Pto* DC3000 EVs suggests that the release of EVs may contribute to the acquisition of iron.

EV yield and likely cargo composition are affected by the environment, in which bacteria grow (25). Having identified proteins enriched in EVs collected from cultured *Pto* DC3000 bacteria, this could limit evidence on the role of EV-enriched proteins during plant infection. If EV-enriched proteins would be involved in infection, we assumed that (i) proteins enriched in EVs from cultured bacteria would be present in bacteria *in planta* and, thus, (ii) genes coding for EV-enriched proteins would be expressed in bacteria *in planta*, and (iii) genes coding for EV-enriched proteins could respond to the plant’s immune status. We, therefore, inspected available *Pto* DC3000 transcriptome data (33).

The expression patterns of genes coding for EV-enriched proteins differed mostly between *Pto* DC3000 cultured *in vitro* (in both minimal and rich media), present *in planta* (in both untreated and mock-treated plants), and present in flg22 immune-induced plants (Fig. 3D). We found five clusters of gene expression patterns across these conditions. Of note, genes in cluster II were upregulated in bacteria in response to *in planta* conditions but downregulated in bacteria from flg22-induced plants. It is thus possible that the proteins encoded by the genes in cluster II are also present at EVs produced by *Pto* DC3000 in untreated and mock-treated plants. Since cluster II is enriched in the GO term “siderophore uptake transmembrane transporter activity” (Fig. 3E; Table 1; Table S2), EVs may play roles in iron acquisition (Fig. 2C, orange labeling).

Cluster III contains genes that were similarly expressed in bacteria grown *in vitro* and bacteria from flg22-induced plants but differed in their expression in response to *in planta* conditions (Fig. 3D). This cluster is associated, e.g., with the GO term “bacterial-type flagellum hook” (Fig. 3E), which has been described in the biogenesis of EVs (40). Also, cluster III is associated with the GO term “serine-type D-Ala-D-Ala carboxypeptidase activity,” which has a cross-reference with the term “Penicillin-binding protein 2” in the InterPro database of protein families. It is worth mentioning that genes PSPTO_3987 and PSPTO_4977 both annotated with the “β-lactam resistance” function are also present in cluster III, although not assigned in the above-mentioned GO term.

Purified *Pto* DC3000 EV samples have immunomodulatory activities

Given the presence of flagellin in our *Pto* DC3000 EV samples, we next examined the ability of the *Pto* DC3000 EVs to modulate the outcome of bacterial infection. We pretreated *Arabidopsis thaliana* leaves with *Pto* DC3000 EVs, which limited the growth of subsequently infected *Pto* DC3000 bacteria *in planta* (Fig. 4A). Thus, the immunogenic activity of *Pto* DC3000 EVs is sufficient to restrict bacterial colonization, consistent with recent observations (30). In agreement, seedlings treated with purified EVs showed induction of *pFRK1::GUS* expression, albeit lower when compared with treatments with flg22 (Fig. 4B; Fig. S4A). We also tested whether treatment with *Pto* DC3000 EVs could arrest seedling growth, a prototypic PTI response of plants to continual PAMP stimulation (41). We observed no significant growth reduction in this experiment (Fig. 4C).

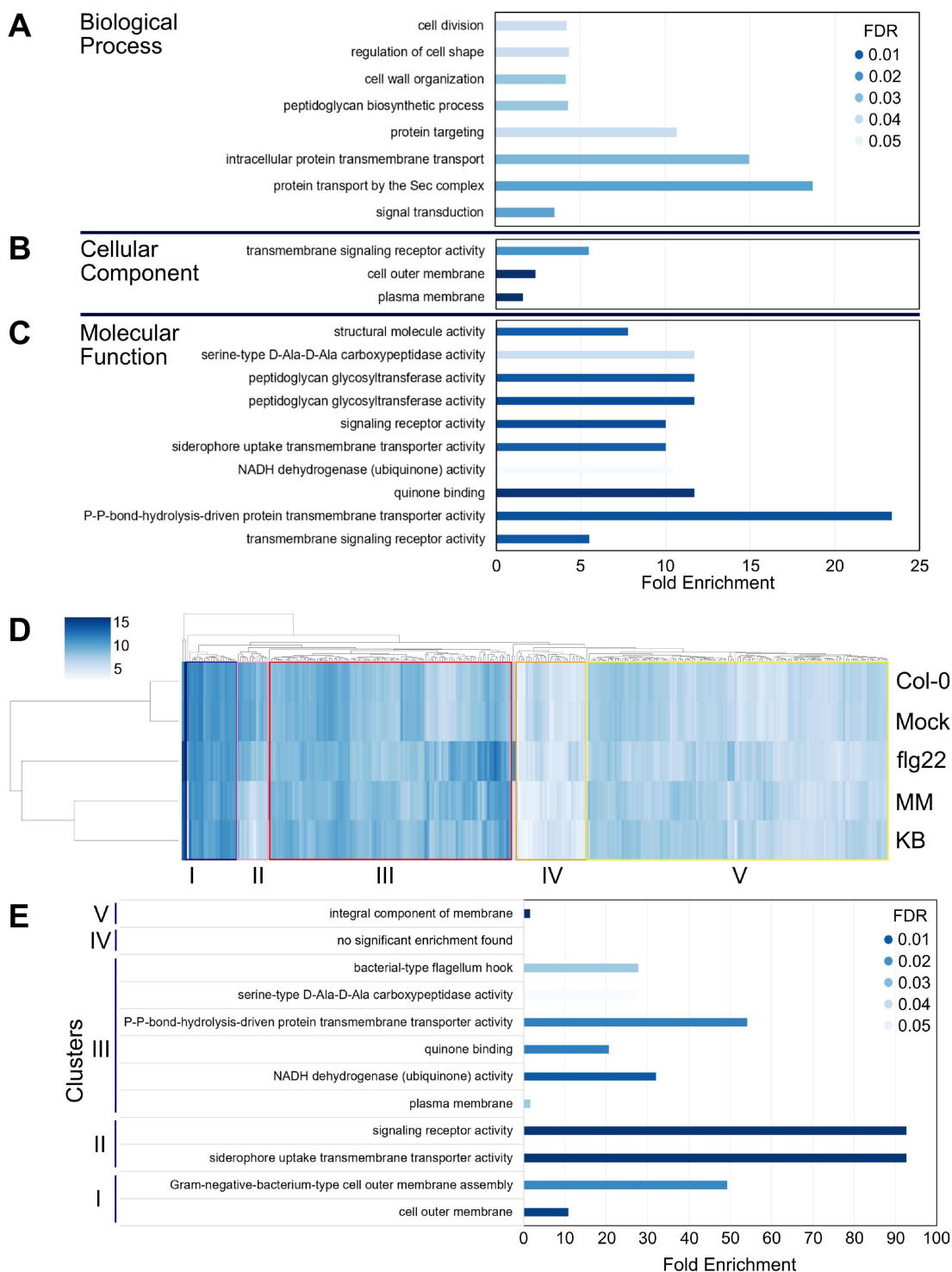


FIG 3 Proteomic composition of *Pto* DC3000 EVs suggests functions in immunomodulation and host adaptation. (A through C) Enriched proteins in biological processes (A), cellular localization (B), and molecular function (C). (D) Heat map representing transcriptional patterns of the genes coding for EV-enriched proteins. Genes with similar expression patterns are indicated as clusters. Five clusters (I–V) were highlighted. Transcriptome data are derived from reference (33). (E) GO terms associated with clusters.

Six flagella-associated proteins were enriched in *Pto* DC3000 EVs, of which flagellin was more than twofold enriched relative to the WC proteome (Table S1). Therefore, to determine the pathway by which the *Pto* DC3000 EVs trigger immune responses, we treated *A. thaliana* mutants of the FLAGELLIN SENSING 2 (FLS2) and EF-Tu receptor (EFR)

TABLE 1 Protein list of the genes present in cluster II and their predicted localization

Locus tag	Subcellular localization	Product description ^a	Other
PSPTO_0577	Unknown	Phage tail sheath subtilisin-like domain-containing protein	
PSPTO_0753	Cytoplasmic membrane	Multidrug efflux MFS transporter	EV unique detected
PSPTO_1207	Outer membrane	TonB-dependent siderophore receptor	EV marker; siderophore transport
PSPTO_1760	Cytoplasmic membrane	HAAAP family serine/threonine permease	
PSPTO_2115	Outer membrane	VacJ family lipoprotein	
PSPTO_3294	Outer membrane	TonB-dependent receptor	EV marker; siderophore transport
PSPTO_3574	Outer membrane	TonB-dependent siderophore receptor	Siderophore transport
PSPTO_4196	Cytoplasmic membrane	Glucose/quinate/shikimate family membrane-bound PQQ-dependent dehydrogenase	
PSPTO_4452	Cytoplasmic	LPS export ABC transporter ATP-binding protein	
PSPTO_4883	Cytoplasmic membrane	PepSY domain-containing protein	
PSPTO_4931	Cytoplasmic membrane	Hypothetical protein	EV unique detected
PSPTO_5391	Outer membrane	OprD family porin	EV marker
PSPTO_5603	Cytoplasmic membrane	F0F1 ATP synthase subunit B	EV "core"

^aMFS = Major Facilitator Superfamily; PQQ = pyrroloquinoline quinone; ABC = ATP-binding cassette.

immune receptors responsible for recognition of flg22 and elf18, respectively (42). The *Pto* DC3000 EVs triggered *FRK1* gene expression in wild-type (WT) and *efr-1* mutants to similar levels (Fig. 4D). No *FRK1* induction was observed in *fls2* mutants. Thus, the EV samples isolated from *Pto* DC3000 cultures must contain bacterial flagellin as the immunogenic molecule.

Notably, SEM analysis of gradient-collected EV samples showed the co-purification of filament-like structures (Fig. 1B), which could represent detached bacterial flagellar or pili. Since flagellin could not be detected in proteinase K-treated EVs and proteinase K-treated EVs did not significantly induce *pFRK1::GUS* expression (Fig. 4E and F; Fig. S4B), taken together, it is possible that flagellin is a co-purifying immunogenic molecule present in *Pto* DC3000 EV samples and recognized in *A. thaliana*. This is consistent with the observation that EVs purified from the *Pto* DC3000 *ΔfliC* mutant did not significantly induce *pFRK1::GUS* expression (Fig. 4G; Fig. S4C). Considering co-purifying flagellin as the major immunogenic molecule in *Pto* DC3000 EV samples, its amount might be insufficient to repress seedling growth over time.

The EV-enriched proteome included proteins related to virulence (Fig. 2C; Table S1), such as MucD (PSPTO_4221) (43), HopAJ2 (PSPTO_4817) (44), and HopAH2-2 (PSPTO_3293) (45, 46). A major function of virulence proteins is the suppression of PTI (47). Recently, the integration of *X. campestris* pv. *campestris* OMVs into plant plasma membranes was observed, which might suggest that vesicle cargoes such as virulence proteins could be discharged into plant cells (48). To test whether *Pto* DC3000 EVs could modulate a prototypic PTI response, we pretreated leaves with EVs from cultured bacteria 24 hours before eliciting an ROS burst with the immunogenic peptides flg22 from bacterial flagellin and elf18 from EF-Tu. EV pretreatments neither significantly reduced nor increased the PAMP-induced ROS production (Fig. 4H). This suggests that under the tested conditions, *Pto* DC3000 EVs are not predominantly involved in inhibiting and/or further enhancing the PAMP-induced ROS responses.

***Pto* DC3000 bacteria produce EVs in planta**

The observation that EVs collected from *Pto* DC3000 cultures may not play major roles in host immune modulation raises the question whether *Pto* DC3000 releases EVs during plant infection. To address this, apoplastic fluids were recovered from *Pto* DC3000-infec-

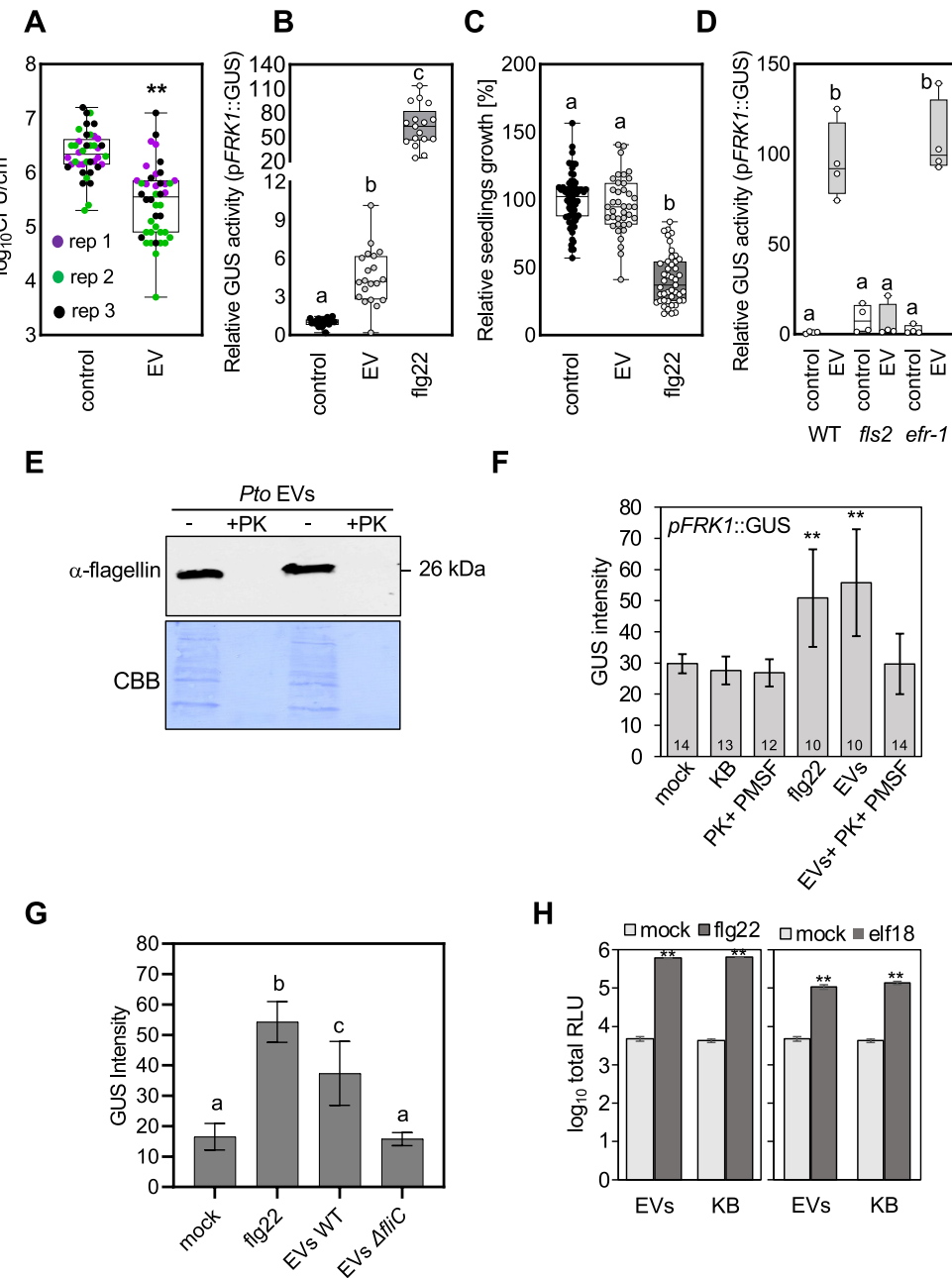


FIG 4 Immunogenic activities of *Pto* DC3000 EVs are mostly dependent on flagellin-induced responses. (A) *Pto* DC3000 growth (cfu) after infection into leaves of *A. thaliana* without and with EV pretreatment (24 hours) at 3 dpi (control = 0.02 mM EDTA). Three biological repeats, each consisting of 12 independent samples were performed. The dots with the same color represent independent samples from one biological repeat. (B) Quantification of *pFRK1::GUS* activity in seedlings incubated without ($n = 20$) and with EVs ($n = 20$) or with 100 nM flg22 ($n = 17$) for 18 hours. The graph represents independent samples from four biological repeats. (C) Fresh weight of seedlings grown without and with EVs for 8 days. For control $n = 69$; for 100 nM flg22 treatment $n = 44$, and EV treatment $n = 39$ of independent samples. The experiment was repeated in six biological repeats with similar results. (D) Relative *FRK1* gene expression in seedlings of the indicated genotypes incubated without and with EVs for 5 hours (control = 0.02 mM EDTA), four independent samples were used for each variant. The experiment was repeated in two biological repeats with similar results. For A, B, C, and D were used EVs for treatments in concentration $\approx 1.10^{10}$ /mL. The boxplots extend from 25th to 75th percentiles, whiskers go down to the minimal value and up to the maximal value, and the line in the middle of the box represents the median. Asterisks indicate statistical significances (two-tailed Welsch's *t*-test; $P < 0.01$) in A; different letters indicate significant differences (Welsch's analysis of variance).

(Continued on next page)

FIG 4 (Continued)

variance with Dunnett's T3 multiple comparisons post hoc test; $P < 0.05$) in B, C, and D. (E) Immunoblot of flagellin in *Pto* DC3000 EVs without and with proteinase K treatment. Flagellin antibodies detect bands in untreated gradient-collected EVs but not proteinase K-treated EVs. Coomassie brilliant blue (CBB) shows protein loading, evidently significantly reduced by proteinase K treatment. (F) Quantification of *pFRK1::GUS* signals in seedlings incubated with gradient-collected *Pto* DC3000 EVs (concentration $\approx 1.10^{10}$) without and with proteinase K treatment (PK+ PMSF [phenylmethylsulfonyl fluoride]), 100 nM flg22, and particles (concentration $\approx 1.10^{10}$) of unconditioned KB medium for 24 hours. The seedling number n is shown in the bars; the bars represent average, and error bars are SD. Asterisks indicate significant differences based on t-test analysis. The experiment was repeated at least twice with similar results. (G) Quantification of *pFRK1::GUS* signals in seedlings (12 days old) incubated with EVs (concentration ranging from 0.75 to 2.5×10^{10} / mL) from *Pto* DC3000 wild-type (WT) and $\Delta fliC$ mutants medium for 18 hours. The bars represent mean, and error bars are SD from $n = 10$ independent samples. The experiment was done in two biological repeats with similar results. (H) Quantification of PAMP-induced reactive oxygen species (ROS) in leaves pre-treated without and with EVs (concentration $\approx 1.10^{10}$) for 24 hours. The bars represent mean, and error bars are SD from $n = 10$ leaf discs. Asterisks indicate significant differences based on t-test analysis. ROS experiments were repeated at least twice with similar results.

ted and control-treated *A. thaliana* leaf tissues at different time points and filtered to remove bacteria.

SEM analysis of apoplastic fluids from control and infected leaves revealed the presence of vesicle-like particles and tiny particles, the latter could resemble ribosomes and/or larger protein complexes (Fig. S5A and B). In apoplastic fluids from infected leaves, we additionally observed structures reminiscent of pili and/or flagellar (Fig. S5B).

The size of apoplastic fluid vesicle-like particles determined by both NTA and SEM did not significantly differ between control and infected leaves (Fig. 5A; Fig. S5C). Particle abundance increased upon infection with *Pto* DC3000 (Fig. 5B), consistent with previous findings (49). Increased particle abundance correlated with both bacterial infection time and titers (Fig. 5B; Fig. S6A and B). We also analyzed EVs from the apoplastic fluids of plants that were co-treated with 100 nM flg22 and *Pto* DC3000. Particle numbers were lower than those recovered from *Pto* DC3000 infection only, consistent with induced plant resistance and not significantly different from plants only stimulated with flg22 (Fig. 5C; Fig. S6C). Taken together, comparing the particle profiles of fluids isolated from *Pto* DC3000-infected plants with flg22 immune-stimulated plants, both the higher particle number and the polydisperse particle size hint at bacterial-derived EVs present in the apoplast of infected *A. thaliana*.

Since *Pto* DC3000 (fluid sample) and *A. thaliana* (apoplastic fluid samples) EVs did not significantly differ in diameter (Fig. 1E and 5A), we focused on the charge of EVs, reflecting the different surface composition of bacterial (prokaryotic) and plant-derived (eukaryotic) EVs. Evaluation of the mean ζ -potential identified significantly less negatively charged EVs recovered from apoplastic fluids of *Pto* DC3000-infected plants at 3 days post-infection (dpi) compared with control treatments and earlier time points (Fig. 5C). This time point correlated with *in planta* bacterial proliferation and depended on bacterial inoculum (Fig. S6A and B). Plotting the relative particle abundance over particle charge, the ζ -potential profiles of EVs recovered from apoplastic fluids of untreated, control-treated, and flg22-treated *A. thaliana* identified major peaks around -32 mV (Fig. 5D; Fig. S6J). By contrast, the ζ -potential profile of EVs recovered from apoplastic fluids of *Pto* DC3000-infected *A. thaliana* had a broader distribution with a similar major peak around -32 mV and an additional shoulder around -10 mV (Fig. 5E; Fig. S6K). Comparison of the different ζ -potential profiles revealed similarities of the major -32 mV peak across all plant samples, likely representing a plant-derived EV pool. Notably, the shoulder around -10 mV detected from apoplastic fluids of *Pto* DC3000-infected plant samples showed an overlay with the ζ -potential profile of EV recovered from *Pto* DC3000 cultures (fluid samples), with a peak from -20 mV to 0 mV (Fig. 5F and G). This could, therefore, represent a bacterial-derived EV pool. Since the ζ -potential profiles of EVs recovered from

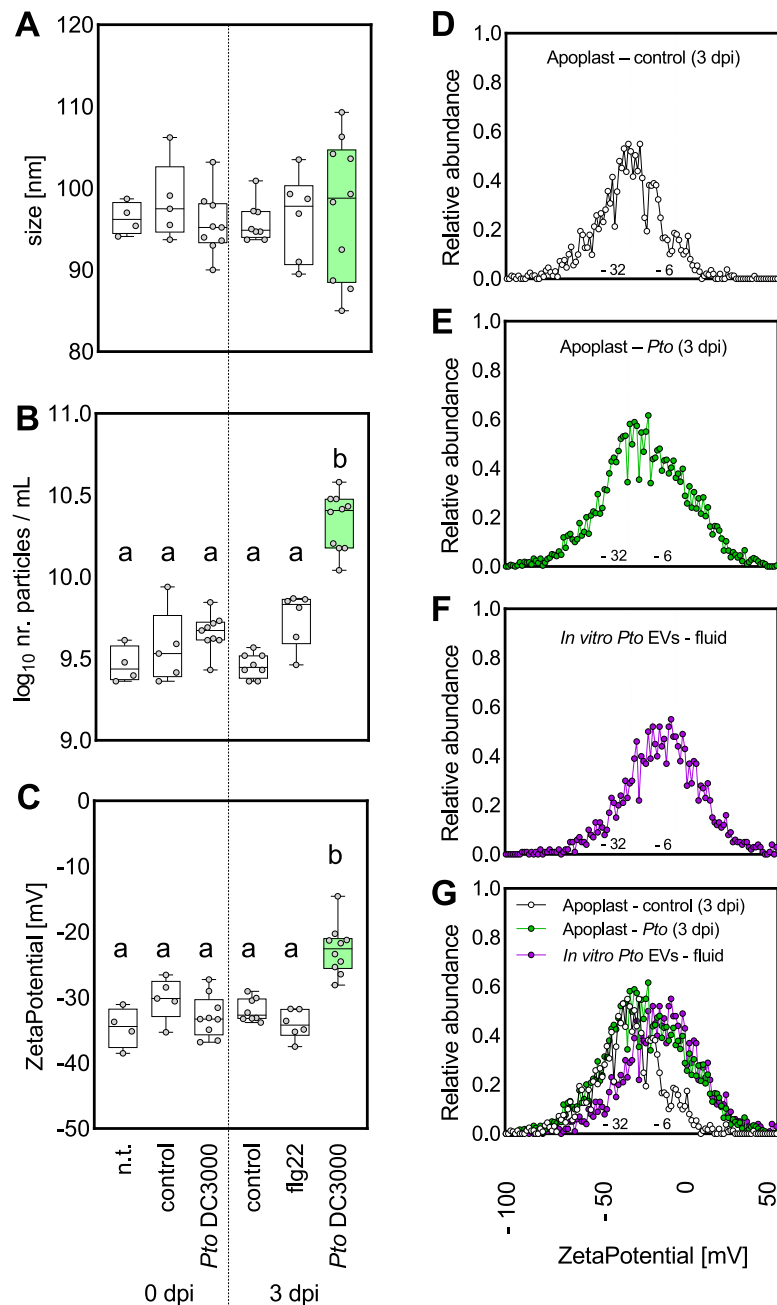


FIG 5 *Pto* DC3000 release EVs *in planta*. Size, concentration, and charge measurements of apoplastic fluids from *A. thaliana* plants (5–6 weeks old) infected with *Pto* DC3000. (A) Size of the particles. (B) Particle concentration in apoplastic fluids. (C) ζ -Potential of the particles. For A–C, the variants represent: n.t., nontreatment ($n = 4$); control, 10 mM MgCl₂ (0 dpi, $n = 5$; 3 dpi, $n = 8$); *Pto* DC3000 (OD₆₀₀ = 0.0006) (0 dpi, $n = 9$; 3 dpi, $n = 10$); 100 nM flg22 (3 dpi, $n = 6$). Experiments A–C were performed in three biological repeats with similar results. (D–G) The profile of ζ -potential for particles detected in *Arabidopsis* apoplast treated with MgCl₂ (control; D) for 3 days, with *Pto* DC3000 (*Pto*; OD₆₀₀ = 0.0006; E) for 3 days and with EVs from *Pto* DC3000 grown in culture (fluid; F). The dots represent the mean from 8 (D and G, white), 10 (E and G, green), and 13 (F and G, purple) biologically independent samples. The boxplots extend from 25th to 75th percentiles, whiskers go down to the minimal value and up to the maximal value, and the line in the middle of the box represents the median. The dots represent values of independent samples. Different letters indicate significant differences (one-way analysis of variance with Tukey post hoc test; $P < 0.05$). The green color is highlighting the particles from *Pto* DC3000-infected plants (3 dpi).

apoplastic fluids of flg22-treated *A. thaliana* did not differ between untreated and control-treated leaves (Fig. S6J), we found no evidence that plant EVs modulate their surface charge during infection.

Pto DC3000 EV-associated proteins are detected during plant infection

We next aimed to identify EV-associated proteins that could be used as markers for *Pto* DC3000 EVs *in planta*. To this end, we addressed whether the protein composition of EVs from *Pto* DC3000 and EVs from related bacteria shares similarities. We focused on three published *P. aeruginosa* PAO1 EV proteomes since a number of EV proteomes have been reported from *P. aeruginosa* (50–52). We found that 103 proteins were identified in the EV proteomes across the three reports (50–52). Of the 103 shared EV proteins from PAO1, we could identify 100 orthologous proteins encoded in the *Pto* DC3000 genome, and 44 proteins were enriched in *Pto* DC3000 EVs (Table 2; Table S1). We refer to these as the EV “core.” These proteins were highly enriched in localization to the OM (44%) and cytoplasmic membrane (26%) (Fig. S7A), consistent with EVs released in the form of OMVs. From these 44 proteins, 20 were putative OM-localized proteins and thus represent good candidate biomarkers for the detection of EVs (Table S1; Fig. 2C, blue labeling). To gain insights into the expression of the EV “core” encoding genes during infection, we searched available transcriptome data (33), which revealed two clusters of generally lower or higher expression levels across the conditions (Fig. S7B). Of the genes coding for EV “core” proteins, a majority encoding OM-localized and cytoplasmic proteins were upregulated *in planta* (Table S1), which suggests their presence during bacterial infection.

One of the predicted EV markers is OprF (Fig. 2C, black labeling), which we used for immunodetection of *Pto* DC3000 EVs *in planta* and purified from *Pto* DC3000 cultures. OprF is a porin integral to the OM and found in EVs of *P. aeruginosa* (53). Using anti-OprF antibodies, we identified specific bands in filtered apoplastic fluids of *A. thaliana* leaves infected with *Pto* DC3000 at 2 and 3 dpi but not in control-treated plants (Fig. 6A). In combination with using anti-TET8 (anti-TETRASPA^N 8) antibodies, we could confirm that the apoplastic fluids of control and infected leaves contain both plant-derived and

TABLE 2 List of candidate EV marker proteins

Locus tag	UniProt ID	Subcellular localization	Name	Other
PSPTO_0554	Q88A43	Outer membrane	Organic solvent tolerance protein	
PSPTO_0569	Q88A28	Outer membrane	Autotransporting lipase, GDSL family	EV unique detected
PSPTO_1207	Q887S9	Outer membrane	Iron(III) dicarboxylate transport protein fecA	Siderophore transport
PSPTO_1296	Q887J6	Outer membrane	Porin B	
PSPTO_1437	Q886Y7	Outer membrane	Lysyl-tRNA synthetase	
PSPTO_1542	Q886N5	Outer membrane	Outer membrane protein	
PSPTO_1720	Q885W1	Outer membrane	Outer membrane protein	
PSPTO_2272	Q883S8	Outer membrane	Outer membrane lipoprotein Oprl	
PSPTO_2299	Q883Q1	Outer membrane	Outer membrane porin OprF	
PSPTO_3229	Q880E1	Outer membrane	Filamentous hemagglutinin, intein containing	
PSPTO_3294	Q87ZX8	Outer membrane	TonB-dependent siderophore receptor	Siderophore transport
PSPTO_3971	Q87Y41	Outer membrane	Peptidoglycan-associated lipoprotein	
PSPTO_3987	Q87Y25	Outer membrane	Porin D	beta-Lactam resistance
PSPTO_4115	Q87XR1	Outer membrane	Lipoprotein SlyB	
PSPTO_4366	Q87X24	Outer membrane	Iron-regulated protein A	
PSPTO_4839	Q87VU6	Outer membrane	Hypothetical protein	
PSPTO_4940	Q87VJ6	Outer membrane	HflK protein	
PSPTO_4977	Q87VG0	Outer membrane	Outer membrane efflux protein TolC	Bacterial secretion system
PSPTO_5031	Q87VA8	Outer membrane	Type IV pilus biogenesis protein PilJ	beta-Lactam resistance; EV unique detected
PSPTO_5391	Q87UB4	Outer membrane	Outer membrane porin, OprD family	

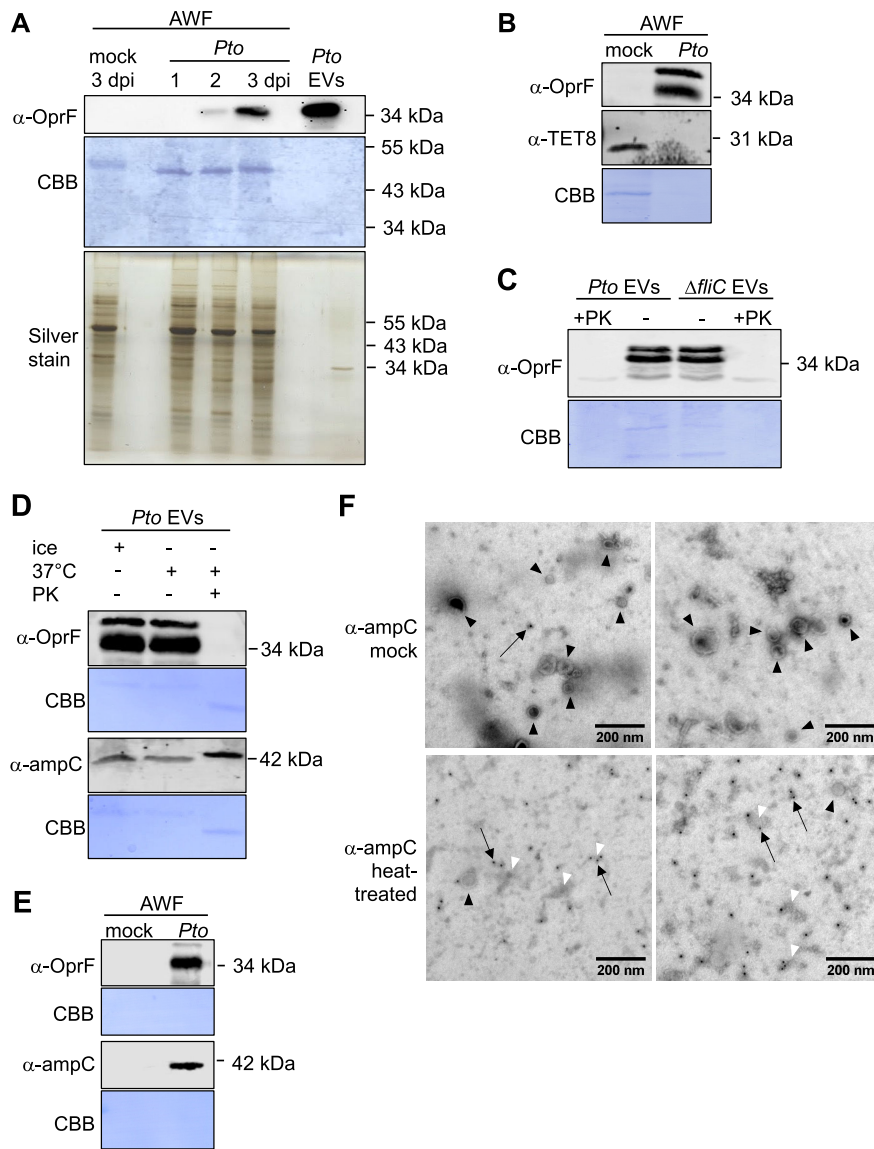


FIG 6 *Pto* DC3000 EV-enriched proteins can be detected in EV samples from filtered apoplastic wash fluids of infected plants. (A) OprF antibodies detect bands in apoplastic fluids (AWF) from *A. thaliana* infected with *Pto* DC3000 and in gradient-collected EVs. Coomassie brilliant blue (CBB) and silver staining show protein loading, evidently lower in gradient-collected EV samples. Similar results were observed in at least three independent experiments. (B) OprF-positive *Pto* DC3000 EVs are detected in apoplastic fluids containing TET8-positive EVs from infected *A. thaliana*. (C) Gradient-collected EVs from *Pto* DC3000 WT and $\Delta fliC$ mutants show proteinase K (PK)-sensitive detection of OprF. (D and E) β -Lactamase antibodies ampC detect bands in gradient-collected EVs independent of PK treatment (D) and in apoplastic fluids from *A. thaliana* infected with *Pto* DC3000 at 3 dpi (E). Here, the blot was incubated with α -ampC antibodies o/n at 4°C. (B through E) CBB shows protein loading, evidently reduced by PK treatment. Similar results were observed in at least three independent experiments. (F) Immunogold staining of gradient-collected *Pto* DC3000 EVs using ampC antibodies. Several intact EVs (black arrowheads) were present in mock-treated samples, mostly not immunogold labeled (black arrow). Only in rare cases, gold particles were found at membranous debris. In heat-treated samples, a large amount of membranous structures (gray areas, white arrowheads) were observed, likely due to the disruption of EVs by the heat treatment. Here, immunogold labeling was observed at the membranous debris (some gold particles are indicated with white arrows). Two representative images are shown for each condition.

bacterial EVs (Fig. 6B). OprF-positive EVs were also detected from the *Pto* DC3000 Δ fliC mutant (Fig. 6C), confirming successful purification of EVs from this strain. However, OprF could not be detected in proteinase K-treated EVs (Fig. 6C). In *P. aeruginosa*, OprF is a general porin of the OM (54) and, consistently, we detected OprF also in the proteome of the OM samples (Table S1). It is thus possible that the immunogenic epitope recognized by the anti-OprF antibodies is located at the external side of the EVs, making it sensitive to proteinase K treatment. It is currently emerging that the EV surface corona plays roles in EV functions (55), and it is possible that OprF might be part of the *Pto* DC3000 EV corona.

We next aimed to identify an EV-enriched protein localized to the EV lumen and explored available antibodies. For example, EVs of *Stenotrophomonas maltophilia* contained β -lactamase (56). Given that two genes annotated with the “ β -lactam resistance” function were present in cluster III and although not detected in our proteome samples, we reasoned that β -lactamase could be present in *Pto* DC3000 EVs. Using anti- β -lactamase antibodies, we identified a specific band in gradient-collected EV samples of cultured *Pto* DC3000, which was also detected after proteinase K treatment (Fig. 6D; Fig. S7C). In addition, a band could be revealed in apoplastic fluids collected from *Pto* DC3000-infected leaves, suggesting the presence of β -lactamase-positive *Pto* DC3000 EVs in these samples (Fig. 6E; Fig. S7C). We explored immuno-negative staining to gain further insights into the localization of β -lactamase in *Pto* DC3000 EVs (Fig. 6F). In mock samples, several intact vesicles were found yet without significant immunogold labeling. Only in rare cases, gold particles were observed at membranous debris. By contrast, after breaking up the vesicles by heat treatment, the membraneous structures showed clear immunogold labeling as several gold particles were observed at these structures. This suggests that β -lactamase was more accessible to ampC immunogold labeling when EVs were disrupted, consistent with β -lactamase present in the lumen of *Pto* DC3000 EVs. Having identified two possible markers for *Pto* DC3000 EVs, membrane-bound OprF and soluble β -lactamase located at the external side and the lumen of EVs, respectively, these data provide additional evidence that *Pto* DC3000 releases EVs *in planta* during infection.

DISCUSSION

A range of activities has been associated with bacterial EVs during infection. This includes modulation of host immunity (PAMPs, effectors, and bacterial cell wall remodeling), elimination of host defenses (antibiotic tolerance and decoys), and acquisition of nutrients from the host (metal ions) (57). In this study, we used a proteomics approach aiming to gain insights into the presence and role of *Pto* DC3000 EVs during plant infection.

PTI responses to *Pto* DC3000 involve recognition by FLS2, EFR, and LIPO-OLIGO-SACCHARIDE-SPECIFIC REDUCED ELICITATION (LORE), which detect immunogenic flg22, elf18, and 3-OH-FAAs, a fatty acid co-purifying with LPS (58). EVs from bacterial phytopathogens are enriched in EF-Tu and LPS (25, 26, 28), suggesting the presence of elf18 and 3-OH-FAAs. Bahar et al. demonstrated that BRI1-ASSOCIATED KINASE 1 (BAK1) and SUPPRESSOR OF BIR 1 (SOBIR1), interacting co-receptors of PRRs (pattern recognition receptors), mediate the immunogenic perception of EVs from *X. campestris* pv. *campestris* (25). We show that vesicle samples from *Pto* DC3000 elicit immune responses that are dependent on FLS2 and the presence of flagellin in EV samples (Fig. 4 thorough G). Since flagella proteins such as FlxC have a specific affinity for EVs and are involved in EV production in *Escherichia coli* (40), they could be considered external EV cargoes. However, filamentous structures were observed in SEM analysis (Fig. 1B). It is, therefore, possible that flagella co-purify with the *Pto* DC3000 EV samples despite depleting extracellular components from EV samples by density gradient centrifugation. Contamination of flagella in EVs was reported to contribute to the detection of FlxC in EVs from *P. aeruginosa* (59).

In contrast to our results, McMillan et al. reported significant seedling growth repression in response to *Pto* DC3000 EVs (30). This disparity in results may be due to several factors, including differences in the growth conditions of both the bacterial cultures and the *A. thaliana* seedlings, the type of biochemical isolation of EVs and vesicle dose, e.g., resulting in different amounts of co-purifying flagella. The stronger protective immune response observed by McMillan et al. may also be due to such differences in experimental procedures (30). Importantly, EVs purified from *Pto* DC3000 *fliC* mutant bacteria did not significantly induce defense gene expression (Fig. 4G). This non-significant immunogenicity of *Pto* DC3000 EVs would be congruous with *Pto* DC3000 releasing EVs in favor of plant infection.

The plant's apoplast, which is the niche colonized by *Pto* DC3000, represents an environment where bacteria are challenged with plant defense molecules, competition with members of the microbiome, and acquisition of nutrients (33). Bacteria respond to environmental stress with the production of EVs, which allows for cell surface remodeling, secretion of degraded and damaged cargo, and uptake of nutrients in bacterial communities, e.g., by packaging transporters in EVs (14, 20, 60). The hypothesis that *Pto* DC3000 may use EVs to adapt to the host environment is evidenced by our finding that *Pto* DC3000 EVs contain β-lactamase (Fig. 6D). Several studies demonstrated that EVs can improve bacterial survival during antibiotic exposure. *S. maltophilia* produced more EVs upon treatment with the β-lactam antibiotic imipenem (56, 61). Its EVs contained β-lactamase and increased *S. maltophilia* survival in the presence of antibiotics (56). Plants defend infection by upregulation of many defense-related genes, including genes coding for antimicrobial peptides (62). Likewise, the host microbiome protects plants against infectious pathogens (63). It is possible that *Pto* DC3000 produces EVs to counter the action of plant- and microbe-derived antimicrobial peptides, i.e., its EVs could improve antimicrobial resistance of *Pto* DC3000 (64, 65).

Proteins involved in siderophore transport were enriched in the EVs from cultured bacteria (Fig. 2C). Siderophores are important virulence factors of bacterial pathogens, directly competing for iron with the host (66). Since the ability of *Pto* DC3000 for iron acquisition is correlated with its growth *in planta* (33), siderophores and their transport are likely to play roles in *Pto* DC3000 infection success. Interestingly, the expression of genes coding for all siderophore transport proteins enriched in EVs was upregulated *in planta* compared with *in vitro* conditions as well as downregulated upon induction of PTI (Fig. 3D). Thus, regulation of siderophore transport proteins can be considered as an adaptive response of *Pto* DC3000 to iron/metal ion availability, and secretion into EVs may allow improved acquisition of iron, analogous to EV secretion of the siderophore mycobactin in *Mycobacterium tuberculosis* (67). In addition, the ability of siderophore uptake into EVs may prevent activation of immunity as siderophores can trigger immune responses (66). Taken together, we propose that *Pto* DC3000 produces EVs to improve its growth ability both in culture and *in planta*. Having identified two markers for *Pto* DC3000 EVs, membrane-bound OprF detected as external EV cargo and β-lactamase as luminal EV cargo, future studies to determine the composition of EVs *in planta* and track their interaction with plant cells are now becoming possible.

MATERIALS AND METHODS

Bacterial strains and growth

Pto DC3000 used in this study was routinely cultured at 28°C in King's B (KB) medium containing 50 µg/mL rifampicin at 180 rpm and on plates with 1% agar without agitation. Planktonic growth was performed in 500 mL cultures, and growth rates were measured over time as OD₆₀₀. *Pto* DC3000 Δ*fliC* was cultivated at 28°C in KB medium containing 50 µg/mL rifampicin and 5 µg/mL chloramphenicol at 180 rpm (68).

Plant material and growth conditions

A. thaliana ecotype Columbia (Col-0), *pFRK1::GUS* (69), *fls2c* (42), and *efr-1* (70) mutants were used in this study. For bacterial infections and ROS assays, Col-0 plants were soil grown at 21°C–22°C and 8-hour photoperiod. For β-glucuronidase (GUS) assays, RT-qPCR (reverse transcription-quantitative polymerase chain reaction) analysis, and induced growth arrest, seedlings were sterile grown on Murashige and Skoog (MS) plates supplemented with 1% sucrose and 1.5% gelrite (Duchefa, the Netherlands) pH 5.8 for 4 days (after 2–4 days stratification in the dark at 4°C), then transferred to 96-well plates containing 150 μL 1/2 MS medium supplemented with 1% sucrose per well and grown for 11–12 days at 22°C and 16-hour photoperiod (120–150 μE·m⁻²·s⁻¹).

Extraction and purification of bacterial EVs

EVs were routinely isolated from planktonic cultures across growth phases (Fig. S8A). The starting inoculum was OD₆₀₀ = 0.01. Samples were taken according to incubation time, evidently slightly differing in the then measured OD₆₀₀, and therefore, we indicate a range of colony-forming units per milliliter bacterial density, from which EVs were collected. One hundred milliliters of planktonic bacteria (grown in liquid cultures) and 10 mL of biofilm bacteria (grown on plates, collected, and resuspended), respectively, were pelleted at 4,500 × g for 2 × 20 minutes, the supernatant was decanted and passed through a 0.22-μm membrane (fluid samples; Fig. S1C). Particles were pelleted from the cell-free supernatant at 100,000 × g for 1.5 hours. The pellet was resuspended in 1.7 mL 1 mM EDTA and loaded on sucrose density step-gradient (1.7 mL of sucrose 25%, 35%, 45%, 50%, and 55%) and centrifuged at 160,000 × g for 18 hours. Two milliliter samples were collected from each of the sucrose density steps and diluted with 1 mM EDTA to 30 mL. Particles were pelleted at 100,000 × g for 2 hours, and the pellets were each resuspended in 0.16 mL 1 mM EDTA (gradient-collected samples; Fig. S1C). EV samples were immediately frozen in liquid nitrogen. Since most EVs migrated to the 55% density fraction (Fig. S8B), we then collected EVs across fractions 3–5, which were less variable in ζ-potential, and size compared to fractions 1 and 2 (Fig. S8C and D).

Extraction of leaf apoplastic fluids

Apoplastic fluids were collected from leaves of 6–7-week-old plants (Col-0 WT, mock treated, and infected with WT *Pto* DC3000). Rosettes of 22–29 plants were vacuum infiltrated with particle-free 1 mM EDTA. After removing the excess buffer, infiltrated leaves were placed into 20 mL syringes and centrifuged in 50 mL conical tubes at 900 × g for 20 minutes at 4°C. The resulting apoplastic wash was passed through a 0.22-μm membrane (apoplastic fluid samples). To confirm the successful filtering of apoplastic fluids, 5 μL was incubated on LB plates containing 50 μg/mL rifampicin. No *Pto* DC3000 colonies were detected after 3 days. For SEM pictures and immunoblots detecting β-lactamase and TET8, apoplastic fluids were additionally ultracentrifuged for 1 hour at 100,000× g. The pellet was resuspended in 100 μL particle-free 1 mM EDTA.

EV quantification, size, charge measurements, and proteinase K treatment

EVs were quantified and had their size and charge measured by NTA using ZetaView BASIC PMX-120 (Particle Metrix, Germany) at room temperature. To detect EVs, we used the manufacturer's default settings for liposomes. Particle quantification and size measurements were performed by scanning 11 cell positions each and capturing 30 frames per position with the following settings: focus: autofocus; camera sensitivity for all samples: 85; shutter: 100; scattering intensity: detected automatically. After capture, the videos were analyzed by the built-in ZetaView Software 8.05.11 (ZNTA) with the following specific analysis parameters: maximum area: 1,000; minimum area: 5; minimum brightness: 25; trace length: 15 ms; hardware: embedded laser: 40 mW at 488 nm; camera: CMOS. For particle charge measurements, the same settings were used except minimum brightness: 30. Statistical analysis was performed using either one-way

analysis of variance (ANOVA) with Tukey post hoc test or Welsch's ANOVA with Dunnett's T3 multiple comparisons post hoc test.

All samples were diluted in particle-free 1 mM EDTA buffer and checked with NTA. Unconditioned KB medium contained up to 1.4×10^9 particles (Fig. S2A). *Pto* DC3000 cultures contained increasing particle numbers with cultivation time: $\approx 2.8 \times 10^9$ particles at $1.5\text{--}2 \times 10^9$ cfu/mL (50% of influence); $\approx 3.7 \times 10^9$ particles at $2.25\text{--}2.75 \times 10^9$ cfu/mL (37% of influence), $\approx 7 \times 10^9$ particles at $3.75\text{--}4.5$ cfu/mL (20% of influence), and $\approx 1.1 \times 10^{10}$ particles at $5\text{--}5.5 \times 10^9$ cfu/mL (13% of influence) (Fig. S2A). We, therefore, focused our measurements on samples collected from $OD_{600} > 7.5$, which shows lower than 20% influence of particles from the medium. We calculated the colony-forming units per milliliter from measured OD_{600} values (71, 72).

For proteinase K treatment, EVs were incubated with 10 µg/mL proteinase K (NEB, P8107S) or mock treated for 30 minutes at 37°C before boiling in Lämmlie buffer at 95°C for 5 minutes.

Propidium iodide staining

The viability assay was done with some modifications according to reference (73). In brief, *Pto* DC3000 cultures were grown until $OD_{600} = 1\text{--}2$ and $OD_{600} = 3\text{--}4$. Propidium iodide (PI) (Sigma-Aldrich) was added to a final concentration of 20 µM. After 10 minutes incubation time, 5 µL of the stained cultures was transferred to a microscopy slide, and pictures were obtained with a Leica 3D Assay THUNDER Imager (Leica, Wetzlar) using an HC PL Fluotar L 40×/0.60 dry objective. PI was excited at 642 nm, and the emission range was 100%. As a negative control, bacteria were boiled in a microwave for several minutes before PI staining. Two technical replicates were performed for $OD_{600} = 1\text{--}2$ and $OD_{600} = 3\text{--}4$, respectively.

Scanning electron microscopy

Planktonic-grown bacteria at $OD_{600} = 3\text{--}4$ ($1.5\text{--}2 \times 10^9$ cfu/mL), gradient-collected EVs ($0.5\text{--}1.5 \times 10^{10}$ particles), and apoplastic fluids passed through 0.2 µm filters were used for SEM. The cells were chemically fixed using 2.5% glutaraldehyde in 50 mM cacodylate buffer (pH 7.0) containing 2 mM MgCl₂. Then, the cells were applied to a glass slide, covered with a cover slip, and plunged frozen in liquid nitrogen. After this, the cover slip was removed, and the cells were placed in a fixation buffer again. After washing four times with buffer, post-fixation was carried out with 1% OsO₄ for 15 minutes. Two additional washing steps with buffer were followed by three times washing with double distilled water. The samples were dehydrated in a graded acetone series, critical point dried, and mounted on an aluminium stub. To enhance conductivity, the samples were sputter coated with platinum. Microscopy was carried out using a Zeiss Auriga Crossbeam workstation at 2 kV (Zeiss, Oberkochen, Germany). The vesicle size was manually measured across five randomly selected SEM micrographs using Fiji software (74).

Transmission electron microscopy

Planktonic-grown *Pto* DC3000 at $OD_{600} = 3\text{--}4$ ($1.5\text{--}2 \times 10^9$ cfu/mL) was used for ultrathin sectioning and subsequent TEM. The cells were concentrated by centrifugation, and the cells were high-pressure frozen using a Leica HPM100 (Leica Microsystems, Wetzlar, Germany). This was followed by freeze substitution with 0.2% osmium tetroxide, 0.1% uranyl acetate, and 9.3% water in water-free acetone in a Leica AFS 2 (Leica Microsystems, Wetzlar, Germany) as described previously (75). After embedding in Epon 812 substitute resin (Fluka Chemie AG, Buchs Switzerland), the cells were ultrathin sectioned (50–100 nm thickness) and post-stained for 1 minute with lead citrate. TEM of ultrathin sections was carried out with a JEOL F200 cryo-S(TEM), which was operated at 200 kV and at room temperature in the TEM mode. Images were acquired using a bottom-mounted XAROSA 20 mega-pixel CMOS camera (EMSI, Münster, Germany).

For immuno-negative staining, freshly purified EVs from *Pto* DC3000 were used. Herein, 15 µL sample was applied to 175 mesh nickel grids, which had been covered with collodium plastic foil and coated with carbon in advance. After incubation for 5 minutes, the grids were blocked for 25 and 30 minutes with 0.1% BSA (bovine serum albumin) in 1× PBS. After this, the grids were incubated with the primary antibody (rabbit anti-*P. aeruginosa* ampC polyclonal antibody, dilution 1:1,000 or 1:5,000 in 1× PBS) for 30 minutes. This was followed by washing six times for 5 minutes with 0.1% BSA in 1× PBS before adding the secondary antibody (goat-anti-rabbit, coupled to 10 nm colloidal gold, dilution: 1:20) for 30 minutes. After this, the grids were washed 2 × 5 minutes with 0.1% BSA in 1× PBS, 2 × 5 minutes with 1× PBS, and 2 × 5 minutes with sterile water. After blocking with a filter paper, the samples were negatively stained with 1% uranyl acetate for 2 minutes, blotted again on a filter paper, and air dried.

As it is expected that the epitope for immunodetection is on the inside of the EVs, we carried out a heat treatment in parallel to break the EVs open. For this, 15 µL of the sample was applied to 400 mesh carbon-coated copper grids and incubated for 20 minutes at 120°C. From this point on, the treatment of the grids was identical to the protocol above.

The immuno-negative stained samples were investigated using a Zeiss EM912 (Zeiss, Oberkochen, Germany) at 80 kV acceleration voltage. Images were acquired using a 2k × 2k slow-speed CCD camera (TRS Tröndle Restlichverstärker-Systeme, Moorenweis, Germany).

Pto DC3000 infection assay

Overnight plate-grown *Pto* DC3000 cells were resuspended in 10 mM MgCl₂ and diluted to OD₆₀₀ = 0.0006. Using a needle-less syringe, the bacterial suspension was infiltrated into mature leaves of 5–6-week-old plants, three leaves per plant. For pretreatments, gradient-collected EVs from planktonic *Pto* DC3000 (concentration ≈1.10¹⁰) and 0.02 mM EDTA as a negative control and 100 nM flg22 (EZbiolabs) as a positive control were syringe infiltrated into leaves 24 hours prior to *Pto* DC3000 inoculation. Discs of the infected leaves (one disc per leaf, 0.6 cm diameter) were excised at 1, 2, or 3 dpi. The three leaf discs from each plant were pooled and ground in 1 mL 10 mM MgCl₂. Serial dilutions were plated on LB medium with rifampicin (50 µg/mL), and bacterial colonies were counted 1 day after incubation at 28°C. Statistical analysis was performed using a two-tailed Welsch's t-test.

Histochemical GUS staining

The histochemical GUS assay was performed with 11-day-old seedlings. Seedlings were treated with gradient-collected *Pto* DC3000 EVs (concentration ≈1.10¹⁰), 100 nM flg22 (EZbiolabs), or as a control with 0.02 mM EDTA for 18 hours. Treated seedlings were immersed in X-Gluc buffer [2 mM X-Gluc (Biosynth), 50 mM NaPO₄, pH 7, 0.5% (vol/vol) Triton-X100, 0.5 mM K-ferricyanide] for 16 hours at 37°C. Chlorophyll was removed by repeated washing in 80% (vol/vol) ethanol. Observations were made on a WHX 6000 digital microscopy (76). The intensity of the GUS signals was quantified using ImageJ software as described in reference (77).

Fluorimetric GUS assay

For fluorimetric GUS assays, 11–12-day-old seedlings were treated with gradient-collected *Pto* DC3000 EVs (concentration ≈1.10¹⁰) or with 100 nM flg22 (EZbiolabs) or as a control with 0.02 mM EDTA for 18 hours. Treated seedlings were frozen in liquid nitrogen in 2 mL conical tubes containing two clean sterile glass beads and liquid nitrogen. The frozen samples were dry homogenized using a Retch mixer mill (Retch). Homogenized samples were kept on ice and cold (4°C). For total protein extraction, GUS extraction buffer was added as described (78) [50 mM sodium phosphate (pH 7); 10 mM 2-mercaptoethanol; 10mM Na₂EDTA; 0.1% Triton X-100; 0.1% sodium lauryl-sarcosine and

PPIC (plant protease inhibitor cocktail)]. GUS activities were measured fluorimetrically in reaction buffer (see below) using methylumbelliferyl- β -D-glucuronic acid dihydrate (MUG) (Biosynth) as a substrate. Reaction buffer was the same solution as extraction buffer with one modification: PPIC was replaced by 1 mM MUG. The fluorescence was measured using TECAN fluorimeter at excitation 360 nm and emission 465 nm. The enzymatic activity of the sample was calculated to protein concentration measured by Bradford protein assay. The absorbance was measured using TECAN spectrometer absorbance at 595 nm. Statistical analysis was performed using one-way ANOVA with Tukey post hoc test.

RNA extraction and RT-qPCR analysis

Gene transcription analysis was performed with 12-day-old seedlings. The seedlings were treated with gradient-enriched EVs (concentration 1.10^{10}) and 0.02 mM EDTA as control for 3 hours, frozen in liquid nitrogen, and ground with 2.5-mm-diameter silica beads using a homogenizer (Retch, Germany). Total RNA was isolated using a TRIzol reagent (Invitrogen, USA) according to the manufacturer's protocol. The extracted RNA was treated with a DNA-free kit (Ambion, USA). Subsequently, 1 μ g of RNA was converted into cDNA with M-MLV RNase H—Point Mutant reverse transcriptase (Promega Corp., USA) and an anchored oligo dT21 primer (Metabion, Germany). Gene transcription was quantified by qPCR using a LightCycler 480 SYBR Green I Master kit and LightCycler 480 (Roche, Switzerland). The PCR conditions were 95°C for 10 minutes followed by 45 cycles of 95°C for 10 seconds, 55°C for 20 seconds, and 72°C for 20 seconds. Melting curve analyses were then carried out. Relative transcription was normalized to the housekeeping gene AtTIP41 (79). Primers were designed using PerlPrimer v1.1.21 (80). The primers used are AtFRK1_FP, GCCAACGGAGACATTAGAG and AtFRK1_RP, CCATAACGACCTGACT-CATC. Statistical analysis was performed using one-way ANOVA with Tukey post hoc test.

Seedling growth analysis

Four-day-old seedlings were transferred from MS solid media into the liquid MS media in transparent 96-well microplates. Each well contained 100 μ L of media either containing 0.02 mM EDTA as a control or gradient-collected *Pto* DC3000 EVs (concentration $\approx 1.10^{10}$) or with 100 nM flg22 (EZbiolabs) as a positive control. After 8 days, the treated seedlings were dried using a paper towel and then the fresh weight was measured. Based on the weight of each seedling, relative seedling growth (%) to control seedlings was calculated. Statistical analysis was performed using Welsch's ANOVA with Dunnett's T3 multiple comparisons post hoc test two-tailed Student t-test.

ROS measurements

ROS production was determined using the luminol-based assay as previously described (81). Briefly, leaves of 5–6-week-old *A. thaliana* plants were infiltrated with gradient-collected EVs (concentration $\approx 1.10^{10}$) or particles isolated from KB. After 2 hours, discs were excised from the infiltrated leaves and 24 hours incubated in ddH₂O at 22°C. Then, the leaf discs were treated with water as mock and with 100 nM flg22 or 100 nM elf18 (EZbiolabs) to induce the production of ROS. The total photon count was collected for 45 min using a TECAN luminometer. Statistical analysis was performed using a two-tailed Student t-test.

Proteomics

We isolated proteins in parallel from *Pto* DC3000 WC lysates and OM and EVs as described previously (51, 82) and above, respectively. WC, OM, and EVs were isolated from *Pto* DC3000 liquid cultures ($OD_{600} = 3\text{--}4$ ($1.5\text{--}2 \times 10^9$ cfu/mL)). The cells were pelleted via centrifugation ($12,000 \times g$ for 10 minutes).

Briefly, for WC, the pellet was resuspended in 1 mL of 20 mM Tris-HCl (pH 8.0), frozen in liquid nitrogen, three times thawing-freezing, and three times sonicated for

10 minutes at 4°C. The samples were centrifuged at 6,000 $\times g$ for 10 minutes at 4°C, and supernatants were collected and frozen in liquid nitrogen.

For OM preparations, the pellet was resuspended in 1 mL 20 mM Tris-HCl (pH 8.0), sucrose (20%), followed by adding 5 μ L lysozyme (15 mg/mL) and 10 μ L 0.5 M EDTA, incubation for 40 minutes on ice, and adding 20 μ L 0.5 M MgCl₂. After centrifugation at 9,500 $\times g$ for 20 minutes at 4°C, the pellet was resuspended in 1 mL ice-cold 10 mM Tris-HCl (pH 8.0) followed by sonication three times for 10 minutes on ice. The samples were then centrifuged at 8,000 $\times g$ for 5 minutes at 4°C, washed with cold 10 mM Tris-HCl (pH 8.0), resuspended in cold, sterile MilliQ water followed by three times freezing thawing in liquid nitrogen, incubation for 20 minutes at 25°C, and adding the sarcosyl to final concentration 0.5%. The samples were then centrifuged at 40,000 $\times g$ for 90 minutes at 4°C, the pellet was resuspended in ice-cold 10 mM Tris-HCl (pH 8.0), and frozen in liquid nitrogen.

Gradient-collected EVs were isolated from the bacteria cultures as described above (Fig. S1C). The protein concentration in the samples was measured using Bio-Rad Protein Assay which is based on Bradford method (83).

For proteomics, the samples were denatured by addition of 1× SDS loading buffer. In-gel trypsin digestion was performed according to standard procedures (84). Briefly, 2 μ g of EV and OM samples and 20 μ g of WC samples were loaded on a NuPAGE 4%–12% Bis-Tris Protein gels (Thermofisher Scientific, USA), and the gels were run for 3 minutes only. Subsequently, the still not size-separated single protein band per sample was cut, reduced (50 mM DTT), alkylated (55 mM CAA, chloroacetamide), and digested overnight with trypsin (trypsin-gold, Promega).

LC-MS/MS data acquisition

Peptides generated by in-gel trypsin digestion were dried in a vacuum concentrator and dissolved in 0.1% formic acid (FA). LC-MS/MS measurements were performed on a Fusion Lumos Tribrid mass spectrometer (Thermo Fisher Scientific) equipped with an Ultimate 3000 RSLC nano system. Peptides were delivered to a trap column (ReproSil-pur C18-AQ, 5 μ m, Dr Maisch, 20 mm \times 75 μ m, self-packed) at a flow rate of 5 μ L/minute in 100% solvent A (0.1% FA in HPLC grade water). After 10 minutes of loading, peptides were transferred to an analytical column (ReproSil Gold C18-AQ, 3 μ m, Dr Maisch, 400 mm \times 75 μ m, self-packed) and separated using a 50-minute gradient from 4% to 32% of solvent B [0.1% FA in acetonitrile and 5% (vol/vol) DMSO] at 300 nL/minute flow rate. Both nanoLC solvents contained 5% (vol/vol) DMSO.

The Fusion Lumos Tribrid mass spectrometer was operated in data-dependent acquisition and positive ionization mode. MS1 spectra (360–1,300 m/z) were recorded at a resolution of 60,000 using an automatic gain control (AGC) target value of 4e⁵ and maximum injection time (maxIT) of 50 ms. After peptide fragmentation using higher-energy collision-induced dissociation, MS2 spectra of up to 20 precursor peptides were acquired at a resolution of 15,000 with an AGC target value of 5e⁴ and maxIT of 22 ms. The precursor isolation window width was set to 1.3 m/z and normalized collision energy to 30%. Dynamic exclusion was enabled with 20-second exclusion time (mass tolerance \pm 10 ppm).

Computational analysis of proteomes

LFQ values were used in the statistical analysis of proteome data. To select EV-enriched proteins, Welch t-test was used to compare protein intensities between EV and WC samples. The resulting P-values were corrected using the Benjamini–Hochberg (BH) method to control the FDR. The proteins with FDR <0.05 and with the intensity in EV at least twice higher than in WC were selected as EV-enriched proteins ($n = 207$). In addition, we selected proteins that were exclusively identified in at least three (out of four) replicates of EV ($n = 162$). A complete list of EV-enriched proteins is given in Table S1. The functional enrichment analysis of the EV proteins was performed using the DAVID functional annotation tool (36, 37). Cluster maps were generated

using the SEABORN python library (<https://seaborn.pydata.org/>), with small cosmetic changes based on its documentation. Gene clusters were generated by SEABORN default method of hierarchical clustering. These gene clusters were also subjected to functional enrichment analysis using the DAVID functional annotation tool (36, 37).

Database searches

Peptide identification and quantification were performed using MaxQuant (version 1.6.3.4) with its built-in search engine Andromeda (85, 86). MS2 spectra were searched against a *Pto* protein database (UP000002515, downloaded from Uniprot 04.05.2020) supplemented with common contaminants (built-in option in MaxQuant). For all MaxQuant searches, default parameters were employed. Those included carbamidomethylation of cysteine as a fixed modification and oxidation of methionine and N-terminal protein acetylation as variable modifications. Trypsin/P was specified as a proteolytic enzyme. Precursor tolerance was set to 4.5 ppm, and fragment ion tolerance to 20 ppm. Results were adjusted to 1% FDR on peptide spectrum match and protein level, employing a target-decoy approach using reversed protein sequences. LFQ algorithm was enabled. The minimal peptide length was defined as seven amino acids, and the "match-between-run" function was not enabled. Each sample type (EV, OM, WC) was analyzed in biological quadruplicates (Table S1).

We used available localization prediction data from the *Pseudomonas* genome database (*pseudomonas.com*) (87). Predicted protein localizations are presented as stacked bar charts (made in MS Excel) as a percentage of the total number of proteins in the analyzed sample. We used the available software DAVID bioinformatic resource 6.8 (<https://david.ncifcrf.gov/>) for GO term and KEGG (Kyoto Encyclopedia of Genes and Genomes) pathway analysis, and the adjusted *P*-value cutoff was set to 0.05 (36, 37). We compared the EV-enriched proteins from *Pto* DC3000 with EV proteomes from planktonic-grown *P. aeruginosa* PAO1 (51, 52, 82). We focused on the proteins that were identified in OMVs from *P. aeruginosa* PAO1 across all three studies and identified their gene orthologs in *Pto* DC3000 using the *Pseudomonas* genome database (*pseudomonas.com*) (87). This set of proteins was compared with the *Pto* DC3000 EV-enriched proteins to predict EV biomarkers. The EV-enriched proteins were also compared with available *in planta* *Pto* DC3000 transcriptome and proteome datasets (11, 33).

Immunoblot analysis

Immunoblot analysis was performed according to Sambrook and Russel (1989) (88). And 10% SDS-PAGE gels were blotted onto PVDF Immobilon-P membranes (Millipore). *Pto* DC3000 OprF was detected using 1:2,000 diluted rabbit polyclonal antibody against OprF from *P. aeruginosa* (Cusabio Biotech Co.; CSB-PA318417LA01EZK); flagellin was detected using 1:300 diluted antibody (68); β-lactamase was detected using 1:2,000 diluted rabbit polyclonal antibody against ampC from *P. aeruginosa* (Cusabio Biotech Co.; CSB-PA326492HA01EZK); and TET8 was detected using 1:500 diluted rabbit polyclonal antibody against TET8 from *Arabidopsis* (PhytoAB, PHY1490S). As secondary antibody, we used a 1:50,000 dilution of the anti-rabbit IgG-peroxidase polyclonal antibody (Sigma-Aldrich, A0545) and 1:5,000 dilution of IRDye 800CW Goat anti-Rabbit IgG Secondary Antibody (LI-COR Biosciences, 926-32211). Signal detection was done using SuperSignal West FemtoMaximum Sensitivity Substrate (Pierce, Thermo Scientific), according to the manufacturer's instructions, and the images were captured using Vilber Lourmat Peqlab FUSION SL Gel Chemiluminescence Documentation System. For detection of the IRDye 800CW Goat anti-Rabbit IgG Secondary Antibody, we used the Odyssey CLx Near-Infrared Fluorescence Imaging System Odyssey CLx (LI-COR, Biosciences).

Coomassie brilliant blue and silver staining

Proteins were separated on 10% SDS-PAGE gels using Hoefer's vertical electrophoresis system (SE250, Hoefer). The gels were subsequently either incubated with Coomassie brilliant blue G-250 staining buffer at room temperature, or the silver staining was performed using ROTI Black P kit (L533, Carl Roth) following the protocol provided by the manufacturer.

Statistical analysis

Student *t*-test, Welsch's *t*-test, one-way ANOVA followed by Tukey multiple comparisons test, and Welsch's ANOVA with Dunnett's T3 multiple comparisons post hoc test were performed using GraphPad Prism version 8.3 for Windows, GraphPad Software, San Diego, CA, USA, www.graphpad.com.

ACKNOWLEDGMENTS

We'd like to thank members of the Robatzek laboratory for fruitful discussions and Eliana Mor for support with sampling. We acknowledge Youssef Belkadir (GMI) for sharing the anti-flagellin antibody and the Pto DC3000 ΔfliC mutant, Lucia Grenga and Catriona Thompson (JIC), Franziska Hackbarth and Hermine Kienberger (BayBioMS) for their laboratory assistance, Miriam Abele for her mass spectrometric support at the BayBioMS as well as Jennifer Grünert and Cornelia Niemann (LMU Biocenter) for technical assistance in electron microscopy, and Oksana Iakovenko (USB) for help with taking seedling pictures.

This research was supported by the Deutsche Forschungsgemeinschaft (to S.R.) through a Heisenberg fellowship (RO 3550/14-1) and the SFB924 "Yield" (TP B15). M.J. was supported by the European Structural and Investment Funds, OP RDE-funded project "CHEMFELLS4UCTP" (no. CZ.02.2.69/0.0/0.0/17_050/0008485) and MEYS (from EU Operational Programme) the nr. CZ.02.2.69/0.0/0.0/18_053/0016975.

A.K. was funded by the DFG (INST 86-1852-1 and project number 491090170). Initial stages of this research were supported by the Gatsby Foundation (to S.R., E.S., F.M., J.S.).

M.J. and S.R. designed research; M.J., K.R., L.K., C.M., A.K., and C.L. performed research; M.J., K.R., L.K., C.M., O.F.-J., B.S., A.B., A.K., C.L., and S.R. analyzed data; E.S., J.S., F.M., and J.M. developed protocols; M.J. and S.R. wrote the paper with inputs from all authors.

AUTHOR AFFILIATIONS

¹LMU Munich Biocenter, Ludwig-Maximilian-University of Munich, Munich, Germany

²Department of Biochemistry and Microbiology, University of Chemistry and Technology Prague, Prague, Czechia

³Faculty of Science, University of South Bohemia in České Budějovice, České Budějovice, Czechia

⁴Bavarian Center for Biomolecular Mass Spectrometry (BayBioMS), Technical University of Munich, Gregor-Mendel-Strasse, Freising, United Kingdom

⁵The Sainsbury Laboratory, Norwich Research Park, Norwich, United Kingdom

⁶John Innes Centre, Norwich Research Park, Norwich, United Kingdom

⁷University of East Anglia, Norwich Research Park, Norwich, United Kingdom

AUTHOR ORCIDs

Silke Robatzek  <http://orcid.org/0000-0002-9788-322X>

FUNDING

Funder	Grant(s)	Author(s)
Deutsche Forschungsgemeinschaft (DFG)	RO 3550/14-1,SFB924/TP B15	Silke Robatzek

Funder	Grant(s)	Author(s)
European structural funds to Czech Republic	CZ.02.2.69/0.0/0.0/17_050/0008485, CZ.02.2.69/0.0/0.0/18_053/0016975	Martin Janda
Deutsche Forschungsgemeinschaft (DFG)	INST 86-1852-1 and project number 491090170	Andreas Klingl

AUTHOR CONTRIBUTIONS

Martin Janda, Data curation, Formal analysis, Investigation, Writing – review and editing, Methodology | Katarzyna Rybak, Data curation, Formal analysis, Investigation, Methodology | Laura Krassini, Formal analysis, Investigation, Methodology | Chen Meng, Data curation, Formal analysis, Investigation, Methodology | Oséias Feitosa-Junior, Formal analysis, Visualization | Egidio Stigliano, Investigation, Methodology | Beata Szulc, Investigation | Jan Sklenar, Methodology | Frank L.H. Menke, Methodology | Jacob G. Malone, Investigation | Andreas Brachmann, Investigation | Andreas Klingl, Formal analysis, Investigation, Methodology | Christina Ludwig, Data curation, Formal analysis, Investigation, Methodology, Writing – review and editing | Silke Robatzek, Conceptualization, Funding acquisition, Project administration, Supervision, Visualization, Writing – original draft, Writing – review and editing

DATA AVAILABILITY

The mass spectrometry proteomics data have been deposited to the ProteomeXchange Consortium via the PRIDE (89) partner repository with the dataset identifier [PXD023971](#).

ADDITIONAL FILES

The following material is available [online](#).

Supplemental Material

Supplemental legends and Figure S1 (Supplemental Information and Figure S1.pdf).

Supplemental legends; observation and isolation of *Pto* DC3000 EVs.

Figure S2 (mBio03589-22-s0002.pdf). Characteristics of *Pto* DC3000 EV isolation.

Figure S3 (mBio03589-22-s0003.pdf). Characteristics of the proteomic analysis.

Figure S4 (mBio03589-22-s0004.pdf). Immunogenicity of *Pto* DC3000 EVs.

Figure S5 (mBio03589-22-s0005.pdf). Isolation and observation of vesicles in apoplastic fluids.

Figure S6 (mBio03589-22-s0006.pdf). Biophysical parameters of particles in apoplastic fluids from *A. thaliana* plants infected with *Pto* DC3000.

Figure S7 (mBio03589-22-s0007.pdf). Selecting candidate EV biomarkers.

Figure S8 (mBio03589-22-s0008.pdf). Biophysical parameters of *Pto* DC3000 EVs across fractions from gradient enrichment.

Table S1 (mBio03589-22-s0009.xlsx). Proteomics data.

Table S2 (mBio03589-22-s0010.xlsx). GO analysis.

REFERENCES

- Büttner D, Bonas U. 2010. Regulation and secretion of *Xanthomonas* virulence factors. *FEMS Microbiol Rev* 34:107–133. <https://doi.org/10.1111/j.1574-6976.2009.00192.x>
- Mansfield J, Genin S, Magori S, Citovsky V, Sriariyanum M, Ronald P, Dow M, Verdier V, Beer SV, Machado MA, Toth I, Salmon G, Foster GD. 2012. Top 10 plant pathogenic bacteria in molecular plant pathology. *Mol Plant Pathol* 13:614–629. <https://doi.org/10.1111/j.1364-3703.2012.00804.x>
- Wilson M, Campbell HL, Ji P, Jones JB, Cuppels DA. 2002. Biological control of bacterial speck of tomato under field conditions at several locations in North America. *Phytopathology* 92:1284–1292. <https://doi.org/10.1094/PHYTO.2002.92.12.1284>
- Melotto M, Underwood W, Koczan J, Nomura K, He SY. 2006. Plant stomata function in innate immunity against bacterial invasion. *Cell* 126:969–980. <https://doi.org/10.1016/j.cell.2006.06.054>
- Xin XF, He SY. 2013. *Pseudomonas syringae* pv. *tomato* DC3000: a model pathogen for probing disease susceptibility and hormone signaling in plants. *Annu Rev Phytopathol* 51:473–498. <https://doi.org/10.1146/annurev-phyto-082712-102321>
- Xin XF, Kvitko B, He SY. 2018. *Pseudomonas syringae*: what it takes to be a pathogen. *Nat Rev Microbiol* 16:316–328. <https://doi.org/10.1038/nrmicro.2018.17>

7. Yuan M, Jiang Z, Bi G, Nomura K, Liu M, Wang Y, Cai B, Zhou JM, He SY, Xin XF. 2021. Pattern-recognition receptors are required for NLR-mediated plant immunity. *Nature* 592:105–109. <https://doi.org/10.1038/s41586-021-03316-6>
8. Couto D, Zipfel C. 2016. Regulation of pattern recognition receptor signalling in plants. *Nat Rev Immunol* 16:537–552. <https://doi.org/10.1038/nri.2016.77>
9. Dodds PN, Rathjen JP. 2010. Plant immunity: towards an integrated view of plant-pathogen interactions. *Nat Rev Genet* 11:539–548. <https://doi.org/10.1038/nrg2812>
10. Kvitko BH, Park DH, Velásquez AC, Wei C-F, Russell AB, Martin GB, Schneider DJ, Collmer A. 2009. Deletions in the repertoire of *Pseudomonas syringae* pv. *tomato* DC3000 type III secretion effector genes reveal functional overlap among effectors. *PLoS Pathog* 5:e1000388. <https://doi.org/10.1371/journal.ppat.1000388>
11. Nobori T, Wang Y, Wu J, Stolze SC, Tsuda Y, Finkemeier I, Nakagami H, Tsuda K. 2020. Multidimensional gene regulatory landscape of a bacterial pathogen in plants. *Nat Plants* 6:1064. <https://doi.org/10.1038/s41477-020-0746-8>
12. Nobori T, Wang Y, Wu J, Stolze SC, Tsuda Y, Finkemeier I, Nakagami H, Tsuda K. 2019. In planta bacterial multi-omics analysis illuminates regulatory principles underlying plant-pathogen interactions. *Plant Biol*. <https://doi.org/10.1101/822932>
13. Nomura K, Debroy S, Lee YH, Pumplin N, Jones J, He SY. 2006. A bacterial virulence protein suppresses host innate immunity to cause plant disease. *Science* 313:220–223. <https://doi.org/10.1126/science.1129523>
14. Schwechheimer C, Kuehn MJ. 2015. Outer-Membrane vesicles from Gram-negative bacteria: biogenesis and functions. *Nat Rev Microbiol* 13:605–619. <https://doi.org/10.1038/nrmicro3525>
15. Bielska E, Birch PRJ, Buck AH, Abreu-Goodger C, Innes RW, Jin H, Pfaffl MW, Robatzek S, Regev-Rudzki N, Tisserant C, Wang S, Weiberg A. 2019. Highlights of the mini-symposium on extracellular vesicles in inter-organismal communication, held in Munich, Germany, August 2018. *J Extracell Vesicles* 8:1590116. <https://doi.org/10.1080/20013078.2019.1590116>
16. Rybak K, Robatzek S. 2019. Functions of extracellular vesicles in immunity and virulence. *Plant Physiol* 179:1236–1247. <https://doi.org/10.1104/pp.18.01557>
17. Raposo G, Stoorvogel W. 2013. Extracellular vesicles: exosomes, microvesicles, and friends. *J Cell Biol* 200:373–383. <https://doi.org/10.1083/jcb.201211138>
18. Roier S, Zingl FG, Cakar F, Durakovic S, Kohl P, Eichmann TO, Klug L, Gadermaier B, Weinzerl K, Prassl R, Lass A, Daum G, Reidl J, Feldman MF, Schild S. 2016. A novel mechanism for the biogenesis of outer membrane vesicles in gram-negative bacteria. *Nat Commun* 7:10515. <https://doi.org/10.1038/ncomms10515>
19. Pérez-Cruz C, Delgado L, López-Iglesias C, Mercade E. 2015. Outer-inner membrane vesicles naturally secreted by gram-negative pathogenic bacteria. *PLoS One* 10:e0116896. <https://doi.org/10.1371/journal.pone.0116896>
20. Toyofuku M, Nomura N, Eberl L. 2019. Types and origins of bacterial membrane vesicles. *Nat Rev Microbiol* 17:13–24. <https://doi.org/10.1038/s41579-018-0112-2>
21. Roszkowiak J, Jajor P, Guła G, Gubernator J, Źak A, Drulis-Kawa Z, Augustyniak D. 2019. Interspecies outer membrane vesicles (Omvs) modulate the sensitivity of pathogenic bacteria and pathogenic yeasts to Cationic peptides and serum complement. *Int J Mol Sci* 20:5577. <https://doi.org/10.3390/ijms20225577>
22. Kaparakis-Liaskos M, Ferrero RL. 2015. Immune modulation by bacterial outer membrane vesicles. *Nat Rev Immunol* 15:375–387. <https://doi.org/10.1038/nri3837>
23. McMillan HM, Kuehn MJ. 2021. The extracellular vesicle generation paradox: a bacterial point of view. *EMBO J* 40:e108174. <https://doi.org/10.1525/embj.2021108174>
24. McMillan HM, Rogers N, Wadle A, Hsu-Kim H, Wiesner MR, Kuehn MJ, Hendren CO. 2021. Microbial vesicle-mediated communication: convergence to understand interactions within and between domains of life. *Environ Sci Process Impacts* 23:664–677. <https://doi.org/10.1039/d1em00022e>
25. Bahar O, Mordukhovich G, Luu DD, Schwessinger B, Daudi A, Jehle AK, Felix G, Ronald PC. 2016. Bacterial outer membrane vesicles induce plant immune responses. *Mol Plant Microbe Interact* 29:374–384. <https://doi.org/10.1094/MPMI-12-15-0270-R>
26. Feitosa-Junior OR, Stefanello E, Zaini PA, Nascimento R, Pierry PM, Dandekar AM, Lindow SE, da Silva AM. 2019. Proteomic and metabolomic analyses of *Xylella fastidiosa* OMV-enriched fractions reveal association with virulence factors and signaling molecules of the DSF family. *Phytopathology* 109:1344–1353. <https://doi.org/10.1094/PHYTO-03-19-0083-R>
27. Chowdhury C, Jagannadham MV. 2013. Virulence factors are released in association with outer membrane vesicles of *Pseudomonas syringae* pv. *tomato* T1 during normal growth. *Biochim Biophys Acta* 1834:231–239. <https://doi.org/10.1016/j.bbapap.2012.09.015>
28. Sidhu VK, Vorhölter F-J, Niehaus K, Watt SA. 2008. Analysis of outer membrane vesicle associated proteins isolated from the plant pathogenic bacterium *Xanthomonas campestris* pv. *campestris*. *BMC Microbiol* 8:87. <https://doi.org/10.1186/1471-2180-8-87>
29. Mitre LK, Teixeira-Silva NS, Rybak K, Magalhães DM, de Souza-Neto RR, Robatzek S, Zipfel C, de Souza AA. 2021. The *Arabidopsis* immune receptor EFR increases resistance to the bacterial pathogens *Xanthomonas* and *Xylella* in transgenic sweet orange. *Plant Biotechnol J* 19:1294–1296. <https://doi.org/10.1111/pbi.13629>
30. McMillan HM, Zebell SG, Ristaino JB, Dong X, Kuehn MJ. 2021. Protective plant immune responses are elicited by bacterial outer membrane vesicles. *Cell Rep* 34:108645. <https://doi.org/10.1016/j.celrep.2020.108645>
31. Klimentová J, Stulík J. 2015. Methods of isolation and purification of outer membrane vesicles from gram-negative bacteria. *Microbiol Res* 170:1–9. <https://doi.org/10.1016/j.micres.2014.09.006>
32. Bachurski D, Schuldner M, Nguyen P-H, Malz A, Reiners KS, Grenzi PC, Babatz F, Schauss AC, Hansen HP, Hallek M, Pogge von Strandmann E. 2019. Extracellular vesicle measurements with nanoparticle tracking analysis - an accuracy and repeatability comparison between Nanosight NS300 and Zetaview. *J Extracell Vesicles* 8:1596016. <https://doi.org/10.1080/20013078.2019.1596016>
33. Nobori T, Velásquez AC, Wu J, Kvitko BH, Kremer JM, Wang Y, He SY, Tsuda K. 2018. Transcriptome landscape of a bacterial pathogen under plant immunity. *Proc Natl Acad Sci U S A* 115:E3055–E3064. <https://doi.org/10.1073/pnas.1800529115>
34. Ashburner M, Ball CA, Blake JA, Botstein D, Butler H, Cherry JM, Davis AP, Dolinski K, Dwight SS, Eppig JT, Harris MA, Hill DP, Issel-Tarver L, Kasarskis A, Lewis S, Matese JC, Richardson JE, Ringwald M, Rubin GM, Sherlock G. 2000. Gene ontology: tool for the unification of biology. The Gene Ontology Consortium. *Nat Genet* 25:25–29. <https://doi.org/10.1038/75556>
35. The Gene Ontology Consortium. 2019. The gene ontology resource: 20 years and still going strong. *Nucleic Acids Res* 47:D330–D338. <https://doi.org/10.1093/nar/gky1055>
36. Huang DW, Sherman BT, Lempicki RA. 2009. Systematic and integrative analysis of large gene Lists using DAVID bioinformatics resources. *Nat Protoc* 4:44–57. <https://doi.org/10.1038/nprot.2008.211>
37. Huang DW, Sherman BT, Lempicki RA. 2009. Bioinformatics enrichment tools: paths toward the comprehensive functional analysis of large gene Lists. *Nucleic Acids Res* 37:1–13. <https://doi.org/10.1093/nar/gkn923>
38. Kulp A, Kuehn MJ. 2010. Biological functions and biogenesis of secreted bacterial outer membrane vesicles. *Annu Rev Microbiol* 64:163–184. <https://doi.org/10.1146/annurev.micro.091208.073413>
39. Kramer J, Özkaya Ö, Kümmel R. 2020. Bacterial siderophores in community and host interactions. *Nat Rev Microbiol* 18:152–163. <https://doi.org/10.1038/s41579-019-0284-4>
40. Manabe T, Kato M, Ueno T, Kawasaki K. 2013. Flagella proteins contribute to the production of outer membrane vesicles from *Escherichia coli* W3110. *Biochem Biophys Res Commun* 441:151–156. <https://doi.org/10.1016/j.bbrc.2013.10.022>
41. Bredow M, Sementchoukova I, Siegel K, Monaghan J. 2019. Pattern-triggered oxidative burst and Seedling growth inhibition assays in *Arabidopsis Thaliana*. *J Vis Exp*. <https://doi.org/10.3791/59437>
42. Zipfel C, Robatzek S, Navarro L, Oakeley EJ, Jones JDG, Felix G, Boller T. 2004. Bacterial disease resistance in *Arabidopsis* through flagellin perception. *Nature* 428:764–767. <https://doi.org/10.1038/nature02485>
43. Wang Y, Garrido-Oter R, Wu J, Winkelmüller TM, Agler M, Colby T, Nobori T, Kemen E, Tsuda K. 2019. Site-specific cleavage of bacterial Mucd by

- secreted proteases mediates Antibacterial resistance in Arabidopsis. *Nat Commun* 10:2853. <https://doi.org/10.1038/s41467-019-10793-x>
44. Vinatzer BA, Teitzel GM, Lee MW, Jelenska J, Hotton S, Fairfax K, Jenrette J, Greenberg JT. 2006. The type III effector repertoire of *Pseudomonas syringae* pv. *syringae* B728a and its role in survival and disease on host and non-host plants. *Mol Microbiol* 62:26–44. <https://doi.org/10.1111/j.1365-2958.2006.05350.x>
45. Lovelace AH, Smith A, Kvittko BH. 2018. Pattern-triggered immunity alters the transcriptional regulation of virulence-associated genes and induces the sulfur starvation response in *Pseudomonas syringae* pv. *tomato* DC3000. *Mol Plant Microbe Interact* 31:750–765. <https://doi.org/10.1094/MPMI-01-18-0008-R>
46. Schechter LM, Vencato M, Jordan KL, Schneider SE, Schneider DJ, Collmer A. 2006. Multiple approaches to a complete inventory of *Pseudomonas syringae* pv. *tomato* DC3000 type III secretion system effector proteins. *Mol Plant Microbe Interact* 19:1180–1192. <https://doi.org/10.1094/MPMI-19-1180>
47. Block A, Alfano JR. 2011. Plant targets for *Pseudomonas syringae* type III effectors: virulence targets or guarded decoys? *Curr Opin Microbiol* 14:39–46. <https://doi.org/10.1016/j.mib.2010.12.011>
48. Tran TM, Chng CP, Pu X, Ma Z, Han X, Liu X, Yang L, Huang C, Miao Y. 2022. Potentiation of plant defense by bacterial outer membrane vesicles is mediated by membrane nanodomains. *Plant Cell* 34:395–417. <https://doi.org/10.1093/plcell/kocab276>
49. Rutter BD, Innes RW. 2017. Extracellular vesicles isolated from the leaf apoplast carry stress-response proteins. *Plant Physiol* 173:728–741. <https://doi.org/10.1104/pp.16.01253>
50. Couto N, Schooling SR, Dutcher JR, Barber J. 2015. Proteome profiles of outer membrane vesicles and extracellular matrix of *Pseudomonas aeruginosa* biofilms. *J Proteome Res* 14:4207–4222. <https://doi.org/10.1021/acs.jproteome.5b00312>
51. Choi DS, Kim DK, Choi SJ, Lee J, Choi JP, Rho S, Park SH, Kim YK, Hwang D, Gho YS. 2011. Proteomic analysis of outer membrane vesicles derived from *Pseudomonas aeruginosa*. *Proteomics* 11:3424–3429. <https://doi.org/10.1002/pmic.201000212>
52. Reales-Calderón JA, Corona F, Monteoliva L, Gil C, Martínez JL. 2015. Quantitative proteomics unravels that the post-transcriptional regulator CRC modulates the generation of vesicles and secreted virulence determinants of *Pseudomonas aeruginosa*. *Data Brief* 4:450–453. <https://doi.org/10.1016/j.dib.2015.07.002>
53. Toyofuku M, Roschitzki B, Riedel K, Eberl L. 2012. Identification of proteins associated with the *Pseudomonas aeruginosa* biofilm extracellular matrix. *J Proteome Res* 11:4906–4915. <https://doi.org/10.1021/pr300395j>
54. Tamber SH, Robert EWH. 2004. The outer membranes of pseudomonads. In Ramos J (ed), *Pseudomonas*. Springer. <https://doi.org/10.1007/978-1-4419-9086-0>
55. Buzas EI. 2022. Opportunities and challenges in studying the extracellular vesicle corona. *Nat Cell Biol* 24:1322–1325. <https://doi.org/10.1038/s41556-022-00983-z>
56. Devos S, Van Putte W, Vitse J, Van Driessche G, Stremersch S, Van Den Broek W, Raemdonck K, Braeckmans K, Stahlberg H, Kudryashev M, Savvides SN, Devreese B. 2017. Membrane vesicle secretion and prophage induction in multidrug-resistant *Stenotrophomonas maltophilia* in response to ciprofloxacin stress. *Environ Microbiol* 19:3930–3937. <https://doi.org/10.1111/1462-2920.13793>
57. Orench-Rivera N, Kuehn MJ. 2016. Environmentally controlled bacterial vesicle-mediated export. *Cell Microbiol* 18:1525–1536. <https://doi.org/10.1111/cmi.12676>
58. Wan W-L, Fröhlich K, Pruitt RN, Nürnberger T, Zhang L. 2019. Plant cell surface immune receptor complex signaling. *Curr Opin Plant Biol* 50:18–28. <https://doi.org/10.1016/j.pbi.2019.02.001>
59. Bauman SJ, Kuehn MJ. 2006. Purification of outer membrane vesicles from *Pseudomonas aeruginosa* and their activation of an IL-8 response. *Microbes Infect* 8:2400–2408. <https://doi.org/10.1016/j.micinf.2006.05.001>
60. Zingl FG, Kohl P, Cakar F, Leitner DR, Mitterer F, Bonnington KE, Rechberger GN, Kuehn MJ, Guan Z, Reidl J, Schild S. 2020. Outer membrane vesiculation facilitates surface exchange and in vivo adaptation of *Vibrio cholerae*. *Cell Host Microbe* 27:225–237. <https://doi.org/10.1016/j.chom.2019.12.002>
61. Devos S, Van Oudenhoove L, Stremersch S, Van Putte W, De Rycke R, Van Driessche G, Vitse J, Raemdonck K, Devreese B. 2015. The effect of imipenem and diffusible signaling factors on the secretion of outer membrane vesicles and associated Ax21 proteins in *Stenotrophomonas maltophilia*. *Front Microbiol* 6:298. <https://doi.org/10.3389/fmicb.2015.00298>
62. Campos ML, de Souza CM, de Oliveira KBS, Dias SC, Franco OL. 2018. The role of antimicrobial peptides in plant immunity. *J Exp Bot* 69:4997–5011. <https://doi.org/10.1093/jxb/ery294>
63. Vogel CM, Potthoff DB, Schäfer M, Barandun N, Vorholt JA. 2021. Protective role of the *Arabidopsis* leaf microbiota against a bacterial pathogen. *Nat Microbiol* 6:1537–1548. <https://doi.org/10.1038/s41564-021-00997-7>
64. Manning AJ, Kuehn MJ. 2011. Contribution of bacterial outer membrane Vesicles to innate bacterial defense. *BMC Microbiol* 11:258. <https://doi.org/10.1186/1471-2180-11-258>
65. Park J, Kim M, Shin B, Kang M, Yang J, Lee TK, Park W. 2021. A novel decoy strategy for polymyxin resistance in *Acinetobacter baumannii*. *eLife* 10:e66988. <https://doi.org/10.7554/eLife.66988>
66. Aznar A, Dellagi A. 2015. New insights into the role of siderophores as triggers of plant immunity: what can we learn from animals? *J Exp Bot* 66:3001–3010. <https://doi.org/10.1093/jxb/erv155>
67. Prados-Rosales R, Weinrick BC, Piqué DG, Jacobs WR, Casadevall A, Rodriguez GM. 2014. Role for *Mycobacterium tuberculosis* membrane vesicles in iron acquisition. *J Bacteriol* 196:1250–1256. <https://doi.org/10.1128/JB.01090-13>
68. Parys K, Colaianni NR, Lee H-S, Hohmann U, Edelbacher N, Trgovcic A, Blahovska Z, Lee D, Mechtler A, Muhari-Portik Z, Madalinski M, Schandry N, Rodríguez-Arévalo I, Becker C, Sonnleitner E, Korte A, Bläsi U, Geldner N, Hothorn M, Jones CD, Dangl JL, Belkhadir Y. 2021. Signatures of antagonistic pleiotropy in a bacterial flagellin epitope. *Cell Host Microbe* 29:620–634. <https://doi.org/10.1016/j.chom.2021.02.008>
69. Kunze G, Zipfel C, Robatzek S, Niehaus K, Boller T, Felix G. 2004. The N terminus of bacterial elongation factor Tu elicits innate immunity in *Arabidopsis* plants. *Plant Cell* 16:3496–3507. <https://doi.org/10.1105/tpc.104.026765>
70. Zipfel C, Kunze G, Chinchilla D, Caniard A, Jones JDG, Boller T, Felix G. 2006. Perception of the bacterial PAMP EF-Tu by the receptor EFR restricts Agrobacterium-mediated transformation. *Cell* 125:749–760. <https://doi.org/10.1016/j.cell.2006.03.037>
71. Jones AM, Wildermuth MC. 2011. The phytopathogen *Pseudomonas syringae* pv. *tomato* DC3000 has three high-affinity iron-scavenging systems functional under iron limitation conditions but dispensable for pathogenesis. *J Bacteriol* 193:2767–2775. <https://doi.org/10.1128/JB.00069-10>
72. Katagiri F, Thilimony R, He SY. 2002. The *Arabidopsis thaliana*-*Pseudomonas Syringae* interaction. *Arabidopsis Book* 1:e0039. <https://doi.org/10.1199/tab.0039>
73. Liang J, Klingl A, Lin Y-Y, Boul E, Thomas-Oates J, Marín M. 2019. A subcompatible rhizobium strain reveals infection duality in *Lotus*. *J Exp Bot* 70:1903–1913. <https://doi.org/10.1093/jxb/erz057>
74. Schindelin J, Arganda-Carreras I, Frise E, Kaynig V, Longair M, Pietzsch T, Preibisch S, Rueden C, Saalfeld S, Schmid B, Tinevez JY, White DJ, Hartenstein V, Eliceiri K, Tomancak P, Cardona A. 2012. Fiji: an open-source platform for biological-image analysis. *Nat Methods* 9:676–682. <https://doi.org/10.1038/nmeth.2019>
75. Flechsler J, Heimerl T, Pickl C, Rachel R, Stierhof YD, Klingl A. 2020. 2D and 3D immunogold localization on (epoxy) ultrathin sections with and without osmium tetroxide. *Microsc Res Tech* 83:691–705. <https://doi.org/10.1002/jemt.23459>
76. Krcková Z, Kocourková D, Danek M, Brouzdová J, Pejchar P, Janda M, Pokotylo I, Ott PG, Valentová O, Martinec J. 2018. The *Arabidopsis thaliana* non-specific phospholipase C2 is involved in the response to *Pseudomonas syringae* attack. *Ann Bot* 121:297–310. <https://doi.org/10.1093/aob/mcx160>
77. Béziat C, Kleine-Vehn J, Feraru E. 2017. Histochemical staining of β-glucuronidase and its spatial quantification. *Methods Mol Biol* 1497:73–80. https://doi.org/10.1007/978-1-4939-6469-7_8
78. Andriankaja A, Boisson-Dernier A, Frances L, Sauviac L, Jauneau A, Barker DG, de Carvalho-Niebel F. 2007. AP2-ERF transcription factors mediate

- Nod factor dependent Mt ENOD11 activation in root hairs via a novel cis-regulatory motif. *Plant Cell* 19:2866–2885. <https://doi.org/10.1105/tpc.107.052944>
79. Czechowski T, Stitt M, Altmann T, Udvardi MK, Scheible WR. 2005. Genome-Wide identification and testing of superior reference genes for transcript normalization in *Arabidopsis*. *Plant Physiol* 139:5–17. <https://doi.org/10.1104/pp.105.063743>
80. Marshall OJ. 2004. Perlprimer: Cross-platform, graphical Primer design for standard, Bisulphite and real-time PCR. *Bioinformatics* 20:2471–2472. <https://doi.org/10.1093/bioinformatics/bth254>
81. Mersmann S, Bourdaïs G, Rietz S, Robatzek S. 2010. Ethylene signaling regulates accumulation of the FLS2 receptor and is required for the oxidative burst contributing to plant immunity. *Plant Physiol* 154:391–400. <https://doi.org/10.1104/pp.110.154567>
82. Park AJ, Murphy K, Krieger JR, Brewer D, Taylor P, Habash M, Khursigara CM. 2014. A temporal examination of the planktonic and biofilm proteome of whole cell *Pseudomonas aeruginosa* PAO1 using quantitative mass spectrometry. *Molecular & Cellular Proteomics* 13:1095–1105. <https://doi.org/10.1074/mcp.M113.033985>
83. Bradford MM. 1976. A rapid and sensitive method for the quantitation of microgram quantities of protein utilizing the principle of protein-dye binding. *Anal Biochem* 72:248–254. <https://doi.org/10.1006/abio.1976.9999>
84. Shevchenko A, Tomas H, Havlis J, Olsen JV, Mann M. 2006. In-gel digestion for mass spectrometric characterization of proteins and proteomes. *Nat Protoc* 1:2856–2860. <https://doi.org/10.1038/nprot.2006.468>
85. Cox J, Neuhauser N, Michalski A, Scheltema RA, Olsen JV, Mann M. 2011. Andromeda: a peptide search engine integrated into the MaxQuant environment. *J Proteome Res* 10:1794–1805. <https://doi.org/10.1021/pr101065j>
86. Tyanova S, Temu T, Cox J. 2016. The MaxQuant computational platform for mass spectrometry-based shotgun proteomics. *Nat Protoc* 11:2301–2319. <https://doi.org/10.1038/nprot.2016.136>
87. Winsor GL, Griffiths EJ, Lo R, Dhillon BK, Shay JA, Brinkman FSL. 2016. Enhanced Annotations and features for comparing thousands of *Pseudomonas* Genomes in the *Pseudomonas* genome database. *Nucleic Acids Res* 44:D646–D653. <https://doi.org/10.1093/nar/gkv1227>
88. Sambrook J, Russell DW. 2001. Molecular cloning: A laboratory manual, . In Cold spring harbor laboratory, 3rd ed. Cold Spring Harbor, N.Y.
89. Perez-Riverol Y, Csordas A, Bai J, Bernal-Llinares M, Hewapathirana S, Kundu DJ, Inuganti A, Griss J, Mayer G, Eisenacher M, Pérez E, Uszkoreit J, Pfeuffer J, Sachsenberg T, Yilmaz S, Tiwary S, Cox J, Audain E, Walzer M, Jarnuczak AF, Ternent T, Brazma A, Vizcaíno JA. 2019. The PRIDE database and related tools and resources in 2019: improving support for quantification data. *Nucleic Acids Res* 47:D442–D450. <https://doi.org/10.1093/nar/gky1106>



Changes in actin dynamics are involved in salicylic acid signaling pathway

Jindřiška Matoušková^{a,d}, Martin Janda^a, Radovan Fišer^b, Vladimír Šašek^c, Daniela Kocourková^c, Lenka Burketová^c, Jiřina Dušková^d, Jan Martinec^c, Olga Valentová^{a,*}

^a Department of Biochemistry and Microbiology, Institute of Chemical Technology Prague, Technická 3, 166 28 Prague 6, Czech Republic

^b Charles University in Prague, Faculty of Science, Albertov 2038/6, 128 00 Prague 2, Czech Republic

^c Institute of Experimental Botany, Academy of Science of the Czech Republic, Rozvojová 263, 165 02 Prague 6 – Lysolaje, Czech Republic

^d Charles University in Prague, Faculty of Pharmacy in Hradec Králové, Heyrovského 1203, 500 05 Hradec Králové, Czech Republic

ARTICLE INFO

Article history:

Received 3 December 2013

Received in revised form 7 February 2014

Accepted 1 March 2014

Available online 11 March 2014

Keywords:

Actin dynamics

Salicylic acid

PR genes

Phosphatidic acid

ABSTRACT

Changes in actin cytoskeleton dynamics are one of the crucial players in many physiological as well as non-physiological processes in plant cells. Positioning of actin filament arrays is necessary for successful establishment of primary lines of defense toward pathogen attack, depolymerization leads very often to the enhanced susceptibility to the invading pathogen. On the other hand it was also shown that the disruption of actin cytoskeleton leads to the induction of defense response leading to the expression of PATHOGENESIS RELATED proteins (PR). In this study we show that pharmacological actin depolymerization leads to the specific induction of genes in salicylic acid pathway but not that involved in jasmonic acid signaling. Life imaging of leaves of *Arabidopsis thaliana* with GFP-tagged fimbrin (GFP-fABD2) treated with 1 mM salicylic acid revealed rapid disruption of actin filaments resembling the pattern viewed after treatment with 200 nM latrunculin B. The effect of salicylic acid on actin filament fragmentation was prevented by exogenous addition of phosphatidic acid, which binds to the capping protein and thus promotes actin polymerization. The quantitative evaluation of actin filament dynamics is also presented.

© 2014 Elsevier Ireland Ltd. All rights reserved.

1. Introduction

During coevolution with their natural enemies, plants evolved very complex and multilevel mechanisms to defend themselves, resulting in relatively very low success rate of invaders. Besides the constitutively based defense such as production of antimicrobial metabolites or structural barriers, plants are endowed with wide range of inducible mechanisms leading to the immune response to the invader. These processes are triggered by the recognition of pathogen common structures; pathogen or microbe associated molecular patterns (PAMPs or MAMPs). These structural determinants are perceived by pattern recognition receptors (PRRs) which in turn initiate downstream early events leading to immune response called PAMP-triggered immunity (PTI). Pathogens are able to overcome PTI by introducing effector molecules into the plant cell promoting the virulence of the pathogen. Plants in turn

produce R proteins (resistance proteins) capable to eliminate the effect of effectors [1]. These early events triggered by pathogen attack are followed by the activation of signaling cascades which are regulated by plant hormones; key players in these processes are salicylic acid (SA), jasmonic acid (JA) and/or ethylene (ET) [2]. These hormones regulate signaling pathways which lead to the massive reprogramming of transcriptome and the expression of defense genes (PATHOGENESIS RELATED, PR) [3,4]. In *Arabidopsis* *PR-1* (anti-fungal with unknown function), *PR-2* (beta-1,3-glucanase) and *PR-5* (thaumatin) are induced by salicylic acid, whereas *PR-3* (chitinase), *PR-4* (chitinase) and *PR-12* (defensin, *PDF1.2*) are induced by jasmonic acid [5]. JA responsive gene *PDF1.2* is associated with enhanced resistance to necrotrophic pathogens, the response to mechanical damage leads to the induction of vegetative storage protein (*VSP2*) [6–8]. SA also triggers induction of some WRKY transcription factors [9]. Transcription of two of them, *WRKY38* and *WRKY62* were shown to be induced by SA [10,11].

The actin cytoskeleton is a complex and dynamic filamentous structure of all eukaryotic cells. Besides its structural role, the actin cytoskeleton dynamics plays important roles not only in

* Corresponding author. Tel.: +420 220445102; fax: +420 220445167.

E-mail address: olga.valentova@vscht.cz (O. Valentová).

numerous vitally important physiological processes but it has been shown many times that cytoskeleton undergoes structural changes in plant responses to the internal and external cues. Recent live cell imaging techniques have revealed dynamic features and significant roles of cytoskeleton during defense responses of plant cells after pathogen recognition. Actin filaments (AFs) are focusing at the site of infection and function as tracks for the polar transport of antimicrobial materials [12]. A few pieces of evidence were also given showing the involvement of actin cytoskeleton rearrangement in the signaling pathways involved in the induced resistance. Actin-depolymerizing factor (AtADF4) mediates defense signal in *Arabidopsis* triggered by *Pseudomonas syringae* DC3000 [13]. Reduced and delayed salicylic acid (SA) pathway marker gene *PR-1* induction was observed within 12 hpi in plants silenced in *AtADF4*. Depolymerization of actin by cytochalasin E, the inhibitor of actin microfilament polymerization, led to the increase of HR-like cell death and *PR-1* expression in tobacco leaf discs and this increase correlated with actin polymerization index [14].

Phospholipid signaling is obviously involved in early events triggered by infection or chemicals which mimic invasion of pathogen. Key players of this signaling system comprise phospholipid metabolizing enzymes as well as products of their action. One of the latter is phosphatidic acid, which can be produced by phospholipase D or diacylglycerol kinase. PA notably plays a role in plant stress signaling and is now considered to be one of the principal second messengers in plants. Li et al. [15] observed an increased density of actin filaments in the cortical array of *Arabidopsis* hypocotyl epidermal cells following exogenous PA treatments. This is due to the interaction of PA with capping protein (CP) which binds with high affinity to the barbed ends of actin filaments blocking actin assembly and disassembly. PA negatively regulates binding of CP and this leads to the uncapping of actin filament ends, and thereby allowing assembly of new F-actin [16].

In the presented study we demonstrate that actin cytoskeleton dynamics undergoes significant changes after exogenous treatment of *Arabidopsis* plant with salicylic acid mimicking pathogen attack. We also show that pretreatment of plants with PA abolishes the effect of SA on actin dynamics. Treatment of *Arabidopsis* seedlings with cytoskeleton disrupting drugs leads to the induction of SA responsive genes but not that of JA signaling pathway.

2. Materials and methods

2.1. Plant material

Surface sterilized seeds of *Arabidopsis thaliana*, ecotype Columbia-0 with tagged fimbrin: 35S::GFP-fABD2 [17] were cultivated in Petri dishes in MS medium modified according to Illes [18,19] and solidified with 1.2% agar. Petri dishes were positioned vertically into a growing chamber for 7–10 days and plants were grown in conditions: 22 °C/20 °C, 8/16 h day/night cycle, light 110–150 µmol m⁻² s⁻¹. All solutions were prepared with Milli-Q water.

For transcriptional analysis seedlings of *A. thaliana* ecotype Col-0 were grown in 24-well plates in 400 µL of MS liquid medium [20] for 10 days in a cycle of 10 h day (130 µE m⁻² s⁻¹, 22 °C) and 14 h night (22 °C) at 70% relative humidity. On the 7th day, the medium in wells was changed for a fresh one.

2.2. Plant treatment

For microscopy analyses *Arabidopsis* seedlings were treated with 10 µM cytochalasin E (Sigma–Aldrich) and 200 nM latrunculin B (Sigma–Aldrich). Drugs were solved in DMSO (Sigma–Aldrich) to prepare 1000x concentrated stock solutions which were then

diluted by liquid growing MS medium to final concentrations. Aqueous stock solution of sodium salicylate (SA, Sigma–Aldrich) was diluted with liquid growing medium to final 1 mM concentration.

10 µM 1,2-dioctanoyl-sn-glycerol 3-phosphate sodium salt (PA, Sigma–Aldrich) was solved in 95% ethanol, vacuum evaporated and dissolved in cultivation medium by sonication.

Bion®50WG (Syngenta) pellets containing 50% of active compound – BTB (1,2,3-benzothiadiazole-7-carbothioic acid S-methyl ester) were dissolved in distilled water to obtain 1000x concentrated stock solution. Suspension was centrifuged 1 min at 5000 × g and supernatant was diluted by growing medium to the final 300 µM concentration.

Seedlings for microscopic analyses were positioned onto an inverted platform (with a cover slip at the bottom) and submerged into a drop of MS medium. Chemicals solved in MS medium were applied directly on the microscope stage using pipette or perfusion culture chamber.

For transcription analyses, seedlings were treated by replacing the pure MS medium in growing plate wells with medium containing 200 nM latrunculin B, 10 µM cytochalasin E or 20 µM oryzalin solved in DMSO and diluted as described above.

2.3. Gene expression analysis

Whole seedlings from three independent wells were immediately frozen in liquid nitrogen. Tissue was homogenized in tubes with 1 g of 1.3 mm silica beads using a FastPrep-24 instrument (MP Biomedicals). Total RNA was isolated using a Spectrum Plant Total RNA Kit (Sigma–Aldrich) and treated with a DNA-free Kit (Ambion, Austin, TX, USA). Subsequently, 1 µg of RNA was converted into cDNA with M-MLV RNase H– Point Mutant reverse transcriptase (Promega Corp.) and anchored oligo dT21 primer (Metabion, Martinsried, Germany). An equivalent of 6.25 ng of RNA was loaded into a 10 µL reaction with a qPCR mastermix EvaLine-E1LC (GeneOn, Ludwigshafen am Rhein, Germany). All reactions were performed in polycarbonate capillaries (Genaxxon, Ulm, Germany) and LightCycler 1.5 (Roche). The following PCR program was used for all PCR assays: 95 °C for 10 min; followed by 45 cycles of 95 °C for 10 s, 55 °C for 10 s, and 72 °C for 10 s; followed by a melting curve analysis. Threshold cycles and melting curves were calculated using LightCycler Software 4.1 (Roche). Relative expression was calculated with efficiency correction and normalization to *SAND* [21]. Primers were designed using PerlPrimer v1.1.17 [22]. Following *A. thaliana* genes with corresponding accession numbers and primers were used: *SAND*, AT2G28390, FP: 5' CTG TCT TCT CAT CTC TTG TC 3', RP: 5' TCT TGC AAT ATG GTT CCT G 3', *PR-1*, AT2G14610, FP: 5' AGT TGT TTG GAG AAA GTC AG 3', RP: 5' GTT CAC ATA ATT CCC ACG A 3', *LOX2*, AT3G45140, FP: 5' ATC CCA CCT CAC TCA TTA CT 3', RP: 5' ATC CAA CAC GAA CAA TCT CT 3', *PR-2*, AT3G57260, FP: 5' TAT AGC CAC TGA CAC CAC 3', RP: 5' GCC AAG AAA CCT ATC ACT G 3', *WRKY38*, AT5G22570, FP: 5' GCC CCT CCA AGA AAA GAA AG 3', RP: 5' CCT CCA AAG ATA CCC GTC GT 3', *AOS*, AT5G42650, FP: 5' GGT CAT CAA GTT CAT AAC CG 3', RP: 5' TTT CTC AAT CGC TCC CAT 3', *VSP2*, AT5G24770, FP: 5' CCA AAC AGT ACC AAT ACG AC 3', RP: 5' CTT CTC TGT TCC GTA TCC AT 3'.

2.4. Microscopy and image adjustment

A. thaliana seedlings stably expressing 35S::GFP-fABD2 construct were placed between a microscope slide and a cover slip in a droplet of cultivation medium. Abaxial surface of the first true leaf was set toward the cover slip. The slide with seedling was positioned onto an inverted platform (with a cover slip at the bottom) of a confocal laser scanning microscope Zeiss LSM 5 DUO. The epidermal cells were imaged using an Zeiss C-Apochromat 40×/1,2

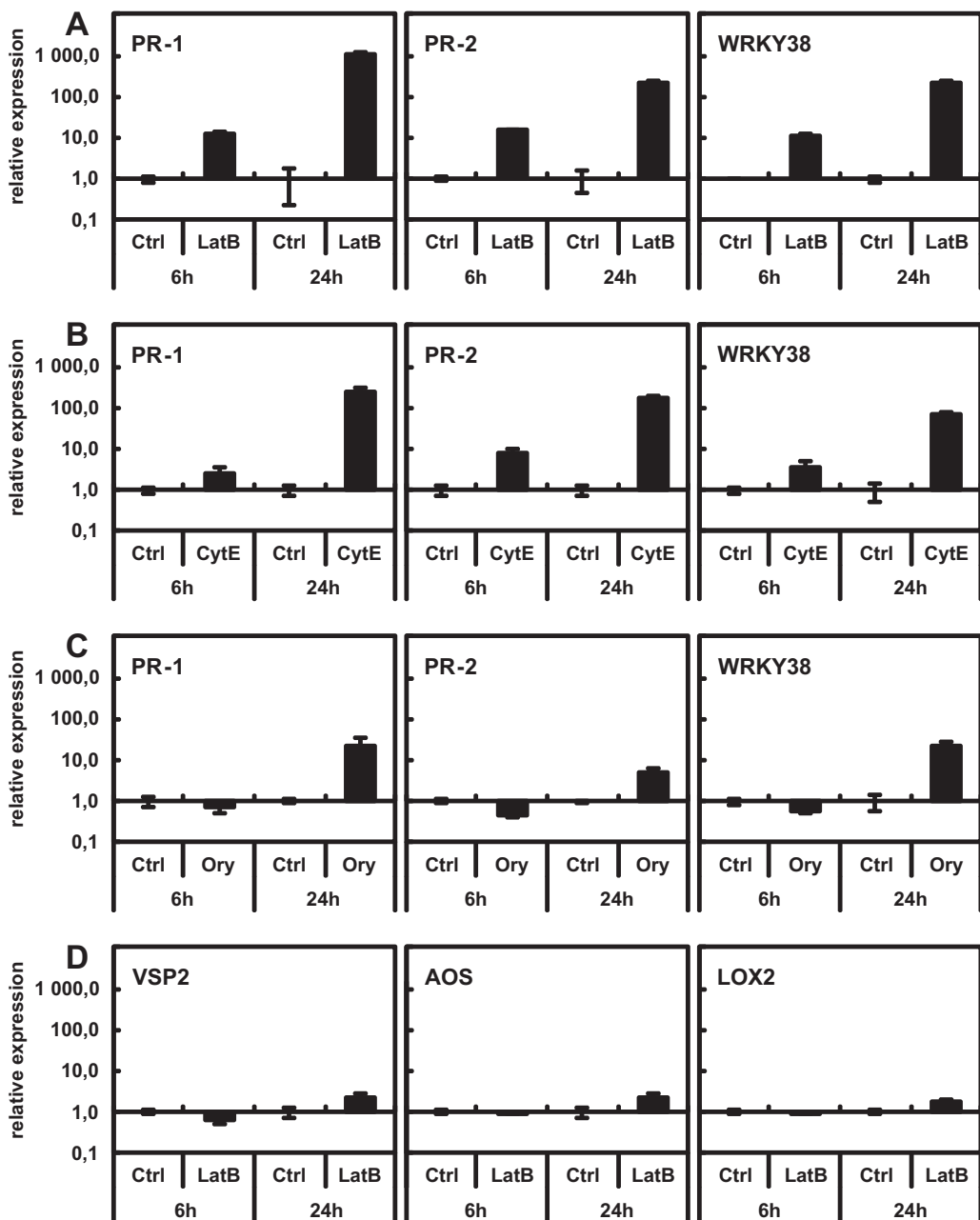


Fig. 1. Effect of cytoskeleton drugs on the expression of genes involved in salicylic acid and jasmonic acid signalling pathways. 10-days-old *Arabidopsis* seedlings grown in liquid MS medium were treated 6 h and 24 h with (A) 200 nM latrunculin B (Lat B), (B) 10 μM cytochalasin E (Cyt E) and (C) 20 μM oryzaline (Ory) and the expression of salicylic acid marker genes (*PR-1*, *PR-2* and *WRKY38*) was measured by qPCR. (D) Seedlings were treated with 200 nM latrunculin B (Lat B) and the expression of jasmonic acid marker genes (*LOX2*, *VSP2* and *AOS*) was measured by qPCR. Control plants were treated with DMSO diluted with liquid growth medium (Ctrl). Values represent means ± SE from three (LatB, Ory) and four (CytE) biological replicates.

UV-VIS-NIR water corrected objective or x63 (Plan-Apochromat 63x/1,40 Oil DIC) objective with 477 nm or 488 nm excitation with argon laser. Emitted light was captured using HFT488 beam splitter and a 505–550 nm band-pass filter.

Images of GFP – tagged actin filaments in epidermal cells were taken before the treatment and in approximately 10 min intervals after the treatment.

The images were usually taken from the tip of leaves in the region with perfectly flattened cells which helped to capture bigger leaf area in a single optical section.

Cytoplasmic streaming in hypocotyls of *A. thaliana* seedlings, was observed by Nomarski differential interference contrast microscopy using Nikon Eclipse E600 microscope (Nikon, Japan)

and time sequences captured with color digital camera (DVC 1310C, USA). Obtained images were processed using LUCIA image analysis software (laboratory Imaging, Prague, Czech Republic), Image J free software and Adobe Photoshop software (Mountain View, CA, USA).

2.5. Image analysis

For the analysis of the lengths of actin filaments (AF) the following method was used. For each experiment one fluorescence image was acquired before any treatment, followed by series of approximately 10 images after addition of chemicals. For each subsequent image acquisition the care was taken to record the same focal plane. The data were obtained with lateral resolution 114 nm/pixel. The

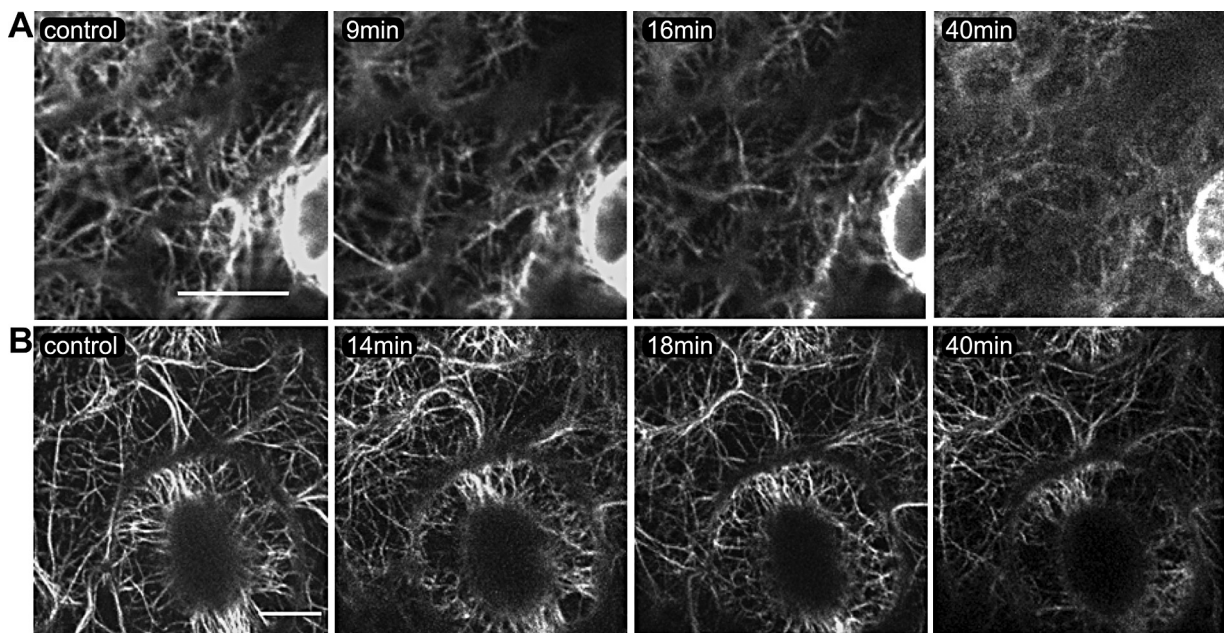


Fig. 2. Changes in actin dynamics in *Arabidopsis thaliana* epidermal leaf cells after treatment with chemical inducers. 7–10-days-old *Arabidopsis* 35S::GFP-fABD2 were treated with (A) 1 mM salicylic acid, (B) 300 µM BTH (benzothiadiazole). Approximately 4 µm of cortical layer beneath the plasma membrane (400 nm steps) of epidermal leaf cells on abaxial side was observed with confocal scanning microscope LSM 5 DUO (Zeiss) before and up to 40 min after treatment. Pictures show single optical sections of the same position and represent typical results from thirty repetitions for treatment with SA and five repetitions for BTH. Bars represent 10 µm.

pictures were processed using Zeiss LSM Image Browser to choose accurate Z-plane and Adobe Photoshop software (Mountain View, CA, USA) to crop images to gain comparable areas in the sequences of images. After recording, images were processed automatically by scripts based on ImageJ, Perl and Gnuplot. The images were filtered using FFT and custom Low Pass filters with specific orientation (step 10°) and individual particles were recognized using automatic threshold. In this way the binary model of all individual AFs (or bundles) with different orientation was generated. After visual control of processed data, the length histograms (with 1 pixel bin size) were calculated. Detailed description of image processing is in Supplemental Method and Figures S1–S6.

3. Results

3.1. Disruption of actin filaments leads to the induction of SA pathway

Kobayashi and Kobayashi [14] showed on tobacco leaf sections treated 48 h with cytochalasin E that the depolymerization of actin filaments correlates with the induction of hypersensitive response-like cell death and with the increased transcription of acidic *PR-1* and *PR-2* defense genes. Both effects are the hallmark of SA signaling pathway. This effect was significantly dependent on the type of cytochalasin used and correlated with the degree or probably the mechanism of depolymerization. While cytochalasins bind to the growing plus ends of actin filaments, latrunculin, another cytoskeletal drug, severely influencing actin dynamics, is binding to the G-actin (monomer) and thus prevents the formation of new filaments. We were interested in the effect of latrunculin B on the activation of early defense responses in *Arabidopsis* plants. Ten days old seedlings grown in liquid MS medium were treated with 200 nM latrunculin B. The increased expression of SA marker genes *PR-1*, *PR-2* and *WRKY38* was observed already 6 h after treatment followed by massive induction after 24 h, more than 1000 times in case of acidic *PR-1* and 100 times for *PR-2* and *WRKY38* (Fig. 1A). The similar effect was observed when plants were treated with 10 µM cytochalasin E (Fig. 1B). The level of the expression of

the genes after 24 h was similar to their expression in plants treated with SA (data not shown). On the other hand we did not observe any change in the expression of jasmonic acid (JA) pathway marker genes *VSP2*, *AOS* and *LOX2* [23] (Fig. 1D). These results indicate that the disruption of actin filaments is specific for SA signaling pathway.

Furthermore it seems that the SA pathway is more specifically connected with actin cytoskeleton dynamics than with the dynamics of microtubules (MT). We treated plants for 6 h and 24 h with 20 µM oryzalin, drug which binds to plant tubulin and depolymerizes MT. We observed some effect on the expression of the SA marker genes only 24 h after treatment. The relative expression was 100 times lower when compared with the level of expression in plants treated with latrunculin B and cytochalasin E (Fig. 1C).

3.2. Salicylic acid causes the disruption of actin filaments

Results of the gene expression pattern in response to cytoskeletal drug treatment led us to the question whether SA itself could have an impact on the actin cytoskeleton dynamics. To study the response of plant cells after treatment with 1 mM sodium salicylate, we imaged actin filament arrays in the leaves of *Arabidopsis* plants by confocal microscopy. Actin filaments were imaged in several time points after submerging the plants in the medium with SA directly on microscopic plates. Surprisingly, actin filaments in the leaves of *A. thaliana* depolymerized rapidly, within minutes, after the treatment (Fig. 2A). Several different but related actin dynamic patterns of actin depolymerization were accompanied by reliable appearance of a few stable thicker bundles of actin filaments after approximately 20 min of the treatment. The decrease of filament number was obvious 10 min after treatment and it continued gradually for next 20 min. While this is true for majority of samples (about 75%), in the remaining experiments the number of filaments in the interval between 10 and 20 min rose almost back to initial values, but it started to decrease later again. Tiny filaments fragmented into dots or short fibers (about 60% of all cases) or simply disappeared after treatment. The region surrounding actin cables was full of tiny speckles or fog-like diffuse signal, usually 40 min after treatment with SA, total number of actin particles of all sizes

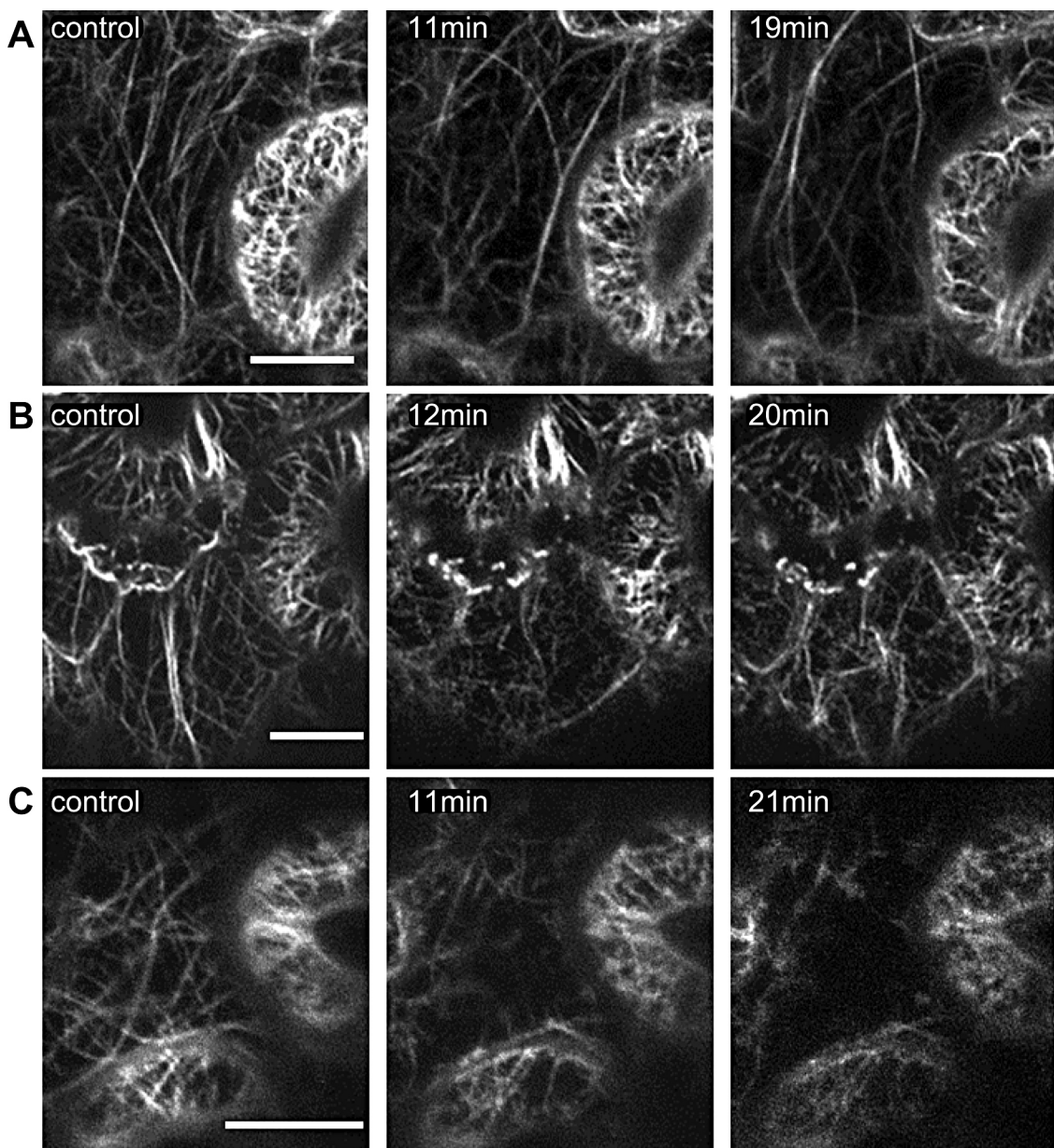


Fig. 3. Changes in actin dynamics in *Arabidopsis thaliana* epidermal leaf cells after treatment with SA in comparison to the effect of cytoskeletal drugs. 7–10-days-old *Arabidopsis* 35S::GFP-fABD2 were treated with (A) 1 mM salicylic acid, (B) 200 nM latrunculin B and (C) 10 μ M cytochalasin E. Approximately 4 μ m of cortical layer beneath the plasma membrane (400 nm steps) of epidermal leaf cells on abaxial side was observed with confocal scanning microscope LSM 5 DUO (Zeiss) before and up to 20 min after treatment. Pictures show single optical sections of the same position and represent typical results from thirty repetitions for treatment with salicylic acid and five repetitions for treatment with latrunculin B and cytochalasin E. Bars represent 10 μ m.

rapidly increased. This is due to the significantly augmented quantity of short, perished filaments with the length below 5.7 μ m, while number of longer filaments decreased (Table 1). Treatment of plants with 300 μ M benzothiodiazole (BTH), functional analog of SA, gave similar results to the effect of salicylic acid (Fig. 2B). To exclude the effect of pH changes caused by SA, we did the experiment with equal concentration of 4-hydroxybenzoic acid, the inactive analog of SA, with similar acid dissociation constant (pKa)

as SA. No specific influence of pH changes on actin cytoskeleton was observed (data not shown).

For comparison, live imaging of actin filaments in response to anti-actin drugs (latrunculin B and cytochalasin E) was also performed. In our experiments the manner of depolymerization of actin filaments after treatment with 200 nM latrunculin B, in contrast to 10 μ M cytochalasin E, mimics more frequently process induced by salicylic acid regarding the fragmentation of actin fibers

Table 1

Distribution of actin filament (AF) length after treatment with 1 mM salicylic acid (SA) \pm SD ($n = 3–7$).

Time after SA [min]	0	1–20	21–40	41–60
Number of AF 0–5.7 μ m [%]	56.5 \pm 0.9	47.3 \pm 5.7	42.1 \pm 3.8	120.3 \pm 16.1
Number of AF >5.7 μ m [%]	43.5 \pm 0.9	39.7 \pm 1.2	34.8 \pm 3.3	28.5 \pm 2.56
Sum [%]	100 \pm 0	87 \pm 6.4	76.9 \pm 6.7	148.8 \pm 18

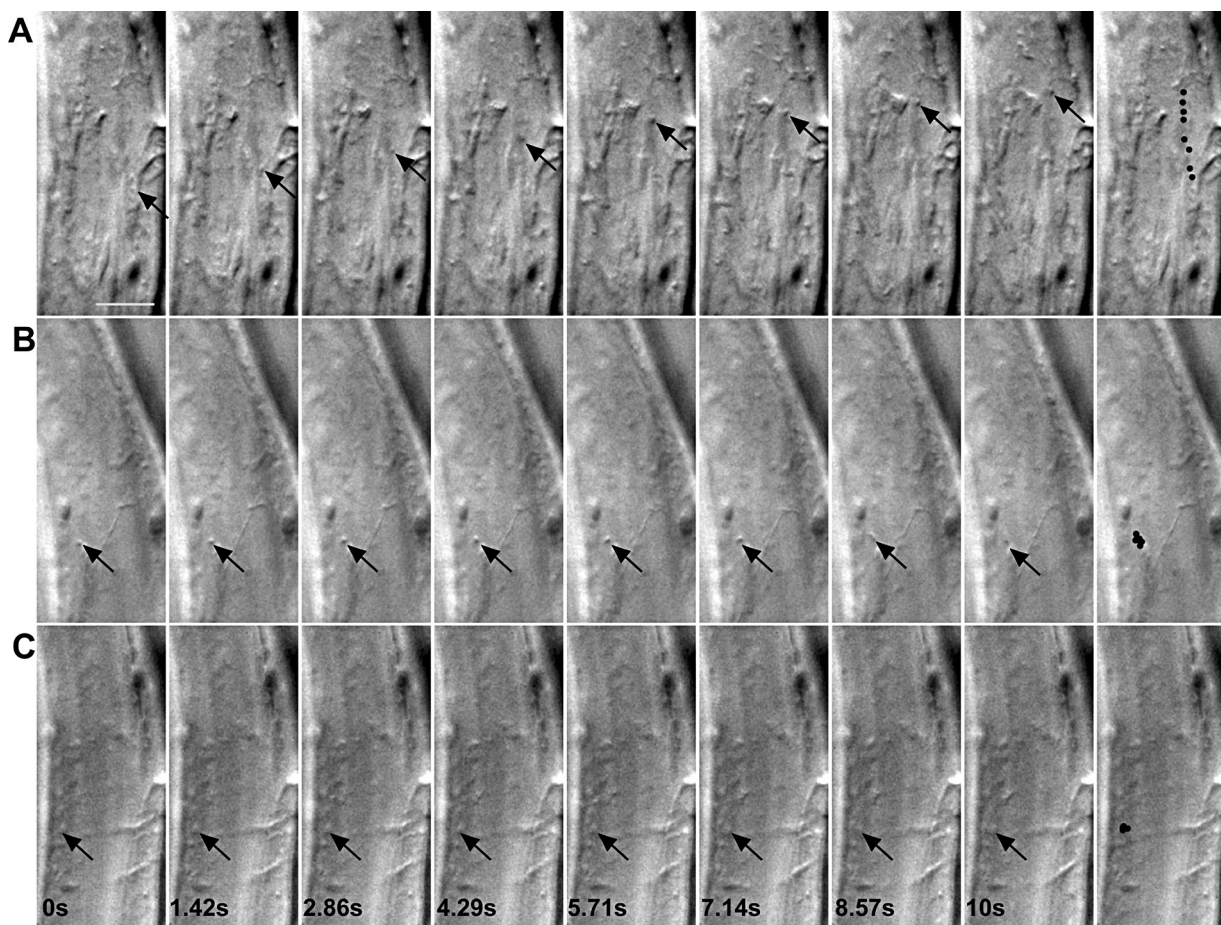


Fig. 4. Effect SA on the cytoplasmic streaming. 7-days-old Arabidopsis 35S::GFP-fABD2 seedlings were treated with 1 mM salicylic acid. Image sequences of hypocotyl cells were captured 10 s by differential interference contrast (DIC) microscopy before treatment (A), 10 min (B) and 40 min (C) after 1 mM salicylic acid treatment. Last picture in each row represents tracking of chosen particle movement during 10 s. Images represent results of typical experiment from three repeats. Bar represents 10 μ m.

but the time course was slightly different. Ten minutes after treatment with latrunculin B many actin filaments disappeared but unlike in salicylate treatment, fragmentation of fibers began earlier, already after 5 min. Formation of thick bundles started also earlier after latrunculin B compared to salicylic acid (Fig. 3).

Dynamics of actin cytoskeleton is tightly connected with cytoplasmic streaming. We therefore measured velocity of cytoplasmic streaming during 40 min after 1 mM SA treatment in anisotropic hypocotyl cells, where streaming is more obvious than in epidermal leaf cells. Movement of the tracked particle in the cytoplasm was nine times faster in the control cell than in treated cells (Fig. 4). In addition, SA caused disappearing of many particles in the cytoplasm. Cytoplasmic strands kept moving for entire experiment period, but speed of motion decreased.

3.3. Phosphatidic acid prevents the effect of SA on the actin filaments

Phosphatidic acid (PA) binds to the capping protein (CP) and this interaction leads to the release of this protein from barbed ends of actin filaments resulting in an increased density of filament arrays [15,24]. In accordance with these findings we observed the increased number of fibers in Arabidopsis leaf epidermal cells approximately 20 min after addition of water soluble 10 μ M diocetyl PA (Fig. 5A). This effect was followed by extensive filament bundling, which was demonstrated by relative decrease of the number of filaments.

Phosphatidic acid is a product of phospholipase D (PLD) reaction and as we observed earlier, SA treatment of Arabidopsis suspension cells leads to the activation of PLD to about 150% within 15 min [11]. Thus we were interested in the effect of PA on SA induced actin filaments disruption. Arabidopsis seedlings were treated with 10 μ M PA, 11–18 min before 1 mM SA addition. This pretreatment totally revoked decrease of actin fiber number, the typical effect caused by SA and moreover bundles or fragmentation did not emerge afterwards (Fig. 5B) and the increase of actin filament number was higher due to the low occurrence of bundles in comparison to treatment with PA itself. To test whether laser beam or the other experimental conditions did not influence systematically actin filaments, we studied actin dynamics in the leaves submerged in growing medium within 40 min in twenty-four parallel experiments as a control. Only slight fluctuations of number of actin filaments were observed every 10 min, without any trend. The changes were in accordance with the usual actin dynamic (data not shown).

3.4. Evaluation of changes in actin dynamics

Eighty parallel experiments after the treatment with 1 mM salicylic acid were performed. In sixty-seven cases depolymerization and actin dynamics as described above were observed, and thirty of them, with special care for accurate optical section, were further used for image analysis.

The observed changes in actin dynamics were quantified as follows. Each time-series of images in parallel experiments was

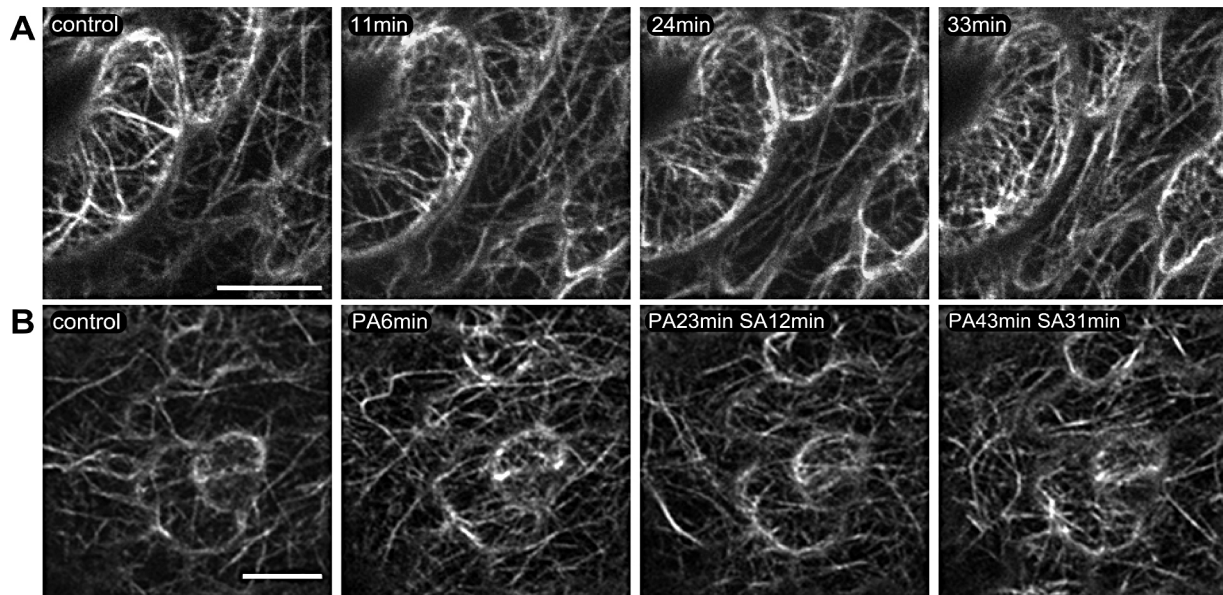


Fig. 5. Phosphatidic acid prevents the effect of salicylic acid on actin filament dynamics in *Arabidopsis thaliana* epidermal leaf cells. 7–10 days old *Arabidopsis* 35S::GFP-fABD2 were treated with (A) 10 μM 1,2-dioctanoyl-sn-glycerol 3-phosphate sodium salt (PA) and (B) pretreated 11 min with 10 μM PA followed by 1 mM salicylic acid application. Approximately 4 μm of cortical layer beneath the plasma membrane (400 nm steps) of epidermal leaf cells on abaxial side was observed with confocal scanning microscope LSM 5 DUO (Zeiss) before and up to 40 min after treatment. Pictures show single optical sections of the same position. Each set of images represents results of typical experiment from fifteen repeats. Bars represent 10 μm.

evaluated by the number of particles, which were counted during image analysis and they differed remarkably in total number of actin particles. In order to make all the experiments comparable, the numbers of actin filaments at time zero (control) in the series was set as 100% and appropriate values for remaining images were calculated.

Discrete values in the plots represent normalized number of actin particles at defined time points before and after treatment. The changes of particle numbers in time were characterized by fitting the data by linear function using least squares method for all parallel experiments. Image evaluation of parallel experiments showed in Fig. 6B confirmed rising population of actin filaments observed up to 25 min after treatment with 10 μM PA.

Fig. 6A is well portraying characteristic parallel experiments with slightly different dynamics of decreasing number of all actin particles after the treatment with 1 mM SA and this tendency after treatment with SA was clearly completely abolished with PA pretreatment. Number of actin particles after PA addition and subsequently within 12–18 min SA treatment of plants tends to increase during the time (Fig. 6C).

4. Discussion

4.1. Disruption of actin filaments leads to the changes in defense genes transcripts

Vast majority of the research focused on the role of actin cytoskeleton in the processes by which plants respond to the pathogen attack was based on the pharmacological attitude using cytochalasins as drugs influencing the actin cytoskeleton dynamics [12]. Actin filament disruption by these drugs typically led to the higher susceptibility mostly toward oomycetes and fungal pathogens. This is probably caused by an inhibitory effect of these drugs on cytoplasmic streaming by the disruption of subcortical actin filaments within 1 h of the treatment [25]. Conversely, latrunculins A and B caused cessation of streaming only after much longer treatment period, over 1 day, and at relatively very high concentrations (200 μM). In accordance with this finding Henty-Ridilla et al.

[26] showed that *Arabidopsis* plants treated with micromolar concentrations of latrunculin B are more susceptible to the attack of *P. syringae* pv. tomato DC3000. On the contrary, we clearly showed that the transcription of three different SA pathway marker genes *PR1*, *PR2* and *WRKY38* was considerably induced by nanomolar concentrations of latrunculin B already 6 h after treatment and the induction steeply increased up to 24 h. Thus we can assume that the disruption of actin filaments in cortical layer triggers pathway leading to defense response. Interestingly we did not see any effect on JA responsive genes *AOS*, *LOX2* and *VSP2*. SA marker genes were not induced 6 h after the treatment of seedlings with oryzalin, microtubules disrupting drug, and only very slightly induced after 24 h. Taken together all these findings led us to the suggestion that actin cytoskeleton dynamics is specifically connected with SA signaling pathway. Kobayashi and Kobayashi [14] also showed on tobacco leaves *PR-1* and *PR-2* induction after depolymerization of actin filaments with cytochalasin E, but they observed the effect after much longer time of treatment (48 h). We can speculate that the observed induced gene transcription could be related to cytoskeletal disassembly, which can liberate transcription factors into the cytoplasm to be available for expression of corresponding genes in the nucleus [27,28].

4.2. Salicylic acid is diminishing number of actin filaments

Levels of salicylic acid in plants are significantly elevated in response to various infection agents as well as to abiotic stress stimuli. Exogenous treatment of plants with SA mimics pathogen attack. Salicylic acid is incorporated within 5 min to the plant cell as it was verified by the uptake of radiolabelled salicylic acid into the maize suspension cells (Skúpa P. and Dobrev P., unpublished results).

Basal level of SA in *A. thaliana* is 250–1000 ng g⁻¹ of fresh weight [29] whereas the SA amount in pathogen challenged leaves was found to be at least 10 times higher [30]. Therefore, to simulate signaling event in pathogen response, we firstly used 250 μM concentration of SA for external treatment of leaves, this concentration is 40 times higher than the basal level in the leaves,

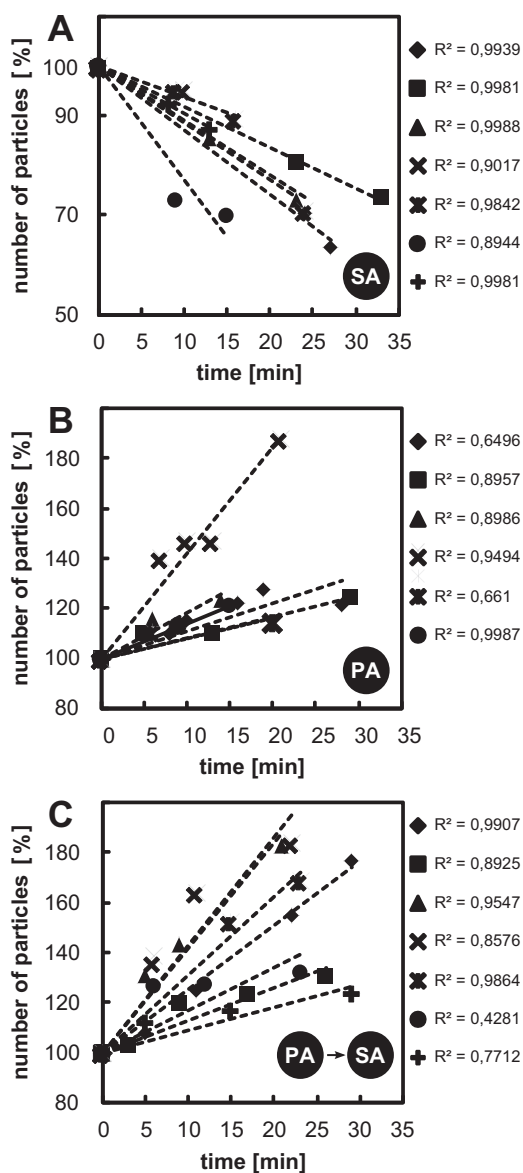


Fig. 6. Quantitative evaluation of micrographs. 7–10 days old *Arabidopsis* 35S::GFP-FABD2 were treated with (A) 1 mM salicylic acid (SA), (B) 10 μ M 1,2-diacyl-sn-glycerol 3-phosphate sodium salt (PA) and (C) 10 μ M PA 11–18 min before 1 mM SA was added. In all series taken to the evaluation (six to eight in each experiment) the number of particles was set to 100% in the time zero. Different symbols represent each experiment. Coefficient of determination R^2 for each experiment is calculated.

nevertheless changes in actin filament network were too feeble (data not shown). Cellular responses to the pathogen, instead of being diffused in the cell, tend to be localized in focused regions where the defense molecules are accumulated [31]. Thus we assumed that SA concentration could be also locally elevated and indeed when 1 mM SA was used for the treatment of leaves, we observed shrinkage and fragmentation of actin filaments within 40 min. In our experiments, three different dynamic patterns of actin depolymerization caused by SA were observed. Nevertheless most often actin filaments fragmented into short fibers or dots and this pattern was similar to the mode of depolymerization caused by latrunculin B rather than the one after cytochalasin E treatment, which we used as a reference. So these changes in actin dynamics after SA treatment might be explained by the mechanism shared with latrunculin B, it means lower assembly rate of G actin units [32]. Different actin filament pattern observed after treatment with latrunculin B or cytochalasin E was also noticed in animal cells [33].

Commonly observed oscillation of actin filament density, called stochastic dynamics [34] is determined by fast growth of tiny filaments, whilst their disassembly is proceeded with a slower rate, balance between growth and shrinkage is then achieved by simultaneous severing of filaments into shorter fibers. Filaments associated in bundles are much more static [35]. Actin dynamics is tuned and realized by many actin binding proteins performing relevant cell needs. With these tools, specific dynamic balance could be shifted to the increased polymerization, disassembly or bundling of filaments, etc.

Both of principal reactions in actin network dynamics – polymerization and depolymerization of actin filaments were described after biotic stress and both lead to the induction of the expression of PR-1 protein, marker of SA signaling pathway [36,37].

Actin dynamics after biotic stress includes local and transient changes with structural defense function reported e.g. after touching *Arabidopsis* leaf cells with micro needle mimicking fungal attack, actin filaments began to cumulate beneath the needle contact site after 3 min [31]. During response to biotic stress, polymerization of actin arrays was described 6 h after bacterial infection with *P. syringae* pv. *tomato* DC 3000 in *Arabidopsis* epidermal leaves [26] as well as depolymerization of actin filaments in cells of *Arabidopsis* suspension culture after 30 min of treatment with *Verticillium dahliae* toxin [38]. Infection with *P. syringae* pv. *tomato* DC 3000 and treatment of cells with *V. dahliae* toxin, both lead to the induction of PR-1 protein expression [36,37]. So transient increasing and also decreasing of actin filament number can be alternately involved in SA signaling pathway, possibly with different timing and localization inside the plant cell.

Interpretation of our results concerning physiological meaning for plant, is stemming from a few information so far. The highest level of PR-1 expression appears 24 h after plant inoculation with bacteria [39], whereas exogenously applied SA triggers expression of the same marker gene up to 6 h after treatment. Interestingly, while Henty-Ridilla and coworkers [26] assumed higher actin filaments density as a way to perform plant defense response to PAMP, they also showed lower AFs density comparing to the control after 18 h after *P. syringae* DC 3000 treatment, which could correlate to SA level increase in the cells. Thus it could be suggested, that only accurate and gradual polymerization or depolymerization of actin cytoskeleton within defense response leads to successful defense. Incessant actin dynamics was hypothesized as plant surveillance tool [26].

Reply to the other important question is more speculative. Why plant cells would need local, short-term depolymerization of AFs? Pathogen threat compels cells to reprogram the flow of cellular energy from growth and development into rescue operations [40], SA for instance inhibits auxin response in plants [41]. During stress-free periods AFs serve like rails allowing delivery of protein cargos for growth and development around the cell. After pathogen attack, not only cargos but maybe also the direction of rails must be changed. It could be expected that it would be much more effective to destroy the whole net and make it *de novo* ready to carry out new tasks, rather than reconstruct the dense actin network step by step.

Further we were able to show that phosphatidic acid (PA) when added to the leaves is capable to prevent the effect of salicylic acid leading to the depolymerization of actin filaments. This is in accordance with finding of Steiger's group showing that PA promotes the growth of actin filaments by binding to the capping protein [24,26] and thus releasing barbed plus ends. F actin prepared *in vitro* activates very significantly one of the isoforms of NtPLD (Nt PLD β), an enzyme producing phosphatidic acid [16]. The activity increased nearly eight times which is much more pronounced activation that was observed for SA itself. The distribution of the filament length formed by *in vitro* polymerization of G-actin is exponential and

the majority of the filament length is within the range from 0.5 to 10 µm [42]. Disruption of actin filaments after SA treatment led to the formation of shorter fragments (Table 1), size of which corresponds to filaments formed *in vitro*. Thus we can speculate that SA can also, in later phases, initiate the process leading to the regeneration of actin network needed for successful defense.

Acknowledgement

This research was supported by the Czech Science Foundation Grant No. 501/11/1654 and Specific University Research (MSMT No. 21/2013 and SVV UK 267 002). We thank Hana Krutinová for her substantial technical support.

Appendix A. Supplementary data

Supplementary data associated with this article can be found, in the online version, at <http://dx.doi.org/10.1016/j.plantsci.2014.03.002>.

References

- [1] S.H. Spoel, X.N. Dong, How do plants achieve immunity? Defence without specialized immune cells, *Nature Reviews Immunology* 12 (2012) 89–100.
- [2] C.M.J. Pieterse, D. Van der Does, C. Zamioudis, A. Leon-Reyes, S.C.M. Van Wees, Hormonal modulation of plant immunity, *Annual Review of Cell and Developmental Biology* Vol28 (28) (2012) 489–521.
- [3] J.P. Metraux, P.A. Goy, T. Staub, J. Speich, A. Steinemann, J. Ryals, E. Ward, Induced systemic resistance in cucumber in response to 2,6-dichloro-isonicotinic acid and pathogens, *Advances in Molecular Genetics of Plant-Microbe Interactions* Vol1 (10) (1991) 432–439.
- [4] J. Sels, J. Mathys, B.M.A. De Coninck, B.P.A. Cammue, M.F.C. De Bolle, Plant pathogenesis-related (PR) proteins: a focus on PR peptides, *Plant Physiology and Biochemistry* 46 (2008) 941–950.
- [5] L.C. van Loon, M. Rep, C.M.J. Pieterse, Significance of inducible defense-related proteins in infected plants, *Annual Review of Phytopathology* 44 (2006) 135–162.
- [6] Y.L. Liu, J.E. Ahn, S. Datta, R.A. Salzman, J. Moon, B. Huyghues-Despointes, B. Pittendrigh, L.L. Murdock, H. Koiwa, K. Zhu-Salzman, Arabidopsis vegetative storage protein is an anti-insect acid phosphatase, *Plant Physiology* 139 (2005) 1545–1556.
- [7] C. Despres, C. DeLong, S. Glaze, E. Liu, P.R. Fobert, The arabidopsis NPR1/NIM1 protein enhances the DNA binding activity of a subgroup of the TGA family of bZIP transcription factors, *Plant Cell* 12 (2000) 279–290.
- [8] H.S. Kim, T.P. Delaney, Arabidopsis SON1 is an F-box protein that regulates a novel induced defense response independent of both salicylic acid and systemic acquired resistance, *Plant Cell* 14 (2002) 1469–1482.
- [9] P.J. Rushton, I.E. Somssich, P. Ringler, Q.X.J. Shen, WRKY transcription factors, *Trends in Plant Science* 15 (2010) 247–258.
- [10] K.C. Kim, Z.B. Lai, B.F. Fan, Z.X. Chen, Arabidopsis WRKY38 and WRKY62 transcription factors interact with histone deacetylase 19 in basal defense, *Plant Cell* 20 (2008) 2357–2371.
- [11] O. Krinke, M. Flemr, C. Vergnolle, S. Collin, J.P. Renou, L. Taconnat, A. Yu, L. Burkettova, O. Valentova, A. Zachowski, E. Ruelland, Phospholipase D activation is an early component of the salicylic acid signaling pathway in arabidopsis cell suspensions, *Plant Physiology* 150 (2009) 424–436.
- [12] T. Higaki, T. Kurusu, S. Hasezawa, K. Kuchitsu, Dynamic intracellular reorganization of cytoskeletons and the vacuole in defense responses and hypersensitive cell death in plants, *Journal of Plant Research* 124 (2011) 315–324.
- [13] M.Y. Tian, F. Chaudhry, D.R. Ruzicka, R.B. Meagher, C.J. Staiger, B. Day, Arabidopsis actin-depolymerizing factor AtADF4 mediates defense signal transduction triggered by the *Pseudomonas syringae* effector AvrPphB, *Plant Physiology* 150 (2009) 815–824.
- [14] Y. Kobayashi, I. Kobayashi, Depolymerization of the actin cytoskeleton induces defense responses in tobacco plants, *Journal of General Plant Pathology* 73 (2007) 360–364.
- [15] J.J. Li, J.L. Henty-Ridilla, S.J. Huang, X. Wang, L. Blanchoin, C.J. Staiger, Capping protein modulates the dynamic behavior of actin filaments in response to phosphatidic acid in Arabidopsis, *Plant Cell* 24 (2012) 3742–3754.
- [16] R. Pleskot, M. Potocky, P. Pejchar, J. Linek, R. Bezvoda, J. Martinec, O. Valentova, Z. Novotna, V. Zarsky, Mutual regulation of plant phospholipase D and the actin cytoskeleton, *Plant Journal* 62 (2010) 494–507.
- [17] B. Voigt, A.C.J. Timmers, J. Šamaj, J. Müller, F. Baluška, D. Menzel, GFP-FABD2 fusion construct allows *in vivo* visualization of the dynamic actin cytoskeleton in all cells of *Arabidopsis* seedlings, *European Journal of Cell Biology* 84 (2005) 595–608.
- [18] T. Murashige, F. Skoog, A revised medium for rapid growth and biosynthesis with tobacco tissue culture, *Physiologia Plantarum* 15 (1962) 473–497.
- [19] P. Illes, M. Schlicht, J. Pavlovkin, I. Lichtscheidl, F. Baluska, M. Ovecka, Aluminium toxicity in plants: internalization of aluminium into cells of the transition zone in *Arabidopsis* root apices related to changes in plasma membrane potential, endosomal behaviour, and nitric oxide production, *Journal of Experimental Botany* 57 (2006) 4201–4213.
- [20] N.K. Clay, A.M. Adio, C. Denoux, G. Jander, F.M. Ausubel, Glucosinolate metabolites required for an *arabidopsis* innate immune response, *Science* 323 (2009) 95–101.
- [21] T. Czechowski, M. Stitt, T. Altmann, M.K. Udvardi, W.R. Scheible, Genome-wide identification and testing of superior reference genes for transcript normalization in *Arabidopsis*, *Plant Physiology* 139 (2005) 5–17.
- [22] O.J. Marshall, PerlPrimer: cross-platform, graphical primer design for standard, bisulphite and real-time PCR, *Bioinformatics* 20 (2004) 2471–2472.
- [23] J.G. Turner, C. Ellis, A. Devoto, The jasmonate signal pathway, *Plant Cell* 14 (2002) S153–S164.
- [24] S.J. Huang, L. Gao, L. Blanchoin, C.J. Staiger, Heterodimeric capping protein from *Arabidopsis* is regulated by phosphatidic acid, *Molecular Biology of the Cell* 17 (2006) 1946–1958.
- [25] I. Foissner, G.O. Wasteneys, Wide-ranging effects of eight cytochalasins and latrunculin A and B on intracellular motility and actin filament reorganization in characean internodal cells, *Plant and Cell Physiology* 48 (2007) 585–597.
- [26] J.L. Henty-Ridilla, M. Shimono, J. Li, J.H. Chang, B. Day, C.J. Staiger, The plant actin cytoskeleton responds to signals from microbe-associated molecular patterns, *PLoS Pathogens* 9 (2013) e1003290.
- [27] S.D.X. Chuong, A.G. Good, G.J. Taylor, M.C. Freeman, G.B.G. Moorhead, D.G. Muench, Large-scale identification of tubulin-binding proteins provides insight on subcellular trafficking, metabolic channeling, and signaling in plant cells, *Molecular & Cellular Proteomics* 3 (2004) 970–983.
- [28] S.J. Winder, K.R. Ayscough, Actin-binding proteins, *Journal of Cell Science* 118 (2005) 651.
- [29] M. Rivas-San Vicente, J. Plasencia, Salicylic acid beyond defence: its role in plant growth and development, *Journal of Experimental Botany* 62 (2011) 3321–3338.
- [30] K. Summhammer, L. Sticher, J.P. Métraux, Systemic responses in *Arabidopsis thaliana* infected and challenged with *Pseudomonas syringae* pv. *syringae*, *Plant Physiology* 108 (1995) 1379–1385.
- [31] A.R. Hardham, D. Takemoto, R.G. White, Rapid and dynamic subcellular reorganization following mechanical stimulation of *Arabidopsis* epidermal cells mimics responses to fungal and oomycete attack, *BMC Plant Biology* 8 (2008) 63.
- [32] B.C. Gibbon, D.R. Kovar, C.J. Staiger, Latrunculin B has different effects on pollen germination and tube growth, *The Plant Cell* 11 (1999) 1363–2349.
- [33] T. Wakatsuki, B. Schwab, N.C. Thompson, E.L. Elson, Effects of cytochalasin D and latrunculin B on mechanical properties of cells, *Journal of Cell Science* 114 (2001) 1025–1036.
- [34] C.J. Staiger, M.B. Sheahan, P. Khurana, X. Wang, D.W. McCurdy, L. Blanchoin, Actin filament dynamics are dominated by rapid growth and severing activity in the *Arabidopsis* cortical array, *Journal of Cell Biology* 184 (2009) 269–280.
- [35] R. Pleskot, J.J. Li, V. Zarsky, M. Potocky, C.J. Staiger, Regulation of cytoskeletal dynamics by phospholipase D and phosphatidic acid, *Trends in Plant Science* 18 (2013) 496–504.
- [36] J.R. Bretz, N.M. Mock, J.C. Charity, S. Zeyad, C.J. Baker, S.W. Hutcheson, A translocated protein tyrosine phosphatase of *Pseudomonas syringae* pv. *tomato* DC3000 modulates plant defence response to infection, *Molecular Microbiology* 49 (2003) 389–400.
- [37] J. Jiang, L.W. Fan, W.H. Wu, Evidences for involvement of endogenous cAMP in *Arabidopsis* defense responses to *Verticillium* toxins, *Cell Research* 15 (2005) 585–592.
- [38] H.Y. Yuan, L.L. Yao, Z.Q. Jia, Y. Li, Y.Z. Li, *Verticillium dahliae* toxin induced alterations of cytoskeletons and nucleoli in *Arabidopsis thaliana* suspension cells, *Protoplasma* 229 (2006) 75–82.
- [39] A.M. Maldonado, P. Doerner, R.A. Dixon, C.J. Lamb, R.K. Cameron, A putative lipid transfer protein involved in systemic resistance signalling in *Arabidopsis*, *Nature* 419 (2002) 399–403.
- [40] D. Walters, M. Heil, Costs and trade-offs associated with induced resistance, *Physiological and Molecular Plant Pathology* 71 (2007) 3–17.
- [41] D. Wang, K. Pajerowska-Mukhtar, A.H. Culler, X. Dong, Salicylic acid inhibits pathogen growth in plants through repression of the auxin signaling pathway, *Current Biology*: CB 17 (2007) 1784–1790.
- [42] D. Sept, J.Y. Xu, T.D. Pollard, J.A. MacCannan, Annealing accounts for the length of actin filaments formed by spontaneous polymerization, *Biophysical Journal* 77 (1999) 2911–2919.

SCIENTIFIC REPORTS



OPEN

Actin depolymerization is able to increase plant resistance against pathogens via activation of salicylic acid signalling pathway

Received: 14 June 2018

Accepted: 20 June 2019

Published online: 18 July 2019

Hana Leontovyčová^{1,2,4}, Tetiana Kalachova¹, Lucie Trdá¹, Romana Pospíchalová², Lucie Lamparová^{1,2}, Petre I. Dobrev¹, Kateřina Malinská¹, Lenka Burketová¹, Olga Valentová¹ & Martin Janda^{1,2,5}

The integrity of the actin cytoskeleton is essential for plant immune signalling. Consequently, it is generally assumed that actin disruption reduces plant resistance to pathogen attack. Here, we demonstrate that actin depolymerization induced a dramatic increase in salicylic acid (SA) levels in *Arabidopsis thaliana*. Transcriptomic analysis showed that the SA pathway was activated due to the action of isochorismate synthase (ICS). The effect was also confirmed in *Brassica napus*. This raises the question of whether actin depolymerization could, under particular conditions, lead to increased resistance to pathogens. Thus, we explored the effect of pretreatment with actin-depolymerizing drugs on the resistance of *Arabidopsis thaliana* to the bacterial pathogen *Pseudomonas syringae*, and on the resistance of an important crop *Brassica napus* to its natural fungal pathogen *Leptosphaeria maculans*. In both pathosystems, actin depolymerization activated the SA pathway, leading to increased plant resistance. To our best knowledge, we herein provide the first direct evidence that disruption of the actin cytoskeleton can actually lead to increased plant resistance to pathogens, and that SA is crucial to this process.

The actin cytoskeleton plays a key role in plant immunity^{1,2}, both by providing a physical barrier and by its involvement in the transport of callose, antimicrobial compounds and cell wall components to an infection site³. Additionally, actin filament reorganization is a very fast response to treatment with conserved microbial compounds, MAMPs (microbe-associated molecular patterns), such as flg22, elf26 and chitin. The recognition of MAMPs triggers a specific set of immune responses, including cytoskeleton reorganization. It underpins the important role of actin cytoskeleton in plant defense^{4,5}. Several studies have shown that when drugs, such as cytochalasins or latrunculin B, depolymerize the actin cytoskeleton, different plant species become more susceptible to pathogens. For example, treatment of *A. thaliana* with latrunculin B resulted in higher susceptibility to infection by *Pseudomonas syringae*⁵⁻⁷. In plants, actin depolymerizing factors serve to sever filamentous actin. The *adf4* (Actin Depolymerizing Factor 4) *A. thaliana* knock out mutant had reduced resistance to *Pseudomonas syringae* pv *tomato* DC 3000 (*Pst* DC3000) expressing the AvrPphB effector⁸. This is because ADF4 is necessary for the expression of RPS5, the resistance protein that recognises AvrPphB⁹. However, in the intact *adf4* mutant, the density and skewness of actin filaments were the same as in control plants, implying that the actin cytoskeleton is not modified before infection¹⁰. ADF4 plays an indispensable role in the actin reorganisation upon elf26, but not in response to chitin⁴. The importance of actin cytoskeleton is also highlighted by the fact that *Pst* DC3000 secretes at least two effectors modulating actin cytoskeleton. The effector HopW1 disrupts the

¹Laboratory of Plant Biochemistry, Department of Biochemistry and Microbiology, University of Chemistry and Technology Prague, Technicka 5, 166 28, Prague 6, Czech Republic. ²Laboratory of Pathological Plant Physiology, Institute of Experimental Botany of The Czech Academy of Sciences, Rozvojova 263, 165 02, Prague 6, Czech Republic. ³Laboratory of Hormonal Regulations in Plants, Institute of Experimental Botany of The Czech Academy of Sciences, Rozvojova 263, 165 02, Prague 6, Czech Republic. ⁴Department of Biochemistry, Faculty of Science, Charles University in Prague, Faculty of Science, 128 44 Hlavova 2030/8, Prague 2, Czech Republic. ⁵Present address: Ludwig-Maximilians-University of Munich (LMU), Faculty of Biology, Biocenter, Department Genetics, Grosshaderner Str. 2-4, D-82152, Martinsried, Germany. Correspondence and requests for materials should be addressed to M.J. (email: martin.janda@vscht.cz)

actin cytoskeleton^{6,7}. Another effector, HopG1, was shown to affect the remodelling of the actin cytoskeleton in *Pst* DC3000-infected *A. thaliana*¹¹. Furthermore, treatment with cytochalasin E increased the penetration of *A. thaliana* plants by *Colletotrichum* species¹² and the rate of entry to barley by *Blumeria graminis* f. sp. *hordei*¹³. Non-host resistance to *Erysiphe pisi* decreased after treatment with cytochalasins in barley, wheat, cucumber and tobacco¹⁴, as did resistance to *Blumeria graminis* f. sp. *tritici* after cytochalasin E treatment of *A. thaliana*. Moreover, treatment with cytochalasin E in the absence of EDS1 (enhanced diseased resistance 1), an upstream component of the salicylic acid (SA) signalling pathway, strongly enhanced the inhibitory effect on non-host resistance¹⁵. However, in tobacco, cytochalasin E induced the transcription of *NtPR-1* (pathogenesis-related 1), a defence-related SA marker gene, and is able to prime cells to HR-like cell death in response to *Erysiphe cichoracearum*¹⁶. Furthermore, both cytochalasin E and latrunculin B induced the transcription of several SA marker genes (*AtPR-1*, *AtPR-2* and *AtWRKY38*) in *A. thaliana* seedlings¹⁷. This suggests that while such drugs do indeed cause actin depolymerization, the effects of such depolymerization may not always be adverse. Could it be that drug-induced actin depolymerization actually triggers processes that induce the SA pathway and thereby increase plant resistance to pathogens?

Results

Actin depolymerization induce salicylic acid biosynthesis via ICS1 dependent pathway. To establish that SA levels can increase upon actin depolymerization, we measured phytohormone content in *A. thaliana* seedlings treated with just 200 nM latrunculin B. Such a low concentration of latrunculin B proved sufficient to depolymerize actin filaments in the seedlings within 24 h (Fig. S1). Additionally, we showed that 24 h treatment with latrunculin B does not induce plant cell death (Fig. S2). Significantly, by that time there was a sevenfold increase in the free SA level of the treated seedlings compared with the control ones. The only other phytohormone to display an increase (twofold) was jasmonic acid (JA). Apart from Indole-3-acetamide (IAM), which showed a threefold decrease, the other tested phytohormones remained largely unaltered (Fig. 1a; Table S1).

Having shown this dramatic rise in SA level in *A. thaliana*, we wondered which of its two SA biosynthetic pathways was responsible for this increase or whether they both contributed to it. One pathway involves phenylalanine ammonia-lyase (PAL, EC 4.3.1.24), which exists in four isoforms, while the other involves isochorismate synthase (ICS; EC 5.4.4.2), which occurs in two isoforms¹⁸. Analysis of the transcription of all *AtPAL* and *AtICS* genes in the seedlings revealed that only the *AtICS* genes were induced by latrunculin B (Fig. 1b). This shows that drug-induced actin depolymerization activates the ICS-dependent pathway and that this pathway alone is responsible for SA biosynthesis under these conditions.

Actin depolymerization leads to induced resistance of *A. thaliana* against *Pst* DC3000. Given that increased resistance to pathogens in *A. thaliana* is associated with SA biosynthesis through the ICS pathway^{19,20}, is it possible that activation of the same pathway invoked by drug-induced actin depolymerization also results in increased resistance? To investigate this, we used Ishiga *et al.*²¹ protocol as a basis for performing two *in vitro* *A. thaliana*-*Pseudomonas syringae* pv. *tomato* DC3000 (*Pst* DC3000) flood-inoculation assays in liquid and solid media²¹. We treated the seedlings with latrunculin B 24 h before inoculation with *Pst* DC3000. Remarkably, under both conditions, the latrunculin B-pretreated seedlings were more resistant than the control ones (Fig. 1c,d,e).

To ensure that this phenomenon is not just associated with *in vitro* conditions, we also performed experiments using four-week-old *A. thaliana* plants cultivated in soil, such plants typically being used for studies of *A. thaliana* resistance to *Pst* DC3000²². Unlike in the seedlings, 24 h treatment with 200 nM latrunculin B did not activate the SA pathway in the adult plants and, thus, no increased resistance was observed (Fig. 2a,b). However, the transcription of SA marker genes (*AtPR-1*, *AtICS1*) was induced after 24 h treatment with 1 μM latrunculin B (Fig. 2a), leading to increased resistance to *Pst* DC3000 (Fig. 2b). This suggests that plant resistance is strongly dependent on latrunculin B concentration, probably due to differences between the efficiency of latrunculin B-induced actin depolymerization in seedlings and in adult plants (Figs S1 and S3). Similar to latrunculin B, pretreatment with cytochalasin E led to both SA-induced gene transcription (Fig. S4a) and increased plant resistance to *Pst* DC3000 (Fig. S4b), thereby strengthening the notion that such resistance is due to the depolymerizing activity of cytoskeletal drugs. It should be noted that we exclude the antibacterial effect of latrunculin B because *Pst* DC3000 grew *in vitro* in the presence of latrunculin B at a similar rate as in the control medium (Fig. S5).

The induced resistance caused by actin depolymerization is dependent on salicylic acid. To further demonstrate the dependence of such resistance on the SA pathway, we performed assays using mutants known to have an impaired SA pathway and thus be more susceptible to *Pst* DC3000: *nahG*, which induces low endogenous SA levels through the expression of SA-hydroxylase²³, and *sid2*, a knock-out mutant of the *AtICS1* gene²⁴. As expected, latrunculin B did not induce resistance in the *nahG* plants (Fig. 2d,e). *Sid2* plants treated with latrunculin B were more resistant compared to *sid2* controls. However, latrunculin B treated *sid2* plants were still more susceptible than WT controls (Fig. 2e). The SA level is not induced in *sid2* plants (Fig. 2f) which correlates with the fact that none of SA biosynthetic genes does have induced transcription (Fig. S6b). Contrarily in seedlings, *ICS2* transcription is induced by latB (Fig. S6a). Altogether these results clearly confirm the crucial role of SA for actin depolymerization-induced resistance. However, increased resistance of latB treated *sid2* mutants uncover a new possible unknown SA independent mechanism triggering immunity.

Actin depolymerization induce SA pathway in *B. napus* and enhance its resistance against *L. maculans*. To show that this phenomenon is neither species-specific nor pathogen-specific, we investigated the effect of latrunculin B on an important crop, oilseed rape (*Brassica napus*). As in the case of *A. thaliana* in *B. napus*, latrunculin B upregulated the transcription of SA marker genes (*BnPR-1*, *BnICS1*) (Fig. 3a). Furthermore,

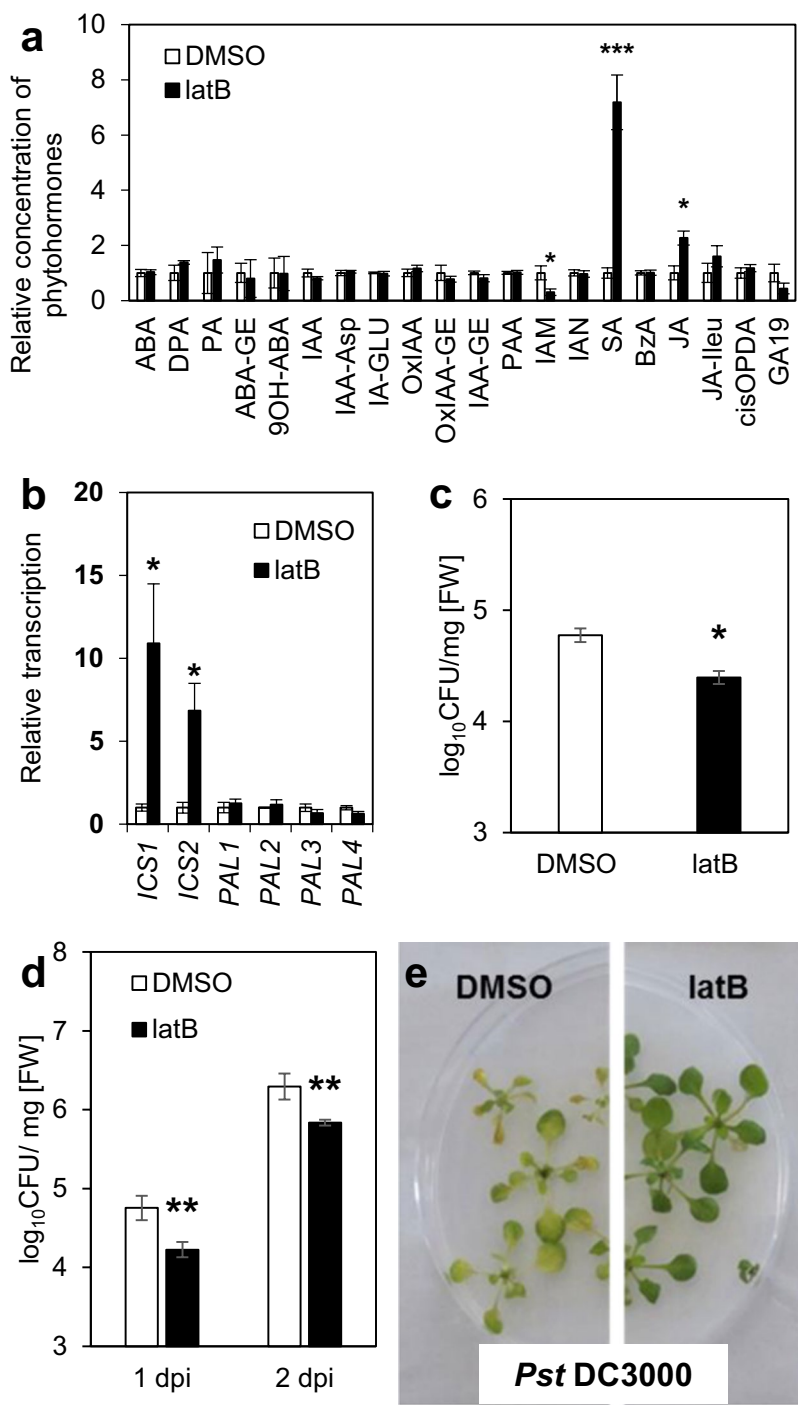


Figure 1. Seedlings of *A. thaliana*: Latrunculin B triggers SA biosynthesis and resistance to *Pst* DC3000. Seedlings were grown *in vitro* in liquid MS medium (**a–c**) and seedlings were grown *in vitro* in solid MS/2 medium (**d,e**). (**a**) Phytohormone analysis. Seedlings were treated for 24 h with 200 nM latrunculin B (latB) or 0.01% DMSO (control). For abbreviations of analyzed phytohormones, see Table S1. (**b**) Transcription of SA biosynthetic genes *ICS1*, *ICS2*, *PAL1*, *PAL2*, *PAL3* and *PAL4*. Seedlings were treated for 24 h with 200 nM latB or 0.01% DMSO. The transcription level was normalized to the reference gene, *SAND*. (**c**) Bacterial titres (liquid medium). Seedlings were pretreated for 24 h with 200 nM latB or 0.01% DMSO before inoculation with *Pst* DC3000. Tissue was harvested 1 day after inoculation with bacteria. (**d**) Bacterial titres (solid medium). Seedlings were pretreated for 24 h with 200 nM latB or 0.01% DMSO before inoculation with *Pst* DC3000. Tissue was harvested 1 and 2 days after inoculation with bacteria. (**e**) Representative photographs of seedlings grown on solid medium 2 days after inoculation with *Pst* DC3000. The values represent mean and error bars (SEM) from four (**a,c**), three to four (**b**) and five (**d**) independent samples. The asterisks represent statistically significant changes in latB-treated samples compared with controls (* $P < 0.05$; ** $P < 0.01$; *** $P < 0.001$; two tailed Student's t-test).

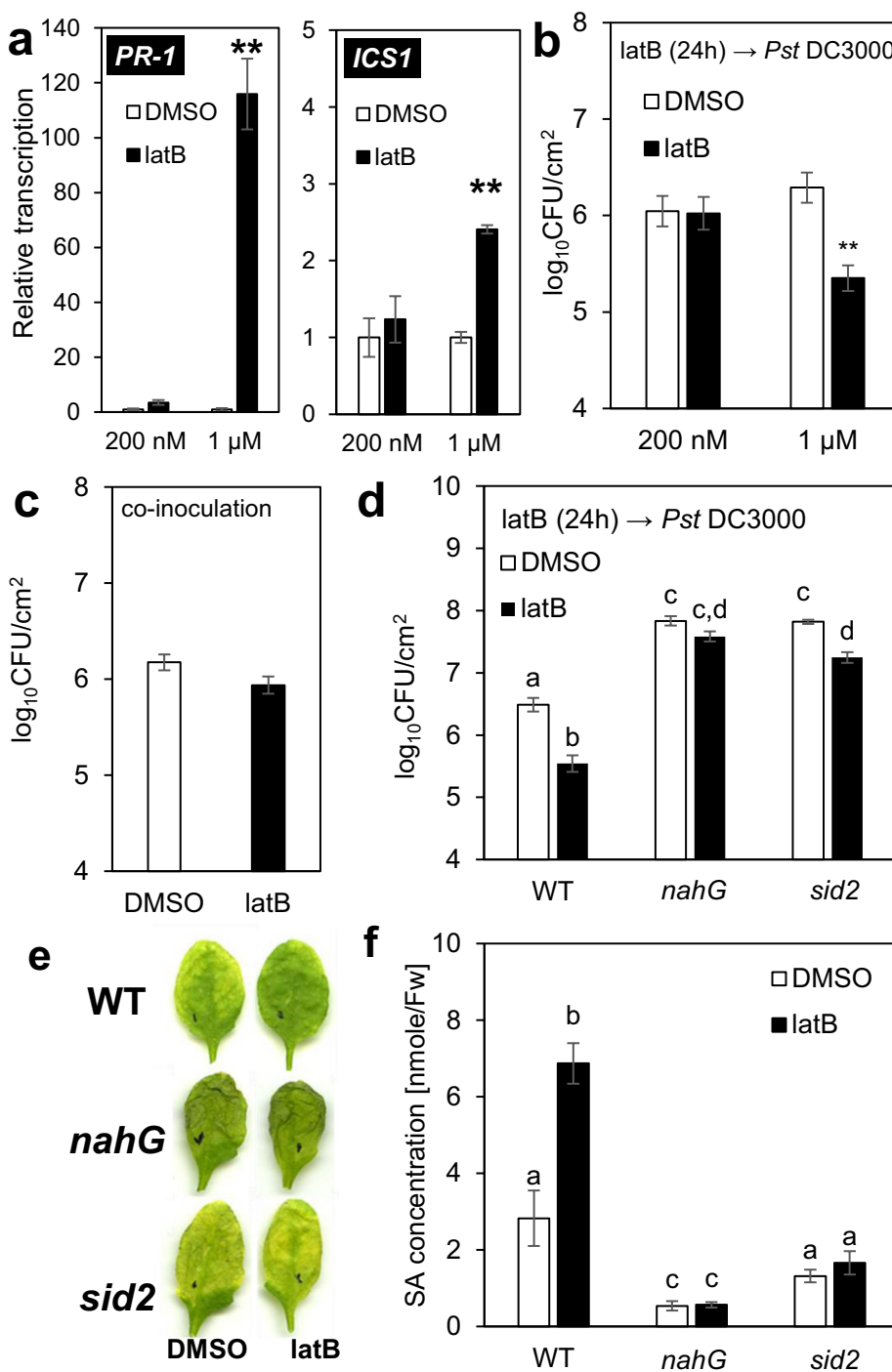


Figure 2. Four-week-old *A. thaliana*: Latrunculin B-triggered SA pathway is necessary for higher resistance to *Pst* DC3000. (a) Transcription of SA marker genes *PR-1* and *ICS1* in four-week-old *A. thaliana* plants. Plants were treated for 24 h with 200 nM or 1 μM latrunculin B (latB). The transcription level was normalized to the reference gene, *TIP41*. (b,c) Bacterial titres in four-week-old plants. (b) Plants were pretreated with 200 nM or 1 μM latB for 24 h before inoculation with *Pst* DC3000. Control plants were pretreated with 0.01 or 0.05% DMSO. (c) Plants were treated with 1 μM latB or 0.05% DMSO, each in a solution containing *Pst* DC3000. (d) Bacterial titres in four-week-old plants. (e) Representative photographs of adult *A. thaliana* leaves infected with *Pst* DC3000 3 days after inoculation. (f) Salicylic acid (SA) concentration after 24 h 1 μM latB treatment. Plants were treated for 24 h with 1 μM latB or 0.05% DMSO before inoculation with *Pst* DC3000. *A. thaliana* WT plants (col-0) and mutants with impaired SA pathways (*nahG* and *sid2*) were used (d, e, f). Tissue was harvested 3 days after inoculation with *Pst* DC3000. The values represent mean and error bars (SEM) from four (a,f) and six (b,c,e) independent samples. The asterisks represent statistically significant changes in latB-treated samples compared with controls (**P < 0.01; two tailed Student's t-test) and statistical differences between the samples (d,f) were assessed using a one-way ANOVA, with a Tukey honestly significant difference (HSD) multiple mean comparison post hoc test. Different letters indicate a significant difference, Tukey HSD, P < 0.01, n = 6.

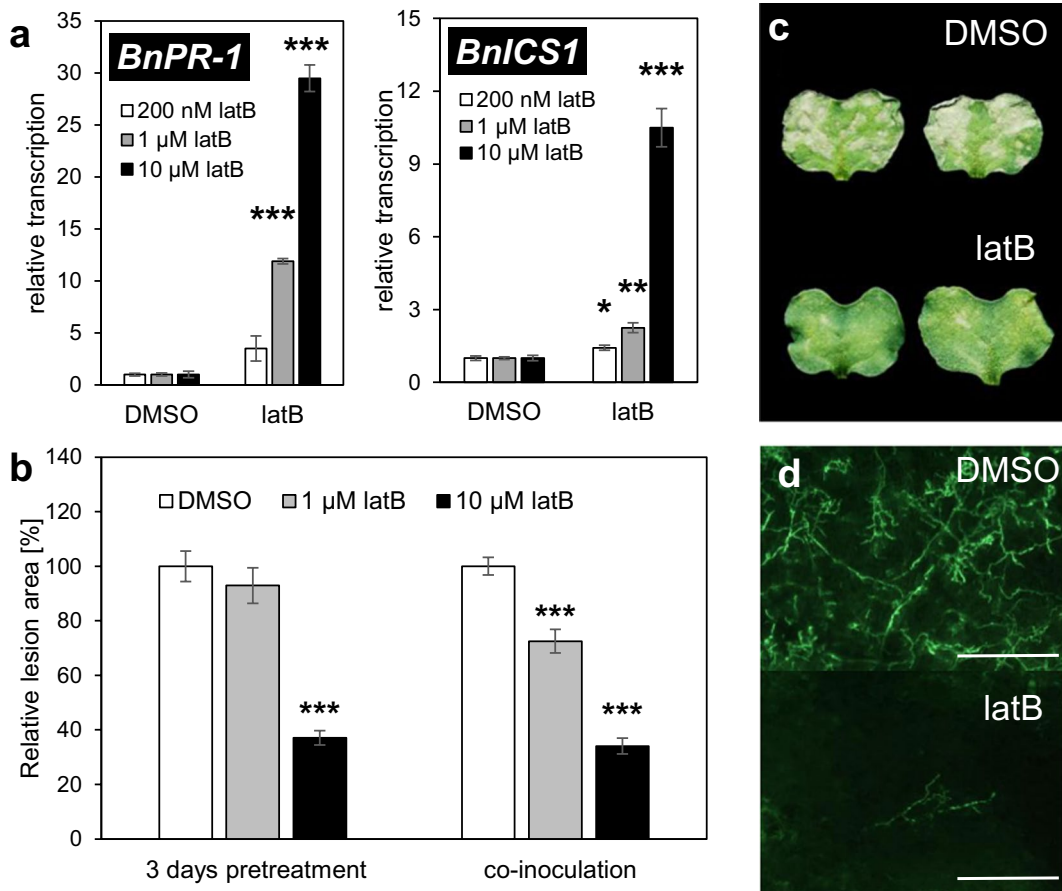


Figure 3. *B. napus* cotyledons: Latrunculin B triggers SA pathway and resistance to *L. maculans* (a). Transcription of SA marker genes *BnPR-1* and *BnICS1* in *B. napus* cotyledons. Cotyledons were treated for 24 h with infiltrations of 0.2, 1 or 10 µM latrunculin B (latB). Control cotyledons were treated for 24 h with a corresponding concentration of DMSO (0.01, 0.05 or 0.5%). The transcription level was normalized to the reference gene, *BnTIP41*. (b) *B. napus* susceptibility to *L. maculans* was evaluated as the relative lesion area (ratio of lesion area to whole leaf area) on the cotyledons. Cotyledons were treated with latrunculin B (latB; 1 µM or 10 µM) or DMSO control (0.05 or 0.5%), either 3 days before inoculation or simultaneously to inoculation by *L. maculans*. Lesions of DMSO controls in each treatment conditions were set as 100%. (c) Representative images of *L. maculans*-infected cotyledons. (d) Representative microscopy images of *L. maculans* hyphae proliferation in *B. napus* cotyledons in response to 10 µM latB or 0.5% DMSO. The bars correspond to 500 µM. The values represent mean and error bars (SEM) from three to four (a) and 60 -142 (b) independent samples. The asterisks represent statistically significant changes in latB-treated samples compared with controls (*P < 0.05; **P < 0.01; ***P < 0.001; two tailed Student's t-test).

as with adult *A. thaliana*, the effect of latrunculin B on *B. napus* was concentration dependent (Fig. 3a). The increased transcription of *BnPR-1* also occurred 72 h after latrunculin B treatment. On the other hand, *BnICS1* was not induced, indicating a transient effect of actin depolymerisation on *BnICS1* transcription (Fig. S7). The treatment of *B. napus* with 10 µM latrunculin B 3 days before inoculation with a hemibiotrophic fungal pathogen, *L. maculans*, efficiently inhibited hyphal colonisation and necrosis formation in the infected cotyledons (Fig. 3b,c,d). Treatment with 1 µM latrunculin B led to much weaker and variable resistance against *L. maculans* (Fig. 3b), corresponding to the weaker transcription of defence-related genes (Fig. 3a). These data are in accordance with our previous study characterizing the importance of SA in the defence of *B. napus* against *L. maculans*²⁵. In addition, we observed significant cytochalasin E-induced resistance to *L. maculans* in *B. napus* (Fig. S8), which suggests that the effect is not compound-specific. Furthermore, neither latrunculin B nor cytochalasin E displayed antifungal activity on *L. maculans* growth *in vitro* (Fig. S9). Interestingly, the co-inoculation of *B. napus* cotyledons with a joint solution of 1 and 10 µM latrunculin B and *L. maculans* conidia also induced resistance (Fig. 3b).

Discussion

Our results indicate that depolymerized actin can trigger resistance to bacterial or fungal pathogens. Thus, we have shown that plant immunity is strongly activated by depolymerised actin and that this phenomenon appears to be generally valid; namely, it seems not to be species specific, pathogen-type specific or drug-type specific. These findings do not negate those of previous studies that showed the susceptibility of plants treated

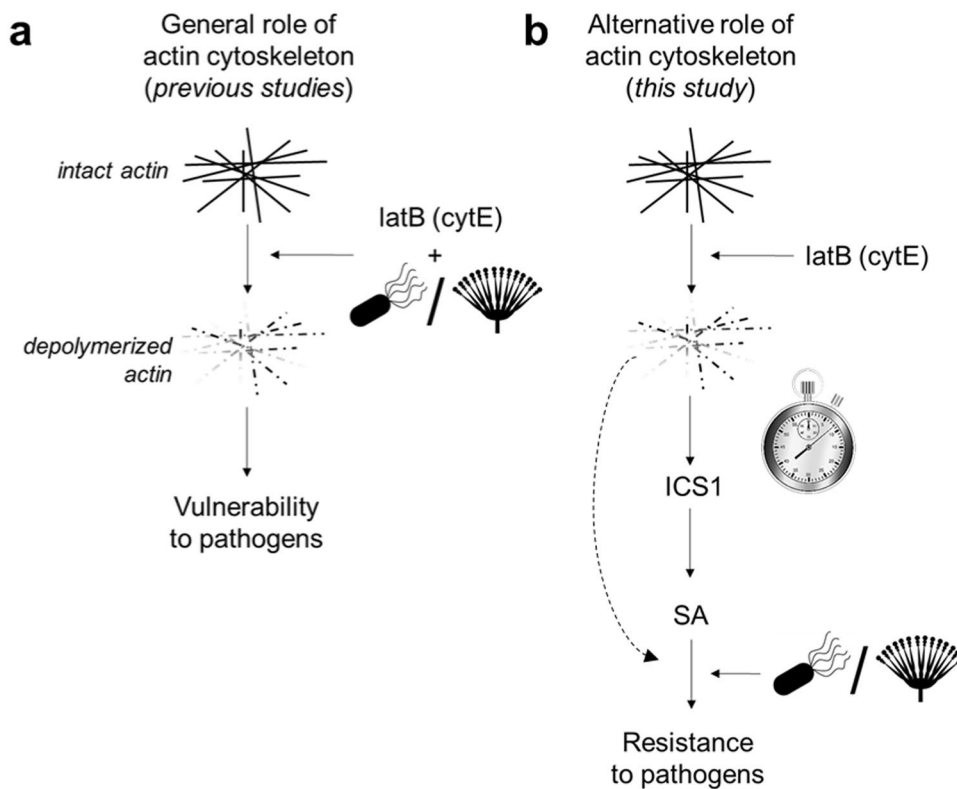


Figure 4. Possible dual role of actin cytoskeleton in plant response to pathogens. **(a)** The widely-published scenario in which depolymerization of the actin cytoskeleton by treatment with latrunculin B or cytochalasin E leads to increased plant vulnerability to pathogens. Studies showing this phenomenon co-inoculated plants with a drug and pathogen. **(b)** The new alternative scenario for the role of the actin cytoskeleton proposed in this manuscript. Plants pretreated with latrunculin B or cytochalasin E before inoculation with a pathogen have time to activate the salicylic acid signalling pathway, resulting in increased resistance to the subsequently inoculated pathogens. latB = latrunculin B; cytE = cytochalasin E; SA = salicylic acid; ICS1 = isochorismate synthase 1; = fungi; = bacteria.

with cytoskeletal drugs to pathogens^{5–7,12,13,15}. Rather, they reveal that the plant disease resistance is strongly dependent on whether the plant has sufficient time to activate SA-mediated immunity (Fig. 4). This was clearly shown by our experiments with *Pst* DC3000, in which pre-infection treatment with cytoskeletal drugs resulted in resistance whilst co-inoculation did not (Fig. 2b,c,e). The co-inoculation of cytochalasin D and *Pst* DC3000 also had no effect on resistance according to Shimono *et al.*¹¹. Other previous studies using actin-depolymerizing drugs showed higher susceptibility to *Pst* DC3000 when co-inoculation was used^{5–7} (Fig. 4). It is also important to mention that actin filaments response to plant immunity is strongly dependent on conditions used in the study. A good example are effects of different MAMPs (flg22 and elf26) on actin reorganization. Using 24 day-old plants infiltrated with MAMPs, Henty-Ridilla *et al.*⁵ showed that treatment with flg22 induces actin reorganization, while elf26 does not⁵. Contradictorily to that, in epidermal cells of hypocotyl grown in the dark, Henty-Ridilla *et al.*⁴ showed that elf26 induces reorganisation and flg22 does not⁴ (an explanation could be that under these conditions, FLS2 receptor of flg22 is not expressed). In this study, we excluded the effect of different conditions on induced resistance of *A. thaliana* against *Pst* DC3000 by testing three different setups (Figs 1c,d and 2b,e). The result was in all cases similar, whereby pretreatment with latrunculin B induced resistance of *A. thaliana* against *Pst* DC3000.

Interestingly, treatment with latrunculin B resulted in increased resistance in both *L. maculans* setups: pretreatment (Fig. 3b) and co-inoculation (Fig. 3b). This suggests that the rapidity of pathogen growth is a crucial factor. In contrast to *Pst* DC3000, which strongly damaged the inoculated leaves within three days, almost no multiplication of *L. maculans* occurred during the same period²⁵. Thus, it appears that the slow growth of *L. maculans* enabled *B. napus* to establish the SA pathway, which was induced within 24 hours of cytoskeletal drug treatment (Fig. 3a). Overall then, while it is true that plant resistance to pathogens is decreased by a disrupted actin cytoskeleton, our results show that, given sufficient time, plants are able to trigger SA-based defence mechanisms to overcome such threats. This could be due to SA antimicrobial activity, accompanied by the SA-induced production of antimicrobial compounds. These powerful SA properties have been nicely demonstrated in relationship to so-called age-related resistance^{26–28}. Our study shows that SA pathway, specifically induced by actin depolymerization, is more powerful despite the missing actin dynamics.

Up to date, some other works suggest the possible positive effect of depolymerization of actin cytoskeleton on plant immunity. Kobayashi and Kobayashi¹⁶ showed that treatment with cytochalins induce *NtPR1* transcription in tobacco. Additionally, cytochalasin E primed tobacco cells to induce HR-like cell death in presence of *Erysiphe cichoracearum*. We can speculate that it could lead to higher resistance against this biotrophic pathogen but it was not explicitly tested¹⁶. We confirmed the induction of *AtPR-1* gene upon treatment with cytoskeletal depolymerizing drugs in *A. thaliana*^{17,29}. Recently it was shown that overexpression of *AtPRF3*, which leads to depolymerization of actin filaments, increased ROS production upon flg22 treatment³⁰. However to our best knowledge, we herein provide the first direct evidence that disruption of the actin cytoskeleton can actually lead to increased plant resistance to pathogens, and that SA is crucial to this process. We strongly believe that our work opens a new and important direction for further research. Is the influence of the actin cytoskeleton on vesicle trafficking involved in SA biosynthesis? For example, when PRRs (pattern recognising receptors) on the plasma membrane recognize MAMPs, it triggers PRRs endocytosis which, in turn, might activate the SA pathway^{31,32}. A well characterised example is the internalization of FLS2, which is dependent on the actin-myosin complex³³. Thus, could an imbalance in PRRs result in constitutively activated immunity and, thereby, induce SA biosynthesis? A hint in support of such a hypothesis is provided by a double mutant with impaired phosphatidylinositol-4-kinase $\beta 1$ and $\beta 2$ (*pi4k $\beta 1\beta 2$*), which has been shown to alter vesicle trafficking and constitutively increase SA concentration^{34,35}. It is also possible that plants have evolved a system for detecting actin cytoskeleton disruption and that the activation of such a system triggers SA-specific immune responses. However, as yet, we are not able to determine if chemically-depolymerised actin is really the triggering event for immune signalling or whether a pleiotrophic event, such as endoplasmic reticulum stress, results in SA induction. For this reason, further research should be focused on deciphering the specific mechanism by which actin depolymerization triggers SA biosynthesis and the ensuing increased plant resistance to pathogens.

Materials and Methods

Plant material. For the *A. thaliana* experiments, the following genotypes were used: Columbia-0 (WT); *sid2-3* (SALK_042603)²⁴; *nahG*²³ and *pUBC:Lifeact-GFP*³⁶. *A. thaliana* seedlings were grown either in liquid MS medium or on solid MS/2 medium. Per litre, the liquid MS medium contained the following: 4.41 g Murashige and Skoog medium including vitamins (Duchefa, Netherlands), 5 g sucrose, 5 g MES monohydrate (Duchefa, Netherlands). Per litre, the solid MS/2 medium contained 2.2 g Murashige and Skoog medium (Duchefa, Netherlands) with 10 g sucrose and 8 g Plant agar (Duchefa, Netherlands). Both media were adjusted to pH 5.7 using 1 M KOH. For cultivation in the liquid, surface-sterilized seeds were sown in 24-well plates containing 400 μ L of liquid MS medium per well. The plants were cultivated for 10 days under a short-day photoperiod (10 h/14 h light/dark regime) at 100–130 μ E m⁻² s⁻¹ and 22 °C. On the 7th day, the medium in the wells was exchanged for a fresh one. For cultivation on the solid MS/2 medium, seedlings were grown in Petri dishes for 12 days under a long-day photoperiod (16 h/8 h light/dark regime) at 100–130 μ E m⁻² s⁻¹ and 22 °C. For *A. thaliana* plants grown for 4 weeks in soil, surface-sterilized seeds were sown in Jiffy 7 peat pellets and the plants cultivated under a short-day photoperiod (10 h/14 h light/dark regime) at 100–130 μ E m⁻² s⁻¹, 22 °C and 70% relative humidity. They were watered with fertilizer-free distilled water as necessary.

For the *B. napus* experiments, plants of the Eurol cultivar were grown hydroponically in perlite in Steiner's nutrient solution (Steiner, 1984) under a 14 h/10 h light/dark regime (25 °C/22 °C) at 150 μ E m⁻² s⁻¹ and 30–50% relative humidity. True leaves were removed from 14-day-old plantlets to avoid cotyledon senescence.

Treatment with chemical compounds. As actin depolymerizing drugs, latrunculin B (Sigma-Aldrich, USA) and cytochalasin E (Sigma-Aldrich, USA) were used. Latrunculin B and cytochalasin E were both dissolved in DMSO; the concentration of the stock solutions were 2 mM and 4 mM, respectively.

For the *Pst* DC3000 resistance assay, the seedlings grown in 24-well plates were treated by replacing the pure liquid MS medium in the plate wells with medium containing 200 nM latrunculin B or 0.01% DMSO control. The seedlings cultivated on the solid medium were treated 24 h by flooding with 10 mL of MS/2 medium containing 200 nM latrunculin B or 0.01% DMSO control. Fully-developed leaves from four-week-old *A. thaliana* grown in soil were infiltrated either with 200 nM or 1 μ M latrunculin B (0.01% or 0.05% DMSO as respective controls) or with 1 μ M or 10 μ M cytochalasin E (0.025% or 0.25% DMSO as respective controls) 24 h before *Pst* DC3000 infection using a needleless syringe.

For the transcriptomic assay, the seedlings of *A. thaliana* grown in 24-well plates were treated 24 h with 200 nM latrunculin B (0.01% DMSO control) or 10 μ M cytochalasin E (0.25% DMSO control). Four-week old *A. thaliana* were infiltrated with 200 nM (0.01% DMSO) or 1 μ M latrunculin B (0.05% DMSO) for 24 h. The 10-day-old cotyledons of *B. napus* were infiltrated either with 1 μ M or 10 μ M latrunculin B or with 10 μ M cytochalasin E (in all cases with corresponding DMSO controls) using a needleless syringe. For infection assay 3 days before infection with *L. maculans*, for transcriptomic assay 24 and 72 h before harvesting tissue.

Inoculation of *A. thaliana* seedlings with *Pst* DC3000. After the *A. thaliana* seedlings had been cultivated in 24-well plates in the liquid MS medium for 10 days, the cultivation medium was exchanged for one containing latrunculin B or cytochalasin E, and incubated for 24 h. On day 11, the medium was replaced with a bacterial suspension of *Pst* DC3000 in 10 mM MgCl₂ (OD₆₀₀ = 0.01). The seedlings were incubated in this bacterial suspension for 1 min. After incubation, the suspension was replaced with the liquid MS medium. On day 12, the seedlings were harvested, each sample taken containing all of the seedlings from three wells. The seedlings were then homogenized in tubes with 1 g of 1.3 mm silica beads using a FastPrep-24 instrument (MP Biomedicals, USA). The resulting homogenate was serially diluted and pipetted onto King B plates. The colonies were counted after 1–2 days of incubation at 28 °C.

The seedlings cultivated on solid medium were flooded with 200 nM latrunculin B solution in water on day 13. Control plants were treated with a corresponding solution of DMSO. On day 14, the solutions were replaced with a suspension of overnight culture of *Pst* DC3000 ($OD_{600} = 0.01$) containing 0.025% Silwet. Samples were harvested at 0, 1 and 2 dpi, with each sample containing the plants from five plates. The seedlings were homogenized in tubes with 1 g of 1.3 mm silica beads using a FastPrep-24 instrument (MP Biomedicals, USA). The resulting homogenate was serially diluted and pipetted onto LB plates containing rifampicin. The colonies were counted after 1–2 days of incubation at 28 °C.

Inoculation of four-week-old *A. thaliana* with *Pst* DC3000. *Pst* DC3000 was grown overnight on King B agar plates at 28 °C, resuspended in 10 mM MgCl₂, and diluted to an OD_{600} of 0.001. Using a needleless syringe, the bacterial suspension was infiltrated into three fully-developed leaves from one plant. After 3 days, the infected tissue was collected as cut leaf discs (one disc per leaf, 0.6-cm diameter); three leaf discs from one plant represent one sample. The discs were homogenized in tubes with 1 g of 1.3 mm silica beads using a FastPrep-24 instrument (MP Biomedicals, USA). The resulting homogenate was serially diluted and pipetted onto King B plates. The colonies were counted after 1–2 days of incubation at 28 °C.

Inoculation of *B. napus* with *L. maculans*. *L. maculans* isolate v23.1.3^{35,37} was used to inoculate *B. napus*. After harvesting, conidia obtained according to Šášek *et al.*²⁵ were washed once with distilled water, diluted to 10^8 spores/ml, and stored at -20 °C for up to 6 months. The cotyledons of 14-day-old plants were infiltrated by conidial suspension (10^5 conidia/ml), with at least 12 plants being used for each inoculation. The leaves were assessed for lesions 10 days after inoculation. The leaf area and the lesion areas therein were measured by image analysis using APS Assess 2.0 software (American Phytopathological Society, USA). The relative lesion area was then calculated as the ratio of lesion area to whole leaf area. For the microscopy studies, the cotyledons infected with GFP-tagged v23.1.3 isolate³⁸ were observed at 10 dpi using a Leica DM5000 B microscope.

Gene expression analysis. The whole seedlings from three independent wells were immediately frozen in liquid nitrogen. The tissue was homogenized in tubes with 1 g of 1.3 mm silica beads using a FastPrep-24 instrument (MP Biomedicals, USA). Total RNA was isolated using a Spectrum Plant Total RNA kit (Sigma-Aldrich, USA) and treated with a DNA-free kit (Ambion, USA). Subsequently, 1 µg of RNA was converted into cDNA with M-MLV RNase H⁻ Point Mutant reverse transcriptase (Promega Corp., USA) and an anchored oligo dT21 primer (Metabion, Germany). Gene expression was quantified by q-PCR using a LightCycler 480 SYBR Green I Master kit and LightCycler 480 (Roche, Switzerland). The PCR conditions were 95 °C for 10 min followed by 45 cycles of 95 °C for 10 s, 55 °C for 20 s, and 72 °C for 20 s. Melting curve analysis was then conducted. Relative expression was normalized to the housekeeping genes *AtSAND* and *BnTIP41*. Primers were designed using PerlPrimer v1.1.21³⁹. A list of the analysed genes and primers is available in Table S2.

Phytohormonal analysis. Hormone analysis was carried out on four samples, each of which contained all seedlings from six of the 24 wells or from the four-week-old *A. thaliana* three leaf discs from every single plant were sampled, three individual plants were sampled as one sample. Plant hormone levels were determined as described by⁴⁰. Briefly, samples were homogenized in tubes with 1.3 mm silica beads using a FastPrep-24 instrument (MP Biomedicals, USA). The samples were then extracted with a methanol/H₂O/formic acid (15:4:1, v:v:v) mixture, which was supplemented with stable isotope-labeled phytohormone internal standards (10 pmol per sample) in order to check recovery during purification and validate the quantification. The clarified supernatants were subjected to solid phase extraction using Oasis MCX cartridges (Waters Co., USA). The eluates were evaporated to dryness and the generated solids dissolved in 30 µl of 15% (v/v) acetonitrile in water. Quantification was performed on an Ultimate 3000 high-performance liquid chromatograph (Dionex, USA) coupled to a 3200 Q TRAP hybrid triple quadrupole/linear ion trap mass spectrometer (Applied Biosystems, USA) as described by⁴¹. Metabolite levels were expressed in pmol/g fresh weight (FW).

Confocal microscopy of actin filaments. For *in vivo* microscopy, a Zeiss LSM 880 inverted confocal laser scanning microscope (Carl Zeiss AG, Germany) was used with either a 40× C-Apochromat objective (NA = 1.2 W) or a 20x Plan-Apochromat objective (NA = 0.8). GFP fluorescence (excitation 488 nm, emission 489–540 nm) was acquired in z-stacks (20–25 µm thickness). The maximum intensity projections obtained from the z-stacks were created using Zeiss ZEN Black software. Actin filaments density analysis was calculated by Fiji software (<https://fiji.sc>)⁴² as the percent occupancy of GFP signal in each Maximum intensity projection. Image threshold was set to include all actin filaments and area fraction was measured. We analysed 7–11 cutouts from 6–7 plants for each variant. Representative images were selected from photos from at least 6 independent plants.

Growth of *Pst* DC3000 and *L. maculans* *in vitro* in presence of latrunculin B or cytochalasin E. *Pst* DC3000 grew overnight on solid LB medium containing rifampicin. From this, a fresh bacterial suspension was prepared ($OD_{600} = 0.01$) in liquid LB or liquid MS medium. To this suspension, latrunculin B (200 nM or 1 µM) or DMSO (0.05% or 0.01%) was added. The OD_{600} was measured 6 and 24 h after suspension preparation. Four independent samples were prepared for each type of treatment.

Conidia of the GFP-tagged v23.1.3 isolate of *L. maculans*³⁸ were grown *in vitro* in Gamborg B5 medium (Duchefa, Netherlands) supplemented with 0.3% (w/v) sucrose and 10 mM MES monohydrate, and adjusted to pH 6.8. This medium contained latrunculin B (1, 10 µM), cytochalasin E (1, 10 µM) or DMSO control (0.5%), and had a final concentration of 2500 conidia per well. The plates (black 96-well plate, Nunc R), covered with lids and sealed with Parafilm®, were incubated in darkness at 26 °C. On day 4, fluorescence was measured using a Tecan F200 fluorescence reader (Tecan, Switzerland) equipped with a 485/20 nm excitation filter and 535/25 nm emission filter. Eight wells were measured for each treatment.

Trypan blue staining. Detached leaves were immersed to the staining solution (10 mL lactic acid (85%, w:w), 10 mL phenol, 10 mL glycerol, 10 mL dH₂O, 40 mg trypan blue (final concentration 10 mg·mL⁻¹) for 30 min due to Fernández-Bautista *et al.*⁴³. Solution was then replaced by ethanol 3 times until leaves were fully decolored from chlorophyll. Leaves were rehydrated by replacing solution with the decreasing ethanol solutions (70%, 50%, 30%, v:v) and kept in water for the microscopy purposes.

Statistical analyses. All experiments were repeated at least three times, except Fig. 3B where we put together data from 3–7 biological repetitions. All statistical analyses were performed with Microsoft Excel 2013. The P values were calculated using a two-tailed Student's t-test or one-way ANOVA followed with Tukey honestly significant difference (HSD) p < 0,01 using software Statistica® v.11 or SigmaPlot11®.

References

- Day, B., Henty, J. L., Porter, K. J. & Staiger, C. J. The pathogen-actin connection: a platform for defense signaling in plants. *Annu Rev Phytopathol* **49**, 483–506, <https://doi.org/10.1146/annurev-phyto-072910-095426> (2011).
- Li, P. & Day, B. Battlefield Cytoskeleton: Turning the Tide on Plant Immunity. *Mol Plant Microbe Interact*, MPMI07180195FI, <https://doi.org/10.1094/MPMI-07-18-0195-FI> (2018).
- Hardham, A. R., Jones, D. A. & Takemoto, D. Cytoskeleton and cell wall function in penetration resistance. *Curr Opin Plant Biol* **10**, 342–348, <https://doi.org/10.1016/j.pbi.2007.05.001> (2007).
- Henty-Ridilla, J. L., Li, J., Day, B. & Staiger, C. J. ACTIN DEPOLYMERIZING FACTOR4 regulates actin dynamics during innate immune signaling in Arabidopsis. *Plant Cell* **26**, 340–352, <https://doi.org/10.1105/tpc.113.122499> (2014).
- Henty-Ridilla, J. L. *et al.* The plant actin cytoskeleton responds to signals from microbe-associated molecular patterns. *PLoS Pathog* **9**, e1003290, <https://doi.org/10.1371/journal.ppat.1003290> (2013).
- Jelenska, J., Kang, Y. & Greenberg, J. T. Plant pathogenic bacteria target the actin microfilament network involved in the trafficking of disease defense components. *Bioarchitecture* **4**, 149–153, <https://doi.org/10.4161/19490992.2014.980662> (2014).
- Kang, Y. *et al.* HopW1 from *Pseudomonas syringae* disrupts the actin cytoskeleton to promote virulence in Arabidopsis. *PLoS Pathog* **10**, e1004232, <https://doi.org/10.1371/journal.ppat.1004232> (2014).
- Tian, M. *et al.* Arabidopsis actin-depolymerizing factor AtADF4 mediates defense signal transduction triggered by the *Pseudomonas syringae* effector AvrPphB. *Plant Physiol* **150**, 815–824, <https://doi.org/10.1104/pp.109.137604> (2009).
- Porter, K., Shimono, M., Tian, M. & Day, B. Arabidopsis Actin-Depolymerizing Factor-4 links pathogen perception, defense activation and transcription to cytoskeletal dynamics. *PLoS Pathog* **8**, e1003006, <https://doi.org/10.1371/journal.ppat.1003006> (2012).
- Inada, N., Higaki, T. & Hasezawa, S. Nuclear Function of Subclass I Actin-Depolymerizing Factor Contributes to Susceptibility in Arabidopsis to an Adapted Powdery Mildew Fungus. *Plant Physiol* **170**, 1420–1434, <https://doi.org/10.1104/pp.15.01265> (2016).
- Shimono, M. *et al.* The *Pseudomonas syringae* Type III Effector HopG1 Induces Actin Remodeling to Promote Symptom Development and Susceptibility during Infection. *Plant Physiol* **171**, 2239–2255, <https://doi.org/10.1104/pp.16.01593> (2016).
- Shimada, C. *et al.* Nonhost resistance in Arabidopsis-Colletotrichum interactions acts at the cell periphery and requires actin filament function. *Mol Plant Microbe Interact* **19**, 270–279, <https://doi.org/10.1094/MPMI-19-0270> (2006).
- Miklis, M. *et al.* Barley MLO modulates actin-dependent and actin-independent antifungal defense pathways at the cell periphery. *Plant Physiol* **144**, 1132–1143, <https://doi.org/10.1104/pp.107.098897> (2007).
- Kobayashi, Y., Yamada, M., Kobayashi, I. & Kunoh, H. Actin microfilaments are required for the expression of nonhost resistance in higher plants. *Plant Cell Physiol* **38**, 725–733, <https://doi.org/10.1093/oxfordjournals.pcp.a029226> (1997).
- Yun, B. W. *et al.* Loss of actin cytoskeletal function and EDS1 activity, in combination, severely compromises non-host resistance in Arabidopsis against wheat powdery mildew. *Plant J* **34**, 768–777 (2003).
- Kobayashi, Y. K. I. Depolymerization of the actin cytoskeleton induces defense responses in tobacco plants. *Journal of General Plant Pathology* **73**, 360–364 (2007).
- Matouskova, J. *et al.* Changes in actin dynamics are involved in salicylic acid signaling pathway. *Plant Sci* **223**, 36–44, <https://doi.org/10.1016/j.plantsci.2014.03.002> (2014).
- Dempsey, D. A., Vlot, A. C., Wildermuth, M. C. & Klessig, D. F. Salicylic Acid biosynthesis and metabolism. *Arabidopsis Book* **9**, e0156, <https://doi.org/10.1199/tab.0156> (2011).
- Vlot, A. C., Dempsey, D. A. & Klessig, D. F. Salicylic Acid, a multifaceted hormone to combat disease. *Annu Rev Phytopathol* **47**, 177–206, <https://doi.org/10.1146/annurev.phyto.050908.135202> (2009).
- Wildermuth, M. C., Dewdney, J., Wu, G. & Ausubel, F. M. Isochorismate synthase is required to synthesize salicylic acid for plant defence. *Nature* **414**, 562–565, <https://doi.org/10.1038/35107108> (2001).
- Ishiga, Y., Ishiga, T., Uppalapati, S. R. & Mysore, K. S. Arabidopsis seedling flood-inoculation technique: a rapid and reliable assay for studying plant-bacterial interactions. *Plant Methods* **7**, 32, <https://doi.org/10.1186/1746-4811-7-32> (2011).
- Katagiri, F., Thilmony, R. & He, S. Y. The Arabidopsis thaliana-pseudomonas syringae interaction. *Arabidopsis Book* **1**, e0039, <https://doi.org/10.1199/tab.0039> (2002).
- Delaney, T. P. *et al.* A central role of salicylic Acid in plant disease resistance. *Science* **266**, 1247–1250, <https://doi.org/10.1126/science.266.5188.1247> (1994).
- Nawrath, C. & Metraux, J. P. Salicylic acid induction-deficient mutants of Arabidopsis express PR-2 and PR-5 and accumulate high levels of camalexin after pathogen inoculation. *Plant Cell* **11**, 1393–1404 (1999).
- Sasek, V. *et al.* Recognition of avirulence gene AvrLm1 from hemibiotrophic ascomycete Leptosphaeria maculans triggers salicylic acid and ethylene signaling in Brassica napus. *Mol Plant Microbe Interact* **25**, 1238–1250, <https://doi.org/10.1094/MPMI-02-12-0033-R> (2012).
- Cameron, R. K. & Zaton, K. Intercellular salicylic acid accumulation is important for age-related resistance in Arabidopsis to *Pseudomonas syringae*. *Physiol. Mol Plant P* **65**, 197–209, <https://doi.org/10.1016/j.pmp.2005.02.002> (2004).
- Kus, J. V., Zaton, K., Sarkar, R. & Cameron, R. K. Age-related resistance in Arabidopsis is a developmentally regulated defense response to *Pseudomonas syringae*. *Plant Cell* **14**, 479–490 (2002).
- Wilson, D. C., Kempthorne, C. J., Carella, P., Liscombe, D. K. & Cameron, R. K. Age-Related Resistance in Arabidopsis thaliana Involves the MADS-Domain Transcription Factor SHORT VEGETATIVE PHASE and Direct Action of Salicylic Acid on *Pseudomonas syringae*. *Mol Plant Microbe Interact* **30**, 919–929, <https://doi.org/10.1094/MPMI-07-17-0172-R> (2017).
- Janda, M., Matouskova, J., Burketova, L. & Valentova, O. Interconnection between actin cytoskeleton and plant defense signaling. *Plant Signal Behav* **9**, e976486, <https://doi.org/10.4161/15592324.2014.976486> (2014).
- Sun, H. *et al.* Profilin Negatively Regulates Formin-Mediated Actin Assembly to Modulate PAMP-Triggered Plant Immunity. *Curr Biol* **28**, 1882–1895 e1887, <https://doi.org/10.1016/j.cub.2018.04.045> (2018).
- Tsuda, K., Glazebrook, J. & Katagiri, F. The interplay between MAMP and SA signaling. *Plant Signal Behav* **3**, 359–361 (2008).
- Tsuda, K., Sato, M., Glazebrook, J., Cohen, J. D. & Katagiri, F. Interplay between MAMP-triggered and SA-mediated defense responses. *Plant J* **53**, 763–775, <https://doi.org/10.1111/j.1365-313X.2007.03369.x> (2008).

33. Beck, M., Zhou, J., Faulkner, C., MacLean, D. & Robatzek, S. Spatio-temporal cellular dynamics of the *Arabidopsis* flagellin receptor reveal activation status-dependent endosomal sorting. *Plant Cell* **24**, 4205–4219, <https://doi.org/10.1105/tpc.112.100263> (2012).
34. Preuss, M. L. *et al.* A role for the RabA4b effector protein PI-4Kbeta1 in polarized expansion of root hair cells in *Arabidopsis thaliana*. *J Cell Biol* **172**, 991–998, <https://doi.org/10.1083/jcb.200508116> (2006).
35. Sasek, V. *et al.* Constitutive salicylic acid accumulation in pi4kIIIbeta1beta2 *Arabidopsis* plants stunts rosette but not root growth. *New Phytol* **203**, 805–816, <https://doi.org/10.1111/nph.12822> (2014).
36. Cvrcikova, F. & Oulehlova, D. A new kymogram-based method reveals unexpected effects of marker protein expression and spatial anisotropy of cytoskeletal dynamics in plant cell cortex. *Plant Methods* **13**, 19, <https://doi.org/10.1186/s13007-017-0171-9> (2017).
37. Rouxel, T. *et al.* Effector diversification within compartments of the *Leptosphaeria maculans* genome affected by Repeat-Induced Point mutations. *Nat Commun* **2**, 202, <https://doi.org/10.1038/ncomms1189> (2011).
38. Trda, L. *et al.* Cytokinin Metabolism of Pathogenic Fungus *Leptosphaeria maculans* Involves Isopentenyltransferase, Adenosine Kinase and Cytokinin Oxidase/Dehydrogenase. *Front Microbiol* **8**, 1374, <https://doi.org/10.3389/fmicb.2017.01374> (2017).
39. Marshall, O. J. PerlPrimer: cross-platform, graphical primer design for standard, bisulphite and real-time PCR. *Bioinformatics* **20**, 2471–2472, <https://doi.org/10.1093/bioinformatics/bth254> (2004).
40. Dobrev, P. I. & Kaminek, M. Fast and efficient separation of cytokinins from auxin and abscisic acid and their purification using mixed-mode solid-phase extraction. *J Chromatogr A* **950**, 21–29 (2002).
41. Dobrev, P. I., Hoyerova, K. & Petrasek, J. Analytical Determination of Auxins and Cytokinins. *Methods Mol Biol* **1569**, 31–39, https://doi.org/10.1007/978-1-4939-6831-2_2 (2017).
42. Schindelin, J. *et al.* Fiji: an open-source platform for biological-image analysis. *Nat Methods* **9**, 676–682, <https://doi.org/10.1038/nmeth.2019> (2012).
43. Fernández-Bautista, N., Domínguez-Núñez, J. A., Moreno, M. M. C. & Berrocal-Lobo, L. Plant Tissue Trypan Blue Staining During Phytopathogen Infection. *BioProtocol* **6**, <https://doi.org/10.21769/BioProtoc.2078> (2016).

Acknowledgements

We would like to thank Dr. Kenichi Tsuda from MPIPZ Cologne for providing the strain of *Pseudomonas syringae* pv. *tomato* DC3000, prof. Silke Robatzek from LMU Munich for her advices about the text and to Andrea Kung Wai for help with English editing. This work was supported by Czech Science Foundation grant no. 17-05151S and GAUK no. 992416. IEB Imaging Facility is supported by OPPK CZ.2.16/3.1.00/21519 and MEYS LM2015062 from (No. CZ.02.1.01/0.0/0.0/16_019/0000738) were supported: Hana Leontovýčová, Tetiana Kalachova, Romana Pospíchalová, Petre I. Dobrev, Burkertová. From Charles University in Prague (project n. SVV260427/2019) was supported Hana Leontovýčová. The pUBC::Lifeact-GFP and 35S::GFP-FABD2 seeds were kindly provided by Dr. Denisa Oulehlová from Žáorský laboratory at IEB ASCR. The image of watches in Figure 4 was downloaded for free from <https://pixabay.com/>.

Author Contributions

H.L., L.T., T.K., M.J. designed the experiments; H.L., L.T., T.K., L.L., R.P., P.I.D., K.M., M.J. performed experiments; H.L., L.T., T.K., L.B., O.V., M.J. analysed the data; H.L., M.J. wrote the manuscript. All the authors discussed the results and commented on the manuscript.

Additional Information

Supplementary information accompanies this paper at <https://doi.org/10.1038/s41598-019-46465-5>.

Competing Interests: The authors declare no competing interests.

Publisher's note: Springer Nature remains neutral with regard to jurisdictional claims in published maps and institutional affiliations.



Open Access This article is licensed under a Creative Commons Attribution 4.0 International License, which permits use, sharing, adaptation, distribution and reproduction in any medium or format, as long as you give appropriate credit to the original author(s) and the source, provide a link to the Creative Commons license, and indicate if changes were made. The images or other third party material in this article are included in the article's Creative Commons license, unless indicated otherwise in a credit line to the material. If material is not included in the article's Creative Commons license and your intended use is not permitted by statutory regulation or exceeds the permitted use, you will need to obtain permission directly from the copyright holder. To view a copy of this license, visit <http://creativecommons.org/licenses/by/4.0/>.

© The Author(s) 2019

Constitutive salicylic acid accumulation in *pi4kIIIβ1β2* Arabidopsis plants stunts rosette but not root growth

Vladimír Šášek¹, Martin Janda^{1,2}, Elise Delage³, Juliette Puyaubert³, Anne Guivarc'h³, Encarnación López Maseda¹, Petre I. Dobrev¹, José Caius⁴, Károly Bóka⁵, Olga Valentová², Lenka Burketová¹, Alain Zachowski^{6,7} and Eric Ruelland^{6,7}

¹Institute of Experimental Botany, Academy of Sciences of Czech Republic, Prague 165 02, Czech Republic; ²Department of Biochemistry and Microbiology, Institute of Chemical Technology, Prague 166 28, Czech Republic; ³Université Paris 6, UR5, Physiologie Cellulaire et Moléculaire des Plantes, 75252 Paris Cedex 05, France; ⁴Unité de Recherche en Génomique Végétale (URGV), Plateforme Transcriptome, UMR INRA 1165, Université d'Evry Val d'Essonne – ERL CNRS 8196, 2 rue G. Crémieux, CP 5708, 91057 Evry Cedex, France; ⁵Department of Plant Anatomy, Eötvös Loránd University, Pázmány Péter sétány 1/C, Budapest H-1117, Hungary; ⁶CNRS, Institut d'éologie et des sciences de l'environnement, 94010 Créteil, France; ⁷Université Paris-Est Créteil, Institut d'éologie et des sciences de l'environnement, 94010 Créteil, France

Summary

Author for correspondence:

Eric Ruelland

Tel: +33 1 44279647

Email: eric.ruelland@upmc.fr

Received: 29 December 2013

Accepted: 22 March 2014

New Phytologist (2014) 203: 805–816

doi: 10.1111/nph.12822

Key words: Arabidopsis, dwarf phenotype, hormone transduction, phosphatidylinositol-4-kinases (PI4Ks), PR-1, resistance, salicylic acid (SA).

- Phospholipids have recently been found to be integral elements of hormone signalling pathways. An *Arabidopsis thaliana* double mutant in two type III phosphatidylinositol-4-kinases (PI4Ks), *pi4kIIIβ1β2*, displays a stunted rosette growth. The causal link between PI4K activity and growth is unknown.
- Using microarray analysis, quantitative reverse transcription polymerase chain reaction (RT-qPCR) and multiple phytohormone analysis by LC-MS we investigated the mechanism responsible for the *pi4kIIIβ1β2* phenotype.
- The *pi4kIIIβ1β2* mutant accumulated a high concentration of salicylic acid (SA), constitutively expressed SA marker genes including *PR-1*, and was more resistant to *Pseudomonas syringae*. *pi4kIIIβ1β2* was crossed with SA signalling mutants *eds1* and *npr1* and SA biosynthesis mutant *sid2* and *NahG*. The dwarf phenotype of *pi4kIIIβ1β2* rosettes was suppressed in all four triple mutants. Whereas *eds1 pi4kIIIβ1β2*, *sid2 pi4kIIIβ1β2* and *NahG pi4kIIIβ1β2* had similar amounts of SA as the wild-type (WT), *npr1 pi4kIIIβ1β2* had more SA than *pi4kIIIβ1β2* despite being less dwarfed. This indicates that *PI4KIIIβ1* and *PI4KIIIβ2* are genetically upstream of *EDS1* and need functional SA biosynthesis and perception through *NPR1* to express the dwarf phenotype. The slow root growth phenotype of *pi4kIIIβ1β2* was not suppressed in any of the triple mutants.
- The *pi4kIIIβ1β2* mutations together cause constitutive activation of SA signalling that is responsible for the dwarf rosette phenotype but not for the short root phenotype.

Introduction

Plants synthesize molecules that trigger adaptive and/or defensive responses when subjected to abiotic or biotic stresses. Salicylic acid (SA) is one of these molecules. This phenolic phytohormone has been much studied because of its role in plant resistance to pathogens. SA is induced in basal defence against pathogens and during responses mediated by *R*-genes. Two subsets of *R*-genes act via pathways that involve *EDS1* or *NDR1*, proteins that regulate SA biosynthesis (Vlot *et al.*, 2009). It is now well established that SA has a role in plant responses to abiotic stresses, such as drought, chilling, heavy metal toxicity, heat, and osmotic stress (Vicente & Plasencia, 2011). SA also regulates developmental and physiological processes such as seed germination (Rajjou *et al.*, 2006; Lee *et al.*, 2010), vegetative growth (Scott *et al.*, 2004), senescence (Vogelmann *et al.*, 2012) and stomatal closure (Khokon *et al.*, 2011; Kalachova *et al.*, 2013).

Salicylic acid is synthesized through two distinct pathways from the precursor chorismate. In one pathway, chorismate is converted into isochorismate by isochorismate synthase (ICS). In the other pathway, phenylalanine, derived from chorismate, is converted to cinnamate by phenylalanine ammonia-lyase (PAL). Both isochorismate and cinnamate are converted into SA in multistep reactions (Vlot *et al.*, 2009). In *Arabidopsis*, ICS and PAL enzymes are encoded by two and four genes, respectively. The *ics1* mutant has 90% less SA than the wild-type (WT) in inducing conditions, showing that the ICS pathway plays a major role in SA biosynthesis in *Arabidopsis*. The remaining portion of SA is synthesized by ICS2 and probably all four PAL gene products (Garcion *et al.*, 2008; Huang *et al.*, 2010).

Exogenous SA treatment of plants induces a signalling pathway leading to changes in gene expression (Krinke *et al.*, 2007; van Leeuwen *et al.*, 2007; Ee *et al.*, 2013). Transcription of the vast majority of SA-regulated genes is dependent on

NONEXPRESSOR OF PR GENES1 (NPR1) (Wang *et al.*, 2006). The NPR1 protein is located in the cytosol in its oxidized oligomeric form. When SA is added and the cell redox status changes, NPR1 oligomers are reduced and monomers translocate into the nucleus. There, NPR1 interacts with TGA transcription factors, thus permitting gene expression (Durrant & Dong, 2004).

Lipid signalling has recently been discovered to be a central mechanism in hormone signal transduction, including for SA (Janda *et al.*, 2013). We previously showed that phosphatidylinositol-4-kinases (PI4Ks) are activated when *Arabidopsis thaliana* suspension cells respond to SA (Krinke *et al.*, 2007). PI4K catalyses the phosphorylation of phosphatidylinositol (PI) at the D4 position of its inositol ring to form phosphatidylinositol 4-phosphate (PI4P). While PI is a major component of eukaryotic membranes, the amount of PI4P and phosphatidylinositol-4,5-bisphosphate (PI4,5P₂) together is <3% of the total amount of PI (Mosblech *et al.*, 2008). Despite their low abundance, PI4P and PI4,5P₂ participate in a plethora of fundamental cellular processes, such as membrane trafficking, cytoskeleton remodelling and signal transduction pathways (Michell, 2008; Ischebeck *et al.*, 2010; Munnik & Nielsen, 2011). Thus PI4K action is a potential central regulation point for signalling events involving these lipids (Delage *et al.*, 2012b). There are two types of PI4Ks, according to their primary sequences and pharmacological sensitivities. Type II PI4Ks are inhibited by adenosine while type III PI4Ks are inhibited by micromolar concentrations of wortmannin, a steroid metabolite produced by the fungi *Penicillium funiculosum* (Delage *et al.*, 2012a). By crossing and characterizing two *Arabidopsis* mutant lines, Preuss *et al.* (2006) produced *pi4kIIIβ1β2*, a double mutant that carries T-DNA insertions in two type III PI4Ks. We recently showed that this double mutant still has 60% of WT PI4K *in vitro* activity that is sensitive to wortmannin. This remaining activity can be attributed to the PI4Kα1 isoform, the only other type III PI4K in *Arabidopsis*. In doing these experiments, we noted the severe growth defects and yellowing of *pi4kIIIβ1β2* plants, as already observed by Preuss *et al.* (2006).

Here, we investigate the mechanisms responsible for the phenotype of *Arabidopsis* double mutant that is defective in the two PI4K genes, *PI4KIIIβ1* and *PI4KIIIβ2*. We show that *pi4kIIIβ1β2* has constitutively high *PR-1* expression and SA concentrations. When the *pi4kIIIβ1β2* was crossed with plants altered in SA signalling or biosynthesis, all the resulting triple mutants showed nearly WT phenotype of the rosettes grown in soil but short-root phenotype of *in vitro* grown *pi4kIIIβ1β2* was not reverted in the triple mutants. Therefore the dwarf phenotype of *pi4kIIIβ1β2* is a complex trait involving SA signalling in shoots but not in roots.

Materials and Methods

Plant material, growth conditions and pharmacological treatments

Plants of WT *Arabidopsis thaliana* Col-0 and *pi4kIIIβ1β2* (SALK_040479 × SALK_098069) were cultivated in Jiffy 7 peat

pellets at 22°C with daily cycles of 16 h of light (130 μmol m⁻² s⁻¹) and 8 h of dark at 70% relative humidity and were watered without fertilizers.

For microarray analysis, plants were grown on 0.5 × Murashige and Skoog (MS) medium basal salt, pH 5.7 (Duchefa, Haarlem, the Netherlands), supplemented with 0.5 g l⁻¹ 2-(N-morpholino) ethanesulphonic acid (MES), 10 g l⁻¹ sucrose and 8 g l⁻¹ agar. Seeds were stratified for 3 d at 4°C. Plates were placed horizontally in continuous light (100 μmol m⁻² s⁻¹) at 22°C. RNA samples were prepared from 15-d-old seedlings.

For root assays, plants were grown in square plates on 0.5 × MS basal salt medium, pH 5.7 (Duchefa), supplemented with 0.5 g l⁻¹ MES and 8 g l⁻¹ agar. Seeds were sterilized with 1.5% sodium hypochlorite and stratified for 3 d at 4°C. Plates were placed vertically under continuous light (100 μmol m⁻² s⁻¹) at 22°C for 3 d and then seedlings were transferred to new plates to assess root growth. Positions of root tips were marked 2, 4 and 7 d after transfer. Primary root length was measured manually using ImageJ software (Schneider *et al.*, 2012).

Quantitative reverse transcription polymerase chain reaction (RT-qPCR) analysis

Plant tissue was homogenized in 2 ml screw-cap tubes containing 1 g of 1.3-mm-diameter silica beads using a FastPrep-24 instrument (MP Biomedicals, Santa Ana, CA, USA). RNA isolation, reverse transcription and qPCR were performed as previously described by Sasek *et al.* (2012). Relative expression was calculated with efficiency correction and normalization to *SAND* expression (Czechowski *et al.*, 2005). The list of qPCR primers is shown in Supporting Information, Table S1.

Transcriptome studies

Microarray analysis was carried out at the Unité de Recherche en Génomique Végétale (Evry, France) using CATMA arrays (Crowe *et al.*, 2003; Hilson *et al.*, 2004). Two independent biological replicates were made. Newly generated microarray data were deposited at Gene Expression Omnibus (<http://www.ncbi.nlm.nih.gov/geo/>; accession no. GSE36624) and at CATdb (<http://urgv.evry.inra.fr/CATdb/>; Projects, AU10-10_Froid) according to the 'Minimum information about a microarray experiment' standards.

Lipid extraction and analysis

Total lipids were extracted as described by Rainteau *et al.* (2012). Phosphoglycerolipids and galactolipids were analysed by mass spectrometry in the multiple reaction mode as previously described (Rainteau *et al.*, 2012; Djafi *et al.*, 2013).

Analysis of plant hormones

Plant hormones were extracted from 100 mg of frozen tissue and the concentrations determined as previously described (Dobrev & Kaminek, 2002; Dobrev & Vankova, 2012) after the addition

of appropriate internal standards. Hormones were quantified with Ultimate 3000 high-performance liquid chromatography equipment (Dionex, Bannockburn, IL, USA) coupled to a 3200 Q TRAP hybrid triple quadrupole/linear ion trap mass spectrometer (Applied Biosystems, Foster City, CA, USA).

Pseudomonas infection assay

Plants for infection assays were grown for 4 wk in soil as indicated earlier, but with daily cycles of 10 h of light ($230 \mu\text{mol m}^{-2} \text{s}^{-1}$) and 14 h of darkness. *Pseudomonas syringae* pv. *maculicola* ES4326 were grown on King B agar plates at 28°C overnight, resuspended in 10 mM MgCl₂ and diluted to an OD₆₀₀ of 0.5. Silwet L77 was added to the bacterial suspension to give a final concentration of 0.02% and plants were sprayed until runoff. Plants were enclosed in a transparent airtight container for 24 h to maintain high relative humidity. Approximately 50 mg of 0.6-mm-diameter leaf discs were homogenized with plastic pestles in 1.5 ml microcentrifuge tubes and the resulting homogenate was serially diluted and loaded on to King B plates. Colonies were counted after 2 d of incubation at 28°C.

Quantification of reactive oxygen species

Plants were grown in soil under standard conditions for 4 wk. Leaf discs (6 mm diameter) were incubated in separate wells of a white 96-well plate containing 50 mM Tris-HCl (pH 8.5) for 1 h. To prepare reaction solution, 7 mg of luminol (Fluka, Switzerland) was dissolved in 100 µl of 1 M NaOH and mixed with 100 µl of 50 mM Tris-HCl (pH 8.5) containing 4 mg horseradish peroxidase (Sigma-Aldrich). The buffer in each well was replaced with 100 µl of reaction solution and the plate was immediately inserted into an Infinite F200 plate reader (Tecan, Männedorf, Switzerland). Chemiluminescence was continuously measured at 26°C for 50 min with a 5 s integration time per well. Luminescence values measured 10 min after initiating reactions were used to calculate relative luminescence.

Light microscopy and scanning electron microscopy

For light microscopy, whole roots excised from seedlings were directly observed under differential interference contrast illumination using ApoTome apparatus and AxioVision software (Zeiss, Oberkochen, Germany). For scanning electron microscopy, 10-d-old soil-grown plants were used. Whole young leaves (rank $n = 3$) and old leaves (rank $n = 7$) were excised and fixed in 4% glutaraldehyde and 1.5% formaldehyde in PBS buffer for 4 h at 4°C. Leaves were then rinsed with PBS buffer, dehydrated in successive baths of 50, 70, 95 and 100% ethanol for 30 min each, and then dried with liquid CO₂ with a CDP7501 critical point dryer (Quorum Technologies Ltd). Samples were sputter-coated with gold and observed with a S260 Cambridge scanning electron microscope at the Service de Microscopie Electronique of Paris 6 University (France).

Transmission electron microscopy

Sample preparation and observation were performed as described by Sasek *et al.* (2012). Micrographs were taken with a Mega View III camera with analySIS Pro 3.2 software (Soft Imaging System GmbH, Münster, Germany). For morphometry, 30 micrographs of plastids and unit areas of plastids ($3.7 \mu\text{m}^2$ at $\times 50\,000$ magnification) from two embedded tissue blocks of three independent samples of WT and mutants were measured. For each plastid image, the length, width, total area and starch area were measured with analySIS software. Granum and stroma thylakoid length were measured with a curvometer. From these data, granum and stroma thylakoid ratio were calculated. Granum number, granum height and starch grain number were determined from micrographs.

Generation of triple mutants

pi4kIIIβ1β2 double mutants were crossed to each of *eds1-2*, *npr1-1*, *NahG* and *sid2-5*. Homozygous plants were identified in the F3 generation using PCR or restriction analysis. T-DNA insertions characteristic of *pi4kIIIβ1β2* plants were detected using the following primers flanking the insertion: for SALK_040479, 5'-AGGACGTAACCAGAGGGGTAG-3' and 5'-CGTTGTGACCCGTATTAATC-3'; and for SALK_098 069, 5'-ATGAACGAAATTGGGTTCTCC-3' and 5'-AAA CCTCCTTATCTTCCGCTG-3' together with the LBB1.3 primer (5'-ATTGGCCGATTTCGGAAC-3') aligning to the left border of the insertion. The T-DNA insertion in *sid2-3* SALK_042603 described by Gross *et al.* (2006) was detected with 5'-ACCCTAATTGGATTGGTGC-3' and 5'-AGCTCTA GGCCTAGTTGCAGC-3' together with the LBB1.3 primer. Plants carrying the *eds1-2* mutation (Falk *et al.*, 1999) were detected with primers flanking a deletion in the mutant, 5'-CCAATGTTACCTTGAGCCTCGT-3' and 5'-ATCCAT TCTCCAAGCATCCCTCT-3'. The PCR product from WT is 1493 bp, whereas the *eds1-2* product is 578 bp. However plants heterozygous for *eds1-2* often lacked the WT product, so an additional set of primers was used to confirm homozygosity, 5'-AACAACTCGGACGCCATTCTCA-3' and 5'-GCAATC ATTCCGTTGGCTTCAGT-3'. These primers amplify an 878 bp product from the WT but no product from *eds1-2*. Plants carrying the *npr1-1* mutation (Cao *et al.*, 1997) were detected with primers flanking a point mutation, 5'-CGTGTGCTCTTC ATTTGCTGT-3' and 5'-GTGCGTTCTACCTTCCAAA GTT-3'. These primers give a PCR product of 209 bp that, if from the WT, can be cleaved with NlaIII/Hin1II but not if from *npr1-1* (New England Biolabs, Ipswich, MA, USA). Plants expressing the bacterial salicylate hydroxylase *NahG* (Delaney *et al.*, 1994) were detected with the primers 5'-GAC-GCCCTAGTAACTCACC-3' and 5'-TGATGATGCCGCC ATTCC-3', which give a PCR product of 370 bp. In the F2 population we identified a *NahG* triple mutant that did not segregate for *NahG* in the F3 generation. Homozygosity of all lines was verified in the two following generations. As a control, sibling *pi4kIIIβ1β2* lines were selected in the F3 of each cross to confirm

that the differences in triple mutant phenotypes were not a result of other genetic elements.

Results

The *pi4kIIIβ1β2* double mutant has a dwarf phenotype

The *pi4kIIIβ1β2* plants (SALK_040479 and SALK_098069) were previously identified and characterized by Preuss *et al.* (2006). In their study and in our previous work (Delage *et al.*, 2012a), these plants were shown to display a stunted rosette growth and short root when grown *in vitro*. Here we investigate this phenotype in more detail. When grown in soil, no major difference between the single *pi4kβ2* mutant and the WT plants was detected. Rosettes of *pi4kβ1* plants were smaller than the WT and occasionally showed leaf yellowing. The *pi4kIIIβ1β2* double mutant had a strong dwarf phenotype and frequent yellowing of older leaves (Fig. 1a). The inflorescence of *pi4kIIIβ1β2* was less than half as tall as the WT (Fig. S1a). The dwarfism of *pi4kIIIβ1β2* is not a result of a delay in development, because the double mutant and WT had the same number of leaves at any time assayed (Fig. S1b). To assess the dwarf phenotype at the cellular level, young (rank $n = 3$) and old (rank $n = 7$) leaves of 10-d-old plants grown in soil were excised and fixed and the epidermal cells were observed by scanning electron microscopy (Fig. 1b). Epidermal cells of both young and old *pi4kIIIβ1β2* leaves were c. 30% smaller than the WT controls (Fig. 1c). The WT had about half as many stomata per unit area of leaf surface as the mutant (Fig. 1d). This indicates that the small size of *pi4kIIIβ1β2* mutant leaves was a result of having fewer and smaller cells.

Root length was assayed in *in vitro* cultured plants. Roots of 8-d-old *in vitro* grown seedlings were visualized by light microscopy (Fig. 1e). As described by Preuss *et al.* (2006), the *pi4kIIIβ1β2* mutant has shorter roots than the WT (Fig. 1f). As already described by Kang *et al.* (2011), the *pi4kIIIβ1β2* double mutant roots have irregular-shaped cortical cells. They also had abnormal root hairs (Fig. 1e). The length of the meristematic zone was 17% shorter in the double mutant (Fig. 1g). In addition, the length of cortical cells in the differentiated zone of the primary root was 40% shorter in *pi4kIIIβ1β2* than in the WT (Fig. 1h). These results indicate that the double mutant has shorter primary roots, because it has fewer and shorter cells partly as a result of reduced cell cycling in the mutant.

Genome-wide analysis reveals that SA-responsive genes are constitutively altered in the *pi4kIIIβ1β2* mutant

Transcripts were extracted from 2-wk-old seedlings grown *in vitro*, and the *pi4kIIIβ1β2* transcriptome was compared with the WT transcriptome (Table S2). We found that 133 genes were down-regulated in the double mutant compared with the WT, while 29 genes were up-regulated. These 29 up-regulated genes and the 29 most down-regulated genes are listed in Table 1. Several well-characterized SA-induced genes are amongst the genes that are overexpressed in the *pi4kIIIβ1β2* double mutant, such as the *PR-1*, *ORG1* (*OBP3-RESPONSIVE PROTEIN 1*),

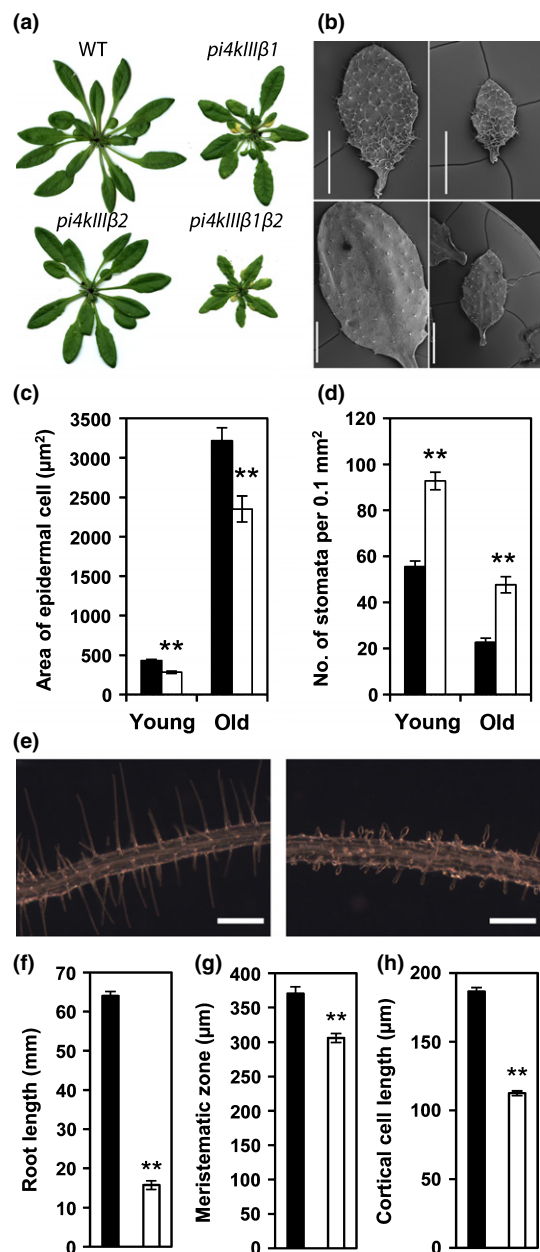


Fig. 1 Morphometric analysis of *Arabidopsis pi4kIIIβ1β2* plants grown in soil (a–d) and *in vitro* (e–h). (a) Photographs of typical wild-type (WT), *pi4kIIIβ1*, *pi4kIIIβ2* and *pi4kIIIβ1β2* plants. (b) Scanning electron micrographs of young rank $n = 3$ (top) and old rank $n = 7$ (bottom) leaves from WT and *pi4kIIIβ1β2* plants. Bars, 2 mm. (c) Epidermal cell area. (d) Frequency of stomata per leaf surface area. (e) Photomicrographs of *in vitro* grown roots of WT (left) and *pi4kIIIβ1β2* (right); bars, 0.5 mm. (f) Root length of *in vitro* grown seedlings. (g) Meristematic zone length. (h) Length of cortical cells. (c, d, f–h) WT, closed bars; *pi4kIIIβ1β2*, open bars. All graphical data are presented as means \pm SE. Statistically significant differences compared with WT plants: **, $P < 0.01$, Student's *t*-test.

ORG2 and *ORG3* genes (Kang *et al.*, 2003). *At2g44240*, *At1g21190* and *At1g14880* were also induced by SA in *Arabidopsis* suspension cells (Krinke *et al.*, 2007). Among the 29 most repressed genes, 22 are encoded in chloroplasts. One of the few nucleus-encoded genes repressed in the double mutant was *PDF1.2* (*PLANT DEFENSIN 1.2A*), a gene positively regulated

Table 1 The 29 upregulated and 29 most downregulated genes in *Arabidopsis pi4kIIIβ1β2* *in vitro* grown seedlings compared with wild type (WT)

Locus	Name	Log ₂ ratio		Locus	Name	Log ₂ ratio	
		Microarray ¹	RT-qPCR ²			Microarray ¹	RT-qPCR ²
At1g47400	Unknown protein	1.40	2.14	At5g64070	PI4K	-1.72	
At3g56970	ORG2	1.36	2.58	Atcg00480	Unknown protein	-1.63	-1.05
At1g47395	Unknown protein	1.34	2.25	Atcg00340	Unknown protein	-1.57	-1.04
At5g53450	ORG1	1.29	0.37	Atcg00470	Unknown protein	-1.50	
At1g13609	Unknown protein	1.27	3.21	Atcg00680	Unknown protein	-1.44	
At2g14610	PR-1	1.17	11.63	Atcg00150	Unknown protein	-1.42	
At2g41240	bHLH100	1.13	3.73	Atcg00340	Unknown protein	-1.40	
At3g18290	EMB2454	1.12		At5g44420	PDF1.2	-1.38	-2.10
At1g18860	WRKY61	1.09	6.07	Atmg00280	Unknown protein	-1.36	
At3g56980	ORG3	1.00	5.07	Atcg00280	Unknown protein	-1.35	
At1g56430	NAS4	0.96		Atcg00540	Unknown protein	-1.35	
At5g56080	NAS2	0.92		Atcg00490	Unknown protein	-1.34	
At5g01870	PR-14	0.90	3.74	Atcg00540	Unknown protein	-1.33	
At1g27120	Galactosyltransferase	0.88		Atcg00790	Unknown protein	-1.32	
At2g43610	Glycoside hydrolase	0.82		Atcg00150	Unknown protein	-1.31	
At1g14880	Unknown protein	0.81		Atcg00270	Unknown protein	-1.30	
At4g19690	IRT1	0.81		Atcg00470	Unknown protein	-1.28	
At5g13740	ZIF1	0.78		At2g07732	Pseudogene	-1.28	-0.85
At1g54010	GDSDL-like Lipase	0.70	5.59	Atcg00160	Unknown protein	-1.27	
At1g21190	LSM3A	0.69		At1g53480	DNA binding	-1.27	
At1g13608	Unknown protein	0.68		Atcg00040	Unknown protein	-1.26	
At5g17220	ATGSTF12	0.65	0.66	At5g51720	Unknown protein	-1.25	
At2g44240	Unknown protein	0.65		Atcg00490	Unknown protein	-1.24	
At3g16660	Unknown protein	0.65		Atcg00140	Unknown protein	-1.23	
At5g67330	ATNRAMP4	0.65	-0.02	Atcg00530	Unknown protein	-1.20	
At3g20470	Pseudogene	0.64		Atcg01040	Unknown protein	-1.20	
At2g23170	GH3.3	0.62	-1.52	Atcg00130	Unknown protein	-1.20	
At2g26695	Binding	0.62		At5g01600	ATFER1	-1.14	
At5g67370	Unknown protein	0.61		Atcg00280	Unknown protein	-1.13	

¹The expression levels are given as the log₂ of the ratio of the intensity in the *pi4kIIIβ1β2* mutant vs the intensity in WT plants.

²Log₂ ratios of selected genes analysed by quantitative reverse transcription polymerase chain reaction (RT-qPCR) in adult soil grown plants.

by jasmonic acid (JA). SA is known to repress the JA pathway (Spoel *et al.*, 2003).

The expression of certain genes was analysed in soil-grown adult plants using RT-qPCR. Out of 13 genes up-regulated in *in vitro* *pi4kIIIβ1β2* seedlings, 12 were also induced in the soil-grown adult plants (Table 1). Generally, the expression of these genes was much stronger in the adult soil-grown plants than in the *in vitro* grown seedlings. We also analysed the expression of the two most suppressed chloroplast and nuclear genes. All four were suppressed in the adult plants of *pi4kIIIβ1β2* in a similar way as in *in vitro* seedlings.

To understand the difference in intensity in gene expression between seedlings grown *in vitro* and soil-grown plants, we monitored *PR-1* expression and rosette FW in soil-grown plants for the first 29 d. We found that, as plants age, more *PR-1* is expressed in the *pi4kIIIβ1β2* double mutant (Fig. 2b). The dwarf phenotype was also more pronounced in older plants (Fig. 2a).

pi4kIIIβ1β2 plants have constitutively high concentrations of SA

The constitutively high expression of SA-induced genes in *pi4kIIIβ1β2* plants made us wonder whether SA metabolism was

also altered. The major phytohormones were analysed in soil-grown adult plants and in all cases the double mutant had different concentrations than the WT. While the fold differences in ABA, IAA, JA, trans-zeatin (tZ) and cis-zeatin (cZ) ranged from 0.4 for ABA to 3.6 for JA, the SA concentration was 14-fold greater in the double mutant than in WT plants (Fig. 3a).

We analysed the expression of genes encoding enzymes thought to be involved in SA biosynthesis in *pi4kIIIβ1β2* mutants. While the expression of *PAL1*, *PAL2*, *PAL3* and *PAL4* genes was not different from that in the WT (data not shown), expression of *ICS1* was significantly induced in *pi4kIIIβ1β2* (Fig. 3b). By contrast, *ICS2* was strongly repressed in the double mutant. Transcription of *ICS1* is regulated by two transcription factors, *SARD1* (*SAR DEFICIENT 1*) and *CBP60g* (*CALMODULIN BINDING PROTEIN 60g*) (Zhang *et al.*, 2010). Expression of these genes was induced in the double mutant. Recently, Zhang *et al.* (2013) described SA-3-hydroxylase (S3H) as a major enzyme involved in SA degradation. This gene was also induced in *pi4kIIIβ1β2*.

Isochorismate synthase-dependent biosynthesis of SA occurs in chloroplasts and most of the genes down-regulated in *pi4kIIIβ1β2* are chloroplast-encoded (Table 1). This prompted us to investigate the ultrastructure of chloroplasts using

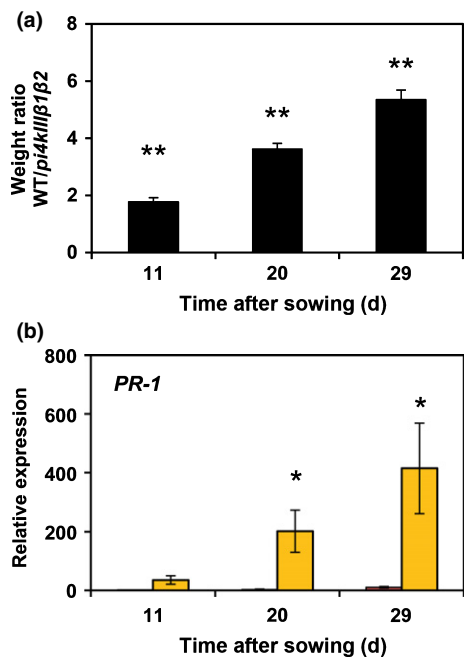


Fig. 2 Kinetics of growth and *PR-1* expression in wild-type (WT) and *pi4kIIIβ1β2* *Arabidopsis thaliana*. Plants were grown in soil for 4 wk and sampled 11, 20 and 29 d later. (a) Weight ratio between WT and *pi4kIIIβ1β2* plants showing increasing differences with time. (b) Quantitative reverse transcription polymerase chain reaction (RT-qPCR) analysis of *PR-1* expression in WT (red bars) and *pi4kIIIβ1β2* (yellow bars) plants. Values are means \pm SE of four biological replicates. Statistically significant differences between WT and *pi4kIIIβ1β2* plants: *, $P < 0.05$; **, $P < 0.01$, Student's *t*-test.

transmission electron microscopy (Fig. S2). Detailed image analysis showed slight differences in the mutant. Granum thylakoids were shorter, the grana were smaller and there were more grana in *pi4kIIIβ1β2*. The number and total area (on electron micrographs) of starch grains were higher in the mutant (Table S3).

pi4kIIIβ1β2 plants have constitutively high ROS concentrations and enhanced basal resistance to *Pseudomonas*

Typically, mutants that accumulate excess SA also produce more reactive oxygen species (ROS) (Mateo *et al.*, 2006) and are more resistant to biotrophic and hemibiotrophic pathogens (Vlot *et al.*, 2009). The ROS concentration was more than seven times higher in *pi4kIIIβ1β2* plants than in WT plants (Fig. 4a). Resistance to pathogens was assessed in the double mutant. Plants were spray-inoculated with *P. syringae* pv. *maculicola* ES4326, thus avoiding potential differences in amount of inoculum as a result of the altered morphology of mutant plants. Three days later, WT plants exhibited leaf necrosis and large zones of yellowing. These symptoms were almost absent in the double mutant (Fig. 4b), except for characteristic yellowing present before inoculation (Figs 1a, 5). The bacterial titres collected 3 d after inoculation from *pi4kIIIβ1β2* leaves were 10 times lower than those collected from WT leaves (Fig. 4c). The equal amounts of inoculum on both genotypes was confirmed by bacteria enumeration just after infection (Fig. 4c).

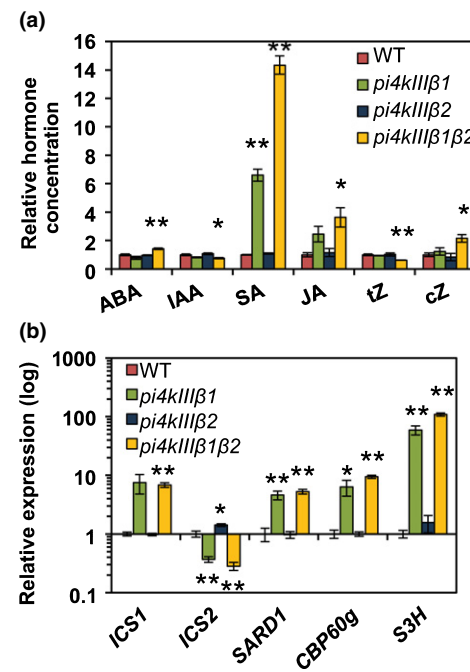


Fig. 3 Effect of *pi4kIIIβ1* and *pi4kIIIβ2* mutations in *Arabidopsis* on phytohormone concentrations and related gene expression. (a) Hormone concentrations determined in 4-wk-old plants grown in soil using LC-MS. SA, salicylic acid; JA, jasmonic acid; tZ, trans-zeatin; cZ, cis-zeatin. (b) Expression analysis of genes involved in SA biosynthesis (*ICS1*, *ICS2*), its regulation (*SARD1*, *CBP60g*) and degradation (*S3H*). Values are means \pm SE of four biological replicates. Statistically significant differences compared with wild-type (WT) plants: *, $P < 0.05$; **, $P < 0.01$, Student's *t*-test.

The lipidomes of *pi4kIIIβ1β2* and *ssi2* plants have some similar features

The phenotype of the *pi4kIIIβ1β2* double mutant is in part reminiscent of the *ssi2* mutant phenotype: enhanced resistance to *P. syringae*, constitutive accumulation of elevated SA concentration and expression of the *PR-1* gene (Shah *et al.*, 2001). *ssi2* is deficient in stearoyl-acyl carrier protein desaturase, and its fatty acid composition is altered (Kachroo *et al.*, 2001). Using multiple reaction monitoring mass spectrometry, the molecular species were analysed. The most apparent changes in *ssi2* were increases in the relative contents of 18:0/18:1-, 18:0/18:2-, 18:0/18:3-molecular species in PI, PE, PC, PG, and of 18:0/18:3- in MGDG and DGDG and decreases in the relative contents of 16:0/18:2- molecular species in PI, PE and PC, and of 16:0/18:1- in PG (Fig. S3) (PI, phosphatidylinositol; PE, phosphatidylethanolamine; PC, phosphatidylcholine; PG, phosphatidylglycerol; MGDG, monogalactosyldiacylglycerol; DGDG, digalactosyldiacylglycerol). None of these differences were detected in *pi4kIIIβ1β2*. However, some altered profiles were found in both *ssi2* and *pi4kIIIβ1β2*. These mutants both contained relatively less 18:1/18:2-, 18:1/18:3-, 18:2/18:2-, and 18:2/18:3- species of PI, 18:1/18:2- species of PC and 16:1/18:3-species of PG, but more 16:0/18:3- species of PG. However, the latter differences were marginal compared with those observed in *ssi2* alone, so overall the molecular species profile of *pi4kIIIβ1β2*

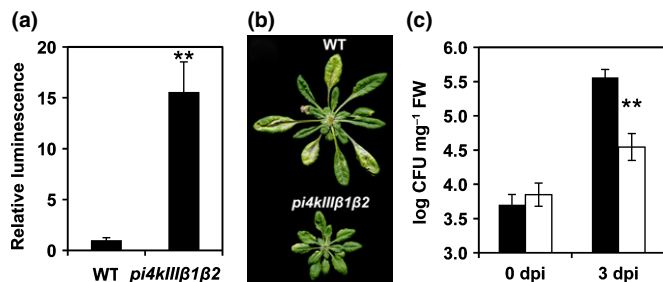


Fig. 4 (a) Reactive oxygen species (ROS) production in *Arabidopsis* *pi4kIIIβ1β2* in leaf discs from 4-wk-old soil-grown plants detected with luminol. Values are averages of eight samples per genotype and error bars, \pm SE. Statistically significant difference from wild-type (WT): ** $P < 0.01$, Student's *t*-test. (b) Symptoms of WT and *pi4kIIIβ1β2* plants 3 d after infection with *Pseudomonas syringae* pv. *maculicola* ES4326. Four-week-old plants were spray-inoculated with bacterial suspension at OD₆₀₀ of 0.5. (c) Bacterial titres in the leaves collected at 0 and 3 d postinfection (dpi) from Col-0 (closed bars) and *pi4kIIIβ1β2* (open bars). Values are averages of five samples per genotype and error bars, \pm SE. Statistically significant difference from WT: **, $P < 0.01$, Student's *t*-test.

does not strongly resemble that of *ssi2*. The most significant molecular species change in *pi4kIIIβ1β2* was that 16:0/18:3-species were increased in PI, PC, PE, PG but not in MGDG and DGDG. In MGDG, but not in DGDG, 18:2/18:3-species were increased in *pi4kIIIβ1β2* (Fig. S3).

Elevated SA concentrations stunt *pi4kIIIβ1β2* rosette growth via an NPR1-dependent pathway

The action of type III PI4K was investigated genetically. NahG plants overexpress a bacterial SA-hydroxylase and so have less SA than the WT (Delaney *et al.*, 1994). The *sid2-3* mutant has a T-DNA insert in the biosynthetic *ICS1/SID2* gene (Gross *et al.*, 2006), and *EDS1* (Falk *et al.*, 1999) encodes a protein upstream of SA biosynthesis so that both mutants accumulate less SA in response to biotic elicitation. NPR1 is the major transcription cofactor that controls the expression of *PR-1* and most other SA-responsive genes (Durrant & Dong, 2004), and so *npr1* mutants have limited SA signalling. The *pi4kIIIβ1β2* double mutant was crossed with these mutants affected in SA biosynthesis, SA accumulation or SA sensitivity. Rosette FW, SA content and *PR-1* expression were determined in the resulting triple mutants.

The only triple mutant with a conspicuously different phenotype was *npr1pi4kIIIβ1β2*. When the plants started to bolt, compact chlorosis appeared in the central part of the rosette (Fig. 5a). All the triple mutants were much less dwarfed than the *pi4kIIIβ1β2* double mutant. Furthermore, the *eds1pi4kIIIβ1β2*, *sid2pi4kIIIβ1β2* and *NahGpi4kIIIβ1β2* rosette weights were not significantly different from WT rosette weights (Fig. 5a). We calculated the effect of introducing the *pi4kIIIβ1β2* double mutation into WT and single mutant genetic backgrounds. The double mutation introduced into the WT background led to a 77% decrease in weight. When introduced into *npr1*, *sid2* and *nahG* backgrounds, the decrease was only 2, 14 and 32%, respectively (Table 2). When introduced into *eds1*, the double mutation led to a 20% increase in rosette weight.

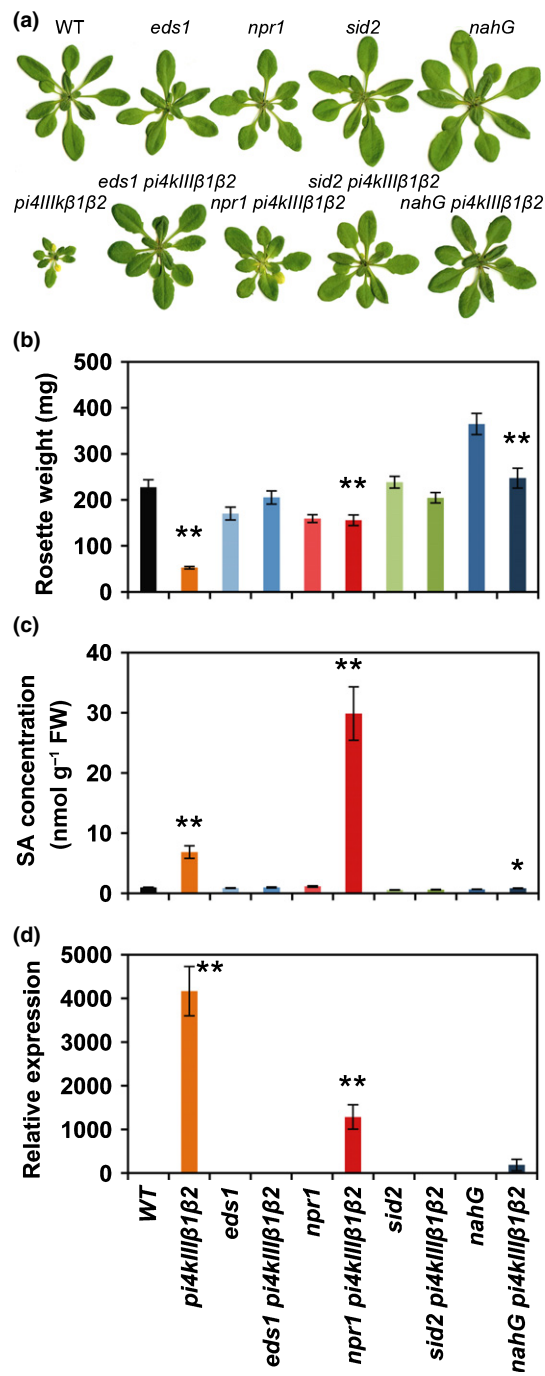


Fig. 5 Analysis of *Arabidopsis* triple mutant plants grown in soil for 4 wk. (a) Representative images of rosettes of all genotypes analysed in the experiment. (b) Average rosette FW. (c) Salicylic acid (SA) concentration determined by LC-MS. (d) Relative expression of *PR-1*. Values are means \pm SE of 12 plants (b) or four biological replicates (c, d). Statistically significant differences compared with the parental single mutants: *, $P < 0.05$; **, $P < 0.01$, Student's *t*-test.

While the *pi4kIIIβ1β2* plants had significantly more SA constitutively than WT plants, the amounts of SA in the single *eds1* and *npr1* mutants were not different from that in the WT. As expected, the SA concentrations were significantly lower in the *sid2* and *NahG* plants. The *eds1pi4kIIIβ1β2*, *sid2pi4kIIIβ1β2* and *NahGpi4kIIIβ1β2* triple mutants had significantly less SA

Table 2 Reduction of shoot weight and root length induced by *pi4kIIIβ1β2* mutation in different background genotypes of Arabidopsis

Background genotype	Trait		
	Shoot mass in soil (%)	Root length in vitro (%)	Plant studied
Wild-type	-76.9	-72.2	<i>pi4kIIIβ1β2</i>
<i>eds1</i>	20.5	-46.0	<i>eds1 pi4kIIIβ1β2</i>
<i>npr1</i>	-2.4	-62.9	<i>npr1 pi4kIIIβ1β2</i>
<i>sid2</i>	-14.2	-44.7	<i>sid2 pi4kIIIβ1β2</i>
<i>nahG</i>	-32.2	-53.1	<i>nahG pi4kIIIβ1β2</i>

than *pi4kIIIβ1β2*. The SA concentration in the *eds1 pi4kIIIβ1β2* and *NahG pi4kIIIβ1β2* triple mutants was not different from that in the WT and was even lower in *sid2 pi4kIIIβ1β2*. By contrast, the *npr1 pi4kIIIβ1β2* triple mutant had fourfold more SA than the *pi4kIIIβ1β2* double mutant (Fig. 5b).

PR-1 expression correlated well with SA concentration in each triple mutant, except for *npr1 pi4kIIIβ1β2*. Although *PR-1* expression is dependent on *NPR1*, the *npr1 pi4kIIIβ1β2* mutant still had a relatively high *PR-1* expression, indicating the existence of an *NPR1*-independent transduction pathway in this mutant (Fig. 5c). When comparing SA concentration and rosette mass, it appeared that when SA concentration was diminished, the rosette weight was increased. However, the *npr1 pi4kIIIβ1β2* triple mutant was bigger than *pi4kIIIβ1β2* despite its high SA content.

High endogenous SA is a minor regulator of *pi4kIIIβ1β2* root length growth *in vitro*

The primary root length of the triple mutants grown *in vitro* in vertical plates was measured and compared with those of *pi4kIIIβ1β2* and the corresponding single mutants (Fig. 6). As already described (Fig. 1g), the *pi4kIIIβ1β2* double mutant roots were shorter than the WT roots. None of the triple mutants had roots as long as the WT or any of the single mutants. In fact, triple mutant roots were only slightly longer than *pi4kIIIβ1β2* roots or, in the case of *npr1 pi4kIIIβ1β2*, were the same length. As for the shoot size, we calculated the effect of introducing the *pi4kIIIβ1β2* mutations into different genotypes (Table 2). The *pi4kIIIβ1β2* double mutation led to a 72% decrease in root length in a WT background. When introduced into *eds1*, *npr1*, *sid2* and *nahG*, the decrease in root length was 46, 63, 45 and 53%, respectively. This means that the single mutations either did not affect or only partially affected the reduction in root length caused by the double mutation.

Discussion

The *pi4kIIIβ1β2* mutation causes stunted rosette growth (Fig. 1), accumulation of excess SA (Fig. 3) and constitutive expression of SA-induced genes (Table 1, Fig. 2). The growth defect and changes in gene expression are more pronounced in adult plants (Fig. 2, Table 1), indicating a link between the phenotype and plant development. Like other SA-overaccumulating plants, *pi4kIIIβ1β2* plants are more resistant to *P. syringae* and produce

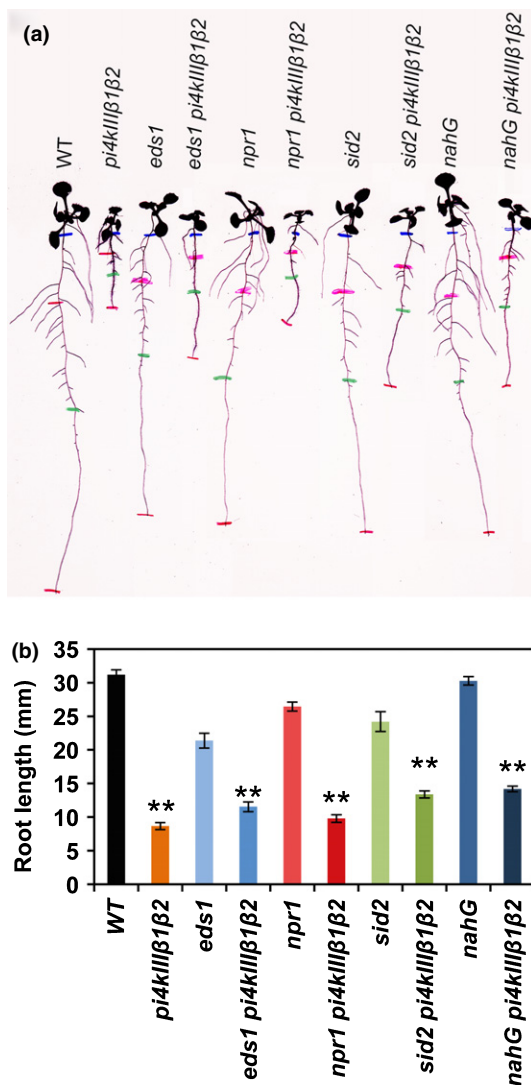


Fig. 6 Analysis of Arabidopsis triple mutant plants grown *in vitro* on vertical plates. (a) Representative image of plantlets of all genotypes analysed in the experiment. Coloured marks indicate the position of root tips at 0 (blue), 2 (pink), 4 (green) and 7 d (red) after transfer to testing plates. (b) Average primary root length determined 4 d after transfer. Values represent means \pm SE of 15 plants. Statistically significant differences compared with the parental single mutant plants: **, $P < 0.01$, Student's *t*-test.

more ROS (Fig. 4). It is important to understand why SA should accumulate in a mutant with less PI4K. SA may accumulate if more is produced and/or less is catabolized. The high concentration of SA was correlated with strong expression of the *ICS1* gene (Fig. 3), recognized as a major biosynthetic gene involved in producing pathogen-induced SA (Wilderthum *et al.*, 2001). As expected with high *ICS1* expression, its two major transcriptional regulators, *SARD1* and *CBP60g*, were also induced (Fig. 3). Interestingly, the expression of *S3H*, a gene involved in SA degradation, was also induced (Fig. 3). However, it is not known if this high expression is correlated with higher amounts of protein and/or activity levels. Most probably, the high expression of *S3H* is the mechanism induced to deal with high SA concentrations.

Many mutants that accumulate high concentrations of SA have been identified, all of which exhibit stunted growth or dwarfism (Bowling *et al.*, 1994, 1997; Yu *et al.*, 1998; Shah *et al.*, 1999; Kachroo *et al.*, 2000; Shirano *et al.*, 2002). To prove that the dwarfism of *pi4kIIIβ1β2* is caused by high SA synthesis, we crossed the double mutant with four different mutants in SA signalling and biosynthesis. The rosette size of all triple mutants was similar to WT, clearly showing that excess SA is responsible for the dwarf phenotype. Combined analysis of shoot size, SA concentration and *PR-1* expression in these mutants allowed us to create a genetic model of *PI4Kβ1/β2* action in the SA signalling pathway (Fig. 7). This model also explains the unusual characteristics of some triple mutants. In WT plants, *PI4Kβ1*, and to a lesser extent *PI4Kβ2*, is a negative regulator of the SA signalling pathway acting upstream of *EDS1* (Fig. 7a). In *pi4kIIIβ1β2* plants, the signalling upstream of *EDS1* is de-repressed and thus *ICS1* expression and subsequently SA biosynthesis increase. This causes *NPR1*-mediated transcriptional reprogramming, which results in stunted rosettes. In these plants, signalling upstream of *ICS1* is negatively regulated through *NPR1*. However, this negative feedback loop is not sufficient to suppress SA to its basal concentration (Fig. 7b). When the *eds1* mutation is introduced into *pi4kIIIβ1β2* plants, the *ICS1* expression and SA concentrations are normal and therefore *eds1 pi4kIIIβ1β2* grows normally (Fig. 7c). Mutation in *ICS1* (*sid2*) or introduction of salicylate hydroxylase (*nahG*) keeps SA at a basal concentration and thus plant growth remains normal, even though the signalling downstream of *EDS1* is activated (Fig. 7d and 7e). In *npr1 pi4kIIIβ1β2* plants, the *ICS1* expression and SA concentration are very high, because the negative feedback loop does not function. The SA signal does not lead to transcriptional reprogramming and the rosette size remains normal (Fig. 7f). The

characteristic bleaching of *npr1 pi4kIIIβ1β2* is probably caused by the high SA concentration and has previously been observed in *cpr5 npr1* plants or when *npr1* plants were supplemented with SA (Bowling *et al.*, 1997).

The positioning of *pi4kIIIβ1β2* upstream of *eds1* in this genetic model is not surprising. Other mutations causing SA overaccumulation, such as *cpr1*, *cpr6*, *bon1* or *bap1*, were also placed upstream of *eds1* in genetic models (Clarke *et al.*, 2001; Yang *et al.*, 2007). Interestingly, *EDS1* and its interacting partners, *PAD4* and *SAG101*, are putative lipases, although it is not known whether they bind lipids (Wiermer *et al.*, 2005). The lipid-binding domains of *EDS1*, *PAD4* and *SAG101* are indispensable for heterodimer formation of these proteins (Wagner *et al.*, 2013). One can easily imagine that these interactions could be regulated by a lipid molecule.

The characteristic short roots and aberrant root hairs of *pi4kIIIβ1β2* grown *in vitro* (Fig. 1) have been previously described by Preuss *et al.* (2006). Kang *et al.* (2011) proposed that the phenotype of roots is caused by changes in early and late *trans* Golgi network morphology and loss of control over secretory vesicle size. We wanted to know whether SA is responsible for the *in vitro* root phenotype. Interestingly, the root lengths of the triple mutants did not significantly revert to WT lengths (Fig. 6). The *PR-1* gene was not induced in *pi4kIIIβ1β2* seedlings grown under the conditions used for root assays (Fig. S4). These data indicate that in the conditions used for *in vitro* root assays, SA signalling is not activated so would not affect the plant phenotype. Taken together, our results show that the mechanisms responsible for small rosettes of adult plants and short roots *in vitro* are different, even though both are caused by *pi4kIIIβ1β2* mutations. Such aberrant roots might be expected to affect shoot growth, but the roots were not investigated in

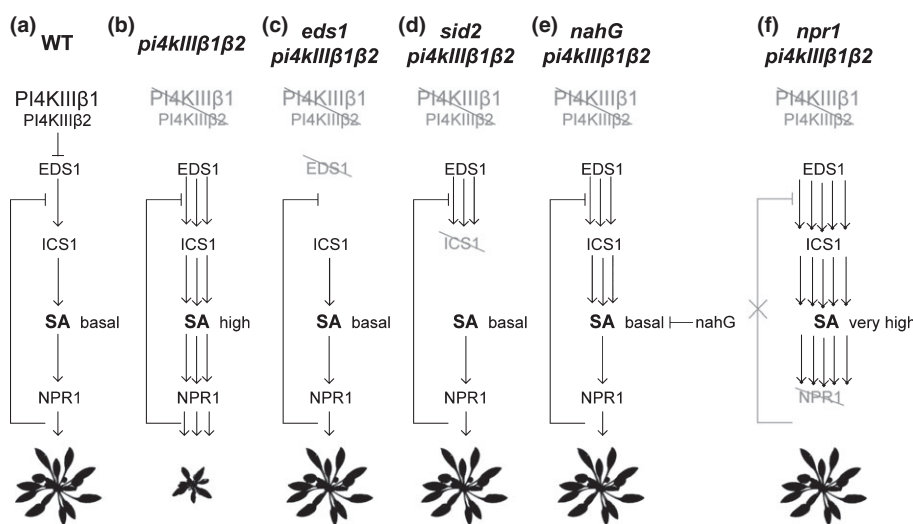


Fig. 7 Genetic model for salicylic acid (SA) signalling pathway in *Arabidopsis thaliana* wild-type (WT), *pi4kIIIβ1β2* and all triple mutants. (a) In the WT, *PI4KIIIβ1* and, to a lesser extent, *PI4KIIIβ2* repress SA signalling upstream of *EDS1*. (b) In *pi4kIIIβ1β2* plants, signalling upstream of *EDS1* is de-repressed, which leads to stronger transcription of the SA biosynthetic gene *ICS1* and thus to high concentrations of SA. This increase stunts rosette growth through *NPR1*-mediated transcriptional reprogramming. (c) In *eds1 pi4kIIIβ1β2* plants, the absence of *EDS1* means that *ICS1* transcription is not induced, and so SA is not in excess and growth is normal. (d, e) In *sid2 pi4kIIIβ1β2* (d) and *nahG pi4kIIIβ1β2* (e) plants, SA biosynthesis is abolished and SA is catabolized, respectively. Thus these plants display normal growth. (f) In *npr1 pi4kIIIβ1β2*, the absence of the *NPR1*-dependent negative feedback loop leads to even higher *ICS1* transcription and SA concentrations. However, the high SA concentration is not transformed to transcriptional reprogramming and the growth remains normal.

adult plants grown in soil. Other mutants with severely defective root hairs do not exhibit other morphological abnormalities (Schiefelbein & Somerville, 1990) and the length of roots does not necessarily determine shoot size (Dhondt *et al.*, 2010).

Using a lipidomic approach, we compared the distribution of fatty acid residues in *pi4kIIIβ1β2* and *ssi2*, a mutant deficient in stearoyl-acyl carrier protein desaturase and which resembles the *pi4kIIIβ1β2* phenotype (Shah *et al.*, 2001). The most obvious characteristic of *ssi2* is high content of 18:0- molecular species (Fig. S3), but this is not true of *pi4kIIIβ1β2*. However, the increase in 18:0 species does not contribute to a constitutively high SA concentration in *ssi2* (Kachroo *et al.*, 2003). The phenotype of *ssi2* is, rather, a result of low oleic acid (Kachroo *et al.*, 2004). We also found decreased relative content of 18:1 (oleic acid) in all phosphoglycerolipids of *ssi2*. There was a decrease of 28% in 18:1 in PC in *pi4kIIIβ1β2*, compared with a decrease of 65% in *ssi2* (Fig. S5). We cannot rule out the possibility that this decrease in 18:1 contributes to the high SA concentration of *pi4kIIIβ1β2*. On the other hand, unlike in *pi4kIIIβ1β2*, the phenotype of *ssi2* does not revert by crossing with *eds1* (Venugopal *et al.*, 2009). This indicates that the mechanism triggering high SA is different in each mutant.

In *pi4kIIIβ1β2*, we did not observe any obvious change in the profile of molecular species of the lipids assessed. The most characteristic change for *pi4kIIIβ1β2* was 16:0/18:3- species that were increased in PI, PC, PE and PG (Fig. S3). The pattern of 16:0/18:3 can be directly related to JA, because 18:3 (linolenic acid) is a precursor in JA biosynthesis (Turner *et al.*, 2002). The concentration of JA was increased almost fourfold in the *pi4kIIIβ1β2* compared with the WT.

We had previously shown that PI4K activity was stimulated when *A. thaliana* suspension cells were treated with exogenous SA. Inhibition of PI4K activity with 30 µM wortmannin inhibited *PR-1* expression (Krinke *et al.*, 2007), suggesting that a type III PI4K is active in the SA signalling pathway downstream of SA biosynthesis. Here we show that *PI4Kβ1* and *PI4Kβ2* operate upstream of SA biosynthesis. Although we cannot exclude the possibility that wortmannin targeted another enzyme activity, PI4K is still the strongest candidate. Besides *PI4Kβ1* and *PI4Kβ2*, there are two other type III PI4Ks in Arabidopsis, *AtPI4KIIIα1* and *AtPI4KIIIα2*. The latter is most probably a pseudogene, as we and others have not been able to detect its transcript (Mueller-Roeber & Pical, 2002). The microsomes extracted from *pi4kIIIβ1β2* still retain 60% of the total PI4K activity as a result of *AtPI4KIIIα1* (Delage *et al.*, 2012a). Therefore, *AtPI4KIIIα1* might be the positive downstream regulator of SA signalling. Unfortunately, we were unable to isolate homozygous plants from three different T-DNA lines of *AtPI4KIIIα1*, which suggests that these mutations cause male or female sterility or homozygous lethality (Delage *et al.*, 2012a).

The *pi4kIIIβ1β2* double mutant is a constitutive overaccumulator of SA. The excess SA concentrations stunt the growth of the mutant. SA is the main factor contributing to this trait in rosettes of soil-grown plants, but not to inhibiting root growth of plants *in vitro*. *PI4Kβ1* and *PI4Kβ2* suppress SA biosynthesis through an EDS1-dependent pathway.

Acknowledgements

This work was supported by grants from the Centre National de la Recherche Scientifique (EAC 7180), Université Pierre et Marie Curie (UR 5) (E.D., J.P., A.G., A.Z. and E.R.) and the Czech Science Foundation (501/11/1654) (V.Š., M.J., P.I.D., O.V. and L.B.), a Specific University research grant (MSMT No 21/2014) (M.J. and O.V.) and a European Union and European Social Fund grant (TÁMOP 4.2.1./B-09/1/KMR 2010-0003) (K.B.). V.Š.'s research stay in the E.R. laboratory was supported by a grant from the French government (729077B). We would like to thank Myrta Pařízková for her excellent technical support, Isabel Le Disquet for microscopic observations (Plateforme imagerie UPMC) and Dr Erik Nielsen who provided us with *pi4kIIIβ1β2* seeds.

References

- Bowling SA, Clarke JD, Liu YD, Klessig DF, Dong XN. 1997. The *cpr5* mutant of *Arabidopsis* expresses both NPR1-dependent and NPR1-independent resistance. *Plant Cell* 9: 1573–1584.
- Bowling SA, Guo A, Cao H, Gordon AS, Klessig DF, Dong X. 1994. A mutation in *Arabidopsis* that leads to constitutive expression of systemic acquired resistance. *Plant Cell* 6: 1845–1857.
- Cao H, Glazebrook J, Clarke JD, Volko S, Dong XN. 1997. The *Arabidopsis NPR1* gene that controls systemic acquired resistance encodes a novel protein containing ankyrin repeats. *Cell* 88: 57–63.
- Clarke JD, Aarts N, Feys BJ, Dong X, Parker JE. 2001. Constitutive disease resistance requires *EDS1* in the *Arabidopsis* mutants *cpr1* and *cpr6* and is partially *EDS1*-dependent in *cpr5*. *Plant Journal* 26: 409–420.
- Crowe ML, Serizet C, Thareau V, Aubourg S, Rouze P, Hilson P, Beynon J, Weisbeek P, van Hummelen P, Reymond P *et al.* 2003. CATMA: a complete *Arabidopsis* GST database. *Nucleic Acids Research* 31: 156–158.
- Czechowski T, Stitt M, Altmann T, Udvardi MK, Scheible WR. 2005. Genome-wide identification and testing of superior reference genes for transcript normalization in *Arabidopsis*. *Plant Physiology* 139: 5–17.
- Delage E, Ruelland E, Guillas I, Zachowski A, Puyaubert J. 2012a. *Arabidopsis* type-III phosphatidylinositol 4-kinases beta1 and beta2 are upstream of the phospholipase C pathway triggered by cold exposure. *Plant and Cell Physiology* 53: 565–576.
- Delage E, Ruelland E, Zachowski A, Puyaubert J. 2012b. Eat in or take away? How phosphatidylinositol 4-kinases feed the phospholipase C pathway with substrate. *Plant Signaling & Behavior* 7: 1197–1199.
- Delaney TP, Uknes S, Vernooij B, Friedrich L, Weymann K, Negrotto D, Gaffney T, Gut-Rella M, Kessmann H, Ward E *et al.* 1994. A central role of salicylic acid in plant disease resistance. *Science* 266: 1247–1250.
- Dhondt S, Coppens F, De Winter F, Swarup K, Merks RM, Inze D, Bennett MJ, Beemster GT. 2010. SHORT-ROOT and SCARECROW regulate leaf growth in *Arabidopsis* by stimulating S-phase progression of the cell cycle. *Plant Physiology* 154: 1183–1195.
- Djafri N, Vergnolle C, Cantrel C, Wietrzynski W, Delage E, Cochet F, Puyaubert J, Soubigou-Taconnat L, Gey D, Collin S *et al.* 2013. The *Arabidopsis* DREB2 genetic pathway is constitutively repressed by basal phosphoinositide-dependent phospholipase C coupled to diacylglycerol kinase. *Frontiers in Plant Science* 4: 307.
- Dobrev PI, Kaminek M. 2002. Fast and efficient separation of cytokinins from auxin and abscisic acid and their purification using mixed-mode solid-phase extraction. *Journal of Chromatography A* 950: 21–29.
- Dobrev PI, Vankova R. 2012. Quantification of abscisic acid, cytokinin, and auxin content in salt-stressed plant tissues. *Methods in Molecular Biology* 913: 251–261.
- Durrant WE, Dong X. 2004. Systemic acquired resistance. *Annual Review of Phytopathology* 42: 185–209.
- El SF, Oh JM, Noor NM, Kwon TR, Mohamed-Hussein ZA, Ismail I, Zainal Z. 2013. Transcriptome profiling of genes induced by salicylic acid and methyl jasmonate in *Polygonum minus*. *Molecular Biology Reports* 40: 2231–2241.

- Falk A, Feys BJ, Frost LN, Jones JDG, Daniels MJ, Parker JE. 1999. EDS1, an essential component of R gene-mediated disease resistance in *Arabidopsis* has homology to eukaryotic lipases. *Proceedings of the National Academy of Sciences, USA* 96: 3292–3297.
- Garcion C, Lohmann A, Lamodiere E, Catinot J, Buchala A, Doermann P, Metraux JP. 2008. Characterization and biological function of the *ISOCHORISMATE SYNTHASE2* gene of *Arabidopsis*. *Plant Physiology* 147: 1279–1287.
- Gross J, Cho WK, Lezhneva L, Falk J, Krupinska K, Shinozaki K, Seki M, Herrmann RG, Meurer J. 2006. A plant locus essential for phylloquinone (vitamin K1) biosynthesis originated from a fusion of four eubacterial genes. *Journal of Biological Chemistry* 281: 17189–17196.
- Hilson P, Allemersch J, Altmann T, Aubourg S, Avon A, Beynon J, Bhalerao RP, Bitton F, Caboche M, Cannoot B et al. 2004. Versatile gene-specific sequence tags for *Arabidopsis* functional genomics: transcript profiling and reverse genetics applications. *Genome Research* 14: 2176–2189.
- Huang J, Gu M, Lai Z, Fan B, Shi K, Zhou YH, Yu JQ, Chen Z. 2010. Functional analysis of the *Arabidopsis PAL* gene family in plant growth, development, and response to environmental stress. *Plant Physiology* 153: 1526–1538.
- Ischebeck T, Seiler S, Heilmann I. 2010. At the poles across kingdoms: phosphoinositides and polar tip growth. *Protoplasma* 240: 13–31.
- Janda M, Planchais S, Djafi N, Martinec J, Burkertova L, Valentova O, Zachowski A, Ruelland E. 2013. Phosphoglycerolipids are master players in plant hormone signal transduction. *Plant Cell Reports* 32: 839–851.
- Kachroo A, Venugopal SC, Lapchyk L, Falcone D, Hildebrand D, Kachroo P. 2004. Oleic acid levels regulated by glycerolipid metabolism modulate defense gene expression in *Arabidopsis*. *Proceedings of the National Academy of Sciences, USA* 101: 5152–5157.
- Kachroo P, Kachroo A, Lapchyk L, Hildebrand D, Klessig DF. 2003. Restoration of defective cross talk in *ssi2* mutants: role of salicylic acid, jasmonic acid, and fatty acids in *SSI2*-mediated signaling. *Molecular Plant-Microbe Interactions* 16: 1022–1029.
- Kachroo P, Shanklin J, Shah J, Whittle EJ, Klessig DF. 2001. A fatty acid desaturase modulates the activation of defense signaling pathways in plants. *Proceedings of the National Academy of Sciences, USA* 98: 9448–9453.
- Kachroo P, Yoshioka K, Shah J, Dooner HK, Klessig DF. 2000. Resistance to turnip crinkle virus in *Arabidopsis* is regulated by two host genes and is salicylic acid dependent but *NPR1*, ethylene, and jasmonate independent. *Plant Cell* 12: 677–690.
- Kalachova T, Lakovenko O, Kretinin S, Kravets V. 2013. Involvement of phospholipase D and NADPH-oxidase in salicylic acid signaling cascade. *Plant Physiology and Biochemistry* 66: 127–133.
- Kang HG, Foley RC, Ofiate-Sánchez L, Lin C, Singh KB. 2003. Target genes for OBP3, a Dof transcription factor, include novel basic helix-loop-helix domain proteins inducible by salicylic acid. *Plant Journal* 35: 362–372.
- Kang BH, Nielsen E, Preuss ML, Mastronarde D, Staehelin LA. 2011. Electron tomography of RabA4b- and PI-4Kβ1-labeled trans Golgi network compartments in *Arabidopsis*. *Traffic* 12: 313–329.
- Khokon MAR, Okuma E, Hossain MA, Munemasa S, Uraji M, Nakamura Y, Mori IC, Murata Y. 2011. Involvement of extracellular oxidative burst in salicylic acid-induced stomatal closure in *Arabidopsis*. *Plant, Cell & Environment* 34: 434–443.
- Krinke O, Ruelland E, Valentova O, Vergnolle C, Renou JP, Taconnat L, Flemm M, Burkertova L, Zachowski A. 2007. Phosphatidylinositol 4-kinase activation is an early response to salicylic acid in *Arabidopsis* suspension cells. *Plant Physiology* 144: 1347–1359.
- Lee S, Kim SG, Park CM. 2010. Salicylic acid promotes seed germination under high salinity by modulating antioxidant activity in *Arabidopsis*. *New Phytologist* 188: 626–637.
- van Leeuwen H, Kliebenstein DJ, West MAL, Kim K, van Poecke R, Katagiri F, Michelmore RW, Doerge RW, Clair DA. 2007. Natural variation among *Arabidopsis thaliana* accessions for transcriptome response to exogenous salicylic acid. *Plant Cell* 19: 2099–2110.
- Mateo A, Funck D, Muhlenbock P, Kular B, Mullineaux PM, Karpinski S. 2006. Controlled levels of salicylic acid are required for optimal photosynthesis and redox homeostasis. *Journal of Experimental Botany* 57: 1795–1807.
- Michell RH. 2008. Inositol derivatives: evolution and functions. *Nature Reviews Molecular Cell Biology* 9: 151–161.
- Mosblech A, Konig S, Stenzel I, Grzeganek P, Feussner I, Heilmann I. 2008. Phosphoinositide and inositolpolyphosphate signalling in defense responses of *Arabidopsis thaliana* challenged by mechanical wounding. *Molecular Plant* 1: 249–261.
- Mueller-Roeber B, Pical C. 2002. Inositol phospholipid metabolism in *Arabidopsis*. Characterized and putative isoforms of inositol phospholipid kinase and phosphoinositide-specific phospholipase C. *Plant Physiology* 130: 22–46.
- Munnik T, Nielsen E. 2011. Green light for polyphosphoinositide signals in plants. *Current Opinion in Plant Biology* 14: 489–497.
- Preuss ML, Schmitz AJ, Thole JM, Bonner HKS, Otegui MS, Nielsen E. 2006. A role for the RabA4b effector protein PI-4Kβ1 in polarized expansion of root hair cells in *Arabidopsis thaliana*. *Journal of Cell Biology* 172: 991–998.
- Rainteau D, Humbert L, Delage E, Vergnolle C, Cantrel C, Maubert MA, Lanfranchi S, Maldiney R, Collin S, Wolf C et al. 2012. Acyl chains of phospholipase D transphosphatidylation products in *Arabidopsis* cells: a study using multiple reaction monitoring mass spectrometry. *PLoS ONE* 7: e41985.
- Rajjou L, Belghazi M, Huguet R, Robin C, Moreau A, Job C, Job D. 2006. Proteomic investigation of the effect of salicylic acid on *Arabidopsis* seed germination and establishment of early defense mechanisms. *Plant Physiology* 141: 910–923.
- Sasek V, Novakova M, Jindrichova B, Boka K, Valentova O, Burkertova L. 2012. Recognition of avirulence gene *AvrLm1* from hemibiotrophic ascomycete *Leptosphaeria maculans* triggers salicylic acid and ethylene signaling in *Brassica napus*. *Molecular Plant-Microbe Interactions* 25: 1238–1250.
- Schiefelbein JW, Somerville C. 1990. Genetic control of root hair development in *Arabidopsis thaliana*. *Plant Cell* 2: 235–243.
- Schneider CA, Rasband WS, Eliceiri KW. 2012. NIH Image to ImageJ: 25 years of image analysis. *Nature Methods* 9: 671–675.
- Scott IM, Clarke SM, Wood JE, Mur LAJ. 2004. Salicylate accumulation inhibits growth at chilling temperature in *Arabidopsis*. *Plant Physiology* 135: 1040–1049.
- Shah J, Kachroo P, Klessig DF. 1999. The *Arabidopsis ssi1* mutation restores pathogenesis-related gene expression in *npr1* plants and renders defensin gene expression salicylic acid dependent. *Plant Cell* 11: 191–206.
- Shah J, Kachroo P, Nandi A, Klessig DF. 2001. A recessive mutation in the *Arabidopsis SSI2* gene confers SA- and *NPR1*-independent expression of *PR* genes and resistance against bacterial and oomycete pathogens. *Plant Journal* 25: 563–574.
- Shirano Y, Kachroo P, Shah J, Klessig DF. 2002. A gain-of-function mutation in an *Arabidopsis* Toll Interleukin1 receptor-nucleotide binding site-leucine-rich repeat type R gene triggers defense responses and results in enhanced disease resistance. *Plant Cell* 14: 3149–3162.
- Spole SH, Koornneef A, Claessens SMC, Korzelius JP, Van Pelt JA, Mueller MJ, Buchala AJ, Metraux JP, Brown R, Kazan K et al. 2003. *NPR1* modulates cross-talk between salicylate- and jasmonate-dependent defense pathways through a novel function in the cytosol. *Plant Cell* 15: 760–770.
- Turner JG, Ellis C, Devoto A. 2002. The jasmonate signal pathway. *Plant Cell* 14(Suppl): S153–S164.
- Venugopal SC, Jeong RD, Mandal MK, Zhu S, Chandra-Shekara AC, Xia Y, Hersh M, Stromberg AJ, Navarre D, Kachroo A et al. 2009. Enhanced disease susceptibility 1 and salicylic acid act redundantly to regulate resistance gene-mediated signaling. *PLoS Genetics* 5: e1000545.
- Vicente MRS, Plasencia J. 2011. Salicylic acid beyond defence: its role in plant growth and development. *Journal of Experimental Botany* 62: 3321–3338.
- Vlot AC, Dempsey DA, Klessig DF. 2009. Salicylic acid, a multifaceted hormone to combat disease. *Annual Review of Phytopathology* 47: 177–206.
- Vogelmann K, Drechsel G, Bergler J, Suberti C, Philippart K, Soll J, Engelmann JC, Engelsdorf T, Voll LM, Hoth S. 2012. Early senescence and cell death in *Arabidopsis saul1* mutants involves the *PAD4*-dependent salicylic acid pathway. *Plant Physiology* 159: 1477–1487.
- Wagner S, Stuttmann J, Rietz S, Guerois R, Brunstein E, Bautista J, Niefind K, Parker JE. 2013. Structural basis for signaling by exclusive EDS1 heteromeric complexes with SAG101 or PAD4 in plant innate immunity. *Cell Host & Microbe* 14: 619–630.

- Wang D, Amornsiripanitch N, Dong X. 2006. A genomic approach to identify regulatory nodes in the transcriptional network of systemic acquired resistance in plants. *PLoS Pathogens* 2: e123.
- Wiermer M, Feys BJ, Parker JE. 2005. Plant immunity: the EDS1 regulatory node. *Current Opinion in Plant Biology* 8: 383–389.
- Wildermuth MC, Dewdney J, Wu G, Ausubel FM. 2001. Isochorismate synthase is required to synthesize salicylic acid for plant defence. *Nature* 414: 562–565.
- Yang H, Yang S, Li Y, Hua J. 2007. The *Arabidopsis BAP1* and *BAP2* genes are general inhibitors of programmed cell death. *Plant Physiology* 145: 135–146.
- Yu IC, Parker J, Bent AF. 1998. Gene-for-gene disease resistance without the hypersensitive response in *Arabidopsis dnd1* mutant. *Proceedings of the National Academy of Sciences, USA* 95: 7819–7824.
- Zhang KW, Halitschke R, Yin CX, Liu CJ, Gan SS. 2013. Salicylic acid 3-hydroxylase regulates *Arabidopsis* leaf longevity by mediating salicylic acid catabolism. *Proceedings of the National Academy of Sciences, USA* 110: 14807–14812.
- Zhang YX, Xu SH, Ding PT, Wang DM, Cheng YT, He J, Gao MH, Xu F, Li Y, Zhu ZH *et al.* 2010. Control of salicylic acid synthesis and systemic acquired resistance by two members of a plant-specific family of transcription factors. *Proceedings of the National Academy of Sciences, USA* 107: 18220–18225.

Supporting Information

Additional supporting information may be found in the online version of this article.

Fig. S1 Morphometric analysis of *pi4kIIIβ1β2* rosettes of plants grown in soil.

Fig. S2 Chloroplast structure investigated by transmission electron microscopy.

Fig. S3 Molecular species analysis of main glycerophospholipids and galactolipids.

Fig. S4 RT-qPCR expression analysis of *PR-1* and *ICS1* genes in seedlings grown *in vitro*.

Table S1 List of qPCR primers used in this study

Table S2 List of genes differentially expressed in *pi4kIIIβ1β2*

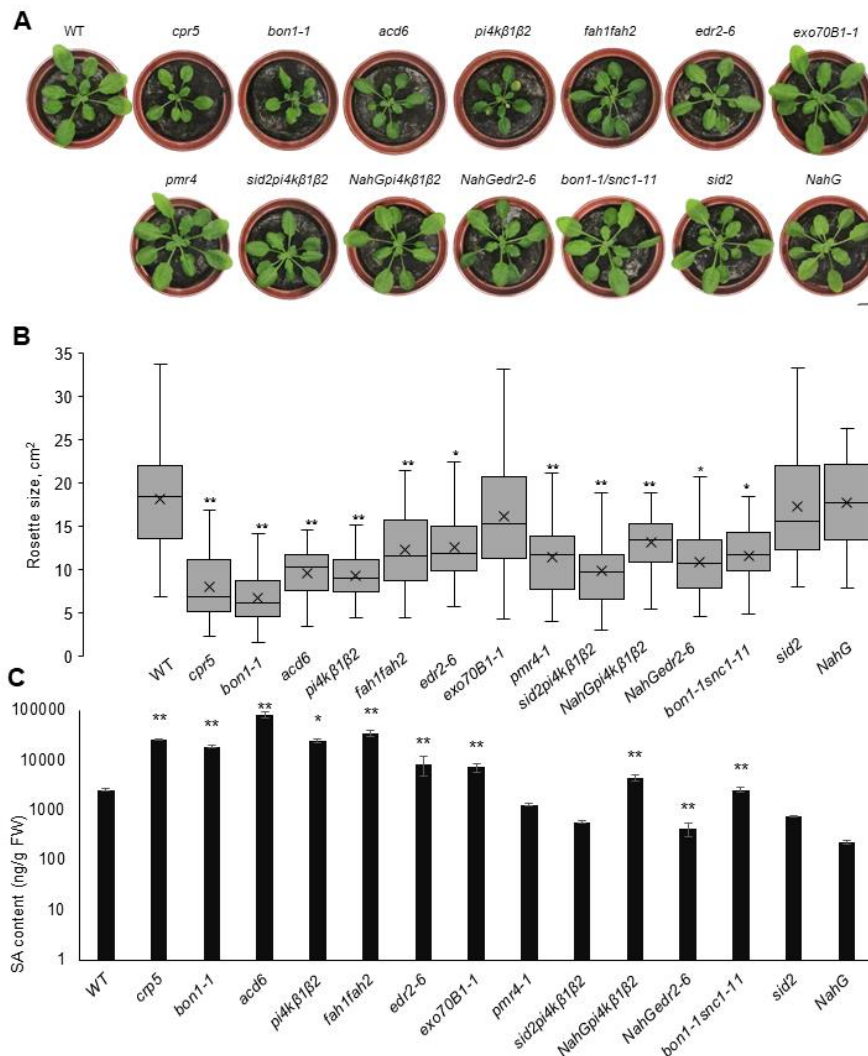
Table S3 Morphometry of plastid structure

Please note: Wiley Blackwell are not responsible for the content or functionality of any supporting information supplied by the authors. Any queries (other than missing material) should be directed to the *New Phytologist* Central Office.

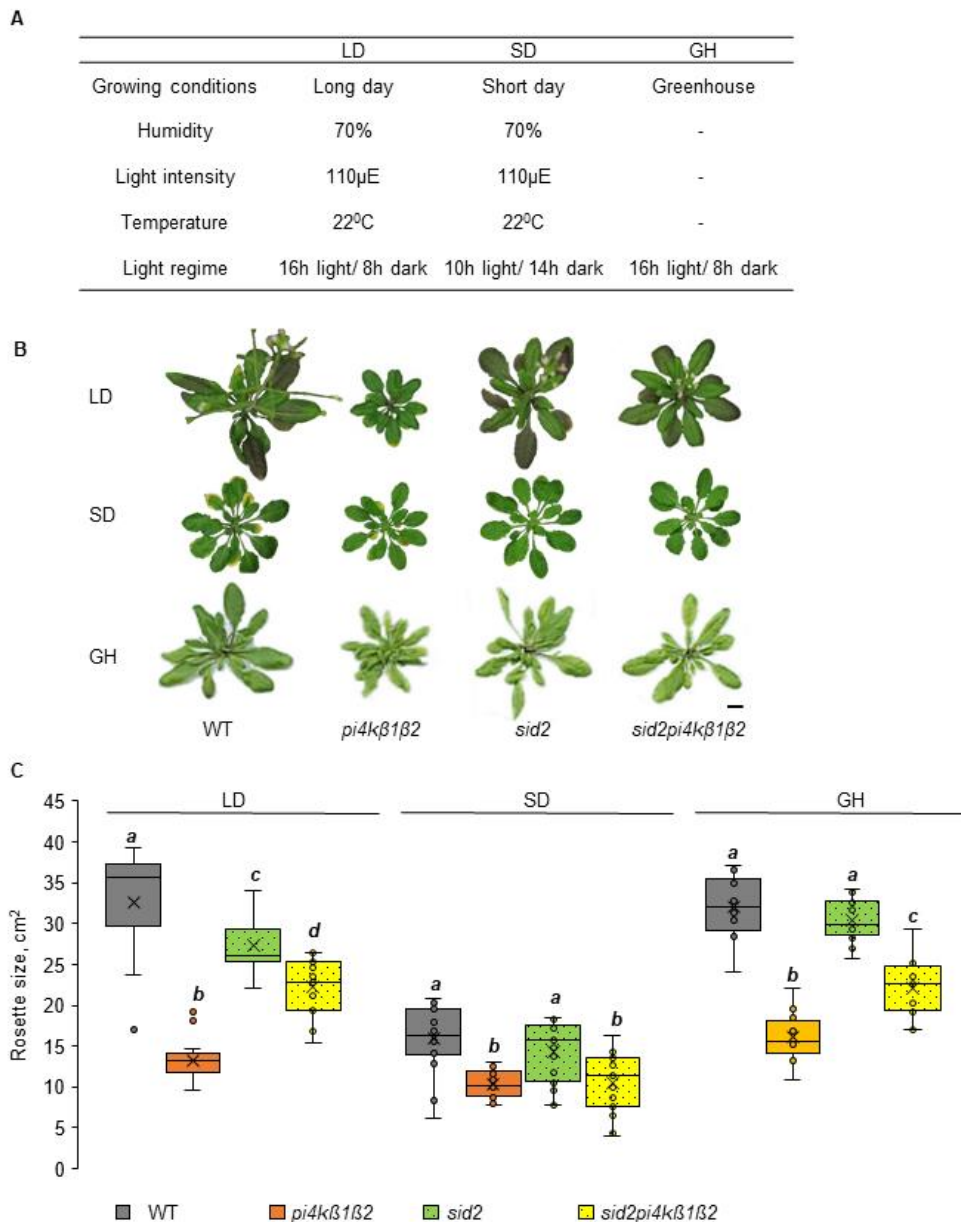


About New Phytologist

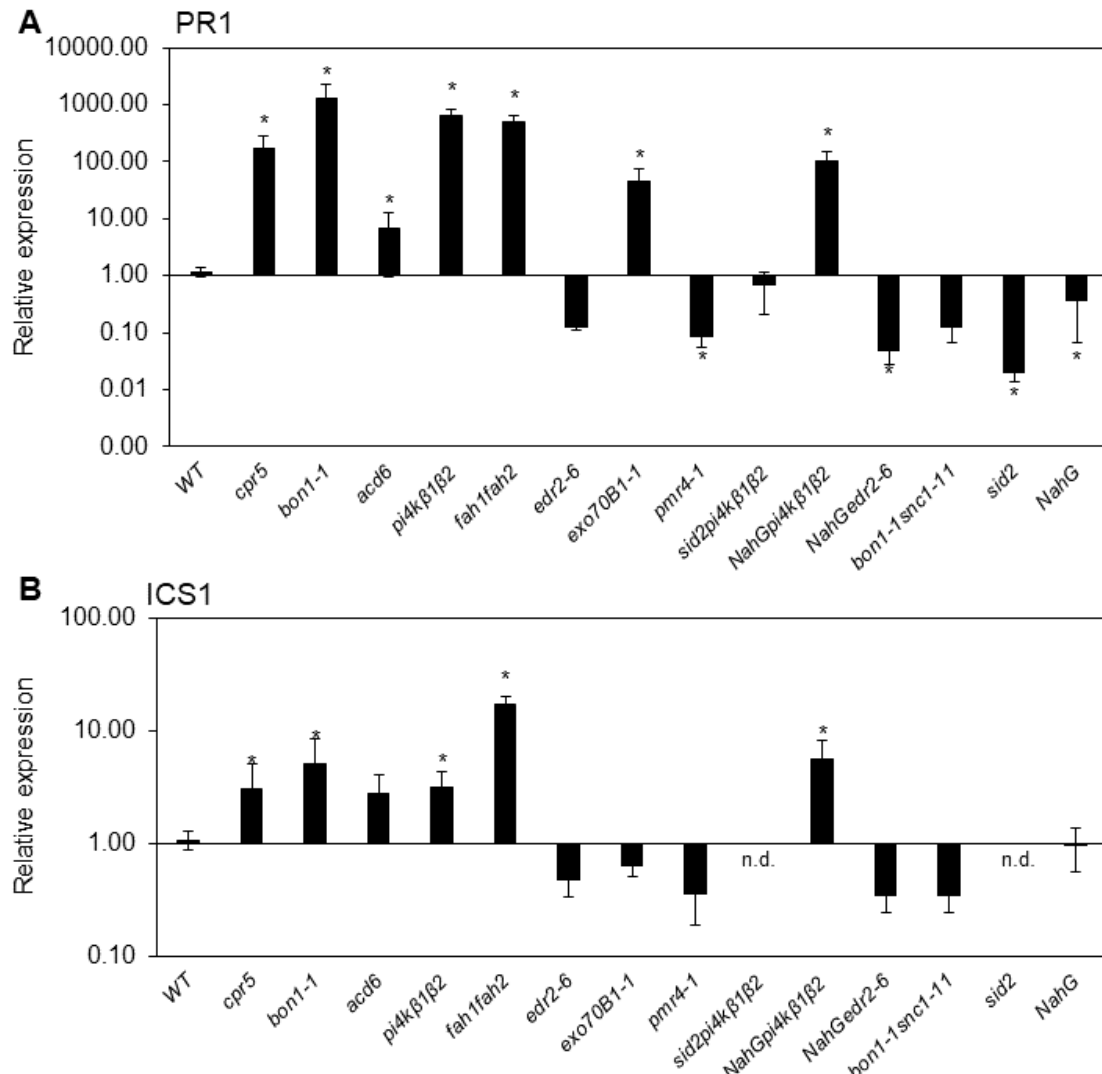
- *New Phytologist* is an electronic (online-only) journal owned by the New Phytologist Trust, a **not-for-profit organization** dedicated to the promotion of plant science, facilitating projects from symposia to free access for our Tansley reviews.
- Regular papers, Letters, Research reviews, Rapid reports and both Modelling/Theory and Methods papers are encouraged. We are committed to rapid processing, from online submission through to publication 'as ready' via *Early View* – our average time to decision is <25 days. There are **no page or colour charges** and a PDF version will be provided for each article.
- The journal is available online at Wiley Online Library. Visit www.newphytologist.com to search the articles and register for table of contents email alerts.
- If you have any questions, do get in touch with Central Office (np-centraloffice@lancaster.ac.uk) or, if it is more convenient, our USA Office (np-usaoffice@ornl.gov)
- For submission instructions, subscription and all the latest information visit www.newphytologist.com

Supplementary Material


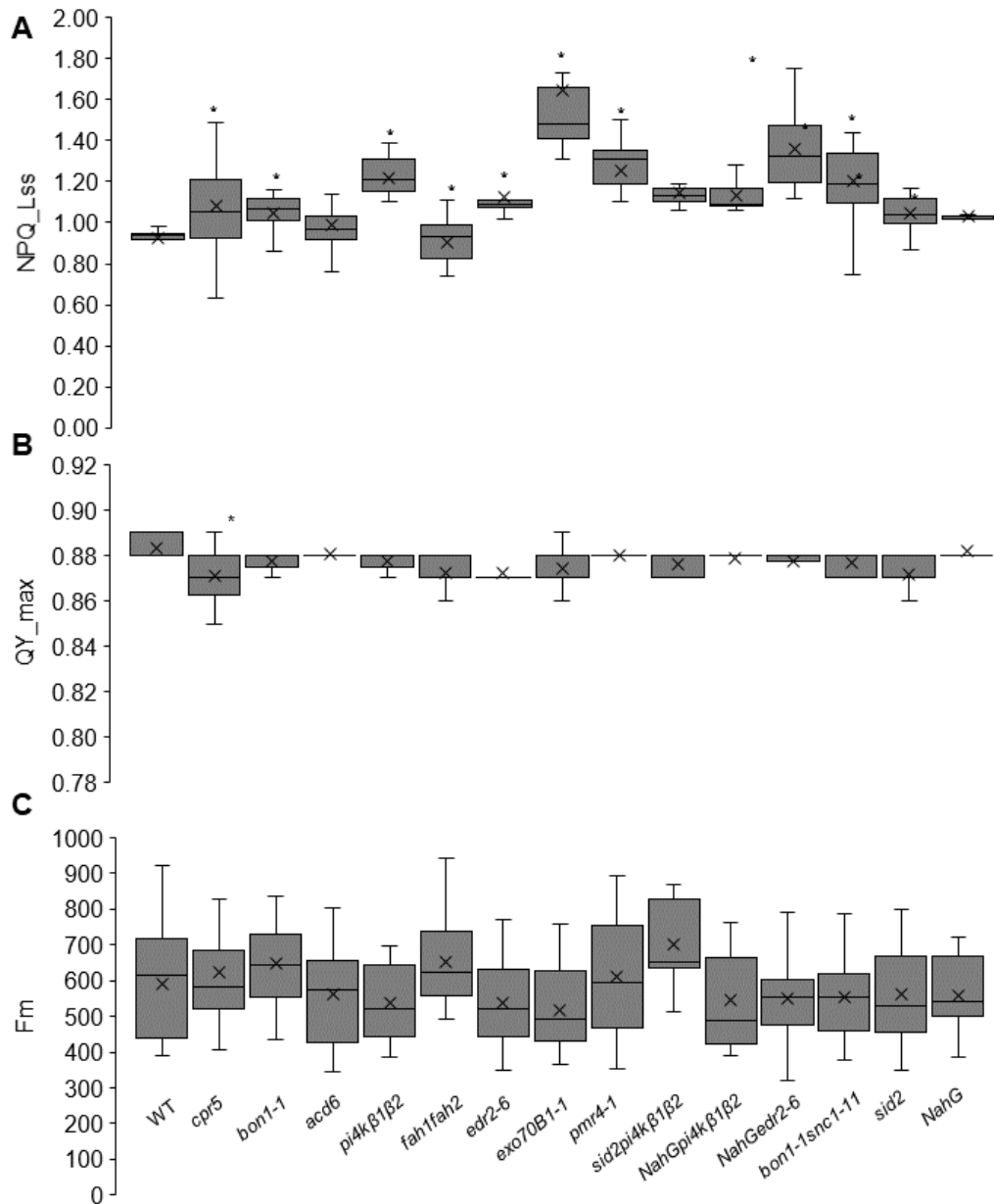
Supplementary Figure S1. Rosette size and salicylic acid (SA) content of plants cultivated under short-day conditions. (A) Representative images of 4 week old plants cultivated at SD conditions: 22 °C, 10 h light/14 h dark. (B) Rosette size. “Immune-related” mutants presented in blue boxes; “phospholipids-related” in red; callose synthase *pmr4* in pink; “reverted” double/triple mutants in yellow and SA-deficient in green. Data are from three biological replicates, $n \geq 70$. Central line of the boxplot represents the median occupancy, cross represents the mean, bottom and top edges of the box are 25 and 75% of distribution and the ends of whiskers are set at 1.5 times the interquartile range. Values outside this range are shown as outliers. Data are from three biological replicates, $n \geq 70$. (C) SA content in the leaves. $n = 4$. Asterisks indicate variants that are different from WT, one-way ANOVA with Tukey’s HSD post hoc test, * $p < 0.05$, ** $p < 0.01$.



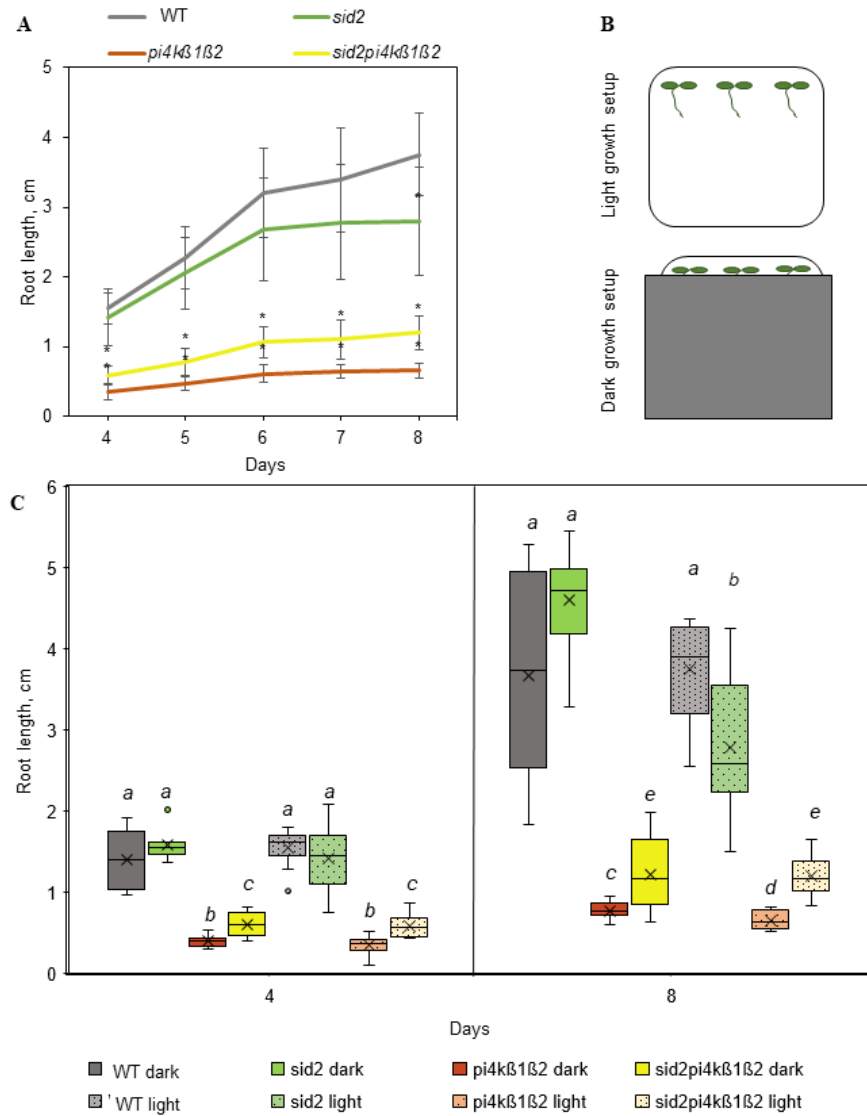
Supplementary Figure S2. Effect of cultivation conditions on rosette size of the *pi4kβ1β2* and *sid2pi4kβ1β2* mutants. (A) Conditions of plant cultivation: LD (long day), SD (short day) and GH (greenhouse). (B) Representative images of 5 week old plants cultivated in different setups, bar 1 cm. (C) Rosette size of the studied mutants grown under different conditions. Different letters indicate variants that were significantly different in every growing condition; one-way ANOVA with Tukey's HSD post hoc test, $p \leq 0.05$. Data are from three biological replicates, $n \geq 12$. Central line of the boxplot represents the median occupancy, cross represents the mean, bottom and top edges of the box are 25% and 75% of distribution and the ends of whiskers are set at 1.5 times the interquartile range.



Supplementary Figure S3. Transcription of *ICS1* and *PR1* in soil-grown plants cultivated under a short-day light regime. Samples were collected from four 4 week old plants. Values were normalized to WT in the respective conditions. *TIP41* was used as a reference gene. Asterisks indicate values different from WT, *t*-test, $p < 0.05$, $n = 4$.



Supplementary Figure S4. Photosynthetic parameters of the studied mutants. Four week old plants were cultivated at 22 °C, 10 h light/ 14 h dark. (A) NPQ-Lss. (B) QY_{max}. (C) Fm. Central line of the boxplot represents the median occupancy, cross represents the mean, bottom and top edges of the box are 25% and 75% of distribution and the ends of whiskers are set at 1.5 times the interquartile range. Values outside this range are shown as outliers. * variants that are different from WT, one-way ANOVA with Tukey's HSD post hoc test. Data are from three biological replicates, $n \geq 70$.



Supplementary Figure S5. Effect of light on primary root elongation of the *pi4kβ1β2* and *sid2pi4kβ1β2* mutants grown in vitro under long day conditions. (A) Dynamics of primary root growth under long-day conditions. * variants that are different from WT, one-way ANOVA with Tukey's HSD post hoc test, $n \geq 10$. (B) Light and dark root setup. (C) Length of primary root grown in light or dark root setup at 4 and 8 days. Central line of the boxplot represents the median occupancy, cross represents the mean, bottom and top edges of the box are 25% and 75% of distribution and the ends of whiskers are set at 1.5 times the interquartile range. Differences calculated separately in each group, 4 and 8 days respectively. Letters correspond to significant differences among groups, $n \geq 10$.

Supplemental Table S1. Primers.

Gene	Accession	Forward Primer	Reverse Primer
<i>TIP41</i>	AT4G34270	GTGAAAACGTGGAGAGAAAGCAA	TCAACTGGATAACCCTTCGCA
<i>PR-1</i>	AT2G14610	AGTTGTTGGAGAAAGTCAG	GTTCACATAATTCCCACGA
<i>ICS1</i>	AT1G74710	GCAAGAACATGTTCCCTACC	AATTATCCTGCTGTTACGAG

Supplemental Table S2. SA content (ng/g FW) of the soil-grown plants.

WT	Short day			Long day		
	251,380	±	15,930	514,591	±	180,327
<i>NahG</i>	225,75	±	17,78	260,36	±	90,84
<i>sid2</i>	741,55	±	24,01	215,81	±	50,57
<i>pmr4</i>	1275,86	±	50,99	994,22	±	107,14
<i>pi4kβ1β2</i>	23851,29	±	1950,85	9410,93	±	982,55
<i>NahGpi4kβ1β2</i>	4458,48	±	659,26	455,29	±	130,99
<i>sid2pi4kβ1β2</i>	567,54	±	31,92	172,26	±	28,88
<i>crp5</i>	25511,32	±	800,46	29118,68	±	17116,81
<i>bon1-1</i>	18437,73	±	964,35	32831,49	±	19690,02
<i>bon1-1snc1-11</i>	2504,99	±	264,97	612,13	±	141,04
<i>edr2-6</i>	8375,98	±	3633,38	2439,16	±	605,55
<i>edr2-6nahG</i>	422,06	±	124,73	1872,03	±	1091,57
<i>fah1fah2</i>	33314,76	±	4732,62	64289,30	±	42158,94
<i>exo70B1-1</i>	7137,93	±	1340,52	1312,63	±	292,41
<i>acd6</i>	80154,83	±	10881,94	61875,90	±	7018,37

PART OF THE FOCUS ISSUE ON PLANT DEFENCE AND STRESS RESPONSE
Identification of salicylic acid-independent responses in an *Arabidopsis* phosphatidylinositol 4-kinase beta double mutant

Tetiana Kalachova^{1,5†}, Martin Janda^{1,2†}, Vladimír Šašek¹, Jitka Ortmannová^{1‡}, Pavla Nováková^{1,2}, I. Petre Dobrev¹, Volodymyr Kravets³, Anne Guivarc'h⁴, Deborah Moura⁵, Lenka Burketová¹, Olga Valentová² and Eric Ruelland^{4,5*}

¹Institute of Experimental Botany, The Czech Academy of Sciences, Prague 160 000, Czech Republic, ²University of Chemistry and Technology, Department of Biochemistry and Microbiology, Prague 166 28, Czech Republic, ³Institute of Bioorganic Chemistry and Petrochemistry, National Academy of Sciences of Ukraine, 02094 Kiev, Ukraine, ⁴CNRS, Institut d'Ecologie et des Sciences de l'Environnement de Paris, UMR 7618, Créteil, France and ⁵Université Paris-Est, UPEC, Institut d'Ecologie et des Sciences de l'Environnement de Paris, Créteil, France

† Equal first authors.

‡ Present address: Department of Plant Biology, Swedish University of Agricultural Sciences, SE-750 07 Uppsala, SWEDEN

* For correspondence. E-mail eric.ruelland@upmc.fr

Received: 4 February 2019 Returned for revision: 13 May 2019 Editorial decision: 23 June 2019 Accepted: 27 June 2019
Published electronically 28 June 2019

• **Background and Aims** We have recently shown that an *Arabidopsis thaliana* double mutant of type III phosphatidylinositol-4-kinases (PI4Ks), *pi4kβ1β2*, constitutively accumulated a high level of salicylic acid (SA). By crossing this *pi4kβ1β2* double mutant with mutants impaired in SA synthesis (such as *sid2* impaired in isochorismate synthase) or transduction, we demonstrated that the high SA level was responsible for the dwarfism phenotype of the double mutant. Here we aimed to distinguish between the SA-dependent and SA-independent effects triggered by the deficiency in *PI4Kβ1* and *PI4Kβ2*.

• **Methods** To achieve this we used the *sid2pi4kβ1β2* triple mutant. High-throughput analyses of phytohormones were performed on this mutant together with *pi4kβ1β2* and *sid2* mutants and wild-type plants. Responses to pathogens, namely *Hyaloperonospora arabidopsis*, *Pseudomonas syringae* and *Botrytis cinerea*, and also to the non-host fungus *Blumeria graminis*, were also determined. Callose accumulation was monitored in response to flagellin.

• **Key Results** We show here the prominent role of high SA levels in influencing the concentration of many other tested phytohormones, including abscisic acid and its derivatives, the aspartate-conjugated form of indole-3-acetic acid and some cytokinins such as *cis*-zeatin. We show that the increased resistance of *pi4kβ1β2* plants to the host pathogens *H. arabidopsis*, *P. syringae* pv. *tomato* DC3000 and *Botrytis cinerea* is dependent on accumulation of high SA levels. In contrast, accumulation of callose in *pi4kβ1β2* after flagellin treatment was independent of SA. Concerning the response to *Blumeria graminis*, both callose accumulation and fungal penetration were enhanced in the *pi4kβ1β2* double mutant compared to wild-type plants. Both of these processes occurred in an SA-independent manner.

• **Conclusions** Our data extensively illustrate the influence of SA on other phytohormone levels. The *sid2pi4kβ1β2* triple mutant revealed the role of PI4Kβ1/β2 *per se*, thus showing the importance of these enzymes in plant defence responses.

Keywords: *pi4kβ1β2/PI4Ks*, callose, salicylic acid, phytohormones, isochorismate synthase 1, biotic stress, pathogens, *Arabidopsis thaliana*.

INTRODUCTION

Salicylic acid (SA) is a phytohormone that has a role in many plant physiological processes, although this has mainly been documented in plant responses to biotic stress when SA accumulates within tissues, both at the site of attack and in a systemic manner (Vlot *et al.*, 2009; Janda and Ruelland, 2015). In plants, SA is biosynthesized via two pathways. One is dependent on phenylalanine ammonia-lyase (PAL; EC 4.3.1.24), which catalyses the conversion of phenylalanine to *trans*-cinnamic acid. In the other pathway, the key enzyme is isochorismate

synthase (ICS; EC 5.4.4.2), which catalyses the isomerization of chorismate to isochorismate (Dempsey *et al.*, 2011). The ICS-dependent pathway was shown to be responsible for most SA accumulation upon pathogen attack. In *Arabidopsis thaliana*, two ICS isoforms exist, but the major role in SA biosynthesis is played by ICS1. The *ICS1* mutant is known as *sid2* for salicylic acid induction deficient 2 (Wildermuth *et al.*, 2001; Wagner *et al.*, 2013; Cui *et al.*, 2017). When SA levels increase, downstream signalling events are triggered, and the best described molecular pathway is dependent on NONEXPRESSOR

OF PATHOGENESIS RELATED 1 (NPR1). Upon SA action, homo-oligomeric NPR1 protein undergoes dissociation by reduction and the resulting monomers move into the nucleus where they interact with TGA-transcription factors to induce the expression of SA responsive genes. An NPR1-independent pathway also exists in response to SA (Janda and Ruelland, 2015). The activation of SA signalling pathways leads to robust changes in the plant transcriptome, including defence-related genes (Seyfferth and Tsuda, 2014). Among the immune responses affected by changes in SA levels or by SA treatments is the accumulation of callose (Kohler *et al.*, 2002; Dong *et al.*, 2008; Antignani *et al.*, 2015), a (1,3)- β -glucan occurring in plant cell walls.

The signalling pathways triggered by SA remain the subject of current research. We have shown that phosphoinositides, the phosphorylated derivatives of phosphatidylinositol (PI), are involved in SA transduction. Indeed, PI can be phosphorylated at the D4 position of the inositol ring by phosphatidylinositol-4-kinases (PI4Ks) thus leading to phosphatidylinositol 4-phosphate (PI4P), which can be phosphorylated further to phosphatidylinositol-4,5-bisphosphate (PI-4,5-P₂). There are two types of PI4Ks according to their primary sequences and pharmacological sensitivities. Type II PI4Ks are inhibited by adenosine while type III PI4Ks are inhibited by micromolar concentrations of wortmannin, a steroid metabolite produced by the fungus *Penicillium funiculosum* (Nakanishi *et al.*, 1995; Balla, 2007; Krinke *et al.*, 2007). From the *A. thaliana* genome, 12 putative PI4K isoforms have been identified. Eight belong to type II (AtPI4K γ 1–8) and four belong to type III (AtPI4K α 1 and α 2, AtPI4K β 1 and β 2) (Delage *et al.*, 2012; Janda *et al.*, 2014). We have shown that type III PI4Ks are activated when *A. thaliana* suspension cells respond to SA, thus leading to an increase in PI4P and PI-4,5-P₂ (Krinke *et al.*, 2007). PI-4,5-P₂ can act as a cofactor to some phospholipase Ds (Pappan *et al.*, 1998). Interestingly, there is overlap between SA-responsive genes controlled by PI4Ks and those controlled by phospholipase Ds, leading to the working model that in response to SA, PI4P and PI-4,5-P₂ are produced with PI-4,5-P₂ acting as a cofactor for a phospholipase D, whose product, PA, will trigger a signalling cascade (Krinke *et al.*, 2009; Kalachova *et al.*, 2016).

To better characterize the role of PI4Ks in the response to SA, we have used *A. thaliana* mutants altered in type III PI4Ks. We previously worked on a double mutant defective in the two PI4K β genes. Surprisingly, *pi4k β 1 β 2* exhibited a constitutively high SA level that resulted in constitutive high transcription of SA-responsive genes such as *PR-1* (PATHOGENESIS RELATED 1). Therefore, PI4Ks are not only involved in SA transduction but they can also impact SA concentration. Furthermore, this double mutant exhibited dwarfism and was more resistant to the bacterial pathogen *Pseudomonas syringae* pv. *maculicola* ES4326 (Sasek *et al.*, 2014). The *pi4k β 1 β 2* plant was crossed with mutants impaired in components of SA synthesis (*sid2*, impaired in *ICS1* expression; *eds1*), SA transduction (*npr1*) or a mutant expressing bacterial SA-hydroxylase (NahG) that degrades SA to catechol. The resulting triple mutants allowed us to conclude that the dwarf phenotype of *pi4k β 1 β 2* plants was dependent on SA accumulation and its transduction via the NPR1 pathway (Janda *et al.*, 2014; Sasek *et al.*, 2014).

In the present study, our aim was to identify amongst the cellular and physiological processes affected by the deficiency of PI4K β 1 β 2 those that were either SA-dependent or SA-independent. To achieve this, we used the *sid2pi4k β 1 β 2* triple mutant that does not accumulate SA and exhibits wild-type-sized rosettes (Sasek *et al.*, 2014). In this mutant, the effects of PI4K β 1 and PI4K β 2 mutations would not be masked by high SA levels. We showed that hormonal levels and pathogen resistance were mainly dependent on SA. However, we could show that *sid2pi4k β 1 β 2* plants accumulated higher amounts of callose in response to *flg22* and wounding. Interestingly, this SA-independent callose accumulation was also observed during early stages of interactions with *Blumeria graminis* when penetration was observed. Our data suggest that PI4Ks are involved in plant immune responses not only through SA accumulation but also via SA-independent processes.

MATERIALS AND METHODS

Plant material, growth conditions

In this study, we used the following genotypes of *A. thaliana*: Columbia-0 (WT), *sid2-3* (Gross *et al.*, 2006), *npr1-1* (Cao *et al.*, 1997), NahG (Delaney *et al.*, 1994), *pi4k β 1 β 2* (SALK_040479/SALK_09069; Preuss *et al.*, 2006), *sid2pi4k β 1 β 2*, NahG π *4k β 1 β 2* and *npr1pi4k β 1 β 2* mutants previously described (Sasek *et al.*, 2014).

All plants were cultivated in Jiffy 7 peat pellets at 22 °C with 70 % relative humidity. All plants were watered without additional fertilizers. Plants were routinely cultivated in daily cycles of 10 h light (100–130 μE m⁻² s⁻¹) and 14 h dark. Plants that would be used for hormonal analysis or transcription analysis were cultivated under 16 h light (130–150 μE m⁻² s⁻¹) and 8 h dark.

Pathogen inoculation

Two-week-old plants grown at high density in one pot were sprayed with *Hyaloperonospora arabidopsis* NoCo2 spores (~100 spores μL⁻¹). The infected plants were cultivated in closed transparent plastic boxes at high humidity for 6 d under 16 h light/8 h dark (100–130 μE m⁻² s⁻¹) at 19 °C. For analysis, leaves collected from one pot were considered as one sample (for each genotype, 11 samples were analysed). Spores were counted under a microscope using a Bürker chamber and expressed as relative spore number (%), where relative spore number for a given control genotype (WT or *sid2*) was set to 100 %. The spores were counted as spores per milligram of tissue fresh weight. The experiments (WT vs. *pi4k β 1 β 2* and *sid2* vs. *sid2pi4k β 1 β 2*) were conducted independently.

Inoculation with *P. syringae* was performed according to Katagiri *et al.* (2002) with modifications. Bacteria were cultivated overnight on King's B medium plates containing rifampicin (50 μg μL⁻¹). *P. syringae* pv. *tomato* DC3000 (*Pst* DC3000) and *P. syringae* pv. *tomato* DC3000 AvrRpt2 (*Pst* DC3000 AvrRpt2) were taken from the respective plate and resuspended in 10 mM MgCl₂ to give an OD₆₀₀ of 0.001. Four-week-old plants were infiltrated with this suspension.

One disc (6 mm) from one leaf, three leaves at a similar developmental stage from one plant and three plants were collected as one sample of one genotype at 0 days post-inoculation (dpi) and 3 dpi (3 dpi only for *Pst* DC3000; 2 dpi for *Pst* DC3000 AvrRpt2). Leaf discs were ground in 10 mM MgCl₂ and decimal dilutions were made. Colony forming units were counted.

Four-week-old *A. thaliana* plants were treated with 6 µL drops containing *Botrytis cinerea* BMM spores (5×10^4 spores mL⁻¹) by applying a single drop to each leaf, with three leaves at a similar developmental stage inoculated for each plant. Treated plants were placed into closed plastic boxes and kept in low light (16 h light/8 h dark, 21 °C; 10–µE m⁻² s⁻¹) for 56 h post-inoculation (hpi).

Blumeria graminis f. sp. *hordei* (*Bgh*) was cultivated continuously on fresh barley ('Golden promise') grown under short day conditions (19 °C, 10/14 h, 50 % humidity, at a light intensity of 70 µmol m⁻² s⁻¹). Plants, ~4 weeks old, were inoculated by spreading spores from infected barley onto the adaxial side of their leaves (from leaf to leaf). The 5th–6th leaves were cut off at selected times hours post-inoculation (hpi) and cleared with 96 % ethanol or chloral hydrate. For penetration rate, fungal structures were stained with 250 mg mL⁻¹ trypan blue in a lactophenol/ethanol solution (Vogel and Somerville, 2000). Stained leaves were observed by classical epifluorescence microscopy or bright-field microscopy using a Zeiss AxioImager ApoTome2 (objective 100×).

Callose deposition

Four-week-old *A. thaliana* plants were treated for 24 h with 100 nM flg22 or infiltrated with *Pst* DC3000. Distilled water infiltration was used as a control (mock) treatment. Infiltrated leaves were decoloured in ethanol/glacial acetic acid (3:1, v/v). The leaves were then rehydrated in successive baths of 70 % ethanol (at least 1 h), 50 % ethanol (at least 1 h), 30 % ethanol (at least 1 h) and water (at least 2 h). Leaves were stained for 4 h with 0.01 % aniline blue in 150 mM K₂HPO₄, pH 9.5. Callose deposition was observed by fluorescence microscopy using a Zeiss AxioImager ApoTome2 (objective 10×). In *Bgh* infection analysis, we calculated only callose spots using the high circularity function of the measurement settings at an interval of 0.5–1 which allowed us to distinguish only the cells with the size exclusion limit for spots corresponding to either encased haustoria or enormous papilla. Images were processed with ImageJ software. At least four leaves from three independent plants were analysed for each variant.

RNA extraction and qPCR analysis

Plant tissues were homogenized in 2-mL screw-cap tubes containing 1 g of 1.3-mm-diameter silica beads using a FastPrep-24 instrument (MP Biomedicals, USA). Total RNA was isolated using a Spectrum Plant Total RNA kit (Sigma-Aldrich, USA) and treated with a DNA-free kit (Ambion, USA). Subsequently, 1 µg of RNA was converted to cDNA with M-MLV RNase H-Point Mutant reverse transcriptase (Promega Corp., USA) and an anchored oligo dT21 primer (Metabion, Germany). Gene transcription was quantified by qPCR using a LightCycler

480 SYBR Green I Master kit and a LightCycler 480 (Roche, Switzerland). The PCR conditions employed were 95 °C for 10 min followed by 45 cycles of 95 °C for 10 s, 55 °C for 20 s and 72 °C for 20 s. Melting curve analyses were then carried out. Relative transcription was normalized to the housekeeping genes *SAND* or *TIP41* (Czechowski et al., 2005). Primers were designed using PerlPrimer v1.1.21 (Marshall, 2004). The primers used were *CalS1_F*, AAGAGCGGAGGGTCACTTG; *CalS1_R*, GGCGACACGAATAGACGGAT; *CalS12_F*, TTCACTCCGTTTCCGAGG; and *CalS12_R*, GGAGAGAGACGCATCTGAGC.

Analysis of plant hormones

Plant hormones were extracted from 100 mg of frozen tissues and their concentrations were determined as previously described (Dobrev and Vankova, 2012; Dobrev and Kaminek, 2002) after the addition of appropriate internal standards. Hormone analysis was carried out on four samples, each taken from three plants. Briefly, samples were homogenized in tubes with 1.3-mm silica beads using a FastPrep-24 instrument (MP Biomedicals). Samples were then extracted with a methanol/H₂O/formic acid (15:4:1, by vol.) mixture, which was supplemented with stable isotope-labelled phytohormone internal standards (10 pmol per sample) in order to check recovery during purification and to validate the quantification. The clarified supernatants were subjected to solid phase extraction using Oasis MCX cartridges (Waters Co., USA). The eluates were evaporated to dryness and the generated solids were dissolved in 30 µL of 15 % (v/v) acetonitrile in water. Hormones were separated and quantified by Ultimate 3000 high-performance liquid chromatography (Dionex, USA) coupled to a 3200 Q TRAP hybrid triple quadrupole/linear ion trap mass spectrometer (Applied Biosystems, USA) as described by Dobrev et al. (2017). Metabolite levels were expressed in pmol/g fresh weight (f. wt).

Statistical analysis

At least three independent biological replicates were performed for all experiments. Statistical analysis was conducted by paired *t*-test or ANOVA with Tukey honestly significant difference (HSD) multiple mean comparison *post hoc* test. The number of analysed samples was specified for each condition. The correlation matrix for hormonal levels was prepared using R-software *Hmisc* and *corrplot* packages based on the Pearson correlation (R Core Team, 2014).

RESULTS

The pi4kβ1β2 double mutant has altered phytohormonal levels

Our goal was to identify SA-dependent and SA-independent processes triggered by the double *pi4kβ1β2* mutation. To do so, we used a *sid2pi4kβ1β2* triple mutant. If a process triggered by the double *pi4kβ1β2* mutation is SA-dependent, then it should disappear in the *sid2pi4kβ1β2* triple mutant. On the

other hand, if a process triggered by the double *pi4kβ1β2* mutation is SA-independent, then it should still be observed in the *sid2pi4kβ1β2* triple mutant.

Because the main effect of the double *pi4kβ1β2* mutation was on the level of SA, we decided to quantify a broad spectrum of phytohormones in the *sid2pi4kβ1β2* triple mutant. The hormone levels obtained were compared to those of *pi4k β1β2*, *sid2* and WT plants. A first look allowed us to establish that the *pi4k β1β2* double mutation does not impact only SA levels. Many hormone-related metabolites showed significantly different levels in *pi4k β1β2* plants when compared to WT plants while most of them remained at WT levels in *sid2pi4kβ1β2*

([Supplementary Data Table S1](#)). In our previous study, we created an additional triple mutant by crossing *pi4kβ1β2* with an *NahG* mutant impaired in SA accumulation: *NahGpi4kβ1β2* ([Sasek et al., 2014](#)). To confirm and to strengthen the results obtained with *sid2pi4kβ1β2*, we also quantified phytohormones in *NahGpi4kβ1β2*, together with their corresponding single mutants ([Table S1](#)). From these data, we built a correlation matrix ([Fig. 1](#)). Many hormone levels were correlated to higher SA levels (Pearson correlation >0.7) as seen for the abscisic acid (ABA) derivatives such as 9-hydroxy-ABA (9OH-ABA), phaseic acid (PA) and dihydrophaseic acid (DPA). However, the high levels of DPA, PA and 9OH-ABA observed in *pi4kβ1β2*

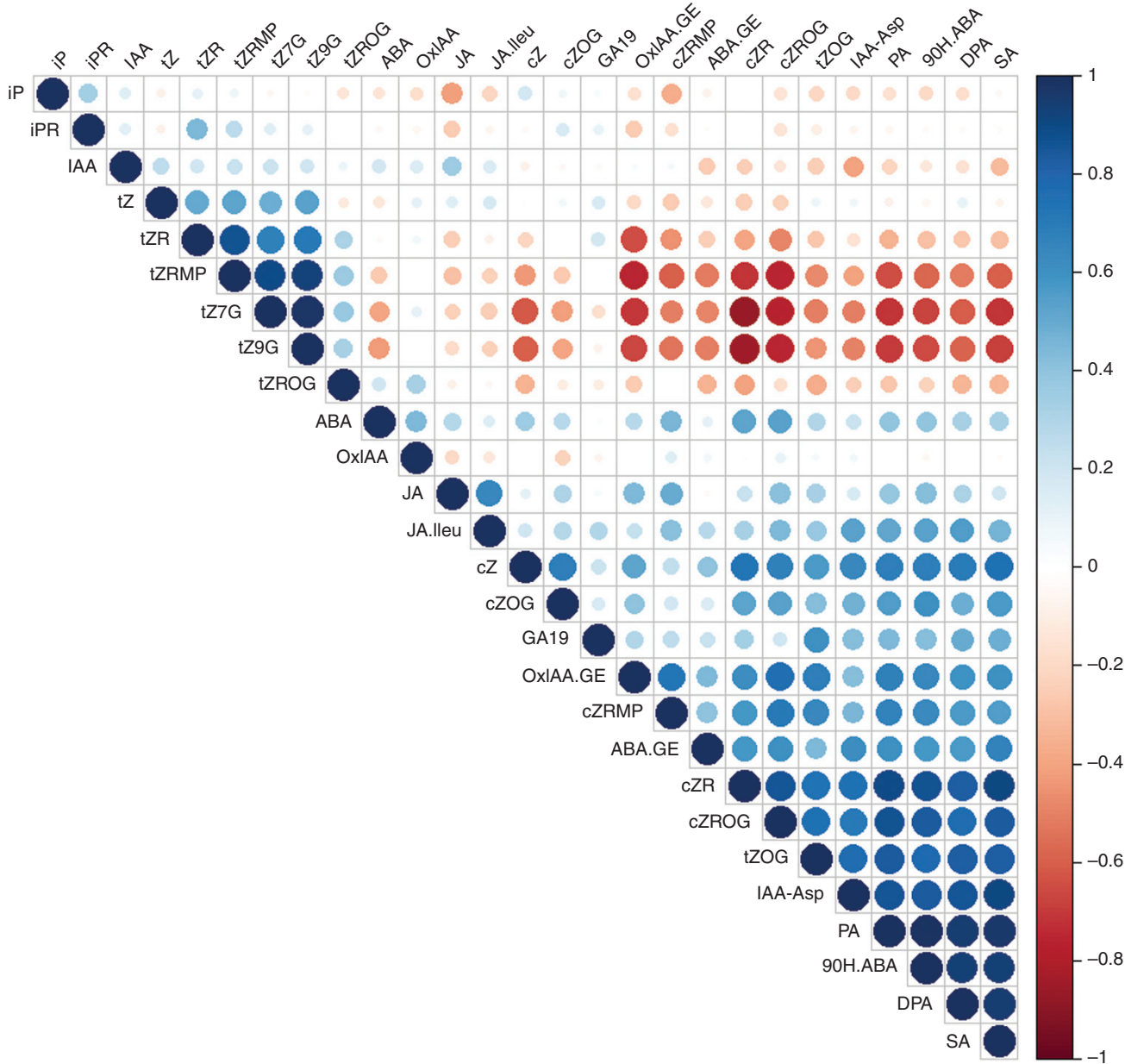


FIG. 1. Correlation matrix between phytohormone levels. The matrix was built using the Pearson correlation of 27 hormone-related metabolites from 24 independent samples corresponding to six genotypes (WT, *sid2*, *NahG*, *pi4kβ1β2*, *sid2pi4kβ1β2* and *NahGpi4kβ1β2*; four plants per genotype). Positive correlations are displayed in blue and negative correlations in red. Colour intensity and the size of the circles are proportional to the correlation coefficients. Red rectangles highlight the correlation between SA and other hormones.

vs. WT were no longer seen in the triple mutants with low SA; therefore, these metabolite levels were controlled by SA in the *pi4kβ1β2* double mutant (Fig. S1A).

Because the main genetic pathway of the SA response is controlled by NPR1, we investigated whether the hormonal control of SA was NPR1-dependent. This was achieved using a previously generated *npr1pi4kβ1β2* triple mutant where the SA level was 30-fold that of the WT and 4-fold that of *pi4kβ1β2*. Interestingly, levels of DPA, PA and 9OH-ABA were still high in *npr1pi4kβ1β2*, showing that the effect of SA on these metabolites was only partially NPR1-dependent. Note that ABA levels did not correlate with SA (Pearson correlation 0.3), indicating that the action of SA on ABA derivatives is probably not directly connected to the biosynthesis of ABA, but with its metabolism.

Other hormones with high Pearson correlations to SA were the Asp conjugated form of indole-3-acetic acid (Asp-IAA) and some cytokinins. The increased level of Asp-IAA observed in *pi4kβ1β2* was no longer observed in the triple mutants with low SA. However, it was still visible in the *npr1pi4kβ1β2* triple mutant, suggesting that this metabolite is controlled by SA but it is only partially NPR1-independent (Supplementary Data Fig. S1B). The pattern of IAA was different from that of Asp-IAA, suggesting that SA control of Asp-IAA is on aspartate conjugation. As for cytokinins, the increase in *cis*-zeatin (cZ), *cis*-zeatin-riboside (cZR), *cis*-zeatin-7-N-glucoside (cZ7G), *cis*-zeatin-riboside-O-glucoside (cZROG) and *trans*-zeatin-O-glucoside (tZOG) and the decrease in *trans*-zeatin-7-N-glucoside (tZ7G) and *trans*-zeatin-9-N-glucoside (tZ9G) in the *pi4kβ1β2* double mutant were SA-driven. In contrast to the other hormones tested, SA's action on tZROG appeared to be partially independent of NPR1 (Fig. S1C).

We identified one hormone for which its level was altered in *pi4kβ1β2* plants independently of SA: the increase in oxIAA-GE observed in *pi4kβ1β2* was still visible in the triple mutants with low SA. Note that oxIAA did not follow the same pattern (Supplementary Data Fig. S2).

Pathogen resistance of *pi4kβ1β2* plants is SA-dependent

At the hormonal level, our data show that the major change induced by the *pi4kβ1β2* double mutation was an increase in SA, with this change determining the levels of many other hormones. Because a major role of SA is related to biotic stress responses, we reasoned that processes related to biotic stress, dependent or not on SA, might also be altered in the double mutant.

Whether the PI4K double mutation *per se* was accompanied by an enhanced resistance to pathogens was investigated. Comparing resistance in *sid2pi4kβ1β2* plants to that in *pi4kβ1β2* or *sid2* would allow us to distinguish between the effectiveness of SA-dependent and SA-independent responses. Therefore, different pathogens with different lifestyles (biotrophs, hemibiotrophs and necrotrophs) were tested (Glazebrook, 2005). The *pi4kβ1β2* double mutant plants were more resistant to the biotroph *H. arabidopsis* NoCo2 compared to WT. However, *sid2pi4kβ1β2* resistance was similar to that of *sid2* plants (Fig. 2A). We then studied resistance to the hemibiotroph *P. syringae* pv. *tomato* DC3000 in its wild type (*Pst* DC3000) or AvrRpt2-expressing form (*Pst* DC3000

AvrRpt2). *Pst* DC3000 AvrRpt2 leads to a strong effector-triggered immunity (ETI) response compared to *Pst* DC3000. With both forms, pathogen development was reduced in *pi4kβ1β2* plants compared to the WT while *sid2pi4kβ1β2* resistance was comparable to that of *sid2* and lower than WT plants (Fig. 2B, Supplementary Data Fig. S3). Unexpectedly, the double mutant also showed an increased resistance to the necrotroph *Botrytis cinerea* which was also SA-dependent as *sid2pi4kβ1β2* resistance was similar to that of *sid2* and WT plants (Fig. 2C). For each pathogenic assay, triple mutant resistance was similar to *sid2*, indicating that SA-dependent pathways were dominant in the immune response. Putative mechanisms regulated by PI4K activity alone were not sufficient to establish pathogen resistance.

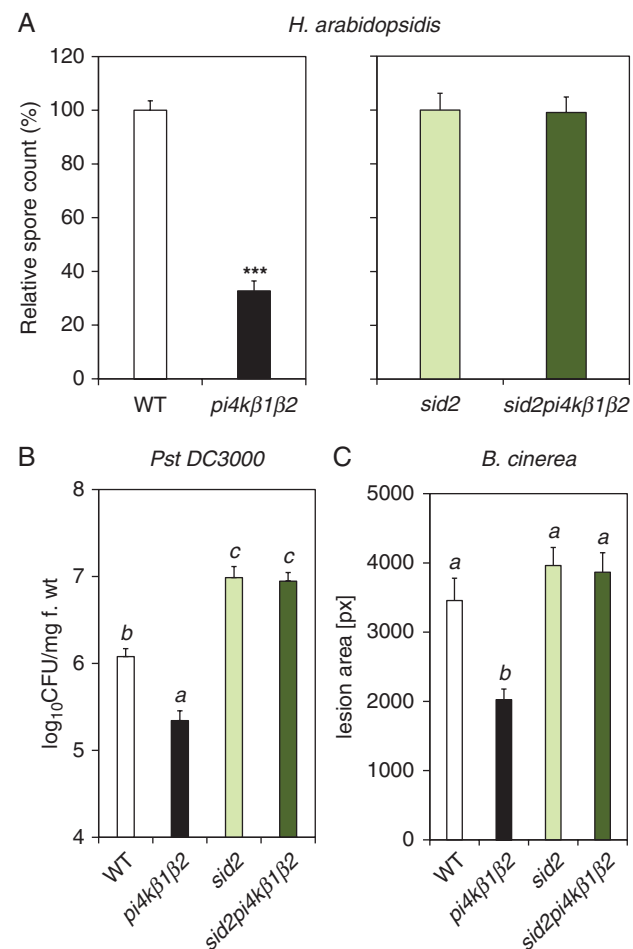


Fig. 2. Resistance to biotic stresses of *pi4kβ1β2* and *sid2pi4kβ1β2* mutants. (A) Resistance to the biotroph *Hyaloperonospora arabidopsis*. (B) Resistance to the hemibiotroph *Pseudomonas syringae* pv. *syringae* DC3000. Infiltration treatment of 4-week-old-plants, with six independent samples. (C) Resistance to the necrotroph *Botrytis cinerea*. Four- to 5-week-old *A. thaliana* were inoculated with a 6-μL drop containing spores of *Botrytis cinerea* (50 000 spores mL⁻¹), placed into a plastic box and kept in the dark for 56 h. Statistical differences between the genotypes for B and C were assessed using ANOVA, with a Tukey honestly significant difference (HSD) multiple mean comparison *post hoc* test. Different letters indicate a significant difference, Tukey HSD, $P < 0.05$, $n = 10$ for A, $n = 7$ for B and $n = 27$ for C. ***Indicate difference from WT, *t*-test, $P < 0.001$.

The enhanced level of basal callose deposition in *pi4kβ1β2* is mainly SA-dependent, while stress-induced callose accumulation is not

SA levels modulate numerous processes associated with immune responses, including the strengthening of leaf tissues and particularly cell walls around the infection site by lignification and callose accumulation (Voigt, 2014). Interestingly, SA pre-treatment also has a positive effect on flagellin-induced callose accumulation (Yi *et al.*, 2014). We therefore studied callose levels, accumulated in leaf tissues in response to treatment with the flagellin epitope (flg22). We first studied callose accumulation in the absence of flg22 treatment (control; Fig. 3A). The *pi4kβ1β2* double mutant exhibited a constitutively high level of callose deposition, as previously shown (Antignani *et al.*, 2015). We were able to show that a spatial pattern in callose accumulation existed, as the examination of different regions of interest (ROI) indicated a higher accumulation in the upper part of the leaf edges (Fig. 3B).

Callose accumulation was then assessed in either mock-infiltrated or flg22-treated plants (Fig. 4). In this case, callose

accumulation was much higher in *pi4kβ1β2* when compared to WT plants (Fig. 4). The *sid2pi4kβ1β2* triple mutant was used to investigate whether high callose deposition in the double mutant depended on its high SA level. For mock treatments, callose deposition was much lower in *sid2pi4kβ1β2* compared to *pi4kβ1β2* plants. This provides arguments for an SA-dependent higher basal callose deposition. This was confirmed by the response to flg22. In WT plants, flg22 induced 20 times more callose compared to control mock infiltrations. Again, the callose level in *pi4kβ1β2* was higher (two-fold) compared to WT plants. This increase was reduced when the *sid2* mutation was introduced into the *pi4kβ1β2* double mutant as the level in the triple mutant was about two-fold lower than in the double mutant and in the same range as the WT level. This indicated that SA was a major inducer of callose accumulation in the *pi4kβ1β2* genotype context. Yet, the *sid2pi4kβ1β2* triple mutant exhibited a higher callose deposition than *sid2* plants. Therefore, the *pi4kβ1β2* double mutation *per se* had a role in the high callose accumulation observed in the *pi4kβ1β2* double mutant.

We also studied callose accumulation in leaf tissues in response to mechanical wounding (Supplementary Data Fig. S4). Again, in response to wounding, the PI4K double mutation enhanced callose accumulation via an SA-dependent pathway.

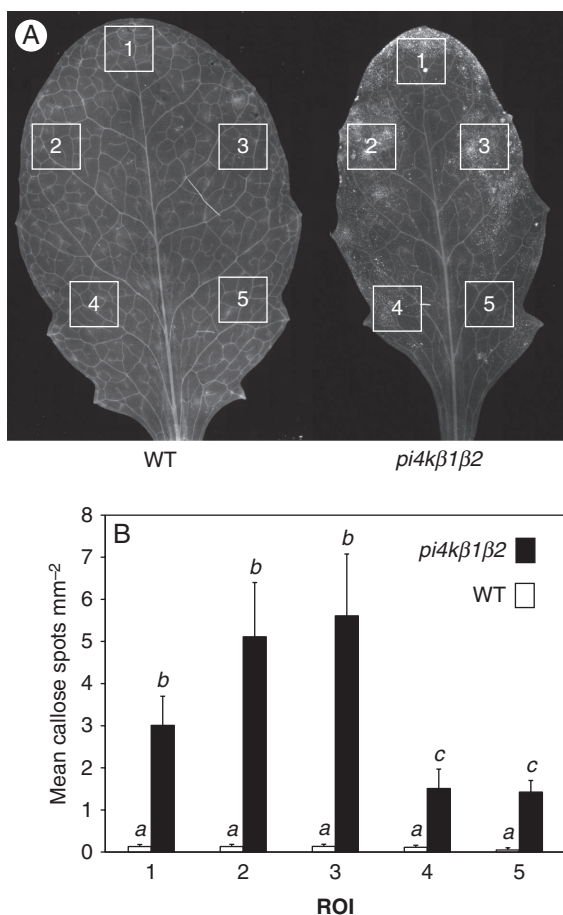


Fig. 3. Pattern of callose accumulation in *pi4kβ1β2* leaves. (A) Aniline blue staining, and fluorescence microscopy. Scale bar = 500 µm. (B) Callose particles accumulated in different ROI. The squares represent the ROI. Data are presented as means \pm s.e.m. Statistical differences were assessed using a two-way ANOVA, with a Tukey honestly significant difference (HSD) multiple mean comparison *post hoc* test. Different letters indicate a significant difference, Tukey HSD, $P < 0.05$. $n = 11$.

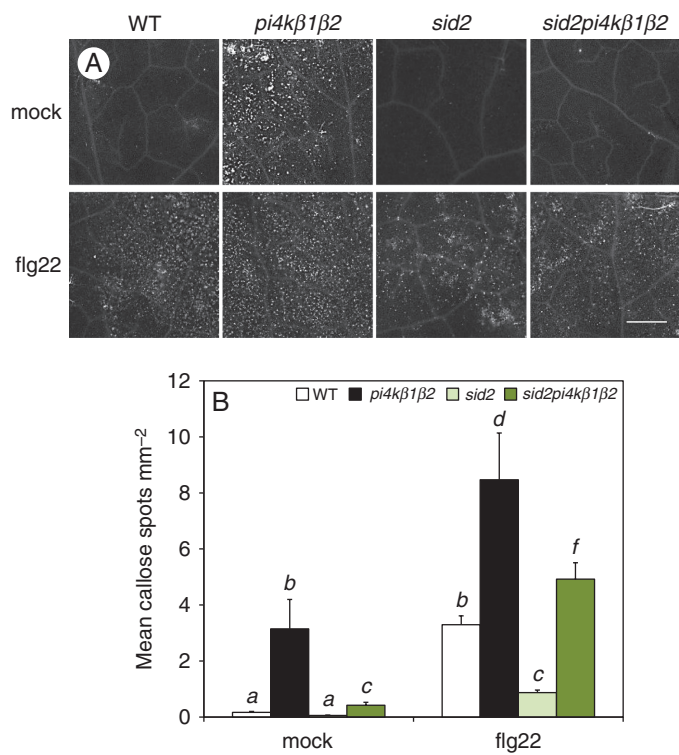


Fig. 4. Callose deposition in response to flagellin. (A) Representative images of callose accumulated in leaves of 4-week-old *A. thaliana* plants by aniline blue staining, 24 h after infiltration with 0.1 µM flg22 or mock infiltration. Scale bar = 1 cm. (B) Quantification of callose particles. Values represent an average of five ROI. Data are presented as means \pm s.d. For each treatment, statistical differences between the genotypes were assessed using a one-way ANOVA, with a Tukey honestly significant difference (HSD) multiple mean comparison *post hoc* test. Different letters indicate a significant difference, Tukey HSD, $P < 0.01$, $n = 4$.

Whether callose overaccumulation correlated with the transcription of callose synthases (*CalSs*) was then investigated. Among 12 callose synthases, *CalS1* and *CalS12* have been shown to be related to SA and/or biotic stresses (Dong *et al.*, 2008). The transcript levels of *CalS1* and *CalS12* were tested by qPCR in WT, *pi4kβ1β2*, *sid2* and *sid2pi4kβ1β2* plants treated or not with flg22. No correlation was observed between *CalS1* and *CalS12* transcript levels and callose accumulation (Supplementary Data Fig. S5).

pi4kβ1β2 has altered non-host resistance that is SA-independent

The establishment of non-host resistance is based on different mechanisms, involving vesicular secretion as well as callose accumulation (Collins *et al.*, 2003; Assaad *et al.*, 2004; Takemoto *et al.*, 2006; Böhnenius *et al.*, 2010; Lee *et al.*, 2017). To study the role of PI4K in such responses, we tested penetration success and callose production in response to the non-host pathogen *Blumeria graminis* f. sp. *hordei* (*Bgh*). In *Bgh/A. thaliana* interactions, callose accumulates in defensive papillae and haustorial encasements or around dead cells (Jacobs *et al.*, 2003; Assaad *et al.*, 2004; Ellinger *et al.*, 2014). The enhanced number of plant cells with developed haustoria

or dead cells reflects the penetration success of fungal hyphae (Fig. 5A). In our experiments a higher penetration correlated with greater callose accumulation in the plant tissue. In particular, the *pi4kβ1β2* double mutant showed an enhanced successful penetration of *Bgh* 24 hpi, as seen by the enhanced number of haustoria and dead cells. A similar defect in penetration resistance was seen in *sid2/pi4kβ1β2*, indicating the SA-independent character of this phenomenon (Fig. 5B). Both *pi4kβ1β2* and *sid2/pi4kβ1β2* accumulated more callose (Fig. 5C) and over larger areas compared to WT plants (Fig. 5C, D). Thus, the lower penetration resistance accompanied by callose accumulation in *pi4kβ1β2* was independent of the SA pathway.

DISCUSSION

The aim of this study was to investigate SA-dependent and SA-independent processes caused by the *pi4k β1β2* double mutation. As previously shown (Sasek *et al.*, 2014), this mutant accumulates a constitutively high level of SA. In *pi4k β1β2*, SA biosynthesis is dependent on ICS1, as demonstrated by an absence of SA accumulation in the *sid2pi4kβ1β2* triple mutant with impaired *ICS1* transcription (Sasek *et al.*, 2014). This was confirmed with the hormone analysis described in

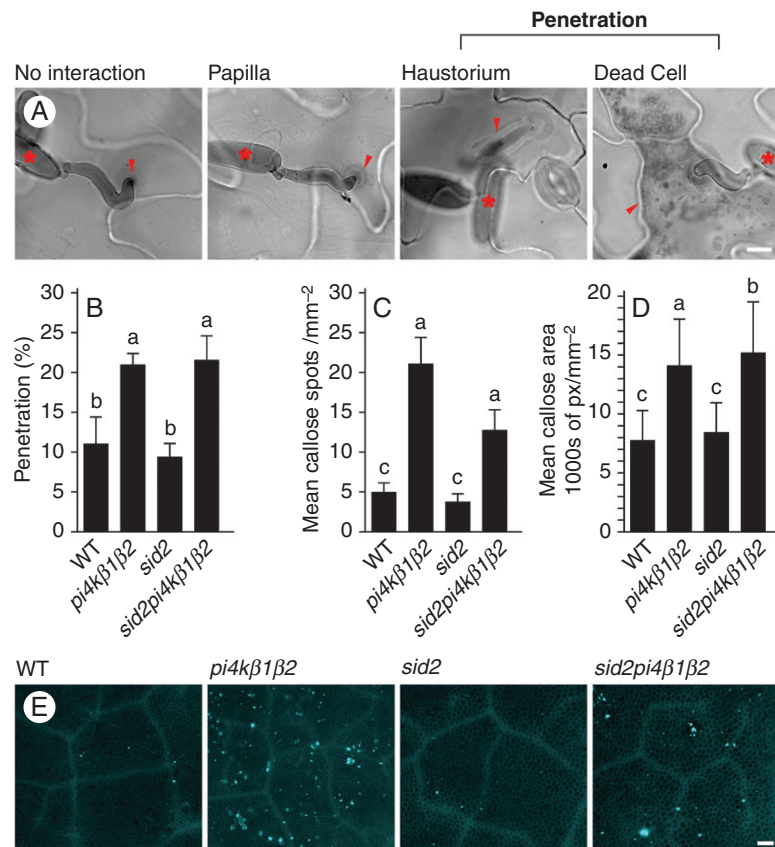


FIG. 5. Resistance of *pi4kβ1β2* to penetration by the non-host pathogen *Blumeria graminis* f. sp. *hordei* (*Bgh*). (A) Four types of interactions counted in the penetration success analysis after trypan blue staining. Scale bar = 5 µm. (B) Data showing penetration success of *Bgh* 24 hpi in each genotype: the mean number of cells with either haustoria or dead cells, respectively. (C) Data showing mean area of a callose spot per mm² at 24 hpi after interaction with *Bgh* spores. (D) Data showing mean area of a callose spot per mm² at 24 hpi after interaction with *Bgh* spores. Data for B, C and D were processed by ANOVA, with a Tukey honestly significant difference (HSD) multiple mean comparison *post hoc* test, the data represent one independent experiment, and the experiment was repeated four times. Letters indicate a significant difference, Tukey HSD, *P* < 0.01. (E) Pictures demonstrating callose staining with aniline blue 24 hpi with *Bgh*. Scale bar = 100 µm.

the present study. The *sid2pi4kβ1β2* triple mutant lacking high SA was used as a tool to distinguish between SA-dependent and SA-independent effects caused by the double mutation in *pi4kβ1β2*.

We first measured phytohormonal levels in fully developed leaves of 4-week-old *A. thaliana* WT, *pi4kβ1β2*, *sid2* and *sid2pi4kβ1β2* plants. To our knowledge, this is the broadest phytohormonal study carried out with an SA over-accumulating mutant (in our case *pi4kβ1β2*) and its comparison with a plant having the same background but with an impaired SA pathway (*sid2pi4kβ1β2*). The level of 15 hormone derivatives (excluding SA) was altered in *pi4k β1β2* compared to WT leaves. For 13 of these, this was SA-dependent. We identified two metabolites, *cis*-zeatin-riboside-5'-monophosphate and glucosylesters of oxindole-3-acetic acid, for which the *pi4k β1β2* double mutation effect was SA-independent. The same conclusions were also reached with another triple mutant, *NahGpi4kβ1β2*. Amongst the hormones controlled by SA were ABA derivatives such as DPA, PA and 9OH-ABA. As ABA levels did not correlate with SA, the action of SA on ABA derivatives did not appear to act on ABA biosynthesis but on its metabolism. Such an effect of SA on ABA catabolism is poorly described. A slight induction of ABA 8'-hydroxylase expression was observed after 24 h of SA treatment of rice seedlings (Mega *et al.*, 2015). In an *A. thaliana* *cpr22* mutant (*constitutive expressor of PR genes 22*), the increase of SA and ABA levels due to a high to low humidity shift was also followed by the SA-dependent expression of genes encoding ABA-metabolizing enzymes (Mosher *et al.*, 2010).

Other hormones displaying a high correlation to SA were Asp-IAA and some cytokinins (SA positively controlled cZROG and tZOG and negatively controlled tZ7G and tZ9G). The pattern of IAA was different from that of Asp-IAA, suggesting that SA control of Asp-IAA was on aspartate conjugation. Aspartate conjugation is catalysed by GH3.2-GH3.6 (Normanly, 2010), with our transcriptome data obtained with *in vitro* grown *pi4kβ1β2* seedlings (Sasek *et al.*, 2014) indicating that GH3.3 (At2g23170) was overexpressed in the double mutant. It would be interesting to investigate whether it was responsible for the Asp-IAA /SA correlation in our double mutant.

Our results demonstrate the major role of hormonal cross-talk between SA and other hormones but only a minor role of impairment of PI4K β 1/ β 2 *per se*. Because a major role of SA is related to responses to biotic stresses, we reasoned that other processes related to biotic stress, whether SA-dependent or not, could also be altered in the double mutant. We tested the resistance of WT, *pi4kβ1β2*, *sid2* and *sid2pi4kβ1β2* plants to representative biotrophic (oomycete *H. arabidopsis* NoCo2), hemibiotrophic (bacteria *Pst* DC3000) and necrotrophic (fungus *Botrytis cinerea*) pathogens. The results clearly showed that resistance to these pathogens was dependent on a high SA content. Resistance to *H. arabidopsis* NoCo2 and *Pst* DC3000 was perhaps not surprising as resistance to such pathogens is generally associated with SA signalling (Glazebrook, 2005). On the other hand, the role of SA in regulating resistance to necrotrophs is rather uncommon. Indeed, plant defence against necrotrophs is commonly associated with jasmonic acid signalling (Ferrari *et al.*, 2003; Glazebrook, 2005). However, Ferrari *et al.* (2003) showed that resistance to *B. cinerea* could be dependent on high SA levels, in accordance with our

observations. A similar finding was reported for defence response to the necrotroph *Sclerotinia sclerotiorum* (Novakova *et al.*, 2014). Moreover, we tested *A. thaliana* ETI by using a bacterial strain highly expressing the AvrRpt2 effector (*Pst* DC3000 AvrRpt2). An ETI response can induce the expression of genes commonly associated with SA, such as *PR-1*, in an SA-independent manner in *A. thaliana* (Tsuda *et al.*, 2013). Yet, we found that the higher resistance of *pi4kβ1β2* plants to *Pst* DC3000 AvrRpt2 was SA-dependent. In conclusion, the higher resistance of the *pi4kβ1β2* mutant to all the host pathogens assayed was strongly SA-dependent.

Non-host resistance, efficient against non-adapted pathogens, does not rely fully on the SA pathway. Here we show that *pi4kβ1β2* exhibited an SA-independent defective resistance towards penetration of the non-host pathogen *Bgh*.

Callose is a linear polysaccharide (1,3- β -glucan) occurring in plant cells where it is important for many plant physiological processes such as cytokinesis (Chen and Kim, 2009). Callose accumulation is triggered in response to pathogens and is used as a common test of pathogen-triggered immunity upon treatment with typical pathogen-associated molecular patterns such as flg22, the epitope of flagellin (Luna *et al.*, 2011). In mock inoculated *pi4k β1β2*, callose deposition was greater than in WT leaves, thus confirming the findings of Antignani *et al.* (2015). Interestingly, this was also true for the *sid2pi4kβ1β2* triple mutant when compared to *sid2* plants, thus indicating an SA-independent phenomenon. Following inoculation with flg22, an increase in callose deposition was observed in all genotypes tested, but this was still higher in *pi4kβ1β2* compared to WT leaves, and callose deposition was higher in *sid2pi4kβ1β2* with respect to *sid2* plants. Therefore, it seems that the *pi4kβ1β2* double mutation *per se* enabled higher callose deposition under biotic stress conditions.

The biosynthesis of callose occurs outside of the cell (Ellinger and Voigt, 2014). Accumulation can be regulated at different levels: transcriptional, translational, or during enzyme transport to the plasma membrane and out of the cell via vesicular trafficking. Phosphorylation and direct translocation of callose synthase is crucial in the regulation of biosynthesis, whereas transcriptional control might have only a minor role (Ellinger and Voigt, 2014). Our data on the transcription levels of *CALS1* and *CALS12* indicate that in *pi4kβ1β2* a transcriptional effect is not involved in the observed over-accumulation of callose. So how is it possible to explain the action on callose of the *pi4kβ1β2* double mutation *per se*? A number of reports indicate that PI4Ks can impact trafficking. In *A. thaliana*, PI4K β 1 was shown to be recruited by the GTP-bound Rab4b GTPase. Both RabA4b and PI4K β 1 localize to budding secretory vesicles in the trans-Golgi network (TGN) and to secretory vesicles *en route* to the cell surface. A *pi4kβ1β2* double mutant produces secretory vesicles of highly variable sizes (Preuss *et al.*, 2006; Kang *et al.*, 2011; Antignani *et al.*, 2015). The product of PI4K activity, PI4P massively accumulates at the plasma membrane and at early endosomes/TGN and Golgi (Platre and Jaillais, 2016; Noack and Jaillais, 2017). Therefore, PI4K β 1/ β 2 are important in vesicle trafficking. Interestingly, inhibiting PI4K with phenylarsine oxide (PAO) suppressed the salt-induced endocytosis of plasma membrane intrinsic protein 2:1 (Ueda *et al.*, 2016). Similarly, inhibiting PI4K led to the internalization of CELLULOSE SYNTHASE3 from the plasma

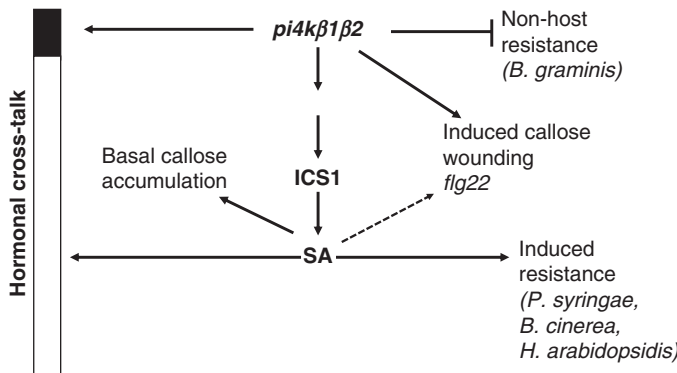


FIG. 6. Schematic representation of the effects of the *pi4kβ1β2* double mutation on *Arabidopsis* plants.

membrane (Fujimoto *et al.*, 2015). Can the impact of PI4K betas on trafficking explain the increased callose accumulation? Callose biosynthesis and accumulation have been shown to be affected by vesicle trafficking (Ellinger and Voigt, 2014). PI4Ks have been shown to play an important role in cytokinesis (Lin *et al.*, 2019), especially in the correct organization of the vesicles at the cell division pla $\beta 1\beta 2$ ne and further formation of a cell plate. During phragmoplast formation, PI4K $\beta 1$ probably interacts with MPK4, a member of the MAP65 protein family that regulates microtubule organization (Lin *et al.*, 2019). Callose is also essential for cytokinesis (Thiele *et al.*, 2009). We can therefore only speculate whether the effects of PI4Ks on callose, cytokinesis and trafficking are interconnected. Interestingly, the role of SA in these processes has not been tested. Because PI4K $\beta 1/\beta 2$ can impact the secretory pathway, they could also impact the translocation of callose synthases. Furthermore, PMR4 (CALS12) binds to small RabA4c GTPase at the TGN and PI4K $\beta 1$ binds to RabA4b GTPase, the most similar small GTPase to RabA4c, at the TGN (Böhnenius *et al.*, 2010). Note that the impact of PI4K betas on trafficking could also explain our non-host resistance data. The *syp121* mutant altered in a SNARE protein involved in trafficking has been reported to accumulate SA and also display defective non-host resistance (Collins *et al.*, 2003).

In conclusion (Fig. 6), the *pi4kβ1β2* double mutant constitutively accumulated a high SA level via ICS1/SID2 and this had considerable impact on other hormone levels and was associated with an increased resistance to several plant pathogens (*P. syringae*, *H. arabidopsidis*, *Botrytis cinerea*). The *pi4kβ1β2* double mutation also affected pathogen-related processes in a high SA-independent manner as seen by differences in callose accumulation in response to *flg22*, to *Bgh* infection, to wounding, and the higher penetration success of *Bgh*. The identification of such processes directly affected by the mutation on PI4Ks will now allow us to better investigate the role of these enzymes, in relation to signalling or trafficking events.

SUPPLEMENTARY DATA

Supplementary data are available online at <https://academic.oup.com/aob> and consist of the following. Table S1: Phytohormone levels in 4-week-old plants. Fig. S1: Levels of hormones controlled

by SA in 4-week-old mutant and WT plants. Fig. S2: Levels of hormones not controlled by SA in 4-week-old mutant and WT plants. Fig. S3: Resistance to *P. syringae* pv. *tomato* DC3000 AvrRpt2. Fig. S4: Callose deposition in response to wounding. Fig. S5: Relative transcription of some *CalS* genes in untreated rosette leaves or 24 h after infiltration with 0.1 μ M *flg22*.

FUNDING

This work was supported by the Czech Science Foundation [grant number 17-05151S]. Collaboration between the Ukrainian and French teams was partially supported by a ‘Projet international de coopération scientifique’ from the ‘Centre National de la Recherche Scientifique’ (2015–2018). T.K. received the Visegrad scholarship (2016–2017) [grant number 51600349]; she also benefited from the Program of Postdoctoral Fellowships of the Czech Academy of Sciences [grant number TK 919220]. This study was also supported by a European Regional Development Fund-Project ‘Centre for Experimental Plant Biology’ [grant number CZ.02.1.01/0.0/0.0/16_019/00000738].

ACKNOWLEDGEMENTS

We thank Lucie Lamparová and Romana Pospíchalová for their technical support and Michael Hodges for language editing.

LITERATURE CITED

- Antignani V, Klocko AL, Bak G, Chandrasekaran SD, Duniniv T, Nielsen E. 2015. Recruitment of PLANT U-BOX13 and the PI4Kbeta1/beta2 phosphatidylinositol-4 kinases by the small GTPase RabA4B plays important roles during salicylic acid-mediated plant defense signaling in *Arabidopsis*. *Plant Cell* 27: 243–261.
- Assaad FF, Qiu JL, Youngs H, *et al.* 2004. The PEN1 syntaxin defines a novel cellular compartment upon fungal attack and is required for the timely assembly of papillae. *Molecular Biology of the Cell* 15: 5118–5129.
- Balla T. 2007. Imaging and manipulating phosphoinositides in living cells. *Journal of Physiology* 582: 927–937.
- Böhnenius H, Mørch SM, Godfrey D, Nielsen ME, Thordal-Christensen H. 2010. The multivesicular body-localized GTPase ARFA1b/1c is important for callose deposition and ROR2 syntaxin-dependent preinvasive basal defense in barley. *The Plant Cell* 22: 3831.
- Cao H, Glazebrook J, Clarke JD, Volko S, Dong X. 1997. The *Arabidopsis* NPR1 gene that controls systemic acquired resistance encodes a novel protein containing ankyrin repeats. *Cell* 88: 57–63.
- Collins NC, Thordal-Christensen H, Lipka V, *et al.* 2003. SNARE-protein-mediated disease resistance at the plant cell wall. *Nature* 425: 973–977.
- Cui H, Gobbato E, Kracher B, Qiu J, Bautista J, Parker JE. 2017. A core function of EDS1 with PAD4 is to protect the salicylic acid defense sector in *Arabidopsis* immunity. *New Phytologist* 213: 1802–1817.
- Czechowski T, Stitt M, Altman T, Udvardi MK, Scheible WR. 2005. Genome-wide identification and testing of superior reference genes for transcript normalization in *Arabidopsis*. *Plant Physiology* 139: 5–17.
- Delage E, Ruelland E, Guillas I, Zachowski A, Puyaubert J. 2012. *Arabidopsis* type-III phosphatidylinositol 4-kinases beta1 and beta2 are upstream of the phospholipase C pathway triggered by cold exposure. *Plant and Cell Physiology* 53: 565–576.
- Delaney TP, Uknes S, Vernooij B, *et al.* 1994. A central role of salicylic Acid in plant disease resistance. *Science* 266: 1247–1250.
- Dempsey DMA, Vlot AC, Wildermuth MC, Klessig DF. 2011. Salicylic Acid biosynthesis and metabolism. *Arabidopsis Book* 9: e0156–e.
- Dobrev PI, Hoyerova K, Petrasek J. 2017. Analytical determination of auxins and cytokinins. *Methods in Molecular Biology* 1569: 31–39.

- Dobrev PI, Kaminek M.** 2002. Fast and efficient separation of cytokinins from auxin and abscisic acid and their purification using mixed-mode solid-phase extraction. *Journal of Chromatography A* **950**: 21–29.
- Dobrev PI, Vankova R.** 2012. Quantification of abscisic acid, cytokinin, and auxin content in salt-stressed plant tissues. *Methods in Molecular Biology* **913**: 251–261.
- Dong X, Hong Z, Chatterjee J, Kim S, Verma DP.** 2008. Expression of callose synthase genes and its connection with Npr1 signaling pathway during pathogen infection. *Planta* **229**: 87–98.
- Ellinger D, Glockner A, Koch J, et al.** 2014. Interaction of the Arabidopsis GTPase RabA4c with its effector PMR4 results in complete penetration resistance to powdery mildew. *Plant Cell* **26**: 3185–3200.
- Ellinger D, Voigt CA.** 2014. Callose biosynthesis in Arabidopsis with a focus on pathogen response: what we have learned within the last decade. *Annals of Botany* **114**: 1349–1358.
- Ferrari S, Plotnikova JM, De Lorenzo G, Ausubel FM.** 2003. Arabidopsis local resistance to Botrytis cinerea involves salicylic acid and camalexin and requires EDS4 and PAD2, but not SID2, EDS5 or PAD4. *Plant Journal* **35**: 193–205.
- Fujimoto M, Suda Y, Vernhettes S, Nakano A, Ueda T.** 2015. Phosphatidylinositol 3-kinase and 4-kinase have distinct roles in intracellular trafficking of cellulose synthase complexes in *Arabidopsis thaliana*. *Plant and Cell Physiology* **56**: 287–298.
- Glazebrook J.** 2005. Contrasting mechanisms of defense against biotrophic and necrotrophic pathogens. *Annual Review of Phytopathology* **43**: 205–227.
- Gross J, Cho WK, Lezhneva L, et al.** 2006. A plant locus essential for phylloquinone (vitamin K1) biosynthesis originated from a fusion of four eubacterial genes. *Journal of Biological Chemistry* **281**: 17189–17196.
- Chen XY, Kim JY.** 2009. Callose synthesis in higher plants. *Plant Signaling and Behaviour* **4**: 489–492.
- Jacobs AK, Lipka V, Burton RA, et al.** 2003. An *Arabidopsis* callose synthase, GSL5, is required for wound and papillary callose formation. *Plant Physiology* **131**: 2503–2513.
- Janda M, Sasek V, Ruelland E.** 2014. The *Arabidopsis* pi4kIIIbeta1beta2 double mutant is salicylic acid-overaccumulating: a new example of salicylic acid influence on plant stature. *Plant Signaling and Behaviour* **9**: e977210.
- Janda M, Ruelland E.** 2015. Magical mystery tour: salicylic acid signalling. *Environmental and Experimental Botany* **114**: 117–128.
- Kalachova T, Puga-Freitas R, Kravets V, et al.** 2016. The inhibition of basal phosphoinositide-dependent phospholipase C activity in *Arabidopsis* suspension cells by abscisic or salicylic acid acts as a signalling hub accounting for an important overlap in transcriptome remodelling induced by these hormones. *Environmental and Experimental Botany* **123**: 37–49.
- Kang BH, Nielsen E, Preuss ML, Mastronarde D, Staehelin LA.** 2011. Electron tomography of RabA4b- and PI-4Kbeta1-labeled trans Golgi network compartments in *Arabidopsis*. *Traffic* **12**: 313–329.
- Katagiri F, Thilimony R, He SY.** 2002. The *Arabidopsis thaliana*-*pseudomonas syringae* interaction. *Arabidopsis Book* **1**: e0039.
- Kohler A, Schwindling S, Conrath U.** 2002. Benzothiadiazole-induced priming for potentiated responses to pathogen infection, wounding, and infiltration of water into leaves requires the NPr1/NIM1 gene in *Arabidopsis*. *Plant Physiology* **128**: 1046–1056.
- Krinke O, Ruelland E, Valentová O, et al.** 2007. Phosphatidylinositol 4-Kinase activation is an early response to salicylic acid in *Arabidopsis* suspension cells. *Plant Physiology* **144**: 1347–1359.
- Krinke O, Flemr M, Vergnolle C, et al.** 2009. Phospholipase D activation is an early component of the salicylic acid signaling pathway in *Arabidopsis* cell suspensions. *Plant Physiology* **150**: 424–436.
- Lee H-A, Lee H-Y, Seo E, et al.** 2017. Current understandings of plant Nonhost Resistance. *Molecular Plant–Microbe Interactions* **30**: 5–15.
- Lin F, Krishnamoorthy P, Schubert V, Hause G, Heilmann M, Heilmann I.** 2019. A dual role for cell plate-associated PI4Kβ in endocytosis and phragmoplast dynamics during plant somatic cytokinesis. *The EMBO Journal* **38**: e100303.
- Luna E, Pastor V, Robert J, Flors V, Mauch-Mani B, Ton J.** 2011. Callose deposition: a multifaceted plant defense response. *Molecular Plant–Microbe Interactions* **24**: 183–193.
- Marshall OJ.** 2004. PerlPrimer: cross-platform, graphical primer design for standard, bisulphite and real-time PCR. *Bioinformatics* **20**: 2471–2472.
- Mega R, Meguro-Maoka A, Endo A, et al.** 2015. Sustained low abscisic acid levels increase seedling vigor under cold stress in rice (*Oryza sativa* L.). *Scientific Reports* **5**: 13819.
- Mosher S, Moeder W, Nishimura N, et al.** 2010. The lesion-mimic mutant cpr22 shows alterations in abscisic acid signaling and abscisic acid insensitivity in a salicylic acid-dependent manner. *Plant Physiology* **152**: 1901–1913.
- Nakanishi S, Catt KJ, Balla T.** 1995. A wortmannin-sensitive phosphatidylinositol 4-kinase that regulates hormone-sensitive pools of inositolphospholipids. *Proceedings of the National Academy of Sciences of the USA* **92**: 5317–5321.
- Noack LC, Jaillais Y.** 2017. Precision targeting by phosphoinositides: how PIs direct endomembrane trafficking in plants. *Current Opinion in Plant Biology* **40**: 22–33.
- Normanly J.** 2010. Approaching cellular and molecular resolution of auxin biosynthesis and metabolism. *Cold Spring Harbor Perspectives in Biology* **2**: a001594.
- Novakova M, Sasek V, Dobrev PI, Valentová O, Burkertova L.** 2014. Plant hormones in defense response of *Brassica napus* to *Sclerotinia sclerotiorum* – reassessing the role of salicylic acid in the interaction with a necrotroph. *Plant Physiology and Biochemistry* **80**: 308–317.
- Pappan K, Austin-Brown S, Chapman KD, Wang X.** 1998. Substrate selectivities and lipid modulation of plant phospholipase D alpha, -beta, and -gamma. *Archives of Biochemistry and Biophysics* **353**: 131–140.
- Platre MP, Jaillais Y.** 2016. Guidelines for the use of protein domains in acidic phospholipid imaging. *Methods in Molecular Biology* **1376**: 175–194.
- Preuss ML, Schmitz AJ, Thole JM, Bonner HK, Otegui MS, Nielsen E.** 2006. A role for the RabA4b effector protein PI-4Kbeta1 in polarized expansion of root hair cells in *Arabidopsis thaliana*. *Journal of Cell Biology* **172**: 991–998.
- R Core Team.** 2014. *R: A language and environment for statistical computing*. Vienna: R Foundation for Statistical Computing.
- Sasek V, Janda M, Delage E, et al.** 2014. Constitutive salicylic acid accumulation in pi4kIIIbeta1beta2 *Arabidopsis* plants stunts rosette but not root growth. *New Phytologist* **203**: 805–816.
- Seyfferth C, Tsuda K.** 2014. Salicylic acid signal transduction: the initiation of biosynthesis, perception and transcriptional reprogramming. *Frontiers in Plant Science* **5**: 697.
- Takemoto D, Jones DA, Hardham AR.** 2006. Re-organization of the cytoskeleton and endoplasmic reticulum in the *Arabidopsis* pen1-1 mutant inoculated with the non-adapted powdery mildew pathogen, *Blumeria graminis f. sp. hordei*. *Molecular Plant Pathology* **7**: 553–563.
- Thiele K, Wanner G, Kindzierski V, et al.** 2009. The timely deposition of callose is essential for cytokinesis in *Arabidopsis*. *The Plant Journal* **58**: 13–26.
- Tsuda K, Mine A, Bethke G, et al.** 2013. Dual regulation of gene expression mediated by extended MAPK activation and salicylic acid contributes to robust innate immunity in *Arabidopsis thaliana*. *PLoS Genetics* **9**: e1004015.
- Ueda M, Tsutsumi N, Fujimoto M.** 2016. Salt stress induces internalization of plasma membrane aquaporin into the vacuole in *Arabidopsis thaliana*. *Biochemical and Biophysical Research Communications* **474**: 742–746.
- Vlot AC, Dempsey DA, Klessig DF.** 2009. Salicylic acid, a multifaceted hormone to combat disease. *Annual Review of Phytopathology* **47**: 177–206.
- Vogel J, Somerville S.** 2000. Isolation and characterization of powdery mildew-resistant *Arabidopsis* mutants. *Proceedings of the National Academy of Sciences USA* **97**: 1897–1902.
- Voigt CA.** 2014. Callose-mediated resistance to pathogenic intruders in plant defense-related papillae. *Frontiers in Plant Science* **5**: 168.
- Wagner S, Stuttmann J, Rietz S, et al.** 2013. Structural basis for signaling by exclusive EDS1 heteromeric complexes with SAG101 or PAD4 in plant innate immunity. *Cell Host & Microbe* **14**: 619–630.
- Wildermuth MC, Dewdney J, Wu G, Ausubel FM.** 2001. Isochorismate synthase is required to synthesize salicylic acid for plant defence. *Nature* **414**: 562–565.
- Yi SY, Shirasu K, Moon JS, Lee SG, Kwon SY.** 2014. The activated SA and JA signaling pathways have an influence on flg22-triggered oxidative burst and callose deposition. *PLoS One* **9**: e88951.